TO MY BELOVED PARENTS

NUMERICAL STUDY OF STABILITY AND TRANSITION OF FREE-CONVECTION BOUNDARY LAYER FLOWS

BY

ABOLFATH SEYEDFATHI, B.Sc.(Eng.)

November, 1974

A thesis submitted for the degree of Doctor of Philosophy of the University of London.

Department of Chemical Engineering
and Chemical Technology,
Imperial College of Science and
Technology,
London, S.W.7.

ABSTRACT

The present work was planned in order to investigate the stability of free-convection boundary layer flows along an isothermal vertical plate.

The disturbance differential equations which describe the stability of free-convection boundary layer flows were derived based upon linear stability theory and on the introduction of a perturbation stream function and a perturbation temperature function. The disturbance equations were rewritten in dimensionless form by the introduction of dimensionless variables.

Quasilinearization and trial-and-error techniques were used to solve the boundary value problem associated with the solution of the disturbance equations for a range of Prandtl numbers 0.733 to 1000.0 and for a range of Grashof numbers 2×10^4 to 10^8. Neutral stability curves were obtained for each Prandtl number.

The unknown boundary conditions and eigenvalues were determined with an accuracy of four decimal places. In order to obtain this accuracy the size of the integration step length, the value of the convergence criterion and the effective boundary layer thickness were optimized.

Comparison of the neutral stability curves for different Prandtl numbers showed that the value of the Prandtl number influences the minimum critical value of the Grashof number. As the Prandtl number was increased it was observed that the minimum critical value of the Grashof number decreased. This effect was more pronounced for Prandtl numbers in the range

0.733 to 6.7 than for the range 6.7 to 1000.0.

A kinetic energy balance equation for the disturbed motion was solved in order to find the importance of the buoyancy term in the disturbance differential equations. The solutions of this equation showed that omission of the temperature fluctuations for the purpose of solving the disturbance differential equations for Prandtl numbers of 0.733 and 1.0 may be justified for wave numbers greater than 0.35 but that for Prandtl numbers of 6.7 and greater the temperature fluctuations could not be omitted.

Comparison of the phase velocities corresponding to the minimum critical Grashof numbers, with the maximum velocities of the basic laminar flows showed that the phase velocities of the disturbance were greater than maximum velocities of the basic laminar flows, consequently asymptotic methods cannot provide a reliable value of the minimum critical Grashof number.

The results of the present work were in good agreement with experimental results obtained by other workers who studied artificially induced disturbances inside the boundary layer.

ACKNOWLEDGEMENTS

I would like to express my sincere thanks and gratitude to Dr. A.R.H. Cornish for his discerning supervision, guidance and encouragement during the course of this study.

The friendship of my departmental colleagues particularly Dr. M. Moayeri and F. Geoola is greatly appreciated, and I would like to thank them for the many discussions which I had with them.

LIST OF CONTENTS

	Page
ABSTRACT	3
ACKNOWLEDGEMENTS	5
LIST OF CONTENTS	6
LIST OF FIGURES	10
LIST OF TABLES	13
LIST OF SYMBOLS	18
CHAPTER 1. INTRODUCTION	22
CHAPTER 2. LITERATURE SURVEY	26
2.1. Introduction	27
2.2. Experimental Investigations	27
2.3. Theoretical Studies	33
CHAPTER 3. THEORETICAL ANALYSIS	40
3.1. The Navier-Stokes, Continuity and Transfer Equation for Free-convective Heat Transfer	41
3.2. The Equations of the Instability of Free-convection Boundary Layer Flows along a Vertical Isothermal Plate	45
3.3. Equations for Free-convection Boundary Layer Flows	57
3.3.1. The Boundary Layer Approximations	58
3.3.2. Free-convection Boundary Layer Equations for Heat Transfer from an Isothermal Vertical Plate	58
3.4. Kinetic Energy Balance of Disturbed Motion	60

CHAPTER 4. NUMERICAL TECHNIQUES 64

4.1. Introduction 65

4.2. Quasilinearization technique 65

4.2.1. Introduction 65

4.2.2. Generalizing the Newton-Raphson Method to Functional Equations 68

4.2.3. Convergence and Monotonicity of the Quasilinearization Technique 70

4.2.4. Application of the Quasilinearization Technique to Systems of Differential Equations 71

4.2.5. Application of the Quasilinearization Technique to Parameter Estimation 78

4.2.6. A Brief Review of the Main Difficulties Arising in the use of the Quasilinearization Technique 79

4.2.7. Application of the Quasilinearization Technique to the Present Problem 81

4.3. Trial-and-error Technique 96

4.3.1. Introduction 96

4.3.2. The Application of Trial-and-error Technique to the Present Problem 96

Page

4.3.3. Simplification of the Present Trial-and-error Technique 101

4.4. Numerical Integration Technique 102

CHAPTER 5. RESULTS AND DISCUSSION 104

5.1. The Accuracy of the Numerical Solutions 105

5.2. Stability Results for Air, Prandtl Number of 0.733, and Prandtl Number of 1.0. 112

5.3. Stability Results for Water, Prandtl Number of 6.7 146

5.4. Stability Results for Prandtl Numbers of 100 and 1000.0 155

5.5. The Influence of the Prandtl Number on the Neutral Stability Curves 172

5.6. The Influence of the Prandtl Number on the Minimum Critical Value of the Grashof Number 178

5.7. Comparison of the Present Results with the Existing Experimental Results 180

CHAPTER 6. CONCLUSIONS 186

APPENDIX A. CONDITIONS TO BE SATISFIED AT THE EDGE OF THE BOUNDARY LAYER 191

APPENDIX B. NEWTON-RAPHSON METHOD 195

APPENDIX C. THE SUPERPOSITION PRINCIPLE 202

APPENDIX D. ORTHOGONALIZATION OF VECTOR SETS 205

Page

APPENDIX E. CAUCHY-RIEMANN EQUATIONS 209

APPENDIX F. TABLES OF RESULTS 212

APPENDIX G. COMPUTER PROGRAMMES 243

BIBLIOGRAPHY 275

LIST OF FIGURES

Figure		Page
3.1	An external free-convection flow.	63
5.1	The plot of phase velocity, c_i, against Grashof number, Gr, at a wave number of 0.76 for a Prandtl number of 0.733.	114
5.2	Neutral stability curve for air, Prandtl number of 0.733, in α, Gr-plane.	115
5.3	Neutral stability curve for air, Prandtl number of 0.733, in c_r, Gr-plane.	117
5.4	Velocity profile for air, Prandtl number of 0.733, from Schmidt and Beckmann equations.	118
5.5 to 5.36	Eigenfunctions for air, Prandtl number of 0.733.	119 to 126
5.37 to 5.52	Energy distributions for air, Prandtl number of 0.733.	128 to 131
5.53	A comparison between the neutral stability curve of the present work with that without temperature fluctuations for a Prandtl number of 0.733.	133
5.54	Neutral stability curve for a Prandtl number of 1.0, in α, Gr-plane.	135
5.55	Neutral stability curve for a Prandtl number of 1.0, in c_r, Gr-plane.	136
5.56	Velocity profile for a Prandtl number of 1.0 from Schmidt and Beckmann equations.	137

Number		Page
5.57 to 5.76	Eigenfunctions for a Prandtl number of 1.0.	138 to 142
5.77 to 5.86	Energy distributions for a Prandtl number of 1.0.	143 to 145
5.87	Neutral stability curve for water, Prandtl number of 6.7, in α, Gr-plane.	147
5.88	Neutral stability curve for water, Prandtl number of 6.7, in c_r, Gr-plane.	148
5.89	Velocity profile for water, Prandtl number of 6.7, from Schmidt and Beckmann equations.	149
5.90 to 5.107	Eigenfunctions for water, Prandtl number of 6.7.	150 to 154
5.108 to 5.115	Energy distributions for water, Prandtl number of 6.7.	156 to 157
5.116	A comparison between the neutral stability curve of the present work with that without temperature fluctuations for a Prandtl number of 6.7.	158
5.117	Neutral stability curve for a Prandtl number of 100.0 in α, Gr-plane.	159
5.118	Neutral stability curve for a Prandtl number of 100.0 in c_r, Gr-plane.	160
5.119	Velocity profile for a Prandtl number of 100.0 from Schmidt and Beckmann equations.	162
5.120 to 5.135	Eigenfunctions for a Prandtl number of 100.0.	163 to 166
5.136 to 5.143	Energy distributions for a Prandtl number of 100.0.	167 to 168

Number		Page
5.144	Neutral stability curve for a Prandtl number of 1000.0 in α, Gr-plane.	169
5.145	Neutral stability curve for a Prandtl number of 1000.0 in c_r, Gr-plane.	170
5.146	Velocity profile for a Prandtl number of 1000.0 from Schmidt and Beckmann equations.	171
5.147 to 5.154	Eigenfunctions for a Prandtl number of 1000.0.	173 to 174
5.155 to 5.158	Energy distributions for a Prandtl number of 1000.0.	175
5.159	Neutral stability curves for Prandtl numbers of 0.733, 1.0, 6.7, 100.0 and 1000.0 in α, Gr-plane.	176
5.160	Neutral stability curves for Prandtl numbers of 0.733, 1.0, 6.7, 100.0 and 1000.0 in c_r, Gr-plane.	179
5.161	A comparison between the neutral stability curve of present work with experimental data for air, Prandtl number of 0.733.	181
5.162	A comparison between the neutral stability curve of present work with experimental data for water, Prandtl number of 6.7.	182
5.163 and 5.164	A comparison between the neutral stability curves of present work using the quasi-linearization technique with those using the trial-and-error technique.	184 and 185
B.1	Newton-Raphson method.	201

LIST OF TABLES

Table		Page
F.1	The effect of the integration step length on the predicted values of $\overset{'''}{\psi}(0)_r$, $\overset{'''}{\psi}(0)_i$, $\overset{'}{\xi}(0)_r$, $\overset{'}{\xi}(0)_i$, c_r and c_i.	213
F.1.(a)	For a Prandtl number of 1.0 at $\alpha Gr = 8.0$ and at $\alpha = 0.02$ with $\eta_{edg} = 8.0$ and a convergence criterion of 1×10^{-4}.	213
F.1.(b)	For a Prandtl number of 1.0 at $\alpha Gr = 75.0$ and at $\alpha = 0.65$ with $\eta_{edg} = 8.0$ and a convergence criterion of 1×10^{-4}.	214
F.1.(c)	For a Prandtl number of 6.7 at $\alpha Gr = 7.0$ and at $\alpha = 0.02$ with $\eta_{edg} = 8.0$ and a convergence criterion of 1×10^{-4}.	215
F.1.(d)	For a Prandtl number of 6.7 at $\alpha Gr = 21.5$ and at $\alpha = 0.60$ with $\eta_{edg} = 8.0$ and a convergence criterion of 1×10^{-4}.	216
F.1.(e)	For a Prandtl number of 100.0 at $\alpha Gr = 11.70$ and at $\alpha = 0.04$ with $\eta_{edg} = 14.0$ and a convergence criterion of 1×10^{-3}.	217
F.1.(f)	For a Prandtl number of 100.0 at $\alpha Gr = 27.0$ and at $\alpha = 0.8$ with $\eta_{edg} = 14.0$ and a convergence criterion of 1×10^{-3}.	218
F.2.	The effect of the value of η_{edg} on the predicted values of $\overset{'''}{\psi}(0)_r$, $\overset{'''}{\psi}(0)_i$, $\overset{'}{\xi}(0)_r$, $\overset{'}{\xi}(0)_i$, c_r and c_i.	219
F.2.(a)	For a Prandtl number of 0.733 at $\alpha Gr = 51.3$ and at $\alpha = 0.45$ with integration step	219

Table		Page
	lengths H = 0.008 ($0<\eta<1$), 0.016 ($1<\eta<8$) and a convergence criterion of 1×10^{-4}.	
F.2.(b)	For a Prandtl number of 0.733 at $\alpha Gr = 6.6$ and at $\alpha = 0.075$ with integration step lengths H = 0.01 ($0<\eta<1$), 0.02 ($0<\eta<8$) and a convergence criterion of 1×10^{-4}.	220
F.2.(c)	For a Prandtl number of 6.7 at $\alpha Gr = 21.0$ and at $\alpha = 0.6$ with integration step lengths H = 0.01 ($0<\eta<1$), 0.02 ($1<\eta<8$) and a convergence criterion of 1×10^{-4}.	221
F.2.(d)	For a Prandtl number of 6.7 at $\alpha Gr = 4.8$ and at $\alpha = 0.04$ with integration step lengths H = 0.0125 ($0<\eta<1$), 0.025 ($1<\eta<8$) and a convergence criterion of 1×10^{-4}.	222
F.2.(e)	For a Prandtl number of 100.0 at $\alpha Gr = 23.60$ and at $\alpha = 0.70$ with integration step lengths H = 0.01 ($0<\eta<1$), 0.02 ($1<\eta<14$) and a convergence criterion of 1×10^{-4}.	223
F.2.(f)	For a Prandtl number of 100.0 at $\alpha Gr = 9.95$ and at $\alpha = 0.04$ with integration step lengths H = 0.0125 ($0<\eta<1$), 0.025 ($1<\eta<14$) and a convergence criterion of 1×10^{-4}.	224
F.2.(g)	For a Prandtl number of 1000.0 at $\alpha Gr = 30.07$ and at $\alpha = 0.90$ with integration step lengths H = 0.01 ($0<\eta<1$), 0.02 ($1<\eta<15$) and a convergence criterion of 1×10^{-4}.	225

Table		Page
F.2.(h)	For a Prandtl number of 1000.0 at $\alpha Gr = 11.35$ and at $\alpha = 0.04$ with integration step lengths H = 0.0125 ($0<\eta<1$), 0.025 ($1<\eta<15$) and a convergence criterion of 1×10^{-4}.	226
F.3	The effect of variation of the convergence criterion on the predicted values of $\overset{'''}{\psi}(0)_r$, $\overset{'''}{\psi}(0)_i$, $\overset{'}{\xi}(0)_r$ and $\overset{'}{\xi}(0)_i$.	227
F.3.(a)	For a Prandtl number of 1.0 at $\alpha Gr = 10.0$ with integration step lengths H = 0.01 ($0<\eta<1$), 0.02 ($0<\eta<1$) and $\eta_{edg} = 8.0$	227
F.3.(b)	For a Prandtl number of 1.0 at $\alpha Gr = 20.0$ with integration step lengths H = 0.01 ($0<\eta<1$), 0.02 ($1<\eta<8$) and $\eta_{edg} = 8.0$.	227
F.3.(c)	For a Prandtl number of 0.733 at $\alpha Gr = 43.2$ with integration step lengths H = 0.01 ($0<\eta<1$), 0.02 ($1<\eta<8$) and $\eta_{edg} = 8.0$.	228
F.3.(d)	For a Prandtl number of 0.733 at $\alpha Gr = 92.6$ with integration step lengths H = 0.008 ($0<\eta<1$), 0.016 ($1<\eta<8$) and $\eta_{edg} = 8.0$.	228
F.3.(e)	For a Prandtl number of 0.733 at $\alpha Gr = 116.8$ with integration step lengths H = 0.008 ($0<\eta<1$), 0.016 ($1<\eta<8$) and $\eta_{edg} = 8.0$.	228

Table		Page
F.3.(f)	For a Prandtl number of 0.733 at $\alpha Gr = 194.0$ with integration step lengths H = 0.008 ($0<\eta<1$), 0.016 ($1<\eta<8$) and $\eta_{edg} = 8.0$.	229
F.3.(g)	For a Prandtl number of 0.733 at $\alpha Gr = 238.0$ with integration step lengths H = 0.008 ($0<\eta<1$), 0.016 ($1<\eta<8$) and $\eta_{edg} = 8.0$.	229
F.3.(h)	For a Prandtl number of 6.7 at $\alpha Gr = 5.4$ with integration step lengths H = 0.0125 ($0<\eta<1$), 0.025 ($1<\eta<8$) and $\eta_{edg} = 8.0$.	229
F.3.(i)	For a Prandtl number of 6.7 at $\alpha Gr = 7.625$ with integration step lengths H = 0.0125 ($0<\eta<1$), 0.025 ($1<\eta<8$) and $\eta_{edg} = 8.0$.	230
F.3.(j)	For a Prandtl number of 6.7 at $\alpha Gr = 10.8$ with integration step lengths H = 0.0125 ($0<\eta<1$), 0.025 ($1<\eta<8$) and $\eta_{edg} = 8.0$.	230
F.3.(k)	For a Prandtl number of 6.7 at $\alpha Gr = 16.0$ with integration step lengths H = 0.01 ($0<\eta<1$), 0.02 ($1<\eta<8$) and $\eta_{edg} = 8.0$.	230
F.3.(l)	For a Prandtl number of 6.7 at $\alpha Gr = 23.0$ with integration step lengths H = 0.01 ($0<\eta<1$), 0.02 ($1<\eta<8$) and $\eta_{edg} = 8.0$.	231
F.3.(m)	For a Prandtl number of 6.7 at $\alpha Gr = 34.0$ with integration step lengths H = 0.01 ($0<\eta<1$), 0.02 ($1<\eta<8$) and $\eta_{edg} = 8.0$.	231

Table		Page
F.3.(n)	For a Prandtl number of 100.0 at αGr = 6.0 with integration step lengths H = 0.0125 ($0<\eta<1$), 0.025 ($1<\eta<8$) and η_{edg} = 14.0	232
F.3.(o)	For a Prandtl number of 100.0 at αGr = 17.55 with integration step lengths H = 0.01 ($0<\eta<1$), 0.02 ($1<\eta<8$) and η_{edg} = 14.0.	232
F.3.(p)	For a Prandtl number of 100.0 at αGr = 32.8 with integration step lengths H = 0.01 ($0<\eta<1$), 0.02 ($1<\eta<8$) and η_{edg} = 14.0.	232
F.4.	The values of α and its corresponding values of Gr, αGr, c_r, c_i and the missing boundary conditions $\psi'''(0)_r$, $\psi'''(0)_i$, $\xi'(0)_r$, $\xi'(0)_i$ on the neutral stability curve.	233
F.4.(a)	For a Prandtl number of 0.733.	233
F.4.(b)	For a Prandtl number of 1.0.	234
F.4.(c)	For a Prandtl number of 6.7.	235
F.4.(d)	For a Prandtl number of 100.0.	236
F.4.(e)	For a Prandtl number of 1000.0.	237
F.5.	Functions f and H and derivatives for various Prandtl numbers from Schmidt and Beckmann equations	238
F.5.(a)	For a Prandtl number of 0.733	238
F.5.(b)	For a Prandtl number of 1.0.	239
F.5.(c)	For a Prandtl number of 6.7	240
F.5.(d)	For a Prandtl number of 100.0.	241
F.5.(e)	For a Prandtl number of 1000.0.	242

LIST OF SYMBOLS

Symbol	Meaning
a	Superposition constant.
b_i	An amplification factor.
b_r	Circular frequency of partial oscillation.
c	Phase velocity.
c^*	Dimensionless phase velocity defined as $cx/2\nu_\infty \sqrt{Gr_x}$.
c_i	An amplification factor.
c_p	Specific heat at constant pressure.
c_r	Velocity of propagation.
e_B	Buoyancy term in equation (3.4.2).
e_D	Dissipation term in equation (3.4.2).
e_{Re}	Reynold stress term in equation (3.4.2).
f	Dimensionless stream function.
$\acute{f}$	Dimensionless velocity function.
$\acute{f}_{max}$	Dimensionless maximum velocity.
Fr	Froude number, $2\nu_\infty^2(Gr_x)/g\delta x^2$.
g	Gravitational acceleration.
$\underline{g}$	Gravity vector.
Gr_x	Grashof number based on x, $g\beta\Delta Tx^3/\nu_\infty^2$.
Gr^*	Modified Grashof number, $2\sqrt{2}(Gr_x)^{1/4}$.
H	Dimensionless temperature function.
J	Jacobian matrix.
K	Coefficient of heat conductivity.
n	Number of missing boundary conditions.
$\underline{n}$	Outward normal vector from the surface.
p	Instantaneous pressure.
P	Pressure of the basic laminar flow.

Symbol	Meaning
$\hat{p}$	Disturbance pressure.
∇p	Pressure gradient
Pr	Prandtl number, $c_p\mu/K$.
Re	Reynolds number $U_{max}\delta/\nu$.
t	time.
T	Temperature of the basic laminar flow.
T_o	Temperature of the surface.
T_∞	Temperature in the stagnant fluid
$\hat{T}$	Disturbance temperature.
$\tilde{T}$	Temperature function.
ΔT	Defined as $T_o - T_\infty$.
u	Vertical component of the instantaneous velocity.
U	Vertical component of velocity of the basic laminar flow.
U_{max}	Maximum vertical component of velocity of the basic laminar flow
$\hat{u}$	Vertical component of the disturbance velocity.
v	Horizontal component of the instantaneous velocity.
V	Horizontal component of the velocity of the basic laminar flow.
$\hat{v}$	Horizontal component of the disturbance velocity.
X	Distance from the leading edge of the plate.
Y	Normal distance from surface.

Greek symbols

α	Wave number
α^*	Dimensionless wave number, $CX/2\nu_\infty \sqrt{Gr_x}$
β	Coefficient of volumetric expansion.
β^*	Defined by equation (3.2.49).
γ^*	Defined by equation (3.2.50).
δ	Boundary-layer thickness.
ζ	Dimensionless distance from the leading edge of the plate.
η	Dimensionless normal distance from the wall.
η_δ	Value of the similarity variable which corresponds to the condition U/U_{max}.
η_{edg}	Effective edge of the boundary layer.
χ	Convergence criterion
λ	Wavelength of the disturbance wave, $2\pi/\alpha$
μ	Fluid viscosity.
ν	Kinematic viscosity.
ξ	Temperature amplitude function.
ξ^*	Dimensionless temperature amplitude function, $\xi/T_o - T_\infty$
ρ	Fluid density.
τ	Instantaneous temperature.
ψ	Velocity amplitude function.
ψ^*	Dimensionless velocity amplitude function, $\psi X/2\nu_\infty \delta \sqrt{Gr_x}$
Ψ	Perturbation stream function.
∇	Vector operator "del"

Symbol	Meaning
Subscripts	
i	Refers to imaginary part.
h,i	The i^{th} homogeneous solutions.
max.	Maximum.
O,S	The value of the variable at the body surface.
r	Refers to real part
∞	The value of the variable at infinity.
Superscripts	
K,K+1	Denotes the iteration number
O,1,2	Denotes the iteration number.
^	Denotes the disturbance quantity
,	Denotes differentiation w.r.t.
*	Dimensionless variable.

CHAPTER 1

INTRODUCTION

1. INTRODUCTION

Free-convective heat transfer manifests itself in different situations in technology and in the natural world around us and it becomes an important mode of heat transfer in many situations in which a hot body is immersed in a quiescent or slowly moving flow, such as a heated plate or cylinder in a stationary atmosphere.

In free-convective heat transfer, temperature gradients in the fluid give rise to density variations and, hence, to fluid motion. Similar types of flow occur in rotating machinery, since centrifugal forces are proportional to fluid density and play a role analogous to that of gravity.

The rate of heat transfer in a free convective situation depends on the nature of the motion of a layer of fluid adjacent to the body. The motion can be either laminar or turbulent. In practice, under certain conditions which favour the growth of small perturbations imposed on the basic laminar free-convective flow, the fluid motion becomes unstable and transition from laminar to turbulent flow occurs. This transition has been studied experimentally as well as theoretically by many investigators throughout the years. These studies will be considered in detail in chapter 2 of this work.

Experimentally, the instability of free-convective flow can be studied by the method of small perturbations. In this method a disturbance with a certain frequency is imposed on the basic laminar flow which is examined to see whether the disturbance is amplified or damped out. This process of amplification or suppression can be described mathematically

by defining such a disturbance in a mathematical form and by inserting it into the equations which govern the disturbed basic flow. The growth or decay of the perturbation can then be determined.

From the earliest studies of problems of instability [1,2,3,4] it can be concluded that the linearized small-perturbation theory used for the prediction of transition from laminar to turbulent flow in forced convection is also applicable to free-convective flow [5,6].

The fundamental assumption that is made is that a perturbation imposed on the basic laminar flow is small and two-dimensional. It is evident [6,7] that this assumption is only true in the early stages of the transition process. Later, when the disturbance amplifies and becomes more complicated, three-dimensional effects emerge.

In free-convective flow an imposed perturbation disturbs both the temperature and velocity distributions, furthermore, a temperature disturbance may amplify a velocity disturbance through density changes.

Mathematically such coupling means that the equations expressing the velocity and temperature fluctuations must be solved simultaneously.

A variety of methods have been used for solving disturbance differential equations for free-convection boundary layer flows. In the earliest work [8,9,10] the temperature fluctuations were assumed to be negligible. This assumption reduced the disturbance differential equations for free-convection boundary layers to the ordinary form of the Orr-Sommerfeld

equation, which was solved by an asymptotic technique. Solutions have been obtained in the form of power series expanded about the location of critical layers in the boundary layers at which the phase velocity of the disturbance is equal to the velocity of the basic laminar flow.

The theoretical results obtained from the asymptotic method were found to be incompatible with the existing experimental data. This shortcoming in the asymptotic method resulted in the adoption of a numerical approach to the problem.

A number of difficulties are associated with the numerical techniques used for solving the problem of the instability of free-convection boundary layer flows [11-12]. However, the availability of high capacity computers invites further consideration of problem, hence the present interest in this work.

The present work was planned in order to investigate the stability of free-convection boundary layer flows along an isothermal vertical plate. A quasilinearization technique and a trial-and-error technique were used to solve the boundary value problem associated with the solution of the derived disturbance differential equations covering a wide range of Prandtl numbers from 0.733 to 1000.

CHAPTER 2

LITERATURE SURVEY

2.1. Introduction

The instability and the transition of fluid motion from laminar to turbulent flow in free-convection boundary layers has been the subject of many theoretical and experimental studies.

These investigations have been mostly concerned with flow along flat plates and the application of linear stability theory to free-convection boundary layer flows. However, because of its complexity the instability of free-convection flows has received less attention than the instability of forced-convection flows and in most cases the effect of temperature fluctuations has been neglected. Also, only certain Prandtl numbers (Pr = 0.73 and 6.7) have been considered in the investigations.

The present literature survey will be confined to instability studies of free-convection boundary layer flows along a vertical plate, although the instability of free-convection boundary layers along inclined and curved surfaces will also be mentioned, whenever appropriate.

2.2. Experimental Investigations

The onset of turbulence in free convection boundary layers along a flat plate occurs when the Grashof number, based on the length in the direction of flow, has reached a critical value. The critical value of the Grashof number has not been obtained unambiguously by experiment. It has been found experimentally that a transition region exists in which the laminar flow starts to become turbulent and that turbulence develops gradually

with increasing distance from the leading edge. Among the earliest experimental studies of the transition from laminar flow to turbulence in free convection boundary layers over heated vertical flat plates, the works of Griffiths and Davis [13], Schmidt and Beckman [14], Schmidt and Forsch [15], Herman [16-17], Saunders [18-19], and Eigenson [20] show that for air and water the transition region extends approximately from a Grashof number of 10^8 to 10^{10}.

Eckert and Soehnghen [21] gave the first detailed description of the transition process in the free-convection boundary layer of air along a heated vertical cylinder. They observed that at a certain value of the Grashof number, the flow in the boundary layer began to develop a wavy motion. This motion then rolled up and finally broke up, causing the boundary layer to become turbulent. These observations were made using a Mach-Zehnder interferometer. The critical Grashof number at which waves first appeared within the boundary layer was reported to be 4×10^8. Their observations were restricted only to a two-dimensional picture, hence only a limited understanding of the transition process was obtained.

Fujii [22] studied the transition of free convection boundary layers of ethyleneglycol and water along a vertical cylinder. He made his observations using the schlieren method and the naked eye with small aluminium particles suspended in the fluid. He reported that at a Rayleigh number (Gr x Pr) of 4×10^9 the laminar boundary layer became unstable and changed to a vortex street layer. Then vortices in the vortex street curled over and broke into a wavy motion and turbulence appeared

at a Rayleigh number of about 10^{10}. He noted that the local heat transfer coefficients were scarcely affected by the development of the vortex street in the boundary layer, but were discontinuously increased by the transition to turbulent flow.

Eckert, Hartnett and Irvine [23] used a smoke-trace technique to study the transition region in air adjacent to an isothermal vertical plate. Vortex formation and break up were studied visually and recorded in motion pictures. They first observed a two-dimensional wavy motion in the range of Grashof numbers of 0.05×10^9 to 6.3×10^9. Later, further along the plate, this wavy motion rolled up and eventually broke up at a Grashof number of 7.3×10^9.

Szewczyk [10] used a dye injection technique to study the stability and transition of free-convection boundary layers. He performed his experiments with a vertical heated plate in a water tank. The temperature profile along the plate was determined from thermocouples imbedded in the plate. He neglected the effect of the small temperature gradient near the leading edge of the plate and observed that the dye streaks were at first continuous but that with increasing height along the plate they began to take on a wave-form before rolling up to form vortices. The vortices which at first appeared to be mainly two-dimensional, now began to take on some three-dimensional character. Several dye streaks with the same character joined together and created a vortex loop. Finally the vortex loop burst into highly random motion. The vortices developed on both sides of the region of maximum

velocity within the boundary layer. The outer region far away from the surface of the plate was seen to become turbulent, while the flow close to the surface remained fairly laminar. Szewczyk suggested that this occurrence must result from the strong instability caused by the point of inflection in the velocity profile outside the region of maximum velocity. From the above mentioned observations, he concluded that the transition zone in a free-convection boundary layer possesses a double-row vortex system and that the instability of the outer layer sets in first and impresses its effect on the inner layer and thus controls the development of the flow.

Tritton [24] used a quartz fibre anemometer to study the transition from laminar to turbulent flow of free-convection boundary layer flows on heated vertical and inclined plates surrounded by air. He reported that the quartz fibre anemometer failed to detect wave-like motion. However he stated that the transition region for a vertical isothermal plate started at a Grashof number of about 9×10^6, which was much lower than the values previously reported by other workers. The region of fully turbulent flow was reached at a Grashof number of about 1.5×10^9.

The experimental investigations mentioned above were concerned with the onset of naturally occurring instability. The measured values of the Grashof number at the onset of transition were considerably different from those predicted by theoretical means. Consequently the available experimental data were not able to confirm either the applicability of linear

stability theory or the importance of temperature-velocity coupling in free-convection boundary layer flows.

Polymeropoulos and Gebhart [5], in order to explain the discrepancy between experimental and theoretical results, reported that in the study of naturally occurring instability, the natural disturbances are too small to be detected at their initial stages of amplification and that these disturbances must be amplified within the boundary layer until they become large enough to be observed. In order to overcome this problem, they used the method of artificially induced disturbances inside the boundary layer. This method had been applied successfully for forced convection flow over a flat plate by Schubauer and Skramstad [4]. In this method the oscillations are large enough to be detected and their wave number can be controlled. The results of an experimental study of the behaviour of artificial disturbances produced by an oscillating ribbon in the free-convection boundary layer over a vertical plate with uniform heat flux in pressurized nitrogen were presented in their paper. The boundary layer was observed using a Mach-Zehnder interferometer. Their results for the location of the neutral stability curve were in good agreement with the available theoretical results based on linear stability theory for air.

Colak-Antic [7] studied the instability of artificially induced disturbances in free-convection boundary layer flows in air and in water over a vertical isothermal plate. The disturbances were introduced by a thin wire which was placed in the boundary layer and pulsed with an electrical signal.

A hot wire anemometer was used for the measurement of the disturbed velocity and for the determination of the amplification rates of the disturbances. Qualitative evidence was obtained for the existence of a temperature-coupling effect at low Grashof and low wave numbers, but no results were given for the region in which the flow was neutrally stable.

Dring and Gebhart [25] investigated experimentally the nature of disturbance amplification in the laminar free-convection boundary layer on a vertical plate with uniform heat flux. The liquid used in the experiments was a silicone fluid (hexamethyldisiloxane). A hot-wire anemometer was used to obtain the amplitude and phase profiles of the disturbance velocities and a Mach-Zehnder interferometer was used to obtain the amplitude and phase profiles of the disturbances in the temperature field, the results of this work were in good agreement with linear stability theory. Dring and Gebhart also measured the amplification rate and disturbance amplitude growth and found that their measurements supported the hypothesis that natural disturbances arise from the frequencies at which the disturbances are amplified the most, rather than from the frequency at which disturbances first begin.

Cheeswright [26] carried out an experimental study of turbulent free-convection from a vertical plate. The first velocity fluctuation appeared in the boundary layer at Grashof number of about 2×10^9. Hence, this Grashof number was considered to correspond to the starting point of transition.

There was no significant change in the temperature distribution within the boundary layer or in the local heat transfer rate until a Grashof number of 5×10^9 was reached. Major changes in the heat transfer rate and in the temperature distribution ended when the Grashof number reached a value of 8×10^9. Further changes in the heat transfer rate and in the characteristics of the turbulent fluctuations were apparent at a Grashof number of 2×10^{10}. These changes were considered by Cheeswright to be the end of the transition region because for $Gr > 2 \times 10^{10}$ the amplitude of the temperature fluctuations remained approximately constant.

Vliet and Liu [27] studied the turbulent free convection boundary layer associated with a vertical plate immersed in water. The heat flux from the plate was uniform. They observed that the transition from laminar to turbulent flow occurred in the range $10^{12} < R_a < 10^{14}$ where $R_a = Pr.Gr_x.Nu_x$. They concluded that the vortex street layer in the transition region decayed into a longitudinal-vortex-type structure and that the flow arising from a plate with uniform heat flux is more stable than that associated with an isothermal plate.

2.3. Theoretical Studies

The equations which govern the stability of free-convection boundary layer flows along heated plates are equivalent to a complex system of linear differential equations of the sixth order involving two eigenvalues and two matching parameters. These equations, which are based upon linear stability theory, were first formulated by Plapp [8-9]

for the case of an inclined plate. He neglected the coupling between velocity and temperature disturbances and obtained the neutral stability curve for free-convective heat transfer from a vertical isothermal wall to air (Pr = 0.72). His solution was based on an asymptotic technique which used a polynomial expression for the velocity of the basic laminar free convection boundary layer flow.

The equations of Plapp were later rederived by Szewczyk [10] for the case of a vertical plate. Szewczyk made a theoretical study of the stability of the free-convection boundary layer arising from an isothermal plate at a Prandtl number of 10. He used an asymptotic technique in which expansions were made about both critical layers, although the coupling between velocity and temperature fluctuations was neglected. His calculations, based on the inner critical layer, showed that the flow in the boundary layer became turbulent at a value of $G = 3.46 \times 10^5$, where $G = 2\sqrt{2}(Gr)^{1/4}$, These results were significantly different from experimental data. He also carried out the instability calculation for the outer critical layer and found that the value of the critical Grashof number was reduced by a factor of 10^3. From these calculations he concluded that the instability arising from the outer critical layer is predominant and sets in well in advance of the onset of any possible instability due to the inner critical layer.

However, the results obtained by the use of asymptotic techniques were found to be incompatible with existing experimental data. This shortcoming of asymptotic techniques

and computational limitations caused a delay in the further treatment of the instability of free-convection boundary layer flows until very large digital computers became available.

Kurtz and Grandall [28] applied a finite-difference technique and integrated the uncoupled disturbance differential equations using a digital computer. The first numerical solutions were obtained for a Prandtl number of 0.733 for the case of an isothermal vertical plate. The results were significantly different from those obtained by Plapp [8-9].

Sparrow, Tsou and Kurtz [29] studied the effect of Prandtl number on the stability characteristics of the laminar free-convection boundary layer adjacent to an isothermal vertical plate. The temperature-velocity coupling was neglected and numerical solutions were obtained, using the method developed by Kurtz and Grandall [28], for Prandtl numbers in the range of 0.733 to 7.0. They also obtained the following empirical relationship for the prediction of the critical Grashof number:

$$Gr = Pr^3 \, Re/2\sqrt{2} - f'_{max} \cdot \eta_\delta$$

where

$Re = U_{max} \cdot \delta/\nu$

U_{max} is the maximum velocity

δ is the boundary layer thickness

ν is the kinematic viscosity

f'_{max} is the dimensionless maximum velocity defined as

$$f'_{max} = U_{max} / \frac{2\nu}{x} \left(\frac{Gr}{Pr}\right)^{\frac{1}{2}}$$

η_δ is the value of the similarity variable which corresponds to the condition $U/U_{max} = .01$.

η is the similarity variable defined as $\eta = \frac{Y}{X}(\frac{GrPr}{4})^{1/4}$.

They concluded that the above relationship is valid for $Pr \geq 5$ and as the Prandtl number tends to infinity the critical Grashof number varies as cube of the Prandtl number.

In the theoretical studies which have been described, the velocity-temperature coupling was neglected. The work of Nachtsheim [11] was the first study which included coupling between velocity and temperature disturbances. He solved the coupled disturbance differential equations for free-convection boundary layer flows over a vertical isothermal plate. His calculations were carried out for Prandtl numbers of 0.733 (air) and 6.7 (water). The solutions were obtained by a numerical step-by-step forward integration procedure. The eigenvalues and missing boundary conditions were guessed and the boundary-value problem was treated as an initial value problem for which not all the proper starting values were known but which had to satisfy conditions at the outer edge of the boundary layer. An analytical asymptotic solution of the disturbance differential equations was obtained for a large distance from the plate. This solution was then employed to provide boundary conditions at the outer edge of the boundary layer. The Newton-Raphson second-order process was used to obtain corrections to the eigenvalues and the starting values in order to satisfy the boundary conditions. Nachtsheim reported that for a Prandtl number of 6.7 and wave numbers greater than 0.75 numerical solution failed to trace the neutral stability curve, because the values of eigenfunctions at

the edge of the boundary layer changed markedly with each run even though the eigenvalues and the starting values were only changing in the eighth decimal place. By comparison of the coupled and uncoupled solutions at the same Prandtl number he found that coupling had a first-order destabilizing effect on the basic laminar free convection flow. However his values of the critical Grashof number were lower than the Grashof number at which finite disturbances had been observed experimentally.

Knowles and Gebhart [30] investigated the effect of a thermal capacity coupling between the fluid and the wall on the instability of free-convection boundary layer flows along a vertical plate. They focused their attention on the boundary conditions for the disturbance temperatures and concluded that in the case of an isothermal plate with a large thermal capacity, the temperature disturbances must be zero at the surface of the plate but, on the other hand, if the plate possesses zero thermal capacity and has a uniform heat flux then the disturbances in the flux tend to zero. In addition they reported that as these two limiting cases cannot be easily attained, many practical situations lie between these two cases. Their calculations were carried out for a plate with uniform heat flux for the range of Prandtl numbers of 0.733 to 6.9. Solutions were also obtained for several values of the relative wall thermal capacity at a Prandtl number of 0.733. The applied numerical technique was similar to that used by Nachtsheim. Their results were in a good agreement with the existing experimental data for the onset of artificially occurring instability.

Hieber and Gebhart [12-31] studied the instability of the free-convection boundary layer flow associated with a vertical plate with uniform heat flux. The problem was solved using a numerical technique which had been employed by Mack [32] in his stability analysis of a compressible forced flow boundary layer. Hieber and Gebhart's study covered a range of Prandtl numbers of 0.01-100 and a large range of Grashof numbers dependent upon the value of Prandtl number. They reported that at small values of the Prandtl number the coupling effect can be ignored in the case of a plate with large thermal capacity, but that when the thermal capacity of the plate is small, coupling has a significant destabilizing effect. For moderate and large values of the Prandtl number, they found that a loop appeared in the neutral stability curve. They attributed the loop to the merging of two unstable modes. Their studies show that the velocity-temperature coupling is the predominant source of instability and that the stability characteristics become independent of the thermal capacity of plate as the Prandtl number tends to infinity. Using their numerical results and the available experimental data, they established an empirical correlation between the results of applying linear stability theory and the onset of naturally occurring instability. The accuracy of their results was within one decimal place.

It may be concluded from the above literature survey that except for Hieber and Gebhart [12], who obtained solutions for a Prandtl number of 100.0, the only Prandtl numbers that have been considered in the investigations are those of air and

water. Unfortunately for a Prandtl number of 100.0, Hieber and Gebhart solved the disturbance equations for only a small part of the neutral stability curve. Although the numerical methods that were used by Nachtsheim [11] and Hieber and Gebhart [12] were complicated and required a lot of computation time, they failed to trace the neutral stability curves for high Prandtl numbers. Furthermore, the accuracy of the results of the above studies was mostly less than two decimal places.

Thus, on the basis of the above study it is clear that since in important application the Prandtl number varies from 10^{-2} in liquid metals to 10^{4} in medium oils, changes in the mechanism of the onset of turbulence may be expected to occur over such a wide range of Prandtl numbers mainly because of the coupling of velocity and temperature fluctuation. Therefore, in any case it is essential to have a knowledge of the neutral stability curves for high Prandtl numbers in order to determine the effect of Prandtl number on the minimum critical value of the Grashof number and its corresponding values of the wave number and the phase velocity. In order to obtain solutions for high Prandtl numbers it is necessary to adopt more sophisticated numerical techniques.

CHAPTER 3

THEORETICAL ANALYSIS

3.1. The Navier-Stokes, Continuity and Transfer Equation for Free-Convective Heat Transfer

The basic differential equations from which the rate of heat transfer may be calculated express the physical concept of conservation. These equations are the momentum (Navier-Stokes) equation, the continuity equation and the transfer equation. The derivations of the appropriate equations may be found in various standard texts [33, 34, 35, 36].

The equations which describe momentum and heat transfer in an incompressible Newtonian fluid when the heat generated by viscous dissipation is negligible and the only body force operating is that of gravity, are as follows:

i) Navier-Stokes equation (for constant viscosity):

$$\rho \frac{D\underline{V}}{Dt} = \rho \underline{g} - \nabla P + \mu \nabla^2 \underline{V} \qquad (3.1.1)$$

ii) Continuity equation:

$$\nabla . \underline{V} = 0 \qquad (3.1.2)$$

iii) Energy equation (for constant thermal conductivity):

$$\frac{DT}{Dt} = \frac{K}{\rho C_p} \nabla^2 T \qquad (3.1.3)$$

where $\underline{V}$ is the velocity vector

$\underline{g}$ is the gravitational vector

ρ is density

μ is viscosity

p is pressure

T is temperature

C_p is the specific heat at constant pressure

K is thermal conductivity

$\frac{D}{Dt}$ is substantial derivative and is defined as

$$\frac{D}{Dt} = \frac{\partial}{\partial t} + (\underline{V}.\nabla) \tag{3.1.4}$$

For steady-state conditions, equations (3.1.1) to (3.1.3) may be written as:

$$\rho(\underline{V}.\nabla)\underline{V} = \rho\underline{g} - \nabla P + \mu\nabla^2\underline{V} \tag{3.1.5}$$

$$\nabla.\underline{V} = 0 \tag{3.1.6}$$

$$(\underline{V}.\nabla)T = \frac{K}{\rho C_p}\nabla^2 T \tag{3.1.7}$$

In free-convective flow, the fluid far from the body is stagnant. In the stagnant region, equation (3.1.5) becomes:

$$\rho_\infty\underline{g} = \nabla P_\infty \tag{3.1.8}$$

where ∞ denotes the value of the variable at infinity.

By the introduction of equation (3.1.8) into equation (3.1.5) the following equation can be written:

$$\rho(\underline{V}.\nabla)\underline{V} = \rho\underline{g} - \rho_\infty\underline{g} - \nabla P + \nabla P_\infty + \mu\nabla^2\underline{V} \tag{3.1.9}$$

if it is assumed that the pressure distribution in the region of the free convective flow is impressed by the pressure distribution in the stagnant fluid, then

$$\nabla(P - P_\infty) = 0 \tag{3.1.10}$$

and equation (3.1.9) becomes:

$$\rho(\underline{V}.\nabla)\underline{V} = (\rho - \rho_\infty)\underline{g} + \mu\nabla^2\underline{V} \qquad (3.1.11)$$

The density, which is a function of temperature, may be expressed in terms of a Taylor's series relative to stagnant fluid conditions,

$$\rho = \rho_\infty + \frac{\partial\rho}{\partial T}\bigg|_{T_\infty}(T - T_\infty) + \ldots\ldots \qquad (3.1.12)$$

thus,

$$\rho - \rho_\infty = \frac{\partial\rho}{\partial T}\bigg|_{T_\infty}(T - T_\infty) \qquad (3.1.13)$$

the coefficient of volumetric expansion is defined by:

$$\beta_\infty = \frac{1}{\rho_\infty}\left(\frac{\partial\rho}{\partial T}\right)\bigg|_{T_\infty} \qquad (3.1.14)$$

Hence, by substitution of equations (3.1.13) and (3.1.14) into equation (3.1.11) the following equation can be obtained:

$$\rho(\underline{V}.\nabla)\underline{V} = \rho_\infty\underline{g}\beta_\infty(T - T_\infty) + \mu\nabla^2\underline{V} \qquad (3.1.15)$$

If it is assumed that temperature variations are not large, then Boussineq's approximation may be applied which enables the density to be treated as a constant ($\rho = \rho_\infty$) in all terms in the equation of motion [3.1.11] except that which arises because of the body force. For the same reason, the viscosity also can be considered as a constant ($\mu = \mu_\infty$). Application of these assumptions results in the following equation:

$$\rho_\infty(\underline{V}.\nabla)\underline{V} = \rho_\infty\underline{g}\beta_\infty(T - T_\infty) + \mu_\infty\nabla^2\underline{V} \qquad (3.1.16)$$

The boundary conditions for equations (3.1.6), (3.1.7) and (3.1.16) for free-convective heat transfer from an isothermal body immersed in a fluid can be expressed as:

i) There is no slip of the fluid at the surface of solid body

ii) The temperature is assumed to be constant at all points on the surface of the immersed body.

iii) As the distance from the body increases, the velocity and temperature become asymptotic to their values in the undisturbed stagnant fluid.

These conditions may be written as:

At $\underline{n} = 0$: $\underline{V} = 0$, $T = T_o$

$\underline{n} \to \infty$: $\underline{V} \to 0$, $T \to T_\infty$

where:

$\underline{n}$ is the outward normal vector from the surface

T_o is the surface temperature

T_∞ is the temperature in the stagnant fluid distant from the body

3.2. The Equations of the Instability of Free-Convection Boundary Layer Flows along a Vertical Isothermal Plate

The method of small perturbations will be applied in order to examine whether a disturbance which satisfies the equations of continuity, motion and energy is amplified or damped out.

A two-dimensional disturbance superimposed upon the basic laminar free-convection boundary layer flow may be expressed in terms of the perturbation quantities:

$$\hat{u}(x,y,t), \quad \hat{v}(x,y,t), \quad \hat{T}(x,y,t) \quad \text{and} \quad \hat{P}(x,y,t) \qquad (3.2.1)$$

The instantaneous velocity components, temperature and pressure are:

$$u = U + \hat{u} \qquad (3.2.2)$$

$$v = V + \hat{v} \qquad (3.2.3)$$

$$\tau = T + \hat{T} \qquad (3.2.4)$$

$$p = P + \hat{P} \qquad (3.2.5)$$

where

- U is the vertical component of velocity of the basic laminar flow
- V is the horizontal component of velocity of the basic laminar flow
- T is temperature of the basic laminar flow
- P is pressure of the basic laminar flow

The governing equations for a disturbed basic flow about a vertical plate, in terms of instantaneous quantities, can be expressed in the coordinate system shown in figure [3.1] as follows:

$$\frac{\partial u}{\partial x} + \frac{\partial v}{\partial y} = 0 \qquad (3.2.6)$$

$$\frac{\partial u}{\partial t} + u\frac{\partial u}{\partial x} + v\frac{\partial u}{\partial y} = -\frac{1}{\rho}\frac{\partial p}{\partial x} + \nu\nabla^2 u + g\beta(\tau - T_\infty) \qquad (3.2.7)$$

$$\frac{\partial v}{\partial t} + u\frac{\partial v}{\partial x} + v\frac{\partial v}{\partial y} = -\frac{1}{\rho}\frac{\partial p}{\partial y} - \nu\nabla^2 v \qquad (3.2.8)$$

$$\frac{\partial \tau}{\partial t} + u\frac{\partial \tau}{\partial x} + v\frac{\partial \tau}{\partial y} = \frac{K}{\rho C_p}\nabla^2\tau \qquad (3.2.9)$$

In order to simplify the problem, the basic laminar flow will be assumed to be a parallel flow so that the mean velocity U will depend only on the y-direction. Thus,

$$\frac{\partial U}{\partial x} = 0 \qquad (3.2.10)$$

and from continuity equation (3.2.6):

$$\frac{\partial V}{\partial y} = 0 \qquad (3.2.11)$$

However, since there is no mass flux normal to the surface at the surface of the body then the velocity component, V, is zero everywhere,

$$V = 0 \qquad (3.2.12)$$

The velocity component V is always non-zero in boundary layer flows [section 3.3.1] but in many cases its magnitude is negligible.

These approximations can also be applied to free convection boundary layer flows [10] in which the dependence of the velocity component U on x-coordinate is much smaller than its dependence on the y-coordinate.

As far as the pressure is concerned, it will be assumed at first that pressure is dependent upon both the x and y directions. The dependence of temperature on the x-coordinate within the boundary layer is also small in comparison with its dependence on the y-coordinate, with these assumptions the quantities U, V, P and T may be expressed as follows:

$$U = U(y); \quad V = 0; \quad P = P(x,y); \quad \text{and } T = T(y) \tag{3.2.13}$$

Hence, equations (3.2.2) to (3.2.5) may be reduced to the following forms:

$$u = U + \hat{u} \tag{3.2.14}$$

$$v = \hat{v} \tag{3.2.15}$$

$$\tau = T + \hat{T} \tag{3.2.16}$$

$$p = P + \hat{P} \tag{3.2.17}$$

It is assumed that the variables (3.2.13) satisfy the Navier-Stokes and energy equations, and it is required that the simplified variables (3.2.14) to (3.2.17) must also satisfy the Navier-Stokes equations.

The superimposed fluctuating velocities (3.2.1) are taken to be "small" in the sense that all quadratic terms in the fluctuating quantities may be neglected with respect to the linear terms.

The next step to be taken for further simplification is the use of the boundary layer assumptions. These assumptions will be discussed in section (3.3.1).

By substitution of equations (3.2.14) to (3.2.17) into equations (3.2.6) to (3.2.9), the following equations can be written:

i) Continuity:

$$\frac{\partial (U + \hat{u})}{\partial x} + \frac{\partial \hat{v}}{\partial y} = 0$$

However,

$$\frac{\partial U}{\partial x} = 0 \qquad \text{(since } U = U(y)\text{)}$$

so that

$$\frac{\partial \hat{u}}{\partial x} + \frac{\partial \hat{v}}{\partial y} = 0 \qquad (3.2.18)$$

ii) Motion equations:

1) x-direction:

$$\frac{\partial (U + \hat{u})}{\partial t} + (U + \hat{u}) \frac{\partial (U + \hat{u})}{\partial x} + \hat{v} \left(\frac{\partial (U + \hat{u})}{\partial y}\right) =$$

$$- \frac{1}{\rho} \frac{\partial (P + \hat{P})}{\partial x} + \nu \left(\frac{\partial^2 (U + \hat{u})}{\partial x^2} + \frac{\partial^2 (U + \hat{u})}{\partial y^2}\right) + g\beta \left((T + \hat{T}) - T_\infty\right)$$

However, because the basic laminar flow is time independent:

$$\frac{\partial U}{\partial t} = 0$$

also:

$$U \frac{\partial U}{\partial x} = 0 \qquad \text{(since } U = U(y)\text{)}$$

$$\hat{u} \frac{\partial U}{\partial x} = 0 \qquad \text{(since } U = U(y)\text{)}$$

$$\hat{u} \frac{\partial \hat{u}}{\partial x} = 0 \qquad \text{(quadratic term)}$$

$$\hat{v}\,\frac{\partial \hat{u}}{\partial y} = 0 \qquad \text{(quadratic term)}$$

$$\frac{\partial^2 U}{\partial x^2} = 0 \qquad \text{(since } U = U(y)\text{)}$$

Hence,

$$\frac{\partial \hat{u}}{\partial t} + U\,\frac{\partial \hat{u}}{\partial x} + \hat{v}\,\frac{\partial U}{\partial y} = -\frac{1}{\rho}\,\frac{\partial P}{\partial x} - \frac{1}{\rho}\,\frac{\partial \hat{P}}{\partial x} + \nu\left(\frac{\partial^2 \hat{u}}{\partial x^2} + \frac{\partial^2 \hat{u}}{\partial y^2}\right)$$

$$+ \nu\,\frac{\partial^2 U}{\partial y^2} + g\beta[(T + \hat{T}) - T_\infty] \qquad (3.2.19)$$

By application of the same procedure to the equation of motion in the y-direction and to the energy equation, the following equations can be obtained:

2) y-direction

$$\frac{\partial \hat{v}}{\partial t} + U\,\frac{\partial \hat{v}}{\partial x} = -\frac{1}{\rho}\,\frac{\partial P}{\partial y} - \frac{1}{\rho}\,\frac{\partial \hat{P}}{\partial y} + \nu\left(\frac{\partial^2 \hat{v}}{\partial x^2} + \frac{\partial^2 \hat{v}}{\partial y^2}\right) \qquad (3.2.20)$$

iii) Energy equation:

$$\frac{\partial \hat{T}}{\partial t} + U\,\frac{\partial \hat{T}}{\partial x} + \hat{v}\,\frac{\partial T}{\partial y} = \frac{K}{\rho C_p}\left(\frac{\partial^2 \hat{T}}{\partial x^2} + \frac{\partial^2 T}{\partial y^2} + \frac{\partial^2 \hat{T}}{\partial y^2}\right) \qquad (3.2.21)$$

Because the variables in (3.2.13) satisfy the Navier-Stokes and energy equations, the following equations can be written:

$$-\frac{1}{\rho}\,\frac{\partial P}{\partial x} + \nu\frac{\partial^2 U}{\partial y^2} + g\beta T - g\beta T_\infty = 0 \qquad (3.2.22)$$

$$-\frac{1}{\rho}\,\frac{\partial P}{\partial y} = 0 \qquad (3.2.23)$$

$$\frac{\partial^2 T}{\partial y^2} = 0 \qquad (3.2.24)$$

By substitution of equations (3.2.22) to (3.2.24) into equations (3.2.19), (3.2.20) and (3.2.21), the governing disturbance partial differential equations for the instability of free-convection boundary layer flows about an isothermal vertical plate become:

$$\frac{\partial \hat{u}}{\partial t} + U\frac{\partial \hat{u}}{\partial x} + \hat{v}\frac{\partial U}{\partial y} = g\beta\hat{T} - \frac{1}{\rho}\frac{\partial \hat{P}}{\partial x} + \nu\left(\frac{\partial^2 \hat{u}}{\partial x^2} + \frac{\partial^2 \hat{u}}{\partial y^2}\right) \tag{3.2.25}$$

$$\frac{\partial \hat{v}}{\partial t} + U\frac{\partial \hat{v}}{\partial x} = -\frac{1}{\rho}\frac{\partial \hat{P}}{\partial y} + \nu\left(\frac{\partial^2 \hat{v}}{\partial x^2} + \frac{\partial^2 \hat{v}}{\partial y^2}\right) \tag{3.2.26}$$

$$\frac{\partial \hat{T}}{\partial t} + U\frac{\partial \hat{T}}{\partial x} + \hat{v}\frac{\partial T}{\partial y} = \frac{K}{\rho C_p}\left(\frac{\partial^2 \hat{T}}{\partial x^2} + \frac{\partial^2 \hat{T}}{\partial y^2}\right) \tag{3.2.27}$$

A perturbation stream function $\Psi(x,y,t)$ which satisfies the continuity equation can be introduced:

$$\Psi(x,y,t) = \psi(y)e^{i(\alpha x - bt)} \tag{3.2.28}$$

where $\psi(y)$ is a complex amplitude function of the disturbance, α is a real positive quantity and represents the wave number of the disturbance, so that the wave length of the disturbance is $\lambda = \frac{2\pi}{\alpha}$, the quantity b is a complex number which is expressed as:

$$b = b_r + ib_i \tag{3.2.29}$$

where b_r is the circular frequency of the partial oscillation and b_i is an amplification factor which expresses the degree of amplification or damping of the disturbance.

Another complex number can be defined as:

$$c = \frac{b}{\alpha} = c_r + ic_i \tag{3.2.30}$$

where c_r denotes the velocity of propagation of the wave in x-direction or the phase velocity and c_i again represents the degree of damping or amplification of the disturbance.

In a similar manner a temperature perturbation may be expressed as:

$$\tilde{T}(x,y,t) = \xi(y)e^{i(\alpha x-bt)} \qquad (3.2.31)$$

The amplitude functions of fluctuation ψ and ξ are assumed to depend only on the y-direction because it has been assumed that the basic laminar flow depends on the y-direction alone.

From equation (3.2.28) the components of the perturbation velocity can be obtained as follows:

$$\hat{u} = \frac{\partial\psi}{\partial y} = \psi'(y)e^{i(\alpha x-bt)} \qquad (3.2.32)$$

$$\hat{v} = -\frac{\partial\psi}{\partial x} = -i\alpha\psi(y)e^{i(\alpha x-bt)} \qquad (3.2.33)$$

The derivatives of the components of the perturbation velocity and temperature with respect to time, and the x and y directions can be written as:

$$\frac{\partial\hat{u}}{\partial t} = -ibe^{i(\alpha x-bt)}\psi'(y)$$

$$\frac{\partial\hat{u}}{\partial x} = i\alpha e^{i(\alpha x-bt)}\ \psi'(y)$$

$$\frac{\partial^2\hat{u}}{\partial x^2} = -\alpha^2 e^{i(\alpha x-bt)}\ \psi'(y)$$

$$\frac{\partial^2 \hat{u}}{\partial y^2} = \frac{\partial}{\partial y}\left(\frac{\partial \hat{u}}{\partial y}\right) = \frac{\partial}{\partial y}\left(\psi''(y)e^{i(\alpha x-bt)}\right) = e^{i(\alpha x-bt)}\ \psi'''(y)$$

$$\frac{\partial \hat{v}}{\partial t} = -\alpha b e^{i(\alpha x-bt)}\psi(y)$$

$$\frac{\partial \hat{v}}{\partial x} = \alpha^2 e^{i(\alpha x-bt)}\psi(y)$$

$$\frac{\partial^2 \hat{v}}{\partial x^2} = \frac{\partial}{\partial x}\left(\frac{\partial \hat{v}}{\partial x}\right) = \frac{\partial}{\partial x}\left(\alpha^2 e^{i(\alpha x-bt)}\psi(y)\right) = i\alpha^3 e^{i(\alpha x-bt)}\ \psi(y)$$

$$\frac{\partial^2 \hat{v}}{\partial y^2} = \frac{\partial}{\partial y}\left(\frac{\partial \hat{v}}{\partial y}\right) = \frac{\partial}{\partial y}\left(-i\alpha e^{i(\alpha x-bt)}\psi'(y)\right) = -i\alpha e^{i(\alpha x-bt)}\ \psi''(y)$$

$$\frac{\partial \hat{T}}{\partial t} = -ibe^{i(\alpha x-bt)}\xi(y)$$

$$\frac{\partial \hat{T}}{\partial x} = i\alpha e^{i(\alpha x-bt)}\ \xi(y)$$

$$\frac{\partial^2 \hat{T}}{\partial x^2} = \frac{\partial}{\partial x}\left(\frac{\partial \hat{T}}{\partial x}\right) = -\alpha^2 e^{i(\alpha x-bt)}\ \xi(y)$$

$$\frac{\partial^2 \hat{T}}{\partial y^2} = \frac{\partial}{\partial y}\left(\frac{\partial \hat{T}}{\partial y}\right) = e^{i(\alpha x-bt)}\ \xi''(y) \qquad (3.2.34)$$

By substitution of the relations (3.2.34) into the disturbance partial differential equations (3.2.25), (3.2.26) and (3.2.27), the following equations can be obtained:

$$-ibe^{i(\alpha x-bt)}\psi'(y) + Ui\alpha e^{i(\alpha x-bt)}\psi'(y) + \hat{v}\frac{\partial U}{\partial y} =$$

$$g\beta\hat{T} - \frac{1}{\rho}\frac{\partial \hat{P}}{\partial x} + \nu\left(-\alpha^2 e^{i(\alpha x-bt)}\psi'(y) + e^{i(\alpha x-bt)}\ \psi'''(y)\right) \qquad (3.2.35)$$

$$-\alpha b e^{i(\alpha x-bt)}\psi(y) + U\alpha^2 e^{i(\alpha x-bt)}\psi(y) = -\frac{1}{\rho}\frac{\partial \hat{P}}{\partial y} +$$

$$\nu(i\alpha^3 e^{i(\alpha x-bt)}\psi(y) + i\alpha e^{i(\alpha x-bt)}\psi''(y)) \qquad (3.2.36)$$

$$-ib e^{i(\alpha x-bt)}\int_{\Lambda}^{\xi(y)} + U(i\alpha e^{i(\alpha x-bt)})\int_{\Lambda}^{\xi(y)} + \hat{v}\frac{\partial T}{\partial y} = \frac{K}{\rho C_p}($$

$$-\alpha^2 e^{i(\alpha x-bt)}\xi(y) + e^{i(\alpha x-bt)}\xi''(y)) \qquad (3.2.37)$$

The pressure terms in equations (3.2.35) and (3.2.36) can be eliminated by differentiation of equation (3.2.35) with respect to y and equation (3.2.36) with respect to x and by subtraction of the two resultant equations. Furthermore, with algebraic manipulation the above mentioned equations may be simplified to the following linear differential equations for the disturbed quantities.

$$(U-c)(\psi''-\alpha^2\psi) - \psi U'' = -\frac{i\nu}{\alpha}(\psi'''' - 2\alpha^2\psi''+\alpha^4\psi) - \frac{ig\beta}{\alpha}\xi' \qquad (3.2.38)$$

$$\xi(U-c) - \psi\left(\frac{\partial T}{\partial y}\right) = \frac{-iK}{\rho C_p \alpha}(\xi'' - \alpha^2\xi) \qquad (3.2.39)$$

Equations (3.2.38) and (3.2.39) can be rewritten in dimensionless form by the introduction of the following dimensionless variables:

$$\eta = \frac{y}{\delta}$$

$$\zeta = \frac{x}{\delta}$$

$$\delta = x\sqrt{2}/(Gr_x)^{1/4}$$

$$Gr_x = g\beta\Delta T\, x^3/\nu_\infty^2$$

$$f' = Ux/2\nu_\infty\sqrt{Gr_x}$$

$$H = \frac{T - T_\infty}{T_o - T_\infty}$$

$$\psi^* = \psi x/2\nu_\infty\delta\sqrt{Gr_x}$$

$$\xi^* = \xi/(T_o - T_\infty)$$

$$c^* = cx/2\nu_\infty\sqrt{Gr_x}$$

$$\alpha^* = \alpha\delta \qquad (3.2.40)$$

After substitution of the above dimensionless variables into equations (3.2.38) and (3.2.39), followed by further rearrangement, the following equations can be obtained [8-10].

$$(f'-c^*)(\psi^{*''} - \alpha^{*2}\psi^*) - \psi^* f''' = -\frac{i}{\alpha^* Gr^*}(\psi^{*''''} - 2\alpha^{*2}\psi^{*''} + \alpha^{*4}\psi^*) - \frac{i\beta\Delta t}{\alpha^* Fr}\xi'^* \qquad (3.2.41)$$

$$(f'-c^*)\xi^* - \psi^* H' = -\frac{i}{Pr\alpha^* Gr^*}(\xi^{*''} - \alpha^{*2}\xi^*) \qquad (3.2.42)$$

where

$Gr^* = 2\sqrt{2}\,(Gr_x)^{1/4}$ is the modified Grashof number

$Fr = 4\nu_\infty^2(Gr_x)/g\delta x^2$ is the Froude number

$Pr = \mu\frac{C_p}{K}$ is the Prandtl number

and

$$\frac{\beta \Delta t}{\alpha^* Fr} = \frac{1}{\alpha^* Gr^*}$$

In equations (3.2.41) and (3.2.42), the effect of the temperature fluctuation appears in the function ξ^* which couples the equations. If ξ^* is set equal to zero, equation (3.2.41) reduces to the Orr-Sommerfeld equation.

Equations (3.2.41) and (3.2.42) will be solved for the velocity disturbance, $\psi(\eta)$, and the temperature disturbance, $\xi(\eta)$, across the boundary layer. In order to solve these equations a knowledge of the basic flow quantities $f'(\eta)$, $f'''(\eta)$, $H'(\eta)$ is required. These quantities can be obtained from the well-known Schmidt and Beckmann equations which will be described in section (3.3.2).

The six complex boundary conditions required for the solution of equations (3.2.41) and (3.2.42) may be expressed as follows: It will be assumed that the no slip condition may be applied at the surface of plate, i.e.

$$\text{at } \eta = 0: \quad \psi^* = 0; \quad \psi'^* = 0; \quad \xi^* = 0 \qquad (3.2.43)$$

At large distances away from the wall ($\eta \to \infty$) the velocity and temperature disturbances tend to zero, i.e.

$$\eta \to \infty: \quad \psi^* \to 0; \quad \psi'^* \to 0; \quad \xi^* \to 0 \qquad (3.2.44)$$

The latter boundary conditions (3.2.44) cannot be used directly, because numerical integration cannot be made over an infinite distance. Thus the boundary conditions which apply at an infinite distance from the plate must be replaced or approximated

by conditions which apply at a finite distance from the plate. In order to obtain these conditions, the outer edge of the basic laminar boundary layer flow is chosen to be at a finite distance, $\eta = \eta_{edg}$, at which the values of f, f''', H' approach to within a specified deviation from zero. Therefore, at $\eta \geq \eta_{edg}$, equations (3.2.41) and (3.2.42) can be simplified to the following form:

$$\psi^{*'''} - 2\alpha^{*2}\psi^{*''} + \alpha^{*4}\psi^{*} + \xi^{*} = -i\alpha^{*}c^{*}Gr^{*}(\psi^{*''} - \alpha^{*2}\psi^{*}) \quad (3.2.45)$$

$$\xi^{*''} - \xi^{*}(\alpha^{*2} - ic^{*}\alpha^{*}Gr^{*}Pr) = 0 \quad (3.2.46)$$

The general solutions of the system of equations (3.2.45) and (3.2.46) are [28]:

$$\psi = c_1\exp(\alpha^{*}\eta) + c_2\exp(-\alpha^{*}\eta) + c_3\exp(\beta^{*}\eta) + c_4\exp(-\beta^{*}\eta) + c_5\exp(\gamma^{*}\eta) + c_6\exp(-\gamma^{*}\eta) \quad (3.2.47)$$

$$\xi = \frac{-c_5(\gamma^{*2} - \alpha^{*2})(\gamma^{*2} - \beta^{*2})}{\gamma^{*}}\exp(\gamma^{*}\eta) + c_6\frac{(\gamma^{*2} - \alpha^{*2})(\gamma^{*2} - \beta^{*2})}{\gamma^{*}}\exp(-\gamma^{*}\eta) \quad (3.2.48)$$

where $$\beta^{*2} = \alpha^{*2} - i\alpha^{*}Gr^{*}c^{*} \quad (3.2.49)$$

$$\gamma^{*2} = \alpha^{*2} - i\alpha^{*}Gr^{*}c^{*}Pr \quad (3.2.50)$$

and c_1, c_2, ...c_6 are arbitrary constants.

By elimination of the arbitrary constants in equations (3.2.47) and (3.2.48) a set of linear and homogeneous relations in the dependent variables and their derivatives can be obtained which are to be satisfied at the outer edge of the boundary layer [see appendix A]. These relations are:

$$\xi'^* + \gamma\xi^* = 0 \qquad (3.2.51)$$

$$\psi'''^* - \alpha^{*2}\psi' + \beta^*(\psi''^* - \alpha^{*2}\psi) + \frac{\gamma^*}{\gamma^* + \beta^*}\xi^* = 0 \qquad (3.2.52)$$

$$\psi'''^* + \alpha^*\psi''^* - \beta^{*2}(\psi'^* + \alpha^*\psi^*) + \frac{\gamma^*}{\gamma^* + \alpha^*}\xi^* = 0 \qquad (3.2.53)$$

In the present work numerical integration was started from the surface of the plate using boundary conditions (3.2.43) and was terminated at the outer edge of the boundary layer using the relations (3.2.51) to (3.2.53).

3.3. Equations for Free-convection Boundary Layer Flows

The Navier-Stokes, continuity and transfer equations are extremely difficult to solve in the form in which they have been stated in section 3.1. The problem for free convection flows is more complicated than for forced convection flows, inasmuch as the governing equations are strongly coupled and must be solved simultaneously. In order to simplify the equations, the boundary layer assumptions can be introduced.

3.3.1. The Boundary Layer Approximations.

The boundary layer approach [37] has proved to be useful in a variety of problems in fluid mechanics and has been successfully applied to free-convection flows [38,39,40,41,42]. The major assumptions of boundary layer theory are:

i) The layer in the neighbourhood of the body in which the velocity and the temperature changes occur is assumed to be thin. The validity of this assumption depends upon the magnitude of the Grashof and Prandtl numbers.

ii) This layer (to be more precise two layers, one for velocity and one for temperature) is much thinner than the dimensions of the body.

These assumptions enable the Navier-Stokes and transfer equations to be simplified so that the resulting boundary layer equations are in a more readily solvable form.

3.3.2. Free-convection Boundary Layers Equations for Heat Transfer from an Isothermal Vertical Plate.

By the means of the above mentioned assumptions, the steady-state equations for the free-convection boundary layer flows associated with an isothermal vertical plate can be derived by making an estimate of the order of magnitude of each term in the dimensionless form of the momentum, continuity and transfer equations. Using the co-ordinate system shown in figure [3.1], equations (3.1. 6), (3.1.6) and (3.1.7) can be written in boundary layer form as follows:

$$\rho_\infty U \frac{\partial U}{\partial x} + \rho_\infty V \frac{\partial U}{\partial y} = \rho_\infty g \beta_\infty (T - T_\infty) + \mu_\infty \frac{\partial^2 U}{\partial y^2} \tag{3.3.1}$$

$$\frac{\partial U}{\partial x} + \frac{\partial V}{\partial y} = 0 \tag{3.3.2}$$

$$U \frac{\partial T}{\partial x} + V \frac{\partial T}{\partial y} = \frac{K}{\rho C_p} \frac{\partial^2 T}{\partial y^2} \tag{3.3.3}$$

Furthermore, a stream function in the form of $U = \frac{\partial \psi}{\partial y}$ and $V = -\frac{\partial \psi}{\partial x}$ can be introduced which satisfies the continuity equation. The resulting partial differential equations for momentum and energy in terms of the dependent variables ψ and T can be reduced to ordinary differential equations by the similarity transformation:

$$\eta = c \frac{y}{4\sqrt{x}}$$

$$\psi = 4\nu c x^{3/4} f(\eta) \tag{3.3.4}$$

$$T^* = H(\eta)$$

where ν is the kinematic viscosity of the fluid, $c = \sqrt[4]{\frac{\beta g (T_o - T_\infty)}{4\nu^2 T_\infty}}$ and T_o is the temperature of the heated body.

The ordinary differential equations obtained by this procedure are [43]:

$$f''' + 3ff'' - 2f'^2 + H = 0 \tag{3.3.5}$$

$$H'' + 3PrfH' = 0 \tag{3.3.6}$$

The associated boundary conditions are:

$$\begin{aligned} \eta = 0: \quad & f' = 0; \quad f = 0; \quad H = 1 \\ \eta \to \infty: \quad & f' \to 0; \quad H \to 0 \end{aligned} \tag{3.3.7}$$

Equations (3.3.5) and (3.3.6) will be solved in order to provide the basic laminar flow properties, $f(\eta)$, $\xi(\eta)$ and their derivatives, which are required for solving equations (3.2.41) and (3.2.42).

3.4. Kinetic Energy Balance of Disturbed Motion

By application of the technique used by Schlichting [44] for forced convection boundary layer flows, an equation which governs the time rate of increase of the disturbance kinetic energy for unit volume of fluid moving with the basic flow can be obtained by multiplying equations (3.2.25) and (3.2.26) by $\hat{u}$ and $\hat{v}$ respectively, adding these equations, and using equation (3.2.18) to simplify the result. The following equation is obtained:

$$\frac{D}{Dt}\left[\frac{\rho}{2}(\hat{u}^2 + \hat{v}^2)\right] = -\rho\hat{u}\hat{v}\frac{dU}{dy} - \left(\frac{\partial \hat{P}\hat{v}}{\partial x} - \frac{\partial \hat{P}\hat{v}}{\partial y}\right) +$$

$$\rho g\beta\hat{u}\hat{T} - \rho\nu\left(\frac{\partial \hat{v}}{\partial x} - \frac{\partial \hat{u}}{\partial y}\right)^2 + \rho\nu\left[\frac{\partial}{\partial x}\left(\frac{\partial \hat{v}}{\partial x} - \hat{v}\frac{\partial \hat{u}}{\partial y}\right) -\right.$$

$$\left.\frac{\partial}{\partial y}\left(\hat{u}\frac{\partial \hat{v}}{\partial x} - \hat{u}\frac{\partial \hat{u}}{\partial y}\right)\right] \tag{3.4.1}$$

Equation (3.4.1) can be transformed to dimensionless form using the relations (3.2.34) and (3.3.40). The resulting equation is then to be integrated with respect to η from $\eta = 0$ to $\eta = \infty$

and with respect to ζ over a wavelength λ of the disturbance. This procedure yields the following energy balance equation for neutral disturbances [28]

$$- \int_0^\infty f'' (\psi_r^* \psi_i^{*\prime} - \psi_i^{*\prime}\psi_r^*)d\eta + \int_0^\infty \frac{1}{\alpha^* Gr^*}(\xi_r^* \psi_r^{*\prime} - \xi_i \psi_i^{*\prime})d\eta +$$

$$- \int_0^\infty \frac{1}{\alpha^* Gr^*} [(\alpha^{*2}\psi_r^* - \psi_r^{*\prime\prime})^2 + (\alpha^{*2}\psi_i^* - \psi_i^{*\prime\prime})]d\eta = 0 \qquad (3.4.2)$$

The first integrand gives the rate at which the basic flow is working against the Reynolds stress arising from the disturbance, while the second integrand represents the work done by the buoyancy force and the last integrand reveals the dissipation of the disturbance motion.

Equation (3.4.2) not only provides a check on the solution of Equations (3.2.41) and (3.2.42) but it will also be very useful for interpretation of the results (Chapter 5).

The following designators are used to abbreviate the integrands in equation (3.4.2):

$$e_{Re} = - (\psi_r^{*\prime}\psi_i^* - \psi_i^{*\prime}\psi_r^*) f'' \qquad (3.4.3)$$

$$e_B = \frac{1}{\alpha^* Gr^*} (\xi_r^* \psi_r^{*\prime} - \xi_i \psi_i^{*\prime}) \qquad (3.4.5)$$

$$e_D = - \frac{1}{\alpha^* Gr^*} (\alpha^{*2}\psi_r^* - \psi_r^{*\prime\prime})^2 + (\alpha^{*2}\psi_i^* - \psi_i^{*\prime\prime}) \qquad (3.4.6)$$

Hence, equation (3.4.2) becomes:

$$\int_0^\infty e_{Re}\, d\eta + \int_0^\infty e_B d\eta + \int_0^\infty e_D d\eta = 0 \qquad (3.4.7)$$

where e_{Re} and e_B and e_D are the local values of the Reynolds stress, the buoyancy and the dissipation terms in energy balance of the disturbed motion respectively.

Figure 3.1

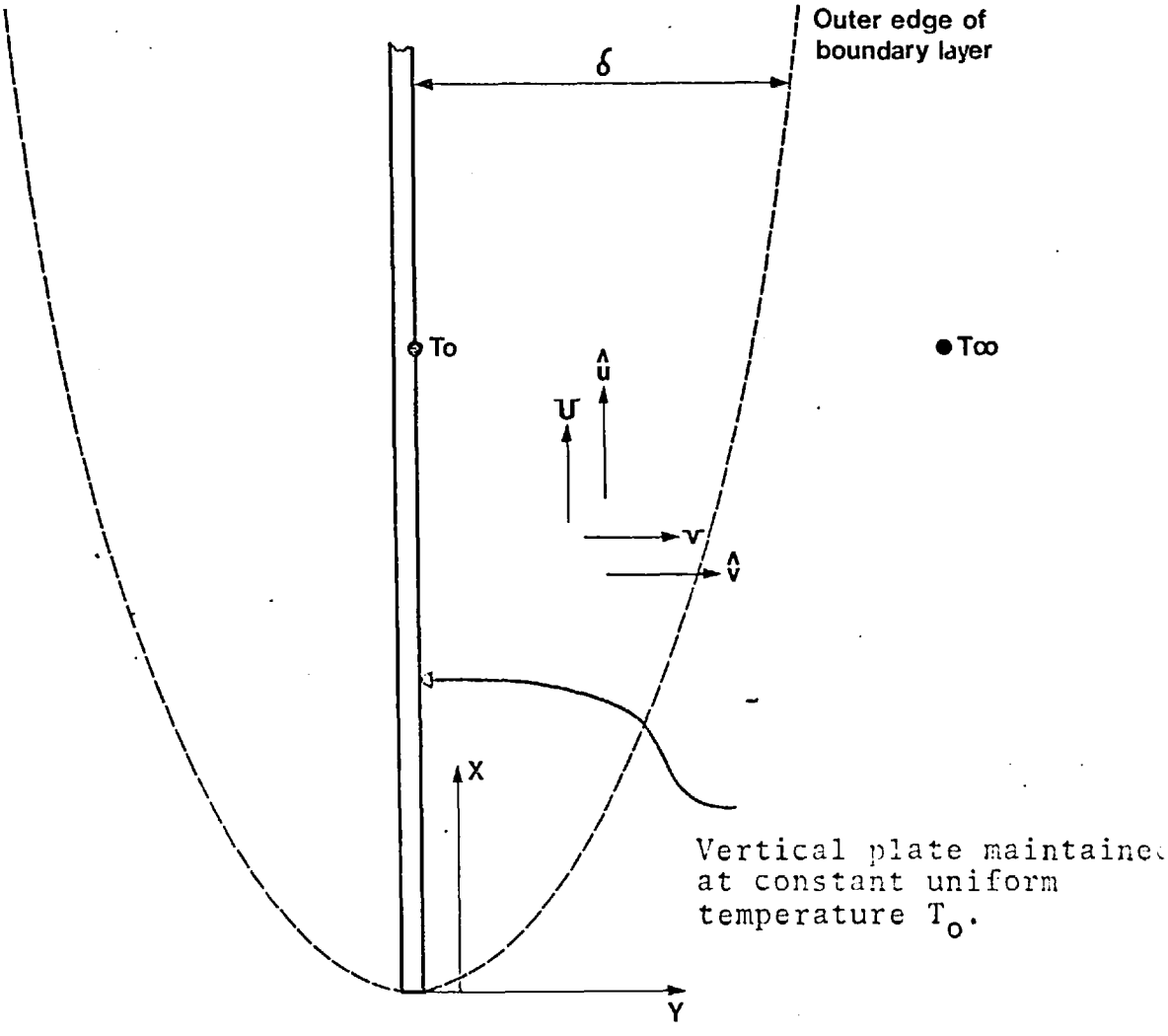

An external free-convection flow

CHAPTER 4

NUMERICAL TECHNIQUES

4.1. Introduction

The system of equations (3.2.41) and (3.2.42) are linear in the y-dependent parts of the perturbation stream function, $\overset{*}{\psi}(y)$, and perturbation temperature function, $\overset{*}{\xi}(y)$, and their derivatives. The equations can be considered to be non-linear in the parameters and eigenvalues that can be varied in the process of solution. Hence, these two equations can be treated as a non-linear set of two coupled ordinary differential equations.

The only method by which the above mentioned equations can be solved is by numerical integration. Unfortunately, all the initial conditions for integration are not known and the problem is a boundary value problem. Hence, it is advantageous to use a quasilinearization technique and a trial-and-error technique in order to solve equations (3.2.41) and (3.2.42). These techniques will be explained in the following sections.

4.2. Quasilinearization Technique

4.2.1. Introduction

Many problems in engineering and applied science are multipoint nonlinear boundary-value problems, in which all the initial conditions for integration are not given. Problems of this type are often very difficult to solve unless a method is used which will obtain the missing initial conditions in an efficient manner.

This section presents a study of the numerical aspects of the use of quasilinearization for obtaining numerical

solutions. Theoretical aspects of the technique can be obtained from references [45,46,47,48].

The quasilinearization technique is essentially a generalized form of the Newton-Raphson method [appendix B] for functional equations. This generalisation will be discussed in section (4.2.2). By using this technique, the non-linear equations are first linearized and then the linearized equations are solved numerically using the superposition principle [appendix C]. The main advantage of this technique is that convergence to the solution of the original equation is quadratic so that very fast convergence can be obtained from poorly guessed initial values of the unknown boundary conditions. Computationally, quadratic convergence means that after a large number of iterations, the number of correct digits for the root X is approximately doubled for each iteration. For example, suppose the approximation to X has an accuracy of 0.01 at K^{th} iteration then for large values of K the approximation at the $(K+1)^{th}$ iteration has an accuracy of 0.0001.

The quasilinearization technique has been used by Lee and Fan [49,50,51], Radhill and McCue [52], Diplock [53], and Harris [54] to solve boundary layer equations and these workers found that, in order to obtain a convergent solution with five figures accuracy only three to six iterations were needed for their problems. Convergence and monotonicity of the technique will be discussed in detail in section (4.2.3).

The quasilinearization technique is generalized to deal with a system of differential equations in section (4.2.4). This technique is applied to problems of parameter estimation

in section (4.2.5). A brief review of difficulties arising in using the quasilinearization technique is presented in section (4.2.6). Finally, the technique is applied to the present problem in section (4.2.7).

4.2.2. Generalizing the Newton-Raphson Method to Functional Equations

As was mentioned in section (4.2.1), the quasilinearization technique is essentially a generalized form of the Newton-Raphson method and may be discussed as follows: First, consider a non-linear first-order differential equation,

$$\frac{dX}{dt} = g(X,t) \tag{4.2.1}$$

Equations (4.2.1) can be expanded in the unknown function $X(t)$ about the approximation $X^o(t)$ as follows:

$$\frac{dX}{dt} - g(X,t) = \frac{dX^o}{dt} - g(X^o,t) + \frac{\partial(\frac{dX^o}{dt})}{\partial X}(X-X^o) -$$

$$\frac{\partial g(X^o,t)}{\partial X}(X-X^o) \tag{4.2.2}$$

where quadratic and higher terms in the Taylor's series have been omitted.

In the same manner $\frac{dX}{dt}$ can be expanded in the following form:

$$\frac{dX}{dt} = \frac{dX^o}{dt} + \frac{\partial(\frac{dX^o}{dt})}{\partial X}(X-X_o) \tag{4.2.3}$$

When this is substituted into equation (4.2.2) the following expression is obtained:

$$\frac{dX}{dt} = g(X^o,t) + \frac{\partial g(X^o,t)}{\partial X}(X-X^o) \tag{4.2.4}$$

Also, the recurrence relation may be employed in order to obtain:

$$(\frac{dX}{dt})^{K+1} = g(X^K,t) + \frac{\partial g(X^K,t)}{X^K}(X^{K+1} - X^K) \qquad (4.2.5)$$

which is the quasilinearization algorithm for the first-order differential equation stated in equation (4.2.1).

The same procedure may be applied to the non-linear second-order differential equation:

$$\frac{d^2X}{dt^2} = g(\frac{dX}{dt},X,t) \qquad (4.2.6)$$

The following relation can be obtained for this case:

$$(\frac{d^2X}{dt^2})^{K+1} = g((\frac{dX}{dt})^K,X^K,t) + ((\frac{dX}{dt})^{K+1} - (\frac{dX}{dt})^K) +$$

$$\frac{\partial g((\frac{dX}{dt})^K,X^K,t)}{\partial(\frac{dX}{dt})^K} + (X^{K+1} - X^K)\frac{\partial g((\frac{dX}{dt})^K,X^K,t)}{\partial X^K} \qquad (4.2.7)$$

where X(t) has been represented as X.

It is obvious that the same procedure can be applied to higher order equations. But, since an I^{th}-order ordinary differential equation can be expressed by a system of I simultaneous first-order ordinary differential equations, it is not necessary to derive the quasilinearization algorithm for higher-order differential equations. This approximation scheme was originally developed by Kantorovich [55,56] and is called the Newton-Raphson-Kantorovich technique.

Bellman [45] and Kalaha [46] developed the Newton-Raphson-Kantorovich technique by using "maximum operation" in order to prove that an original non-linear equation can be transformed into a set of linear equations. They called the method by which the non-linear equation is transformed the quasilinearization technique.

4.2.3. Convergence and Monotonicity of the Quasilinearization Technique

This technique possesses two important properties:

I) Quadratic Convergence

II) Monotonicity

The quadratic convergence of this technique can be proved using an approximation of the Newton-Raphson type. The other property, monotonicity, also can be shown to be abstractly similar to the monotonicity of the Newton-Raphson method. These properties were proved for non-linear second-order differential equations by Bellman and Kalaha [47]. Analytically, for practical problems, these convergence properties cannot easily be obtained. However with the ready availability of modern computers, it is much easier to solve the problem and see if it converges than to try to find convergence properties.

4.2.4. Application of the Quasilinearization Technique to Systems of Differential Equations

The I^{th}-order differential equation can be written as:

$$X^{(I)} = f(t,x,x'....,x^{I-1}) \qquad (4.2.8)$$

where I represents the I^{th} differential. This I^{th}-order ordinary differential equation can be transformed to I first-order ordinary differential equations by the following substitutions:

$$X_1 = X \quad X_2 = X' \quad X_3 = X'',....., X_I = X^{(I-1)} \qquad (4.2.9)$$

The I first-order non-linear ordinary differential equations can be expressed as:

$$\begin{aligned} X_I' &= f(t,X_1,X_2,.....X_I) \\ X_{I-1}' &= X_I \\ &\vdots \\ X_2' &= X_3 \\ X_1' &= X_2 \end{aligned} \qquad (4.2.10)$$

The general form of the equations in the above system can be written as,

$$\frac{dX_i}{dt} = f_i(X_1,X_2,.....X_I,t) \qquad i = 1,2,....I \qquad (4.2.11)$$

With the boundary conditions:

$$\begin{aligned} x_j(0) &= x_{j,0} \qquad j = 1,2,.....m \\ x_q(t_f) &= x_{q,f} \qquad q = m+1,m+2,.....I \end{aligned} \qquad (4.2.12)$$

where $m \leq I$ and t_f denotes the final value of independent variable t.

Equations (4.2.11) and (4.2.12) may be expressed in vector form as:

$$\frac{d\underline{X}}{dt} = \underline{f}(\underline{X},t) \tag{4.2.13}$$

where $\underline{f}$ and $\underline{X}$ are I-dimensional vectors with components $X_1, X_2, \ldots . X_I$ and $f_1, f_2, \ldots . f_I$ respectively.

If it is assumed that $\underline{X}^o$ is an approximate solution of equations (4.2.11), expansions can be made about $\underline{X}^o$ using Taylor's series. If terms of second and higher order are omitted the following equations are obtained:

$$\frac{d\underline{X}}{dt} = \underline{f}(\underline{X}^o,t) + J(\underline{X}^o)(\underline{X} - \underline{X}^o) \tag{4.2.14}$$

where the Jacobian matrix $J(\underline{X}^o)$ is defined by:

$$J(\underline{X}^o) = \begin{bmatrix} \frac{\partial f_1}{\partial X_1^o} & \frac{\partial f_1}{\partial X_2^o} & \cdots & \frac{\partial f_1}{\partial X_I^o} \\ \frac{\partial f_2}{\partial X_1^o} & \frac{\partial f_2}{\partial X_2^o} & \cdots & \frac{\partial f_2}{\partial X_I^o} \\ \vdots & \vdots & & \vdots \\ \frac{\partial f_I}{\partial X_1^o} & \frac{\partial f_I}{\partial X_2^o} & \cdots & \frac{\partial f_I}{\partial X_I^o} \end{bmatrix} \tag{4.2.15}$$

The boundary conditions are still the same as those in equations (4.2.12).

Equation (4.2.14) expresses a set of linear differential equations with variable coefficients which are functions of $\underline{X}^o$. There is no analytical solution of this system but it can be solved numerically with the aid of the superposition principle.

Re-expanding equation (4.2.13) about a known vector $\underline{X}^1$ gives:

$$\frac{d\underline{X}^2}{dt} = \underline{f}(\underline{X}^1,t) + J(\underline{X}^1)(\underline{X}^2 - \underline{X}^1) \qquad (4.2.16)$$

By application of the same procedure to $\underline{X}^2,\underline{X}^3.....$, the following recurrence relation can be obtained:

$$\frac{d\underline{X}^{K+1}}{dt} = \underline{f}(\underline{X}^K,t) + J(\underline{X}^K)(\underline{X}^{K+1} - \underline{X}^K) \qquad (4.2.17)$$

where $J(\underline{X}^K)$ is the following Jacobian matrix:

$$J(\underline{X}^K) = \begin{bmatrix} \frac{\partial f_1}{\partial X_1^K} & \frac{\partial f_1}{\partial X_2^K} & \cdots & \frac{\partial f_1}{\partial X_I^K} \\ \frac{\partial f_2}{\partial X_1^K} & \frac{\partial f_2}{\partial X_2^K} & \cdots & \frac{\partial f_2}{\partial X_I^K} \\ \vdots & \vdots & & \vdots \\ \frac{\partial f_I}{\partial X_1^K} & \frac{\partial f_I}{\partial X_2^K} & \cdots & \frac{\partial f_I}{\partial X_I^K} \end{bmatrix} \qquad (4.2.18)$$

Note that K represents the number of iterations and that the function in the vector $\underline{X}^K$ are considered to be known and the functions in $\underline{X}^{K+1}$ to be unknown.

The boundary conditions for equation (4.2.17) are

$$X_j^{K+1}(0) = X_{j,0} \qquad j = 1,2,....m$$

$$X_q^{K+1}(t_f) = X_{q,f} \qquad q = m+1,m+2,.....I \qquad (4.2.19)$$

As has already been mentioned, a system of linear ordinary differential equations of the boundary value type can be solved numerically with the aid of the principle of superposition.

There exists a set of particular solutions and n sets of homogeneous solutions to the system of equations (4.2.17) and (4.2.19), where n represents the number of missing initial conditions. If the vector $\underline{X}_p^{K+1}(t)$ is any solution of the equations:

$$\frac{d\underline{X}_p^{K+1}}{dt} = \underline{f}(\underline{X}^K,t) + J(\underline{X}^K)(\underline{X}_p^{K+1} - \underline{X}^K) \qquad (4.2.20)$$

which satisfies the conditions:

$$X_{jp}^{K+1}(0) = X_{j,0} \qquad j = 1,2,....m \qquad (4.2.21)$$

and the m vectors $\underline{X}_{hq}^{K+1}$ are m sets of nontrivial and distinct solutions of the m vector equations:

$$\frac{d\underline{X}_{hq}^{K+1}}{dt} = J(\underline{X}^{K})\underline{X}_{hq}^{K+1} \qquad q = m+1, m+2 \ldots I \tag{4.2.22}$$

which satisfy the conditions:

$$\sum_{q=m+1}^{I} a_q^{K+1} X_{jhq}^{K+1}(0) = 0 \tag{4.2.23}$$

Then, the general solution of equation (4.2.17), which satisfies the initial conditions (4.2.19), can be obtained by the use of the principle of superposition as follows:

$$\underline{X}^{K+1}(t) = \underline{X}_p^{K+1}(t) + \sum_{j=1}^{m} \underline{a}_j^{K+1} \underline{X}_{h,j}^{K+1}(t) \tag{4.2.24}$$

where:

$\underline{X}_p^{K+1}(t)$ represents the particular solution of the system of equations (4.2.17) and is denoted by the subscript p.

$\underline{X}_{h,j}^{K+1}(t)$ represents m sets of distinct non-trivial homogeneous solutions. These solutions are designated by the subscript h.

$\underline{a}_j^{K+1}$ is the m-dimensional superposition constant vector which is determined by the use of the conditions which must be satisfied at the end of the region of the integration.

The numerical procedure for obtaining the particular and homogeneous solutions can be explained as follows: The particular solution may be obtained by integrating equation (4.2.20) numerically with the following initial conditions:

$$X_{jp}^{K+1}(0) = X_{j,0} \qquad j = 1,2,....m$$

$$X_{qp}^{K+1}(0) = 0 \qquad q = m+1,m+2,....I \tag{4.2.25}$$

The m homogeneous solutions may be determined by integration of equation (4.2.21) using the following m sets of initial values, which is represented by a matrix with m columns and I rows.

$$\underline{X}_h^{K+1}(0) = \begin{bmatrix} 1 & 0 & 0 & \cdots & 0 \\ 0 & 1 & 0 & \cdots & 0 \\ 0 & 0 & 1 & & \\ \vdots & & & \ddots & \\ 0 & 0 & \cdots & & 1 \\ 0 & 0 & \cdots & & 0 \\ \vdots & & & & \\ 0 & 0 & \cdots & & 0 \end{bmatrix} \tag{4.2.26}$$

These m sets of initial values can also be expressed as:

$$X(i)_{hj}^{K+1}(0) = 1 \quad \text{for } i = j$$

$$X(i)_{hj}^{K+1}(0) = 0 \quad \text{for } i \neq j \tag{4.2.27}$$

where i = 1,2,.....,I and j = 1,2,.....,m.

The subscript i represents the particular variable and j represents a particular set of homogeneous solutions.

Instead of the conditions expressed in equations (4.2.25) and (4.2.27), any other initial conditions can be used as long as the main boundary conditions are satisfied. When the particular and homogeneous solutions have been obtained, the superposition constants ($\underline{a}_j^{k+1}$) can be determined from equation (4.2.24) using the final conditions (4.2.19). At the end of integration, $t = t_f$, the following set of simultaneous algebraic equations can be derived:

$$X_{m,h}^{K+1}(t_f)\ \underline{a}^{K+1} = \underline{c}^{K+1} \tag{4.2.28}$$

where $X_{m,h}^{K+1}(t_f)$ is the mxm square matrix.

$$X_{m,h}^{K+1}(t_f) = \begin{bmatrix} X(1)_{h,1}^{K+1}(t_f) & X(1)_{h,2}^{K+1}(t_f) \cdots\cdots & X(1)_{h,m}^{K+1}(t_f) \\ X(2)_{h,1}^{K+1}(t_f) & X(2)_{h,2}^{K+1}(t_f) \cdots\cdots & X(2)_{h,m}^{K+1}(t_f) \\ \vdots & \vdots & \vdots \\ X(m)_{h,1}^{K+1}(t_f) & X(m)_{h,2}^{K+1}(t_f) \cdots\cdots & X(m)_{h,m}^{K+1}(t_f) \end{bmatrix} \tag{4.2.29}$$

and $\underline{c}^{K+1}$ is the m-dimensional vector.

$$\underline{c}^{K+1} = \begin{bmatrix} X_{1,f} - X(1)_p^{K+1}(t_f) \\ X_{2,f} - X(2)_p^{K+1}(t_f) \\ \vdots \\ X_{m,f} - X(m)_p^{K+1}(t_f) \end{bmatrix} \qquad (4.2.30)$$

Since the matrix $X_{mh}^{K+1}(t_f)$ and the vector $\underline{c}^{K+1}$ are known, the unknown vector $\underline{a}^{K+1}$ can be obtained from equation (4.2.28). Thus,

$$\underline{a}^{K+1} = [X_{m,h}^{K+1}(t_f)]^{-1} \underline{c}^{K+1} \qquad (4.2.31)$$

Equation (4.2.31) can be solved very easily when m is small, otherwise for large m, matrix inversion can be used.

Finally the general solution can be obtained by substitution of the numerical values of the homogeneous and the particular solutions and the superposition constants into equation (4.2.24).

4.2.5. Application of the Quasilinearization Technique to Parameter Estimation

One of the important applications of the quasilinearization technique is parameter estimation [51,52]. This approach is a useful tool for estimating the unknown parameters of systems of equations.

However, as was mentioned in section (4.1) equations (3.2.41) and (3.2.42) are a linear set of two coupled differential equations in which the two eigenvalues and the

two matching parameters are considered to be variables thus giving rise to the nonlinearity of the equations. Hence, the quasilinearization technique will be used for estimating these parameters.

The basic concept of parameter estimation is to consider the unknown parameters as a dependent variables in common with X and as functions of the independent variable, t. Thus, in addition to the governing equations, (4.2.11), the unknown parameters can be represented by the following differential equations:

$$\frac{d\underline{P}}{dt} = 0. \qquad (4.2.32)$$

where $\underline{P}$ is a n-dimensional vector with components $P_1, P_2, \ldots . P_m$. The application of parameter estimation to the present problem will be discussed in section (4.2.7).

4.2.6. A Brief Review of the Main Difficulties Arising in the Use of the Quasilinearization Technique

The main difficulties in using the quasilinearization technique are as follows:

i) Difficulty in using the superposition principle

This difficulty arises from the fact that in using the superposition principle, a set of algebraic equations must be solved. Thus the phenomenon of ill-conditioning in a set of algebraic equations may put a restriction on the use of the superposition principle. The ill-conditioning phenomenon

occurs frequently in physical and engineering problems. Several techniques have been proposed to solve systems of ill-conditioned linear equations [47,51,57]. In the present study, an orthogonalization procedure [appendix D] will be employed for overcoming this difficulty.

ii) Storage and memory

In a number of situations the use of quasilinearization may be limited by the storage capacity of the computer. This difficulty becomes more pronounced when there is need to use complex or double precision arithmetic.

The storage requirements for solving a linear differential equation may be estimated as follows:

If N is the number of grid points, I is the dimension of the dependent variable $\underline{X}$, and n represents the number of missing initial conditions then nxI(N+1) values must be stored in the computer. For example; a typical problem in which 5 initial conditions are missing and I has a rather large value, i.e. 10, the use of double precision or complex arithmetic along with a small integration step corresponding to N = 1000 will give rise to a storage requirement of 100000 locations. This exceeds the available memory of all but the largest computers.

To overcome this problem Belman [47,58,59] suggested that first the guessed initial values $\underline{X}^{o}(t)$, $0 \leq t < t_f$ can be assumed to be constants or simple functions of the independent variable t. These functions should be expressed in a way which requires only a fairly small amount of computer memory. Secondly, instead of storing every calculated value of the previous iteration at every grid point, only the initial values

obtained from the previous iterations need be stored. Then if it is necessary to determine the value of $\underline{X}^K(t)$ at each grid point, the following differential equation can be integrated:

$$\frac{d\underline{X}^K}{dt} = \underline{f}(\underline{X}^{K-1},t) + J(\underline{X}^{K-1})(\underline{X}^K - \underline{X}^{K-1}) \qquad (4.2.33)$$

using the known initial conditions $\underline{X}^K(0)$ which have been determined from the previous iteration and which have been stored in the computer. By application of the above procedure computer memory requirements are reduced at the expense of consuming more computer time.

iii) Monotonic convergence

Theoretically the quasilinearization technique requires positive and convex properties for convergence and this seems to impose a severe limitation on its usefulness. Although this monotonic convergence does not always exist, the technique works well in practice and it converges very rapidly with even poor initial guesses [51,52].

4.2.7. Application of the Quasilinearization Technique to the Present Problem

The quasilinearization technique will now be applied, in order to obtain the solutions of equations (3.2.41) and (3.2.42). The problem is represented by a non-linear set of two coupled ordinary differential equations along with the appropriate boundary conditions. In order to simplify the notation, equations (3.2.41) and (3.2.42) are rewritten without

asterisks as follows:

$$\psi''' = \psi''[i\alpha Gr(f' - c) + 2\alpha^2] - \psi[(f' - c)(i\alpha Gr\alpha^2) + (\alpha^2)^2 + i\alpha Grf'''] - \xi' \quad (4.2.34)$$

$$\xi'' = \xi[(f' - c)(i\alpha GrPr) + \alpha^2] - [i\alpha GrPrH']\psi \quad (4.2.35)$$

with the boundary conditions

$$\psi(0) = 0. \qquad \psi'(0) = 0. \qquad \xi(0) = 0.$$
$$\psi(\infty) \to 0. \qquad \psi'(\infty) \to 0. \qquad \xi(\infty) \to 0. \quad (4.2.36)$$

the eight new variables y can be defined as:

$$\begin{aligned} y(1) &= \psi \\ y(2) &= \psi' \\ y(3) &= \psi'' \\ y(4) &= \psi''' \\ y(5) &= \xi \\ y(6) &= \xi' \\ y(7) &= i\alpha Gr \\ y(8) &= \alpha^2 \end{aligned} \quad (4.2.37)$$

In order to simplify the Jacobian matrix, the parameters α and Gr were replaced by $i\alpha Gr$ and α^2. The quantities $i\alpha Gr$ and α^2 together with c_r and c_i constitute four real parameters in equations (4.2.34) and (4.2.35), of which two must be specified and the other two (eigenvalues) must be determined in the process of solution. The eigenvalues which

were chosen in the computations were (iGr,α^2), but it would have been possible to use other combinations of parameters such as (c_r,c_i) or (c_r,α^2).

The system of equations (4.2.34) and (4.2.35) can now be written as a set of eight first-order ordinary differential equations:

$$\frac{dy(1)}{d\eta} = y(2)$$

$$\frac{dy(2)}{d\eta} = y(3) \qquad (4.2.38)$$

$$\frac{dy(3)}{d\eta} = y(4)$$

$$\frac{dy(4)}{d\eta} = y(3)[y(7)(f'-c) + 2y(8)] - y(1)[(f'-c)y(7)y(8) + (y(8))^2 + y(7)f'''] - y(6)$$

$$\frac{dy(5)}{d\eta} = y(6)$$

$$\frac{dy(6)}{d\eta} = y(5)[(f'-c)((Pr)y(7)) + y(8)] - (Pr)y(7)(H')y(1)$$

$$\frac{dy(7)}{d\eta} = 0.$$

$$\frac{dy(8)}{d\eta} = 0.$$

with the boundary conditions rewritten as:

$$
\begin{aligned}
y(1)_o &= 0. \\
y(2)_o &= 0. \\
y(5)_o &= 0. \\
y(1)_\infty &\to 0. \\
y(2)_\infty &\to 0. \\
y(5)_\infty &\to 0.
\end{aligned}
\qquad (4.2.39)
$$

The subscript in equations (4.2.39) represents the points at which the boundary conditions are known.

Equations (4.2.38) may now be linearized using the recurrence relation (4.2.17). By performing the necessary differentiation, the Jacobian matrix is found to be:

$$
\begin{bmatrix}
0 & 1 & 0 & 0 & 0 & 0 & 0 & 0 \\
0 & 0 & 1 & 0 & 0 & 0 & 0 & 0 \\
0 & 0 & 0 & 1 & 0 & 0 & 0 & 0 \\
-[(\acute{f}-c)y(7) & & [y(7)(\acute{f}-c) & & & & [y(3)(\acute{f}-c)- & [2y(3)-y(1)y(7) \\
y(8)+(y(8))^2 & 0 & +2y(8)] & 0 & 0 & -1 & (\dddot{f})y(1)-y(8) & (\acute{f}-c)-2y(8) \\
+y(7)(\dddot{f})] & & & & & & y(1)(\acute{f}-c)] & y(1)] \\
0 & 0 & 0 & 0 & 1 & 0 & 0 & 0 \\
-(Pr)y(7)(\acute{H}) & 0 & 0 & 0 & [(\acute{f}-c)(Pr) & 0 & [(Pr)y(5)(\acute{f}-c) & -y(5) \\
 & & & & y(7)-y(8)] & & -(Pr)y(1)(\acute{H})] & \\
0 & 0 & 0 & 0 & 0 & 0 & 0 & 0 \\
0 & 0 & 0 & 0 & 0 & 0 & 0 & 0
\end{bmatrix}
$$

(4.2.40)

By substitution of the matrix (4.2.40) into equations (4.2.33) the following set of equations is obtained:

$$\frac{dy(1)^{K+1}}{d\eta} = y(2)^{K+1}$$

$$\frac{dy(2)^{K+1}}{d\eta} = y(3)^{K+1}$$

$$\frac{dy(3)^{K+1}}{d\eta} = y(4)^{K+1}$$

$$\frac{dy(4)^{K+1}}{d\eta} = -y(1)^{K+1}y(7)^{K}y(8)^{K}(f'-c) - y(1)^{K+1}(y(8)^{K})^{2} -$$

$$y(1)^{K+1}y(7)^{K}f''' + y(3)^{K+1}y(7)^{K}(f'-c) + 2y(3)^{K+1}y(8)^{K} - y(6)^{K+1}$$

$$+ y(7)^{K+1}y(3)^{K}(f'-c) - y(7)^{K+1}y(8)^{K}y(1)^{K}(f'-c) - y(7)^{K+1}y(1)^{K}f'''$$

$$- y(7)^{K}y(3)^{K}(f'-c) + y(7)^{K}y(8)^{K}y(1)^{K}(f'-c) + y(7)^{K}y(1)^{K}f'''$$

$$+ 2y(8)^{K+1}y(3)^{K} - y(8)^{K+1}y(1)^{K}y(7)^{K}(f'-c) - 2y(8)^{K+1}y(8)^{K}y(1)^{K}$$

$$- 2y(8)^{K}y(3)^{K} + y(8)^{K}y(1)^{K}y(7)^{K}(f'-c) - 2y(8)^{K}y(8)^{K}y(1)^{K}$$

$$\frac{dy(5)^{K+1}}{d\eta} = y(6)^{K+1}$$

$$\frac{dy(6)^{K+1}}{d\eta} = -y(1)^{K+1}y(7)^{K}(Pr)(H') + y^{K+1}(5)y(7)^{K}(f'-c)(Pr) -$$

$$y(5)^{K+1}y(8)^{K} + y(7)^{K+1}y(5)^{K}(f'-c)(Pr) - y(7)^{K+1}y(1)^{K}(Pr)(H')$$

$$-y(7)^{K}y(5)^{K}(f'-c)(Pr) + y(7)^{K}y(1)^{K}(Pr)(H') - y(5)^{K}y(8)^{K+1} + y(5)^{K}y(8)^{K}$$

$$\frac{dy(7)^{K+1}}{d\eta} = 0. \qquad (4.2.41)$$

$$\frac{dy(8)^{K+1}}{d\eta} = 0.$$

with the boundary conditions

$$y(1)_o^{K+1} = 0.$$

$$y(2)_o^{K+1} = 0.$$

$$y(5)_o^{K+1} = 0.$$

$$y(1)_\infty^{K+1} \to 0.$$

$$y(2)_\infty^{K+1} \to 0.$$

$$y(5)_\infty^{K+1} \to 0. \qquad (4.2.42)$$

This set of linearized equations (4.2.41) and (4.2.42) may now be solved by the superposition principle.

The homogeneous form of equations (4.2.41) can be written as:

$$\frac{dy(1)^{K+1}}{d\eta} = y(2)^{K+1}$$

$$\frac{dy(2)^{K+1}}{d\eta} = y(3)^{K+1}$$

$$\frac{dy(3)^{K+1}}{d\eta} = y(4)^{K+1}$$

$$\frac{dy(4)^{K+1}}{d\eta} = y(1)^{K+1}y(7)^{K}y(8)^{K}(f'-c)-y(1)^{K+1}y(8)^{K}y(8)^{K} -$$

$$y(1)^{K+1}y(7)^{K}f''' + y(3)^{K+1}y(7)^{K}(f'-c) + 2y(3)^{K+1}y(8)^{K} -$$

$$y(6)^{K+1} + y(7)^{K+1}y(3)^{K}(\acute{f}-c) - y(7)^{K+1}y(8)^{K}y(1)^{K}(\acute{f}-c)$$

$$-y(7)^{K+1}y(1)^{K}\dddot{f} + 2y(8)^{K+1}y(3)^{K} - y(8)^{K+1}y(1)^{K}y(7)^{K}(\acute{f}-c)$$

$$-2y(8)^{K+1}y(8)^{K}y(1)^{K}$$

$$\frac{dy(5)^{K+1}}{d\eta} = y(6)^{K+1}$$

$$\frac{dy(6)^{K+1}}{d\eta} = -y(1)^{K+1}y(7)^{K}(Pr)(\acute{H}) + y(5)^{K+1}y(7)^{K}(\acute{f}-c)(Pr) -$$

$$y(5)^{K+1}y(8)^{K} + y(7)^{K+1}y(5)^{K}(\acute{f}-c)(Pr) - y(7)^{K+1}y(1)^{K}(Pr)(\acute{H}) -$$

$$y(5)^{K}y(8)^{K+1}$$

$$\frac{dy(7)^{K+1}}{d\eta} = 0.$$

$$\frac{dy(8)^{K+1}}{d\eta} = 0. \qquad (4.2.43)$$

The boundary conditions for these equations may be arbitrarily chosen but must be non-trivial.

The solution of the system of equations may now be written as:

$$Y(I)^{K+1}(\eta) = y(I)_{p}^{K+1}(\eta) + \sum_{j=1}^{8} a_{j}^{K+1}\, y(I)_{h,j}^{K+1}(\eta) \qquad (4.2.44)$$

where $y(I)_{p}^{K+1}(\eta)$ for I = 1,.....8 is the particular solution and represents one complete solution of the system of equations (4.2.65), and $y(I)_{h,j}^{K+1}(\eta)$ I = 1,2,....8 and j = 1,2,....8, are homogeneous solutions which represent the eight distinct non-trivial solutions of the homogeneous equations (4.2.43). The subscript j denotes the jth homogeneous set of equations and

I the I^{th} variable. Since the system consists of eight first-order differential equations, a_j^{K+1} represents eight superposition constants.

Theoretically, the eight superposition constants can be obtained by the calculation of one particular solution and eight distinct non-trivial homogeneous solutions. However, since three out of eight initial conditions are known, the number of homogeneous solutions can be reduced to five. Thus, the set of homogeneous equations must be integrated five times and five superposition constants are needed.

Applying the above mentioned simplification, equation (4.2.44) becomes:

$$y(I)^{K+1}(\eta) = y(I)_p^{K+1}(\eta) + \sum_{j=1}^{5} a_j^{K+1}\, y(I)_{h,j}^{K+1}(\eta) \qquad (4.2.45)$$

The initial conditions for the particular and homogeneous solutions are:

$$\underline{Y}_p^{K+1}(0) = \begin{bmatrix} y(1)_p^{K+1}(0) \\ y(2)_p^{K+1}(0) \\ y(3)_p^{K+1}(0) \\ y(4)_p^{K+1}(0) \\ y(5)_p^{K+1}(0) \\ y(6)_p^{K+1}(0) \\ y(7)_p^{K+1}(0) \\ y(8)_p^{K+1}(0) \end{bmatrix} = \begin{bmatrix} 0 \\ 0 \\ 0 \\ 0 \\ 0 \\ 0 \\ 0 \\ 0 \end{bmatrix} \qquad (4.2.46)$$

$$\underline{Y}_{h,1}^{K+1}(0) = \begin{bmatrix} y(1)_{h,1}^{K+1}(0) \\ y(2)_{h,1}^{K+1}(0) \\ y(3)_{h,1}^{K+1}(0) \\ y(4)_{h,1}^{K+1}(0) \\ y(5)_{h,1}^{K+1}(0) \\ y(6)_{h,1}^{K+1}(0) \\ y(7)_{h,1}^{K+1}(0) \\ y(8)_{h,1}^{K+1}(0) \end{bmatrix} = \begin{bmatrix} 0 \\ 0 \\ 1 \\ 0 \\ 0 \\ 0 \\ 0 \\ 0 \end{bmatrix} \qquad (4.2.47)$$

$$y^{K+1}_{h,2}(0) = \begin{bmatrix} y(1)^{K+1}_{h,2}(0) \\ y(2)^{K+1}_{h,2}(0) \\ y(3)^{K+1}_{h,2}(0) \\ y(4)^{K+1}_{h,2}(0) \\ y(5)^{K+1}_{h,2}(0) \\ y(6)^{K+1}_{h,2}(0) \\ y(7)^{K+1}_{h,2}(0) \\ y(8)^{K+1}_{h,2}(0) \end{bmatrix} = \begin{bmatrix} 0 \\ 0 \\ 0 \\ 1 \\ 0 \\ 0 \\ 0 \\ 0 \end{bmatrix} \qquad (4.2.48)$$

$$y^{K+1}_{h,3}(0) = \begin{bmatrix} y(1)^{K+1}_{h,3}(0) \\ y(2)^{K+1}_{h,3}(0) \\ y(3)^{K+1}_{h,3}(0) \\ y(4)^{K+1}_{h,3}(0) \\ y(5)^{K+1}_{h,3}(0) \\ y(6)^{K+1}_{h,3}(0) \\ y(7)^{K+1}_{h,3}(0) \\ y(8)^{K+1}_{h,3}(0) \end{bmatrix} = \begin{bmatrix} 0 \\ 0 \\ 0 \\ 0 \\ 0 \\ 1 \\ 0 \\ 0 \end{bmatrix} \qquad (4.2.49)$$

$$\underset{\sim}{y}_{h,4}^{K+1}(0) = \begin{bmatrix} y(1)_{h,4}^{K+1}(0) \\ y(2)_{h,4}^{K+1}(0) \\ y(3)_{h,4}^{K+1}(0) \\ y(4)_{h,4}^{K+1}(0) \\ y(5)_{h,4}^{K+1}(0) \\ y(6)_{h,4}^{K+1}(0) \\ y(7)_{h,4}^{K+1}(0) \\ y(8)_{h,4}^{K+1}(0) \end{bmatrix} = \begin{bmatrix} 0 \\ 0 \\ 0 \\ 0 \\ 0 \\ 0 \\ 1 \\ 0 \end{bmatrix} \qquad (4.2.50)$$

$$\underset{\sim}{y}_{h,5}^{K+1}(0) = \begin{bmatrix} y(1)_{h,5}^{K+1}(0) \\ y(2)_{h,5}^{K+1}(0) \\ y(3)_{h,5}^{K+1}(0) \\ y(4)_{h,5}^{K+1}(0) \\ y(5)_{h,5}^{K+1}(0) \\ y(6)_{h,5}^{K+1}(0) \\ y(7)_{h,5}^{K+1}(0) \\ y(8)_{h,5}^{K+1}(0) \end{bmatrix} = \begin{bmatrix} 0 \\ 0 \\ 0 \\ 0 \\ 0 \\ 0 \\ 0 \\ 1 \end{bmatrix} \qquad (4.2.51)$$

Equations (4.2.46) to (4.2.51) reveal that the original set of boundary conditions at $\eta = 0$ are automatically satisfied.

The next step in obtaining the solution is to search for a procedure which can be used to calculate the five unknown superposition constants. At $\eta \to \infty$, by the use of equations (4.2.42) and (4.2.45), the following relationships can be obtained:

$$y(1)_p^{K+1}(\infty)+a_1^{K+1}y(1)_{h,1}^{K+1}(\infty)+a_2^{K+1}y(1)_{h,2}^{K+1}(\infty)+a_3^{K+1}y(1)_{h,3}^{K+1}(\infty) +$$

$$a_4^{K+1}y(1)_{h,4}^{K+1}(\infty)+a_5^{K+1}y(1)_{h,5}^{K+1}(\infty) = 0 \qquad (4.2.52)$$

$$y(2)_p^{K+1}(\infty)+a_1^{K+1}y(2)_{h,1}^{K+1}(\infty)+a_2^{K+1}y(2)_{h,2}^{K+1}(\infty)+a_3^{K+1}y(2)_{h,3}^{K+1}(\infty) +$$

$$a_4^{K+1}y(2)_{h,4}^{K+1}(\infty)+a_5^{K+1}y(2)_{h,5}^{K+1}(\infty) = 0. \qquad (4.2.53)$$

$$y(5)_p^{K+1}(\infty)+a_1^{K+1}y(5)_{h,1}^{K+1}+a_2^{K+1}y(5)_{h,2}^{K+1}(\infty)+a_3^{K+1}y(5)_{h,3}^{K+1}(\infty) +$$

$$a_4^{K+1}y(5)_{h,4}^{K+1}(\infty)+a_5^{K+1}y(5)_{h,5}^{K+1}(\infty) = 0. \qquad (4.2.54)$$

Equations (4.2.52) to (4.2.54) represent three algebraic equations with five unknowns a_1^{K+1}, a_2^{K+1}, a_3^{K+1}, a_4^{K+1}, a_5^{K+1}. However, it must be noted that, in order to solve this set of algebraic equations, other relationships between the unknown quantities in equations (4.2.42) to (4.2.46) must be introduced. At the surface of plate, $\eta = 0$, the following expressions can be obtained from the seventh and eighth equations of the set of

equations (4.2.45) and from the initial values expressed by expressions (4.2.46) to (4.2.51).

$$y(7)_o^{K+1} = a_4^{K+1} \tag{4.2.55}$$

$$y(8)_o^{K+1} = a_5^{K+1} \tag{4.2.56}$$

Since both $y(7)^{K+1}$ and $y(8)^{K+1}$ are constant functions, it is obvious that the expressions (4.2.55) and (4.2.56) are true not only for $\eta = 0$ but also for $0 < \eta < \infty$:

$$y(7)^{K+1}(\eta) = a_4^{K+1} \tag{4.2.57}$$

$$y(8)^{K+1}(\eta) = a_5^{K+1} \tag{4.2.58}$$

the five superposition constants can now be calculated using the previously obtained particular and homogeneous solutions of equations (4.2.52) to (4.2.54) and (4.2.57) to (4.2.58). After the five superposition constants have been determined, equations (4.2.45) can then be used to determine the "updated" solution $\underset{\sim}{y}^{K+1}(\eta)$ from $\underset{\sim}{y}^{K}(\eta)$. The procedure is then repeated until there is no further change in the values of $y(\eta)$ from one iteration to the next.

From the form of equations (4.2.45), it can easily be concluded that a_1^{K+1}, a_2^{K+1} and a_3^{K+1} are the three unknown initial conditions $y(3)_0^{K+1}$, $y(4)_0^{K+1}$ and $y(6)_0^{K+1}$, respectively.

As was mentioned in section (3.2) it is not always possible to use the boundary conditions at infinity and these

boundary conditions can be replaced by the relationships (3.2.51) to (3.2.53). This problem has been discussed in more detail in Chapter (3).

The procedure for obtaining the required numerical solution can be summarized as follows:

Initial guesses of the solutions for $y(1)^{o}(\eta)$, $y(3)^{o}(\eta)$, $y(5)^{o}(\eta)$, $y(7)^{o}(\eta)$ and $y(8)^{o}(\eta)$ must be chosen (values of $y(2)^{K}(\eta)$, $y(4)^{K}(\eta)$, $y(6)^{K}(\eta)$ are not required during the solution procedure for the $(K+1)^{th}$ iteration). These initial guesses may be arbitrary or may be solutions of a similar problem which happen to be available. Particular and homogeneous solutions can be then computed by integration of the set of equations (4.2.41) and (4.2.43) with the appropriate initial conditions. The integration may be started from the surface of body, $\eta = 0$, to the outer edge of the boundary layer, η_{edg}. In Chapter (5), the effect of choosing different values of the variable, η_{edg}, will be discussed. Furthermore, the five superposition constants can be obtained from equations (4.2.52) to (4.2.58). Then by the use of equations (4.2.45), the new approximation to the solution may be calculated. The procedure can be continued in the same manner described above in order to obtain new particular and homogeneous solutions and new superposition constants. If the difference between the new values of these constants and the values obtained from the previous iteration is within the required accuracy the computation can be stopped.

4.3. Trial-and-error Technique

4.3.1. Introduction

A trial-and-error method based on linear interpolation is frequently used to solve boundary value problems. Green [60] used this technique to find the missing initial conditions for the solution of the boundary layer equations for forced convection. Pandya [61] also employed this technique in an attempt to find two unknown missing boundary conditions for pure free convection. Generally, it has been reported that this technique possesses a relatively slow convergence rate and that for a large number of problems the technique does not converge unless the values of the guessed missing conditions correspond closely to the values of the unknown conditions.

4.3.2. The Application of Trial-and-error Technique to the Present Problem

As was mentioned in section (4.1), the system of equations (3.2.41) and (3.2.42) is linear in the y dependent parts of the perturbation stream function, $\psi(y)$, and perturbation temperature function, $\xi(y)$, and in their derivatives. In section (4.2) the parameters and eigenvalues were considered to be variables during the process of obtaining a solution. In this section parameters and eigenvalues are treated as constants so that equations (3.2.41) and (3.2.42) become a linear fourth-order ordinary differential equation and a linear second-order differential equation, respectively. These equations can be treated as a sixth-order ordinary differential equation. The same procedure and the same notation as was used in

section (4.2.7), can be applied in order to reduce the sixth-order ordinary differential equation into a set of six first-order ordinary differential equations.

The system of equations (3.2.41) and (3.2.42) may be written as:

$$\frac{dy(1)}{d\eta} = y(2)$$

$$\frac{dy(2)}{d\eta} = y(3)$$

$$\frac{dy(3)}{d\eta} = y(4)$$

$$\frac{dy(4)}{d\eta} = y(3)[i\alpha Gr(f'-c)+2\alpha^2] - y(1)[(f'-c)(i\alpha Gr)(\alpha^2) + (\alpha^2)^2 + (f''')(i\alpha Gr)] + y(6)$$

$$\frac{dy(5)}{d\eta} = y(6)$$

$$\frac{dy(6)}{d\eta} = y(5)[(f'-c)(Pr)(i\alpha Gr)+\alpha^2] - (Pr)(i\alpha Gr)(H')y(1) \qquad (4.3.1)$$

The boundary conditions for the above equations are those given in (4.2.39). Since the ordinary differential equations (3.2.41) and (3.2.42) are linear and homogeneous and the boundary conditions (4.2.39) are also homogeneous, it is permissible to put $y(3)_o$ equal to some convenient fixed value. Physically, this means that the arbitrary scale of the disturbance level is fixed. For simplicity $y(3)_o$ will be taken to be unity.

The initial conditions can be written as:

$$\begin{aligned} y(1)_0 &= 0 \\ y(2)_0 &= 0 \\ y(3)_0 &= 1 \\ y(5)_0 &= 0 \end{aligned} \qquad (4.3.2)$$

The system of equations (4.3.1) with the initial conditions (4.3.2) can be solved by the principle of superposition. Solution of equations (4.3.1) can be represented by:

$$y(I)(\eta) = \sum_{j=1}^{6} a_j y(I)_{h,j}(\eta) \qquad (4.3.3)$$

with the initial conditions given by equations (4.3.2). It can be shown that the first, second and fifth integration constants are zero and that the third constant is unity. Thus, only three sets of homogeneous solutions and two superposition constants are needed. Equation (4.3.3) may be simplified as:

$$y(I)(\eta) = y(I)_{h,1}(\eta) + a_2 y(I)_{h,2} + a_3 y(I)_{h,3} \qquad (4.3.4)$$

The initial conditions for the homogeneous equations are:

$$Y_{h,1}(0) = \begin{bmatrix} y(1)_{h,1}(0) \\ y(2)_{h,1}(0) \\ y(3)_{h,1}(0) \\ y(4)_{h,1}(0) \\ y(5)_{h,1}(0) \\ y(6)_{h,1}(0) \end{bmatrix} = \begin{bmatrix} 0 \\ 0 \\ 1 \\ 0 \\ 0 \\ 0 \end{bmatrix} \qquad (4.3.5)$$

$$Y_{h,2}(0) = \begin{bmatrix} y(1)_{h,2}(0) \\ y(2)_{h,2}(0) \\ y(3)_{h,2}(0) \\ y(4)_{h,2}(0) \\ y(5)_{h,2}(0) \\ y(6)_{h,2}(0) \end{bmatrix} = \begin{bmatrix} 0 \\ 0 \\ 0 \\ 1 \\ 0 \\ 0 \end{bmatrix} \qquad (4.3.6)$$

$$Y_{h,3}(0) = \begin{bmatrix} y(1)_{h,3}(0) \\ y(2)_{h,3}(0) \\ y(3)_{h,3}(0) \\ y(4)_{h,3}(0) \\ y(5)_{h,3}(0) \\ y(6)_{h,3}(0) \end{bmatrix} = \begin{bmatrix} 0 \\ 0 \\ 0 \\ 0 \\ 0 \\ 1 \end{bmatrix} \qquad (4.3.7)$$

The initial conditions (4.3.5) to (4.3.7) automatically satisfy the original initial conditions (4.3.2).

The numerical solution procedure is straightforward and is as follows:

For given values of αGr and α^2 a real and imaginary parts of the complex quantity c were guessed and the set of differential equations (4.3.1) integrated across the boundary layer from $\eta = 0$ using the initial conditions (4.3.5) to (4.3.7). When the values of the homogeneous solutions at the edge of boundary layer have been obtained the integration constants a_2 and a_3 are determined by application of the two relationships (3.2.52) and (3.2.53). The remaining relationship (3.2.51) is used to provide a check on the numerical

solutions of equations (4.3.1). The correct values of the real and imaginary parts of c are obtained by the use of an iterative process as follows:

If the left hand side of the relationship (3.2.51) is set to χ (instead of to zero) then:

$$\xi'(\eta_{edg}) + \gamma\xi(\eta_{edg}) = \chi \qquad (4.3.8)$$

If the assumed values of the real and imaginary parts of c give

$$\xi'(\eta_{edg}) + \gamma\xi(\eta_{edg}) = \chi \neq 0$$

The value of c then can be changed to $c + \Delta c_r$, where Δc_r is a small complex quantity. By repeating the integration a new value for χ can be obtained:

$$\xi'(\eta_{edg}) + \gamma\xi(\eta_{edg}) = \chi + \Delta\chi$$

Then, by approximating the partial derivatives to finite differentials:

$$\frac{\partial r}{\partial c_r} = \frac{\Delta \chi}{\Delta c_r}$$

and by applying one of the Cauchy-Riemann relations (appendix D):

$$\frac{\partial(\xi'(\eta_{edg}) + \gamma\xi(\eta_{edg}))_r}{\partial c_r} = \frac{\partial(\xi'(\eta_{edg}) + \gamma\xi(\eta_{edg}))_i}{\partial c_i}$$

so that by using simple linear extrapolation an improved value for c can be obtained.

The process is repeated until χ is within the required accuracy. Values of χ of 1×10^{-2} to 1×10^{-10} were investigated and results will be discussed in Chapter 5.

4.3.3. Simplification of the Present Trial-and-error Technique

The trial-and-error technique has been used by Nachtsheim [11] and by Dring and Gebhart [25] for solving the equations which describe the stability of vertical natural convection boundary layers. Their approach for solving the problem was that for fixed value of wave number, α, and modified Grashof number, Gr, values for two of the complex missing initial conditions and the phase velocity, c, were guessed, and then the governing equations were integrated from surface of the wall to edge of boundary layer, i.e. three complex values were guessed.

Obviously the above approach requires a lot of computation time and complicated procedure must be used to obtain a better approximation to guessed values. In the present work the problem was simplified because only the phase velocity c was guessed rather than guessing three complex values.

4.4. Numerical Integration Technique

The two main integration techniques, which are commonly used for numerical integration, are predictor-corrector type methods and single-step methods.

The single step methods are self-starting but the predictor-corrector techniques require values of the function at a number of previous steps, in order to proceed to the next point. Therefore a single-step technique must be used to calculate the initial points before a switch can be made to the predictor-corrector method. Computationally self starting (single-step) techniques require little storage space when proceeding from one step to the next, since the information from previous steps may be overwritten.

The number of functions that must be evaluated in single step methods are more than in predictor-corrector methods, but, as reported in reference [53], for a given accuracy single-step methods are faster than predictor-corrector methods because the extra function evaluations that are necessary for single-step methods are not the most significant factor in determining the computer time required. Also, changes of integration step length in single-step methods do not require extra programming, and the storage requirements are less than those required for the predictor-corrector method.

The Runge-Kutta method [62] was used in the present work. This method is a fourth order single-step technique in which the truncation error is of the order of h^5, where h is the step length. This method requires four function evaluations for each step.

In the present study the coefficients f', f''' and H' in equations (3.2.41) and (3.2.42) were evaluated implicitly at the point at which the function was evaluated.

CHAPTER 5

RESULTS AND DISCUSSION

Results and Discussion

In this chapter the accuracy of the numerical solutions will be discussed first, this will be followed by a detailed presentation of results and discussion. Finally, the results will be compared with available data.

5.1. The Accuracy of the Numerical Solutions

The accuracy of the numerical solutions depends on the accuracy of the Runge-Kutta numerical integration technique, and on the numerical techniques used to predict the unknown boundary conditions.

The Runge-Kutta integration technique was tested in the usual manner by varying the integration step length. Because of the complexity of the eigenvalue profiles, ψ, ψ', ψ'', ... and because of the limited size of the computer memory, the accuracy of the solutions was chosen to be within four decimal places. Smaller integration step length sizes were used in region $0<\eta<1$ because of the sharp variation of eigenvalue profiles in the region of the wall.

Table F.1.(a) shows the effect of varying the step lengths on the predicted values of the six unknown parameters for a Prandtl number of 1.0 and for a value of the product of the wave number and the Grashof number (αGr) of 8.0. The values of the six unknown parameters $\psi'''(0)_r$, $\psi'''(0)_i$, $\xi'(0)_r$, $\xi'(0)_i$, c_r and c_i are compared for a number of different step lengths. From Table F.1.(a) it can be seen that the solutions for step lengths of 0.1 for $0<\eta<1$ and 0.2 for $1<\eta<8$ are very different to those for step lengths of 0.02 for $0<\eta<1$ and 0.04 for $1<\eta<8$. The differences then become smaller for the subsequent solutions

as step length is reduced. For step lengths of 0.02 for $0<\eta<1$ and 0.04 for $1<\eta<8$ the solutions are close to those for step lengths of 0.01 for $0<\eta<1$ and 0.02 for $1<\eta<8$. A further reduction of step length to 0.008 for $0<\eta<1$ and 0.016 for $1<\eta<8$ brought no further changes in the predicted values up to four decimal places.

Table F.1.(b) shows the solutions for a Prandtl number of 1.0 and for a large value of $\alpha Gr = 75.0$. It can be seen that the solutions for step lengths of 0.008 for $0<\eta<1$ and 0.016 for $1<\eta<8$ are little different to those for step lengths of 0.006 for $0<\eta<1$ and 0.012 for $1<\eta<8$. Therefore, in remaining calculations for values of $\alpha Gr>50.0$ step lengths of 0.01 for $0<\eta<1$ and 0.02 for $1<\eta<8$ were used and for values of $\alpha Gr<50.0$ step lengths of 0.008 for $0<\eta<1$ and 0.016 for $1<\eta<8$ were employed. The need to use smaller step lengths for large values of αGr is not surprising because the oscillatory behaviour of eigenvalue profiles at large values of αGr is more pronounced.

For a Prandtl number of 0.733 because of the similar behaviour of the solutions to those for a Prandtl number of 1.0, step lengths of 0.01 for $0<\eta<1$ and 0.02 for $1<\eta<8$ and 0.008 for $0<\eta<1$ and 0.016 for $1<\eta<8$ were used for values of $\alpha Gr<50.0$ and $\alpha Gr>50.0$ respectively.

The effect of varying the step lengths for a Prandtl number of 6.7 and $\alpha Gr = 7.0$ is shown in Table F.1.(c). It can be seen that the values of the six predicted variables are different for larger step lengths of 0.125 for $0<\eta<1$ and 0.25 for $1<\eta<8$ and 0.0625 for $0<\eta<1$ and 0.125 for $1<\eta<8$. The reduction of step lengths from 0.0125 for $0<\eta<1$ and 0.025 for

$1<\eta<8$ to 0.01 for $0<\eta<1$ and 0.02 for $1<\eta<8$ results in no further change in the predicted values to four decimal places accuracy. For a large value of $\alpha Gr = 21.5$ and a Prandtl number of 6.7, Table F.1.(d) shows that, similar to the case of Prandtl number of 1.0, smaller step lengths are required. Step lengths of 0.0125 for $0<\eta<1$ and 0.025 for $1<\eta<8$ and 0.01 for $0<\eta<1$ and 0.02 for $1<\eta<8$ were used during the calculations for $\alpha Gr<15.0$ and $\alpha Gr>15.0$, respectively.

Because of the results obtained for a Prandtl number of 6.7, step lengths of 0.0125 for $0<\eta<1$ and 0.025 for $1<\eta<8$ and 0.01 for $0<\eta<1$ and 0.02 for $1<\eta<8$ were studied in order to investigate whether the same integration step lengths as had been found satisfactory for a Prandtl number of 6.7 could be used for large values of the Prandtl number of 100.0 and 1000.0. As can be seen in Tables F.1.(e) and F.1.(f), it was found that increasing the Prandtl number had no influence on the step length that was required for integration.

The second important variable in the integration is the value of η at the effective edge of the boundary layer, η_{edg}. As was mentioned in Chapter 4, integration was started from the surface where $\eta = 0$ and terminated at the edge of boundary layer, η_{edg}. In fact, η_{edg} is the effective infinity in solving pure free-convection boundary layer flow equations. In practice, the asymptotic boundary conditions will be satisfied more accurately as η_{edg} becomes progressively larger. However, once a certain value of η_{edg} is reached, there is only a very small improvement in the results when the value of η_{edg} is further increased, and in some cases this even causes instability in numerical integration.

Table F.2.(a) presents the effect of varying the magnitude of η_{edg} for a Prandtl number of 0.733 and a value of the parameter αGr of 51.3. The changes in the values of the six predicted parameters decrease rapidly as the value of η_{edg} is increased and eventually almost constant values are attained for the parameters for values of η_{edg} greater than 7.0.

The corresponding results for the same Prandtl number, Pr = 0.733, but for a different value of αGr of 6.6 are presented in Table F.2.(b). As can be seen from the table, the value of αGr has an influence on the value of η_{edg} that is required for the integration. For the small value of αGr of 6.6 the parameters approach constant values as the value of η_{edg} approaches 8.0.

For a Prandtl number of 6.7 and αGr = 21.0, Table F.2.(c) shows that by increasing the value of η_{edg} the values of the unknown parameters become constant when η_{edg} is greater than 6.0.

Table F.2.(d) presents the effect of varying the magnitude of η_{edg} for a Prandtl number of 6.7 and for a different value of αGr of 4.8. It can be seen that constant values for the parameters are obtained at values of η_{edg} greater than 7.5. Because of these results, values of η_{edg} not smaller than 8.0 were used throughout this work for Prandtl numbers of 0.733, 1.0 and 6.7. This restriction ensured that a small safety margin was included.

For Prandtl numbers of 100.0 and 1000.0, the values of ξ and ξ' were arbitrarily set to zero at a pre-specified value of η for the remainder of the region of integration. This was necessary because of the build-up of round-off errors which

caused the solution to "blow up". The solution "blew up" very rapidly once the round-off errors were transmitted through to hydrodynamic equation (3.2.41). It was found that when ξ and ξ' were set to zero at a value of η less than 4.0 no convergence of the solution could be achieved. Also, the solution "blew up" if a value of η greater than 6.0 was chosen. Therefore, values of η equal to 4.5, 5.0 and 5.5 were examined where the ξ and ξ' were set to zero. It was observed that the rapid convergence was obtained at η = 4.5. Thus, throughout the work, ξ and ξ' were set to zero at η = 4.5 for Prandtl numbers of 100.0 and 1000.0.

It was interesting to note that when ξ and ξ' are set to zero the assumption is made that the buoyancy effect no longer affects the hydrodynamic equation (3.2.41). This is because at high values of the Prandtl number the thermal boundary layer thickness is thinner than the hydrodynamic boundary layer thickness and the velocity-temperature coupling is more noticeable in the region near the wall than regions far from the wall.

The build up of round-off errors was also encountered by Diplock [53] and Harris [54] in their solution of the interaction of free and forced convection and the free convection boundary layer equations respectively for large values of Prandtl number or Schmidt number.

Table F.2.(e) shows the effect of varying the magnitude of η_{edg} for a Prandtl number of 100.0 and for a value of αGr = 23.60 when the values of ξ and ξ' were set to zero at η = 4.5. It can be seen that by increasing the value of η_{edg} the values of the unknown parameters become constant when η_{edg}

is greater than 12.0.

Table F.2.(f) presents the effect of varying the magnitude of η_{edg} for a Prandtl number of 100.0 but for a different value of αGr of 9.95 when the values of ξ and ξ' were set to zero at $\eta = 4.5$. It reveals that for the smaller value of αGr of 9.95 constant values of the parameters are obtained at values of η_{edg} greater than 13.0.

Tables F.2.(g) and F.2.(h) show the effect of varying the magnitude of η_{edg} for a Prandtl number of 1000.0 and for values of $\alpha Gr = 30.07$ and $\alpha Gr = 11.35$, respectively, when the values of ξ and ξ' were set to zero at $\eta = 4.5$. As can be seen from Tables F.2.(g) and F.2.(h), constant values of the parameters were obtained at values of $\eta_{edg} = 13.0$ and $\eta_{edg} = 14.0$, respectively. Because of the above mentioned results, values of η_{edg} not smaller than 14.0 were used for Prandtl numbers of 100.0 and 1000.0.

As was mentioned in section (3.2), equations (3.2.41) and (3.2.42) were integrated from the surface of the plate, $\eta = 0$, to the effective edge of the boundary layer, η_{edg}. In using the trial-and-error method the missing boundary conditions were found at η_{edg} by application of relationships (3.2.52) and (3.2.53). Relationship (3.2.51) was used as the convergence criterion, since it also must be satisfied, i.e. the value of χ, $|\xi'+\gamma\xi| = \chi$, must be sufficiently small [see section (4.3.2)].

In a series of tables F.3.(a) to F.3.(g), the effects of using different convergence criteria for both high and low values of αGr and for Prandtl numbers of 0.733 and 1.0 are

shown. The tabulated results show that for low values of αGr, $\alpha Gr>40.0$, convergence of the missing boundary conditions to five decimal places was achieved when the stated convergence criterion was 1×10^{-3}. Convergence was usually obtained after three or four iterations. For larger values of αGr, $\alpha Gr>40.0$, even a specified convergence criterion of 1×10^{-2} produced extremely accurate predictions of the unknown boundary conditions to an accuracy within six decimal places and convergence was achieved after four or five iterations.

Tables F.3.(h) to C.3.(m) show the effect of using different convergence criteria upon the missing boundary conditions for a Prandtl number of 6.7 and for different values of αGr. It can be seen that a convergence criteria of 1×10^{-3} and 1×10^{-2} yielded very accurate results and convergence was obtained after three or four iterations. For larger values of αGr, $\alpha Gr>25.0$, the number of iterations required increased and eight to ten iterations were needed when the convergence criterion was specified to be 1×10^{-3}. When the value of the convergence criterion was set to less than 1×10^{-3} convergence could not be achieved.

In Tables F.3.(n) to F.3.(p) the effects of using different convergence criteria for a Prandtl number of 100 and for different values of αGr are studied. Once again for $\alpha Gr<20.0$ convergence of the missing boundary conditions to four decimal places was achieved with a convergence criterion of 1×10^{-2}. Similar to the case of a Prandtl number of 6.7 and for values of $\alpha Gr>20.0$ the number of iterations increased and for a specified convergence criterion of 1×10^{-2},

at least ten iterations were needed. For a Prandtl number of 1000.0 because of the similar behaviour of the solution to Prandtl number of 100.0, a convergence criterion of 1×10^{-2} was used.

In using the quasilinearization technique, the superposition constants were calculated using relationships (3.2.51) and (3.2.52). These constants were compared with those of the previous iteration. If they were within the required accuracy the computation was stopped. The accuracy was chosen to be within four decimal places. The effects of instability in the numerical solution procedure were found to be much greater for high Prandtl numbers than for low Prandtl numbers. Stability was achieved for Prandtl numbers greater than 100.0 and for large values of $\alpha Gr > 20.0$ by initial integration of the equations out to a small value of η_{edg}. Then, once convergence had been obtained, the value of η_{edg} was increased and the quasilinearization method applied again.

5.2. Stability Results for Air, Prandtl Number of 0.733, and Prandtl Number of 1.0

The results of a stability analysis are usually presented in the wave number, Grashof number-plane (α, Gr-plane) on which the neutral stability curve, $c_i = 0$, is drawn. The minimum value of the Grashof number for points on this curve is called the minimum critical Grashof number. If a Grashof number, Gr, and disturbance wave number, α, are chosen, reference to the α, Gr-plane shows whether or not the disturbance will be amplified.

In the present study the points on the neutral stability curve were obtained by plotting the imaginary part of the phase velocity, c_i, against the Grashof number, Gr, while holding the disturbance wave number constant [see figure 5.1]. Although this method is easy to apply, it is an indirect method of obtaining points on the neutral stability curve. This disadvantage can be attributed to the choice of the phase velocity, c, as an eigenvalue. A direct procedure would be to set the imaginary part of phase velocity, c_i, to zero, and then to attempt to find the proper relationship between the remaining parameters; wave number, α, the real part of phase velocity, c_r, and the Grashof number, Gr, by solving the disturbance equations (3.2.41) and (3.2.42). This procedure possesses two major disadvantages: first, since the value of the imaginary part of the phase velocity, c_i, is set to zero, there is no longer a relationship between remaining parameters which are chosen as eigenvalues. But, if for example, the real part of the phase velocity, c_r, and the imaginary part of the phase velocity, c_i, were taken as eigenvalues, the Cauchy-Riemann relation could be used for improving the values of the eigenvalues for the next iteration [see section (4.3)]. Secondly, the disturbance equations may not have any solutions which satisfy the condition $c_i = 0$. For example; for the case of plane Couette flow, the disturbance equations have no solution for $c_i = 0$ [11]. In the present work reference to figure 5.2 shows that solutions for $c_i = 0$ exist only for certain ranges of values of the wave number, α.

Figure 5.2 shows the neutral stability curve for the case of a Prandtl number of 0.733. It can be seen that the

Figure 5.1. The plot of phase velocity, c_i, against Grashof number, Gr, at a wave number, α, of 0.76 for a Prandtl number, Pr, of 0.733.

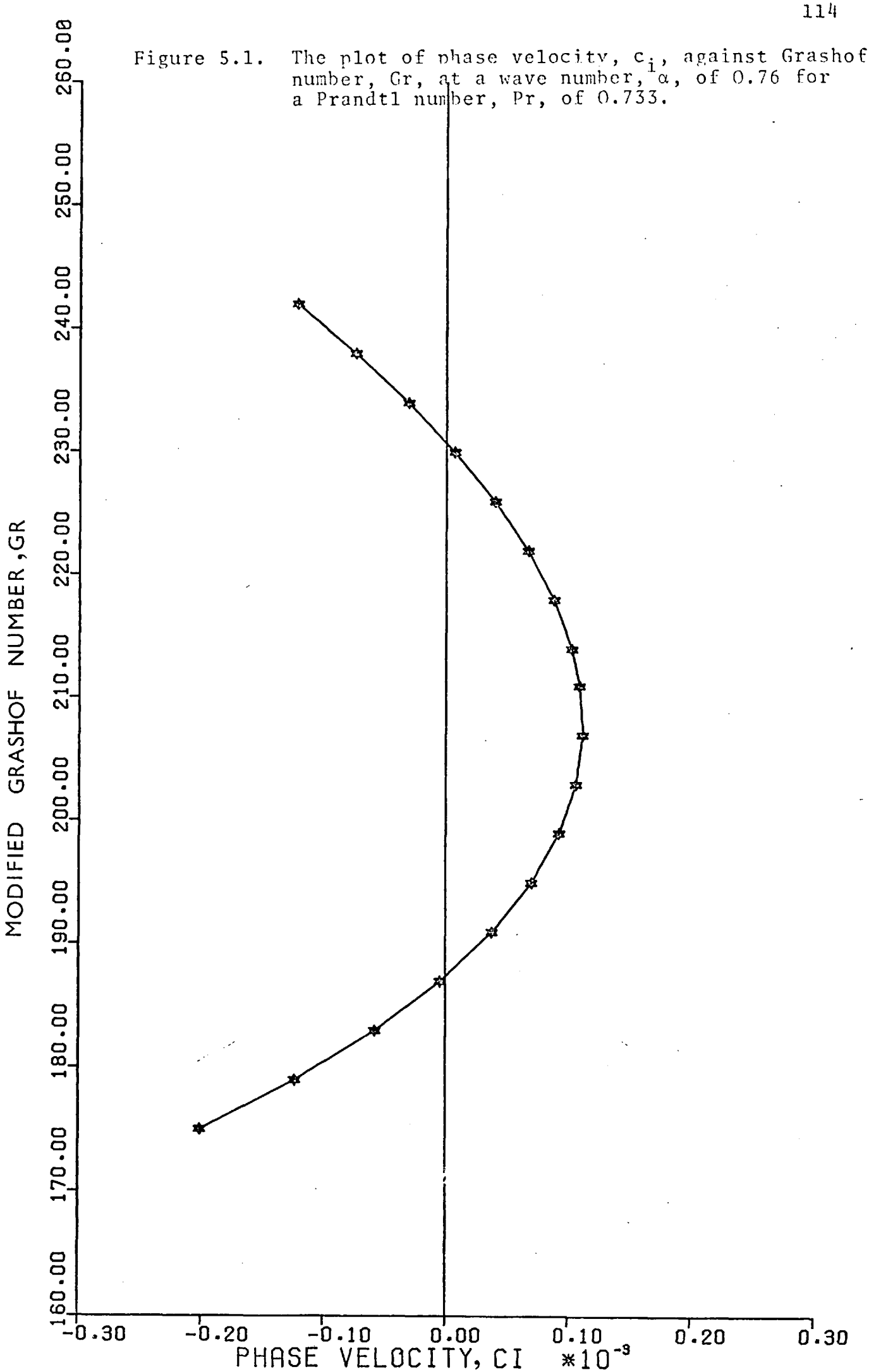

Figure 5.2. Neutral stability curve for a Prandtl number of 0.733 in α, Gr-plane.

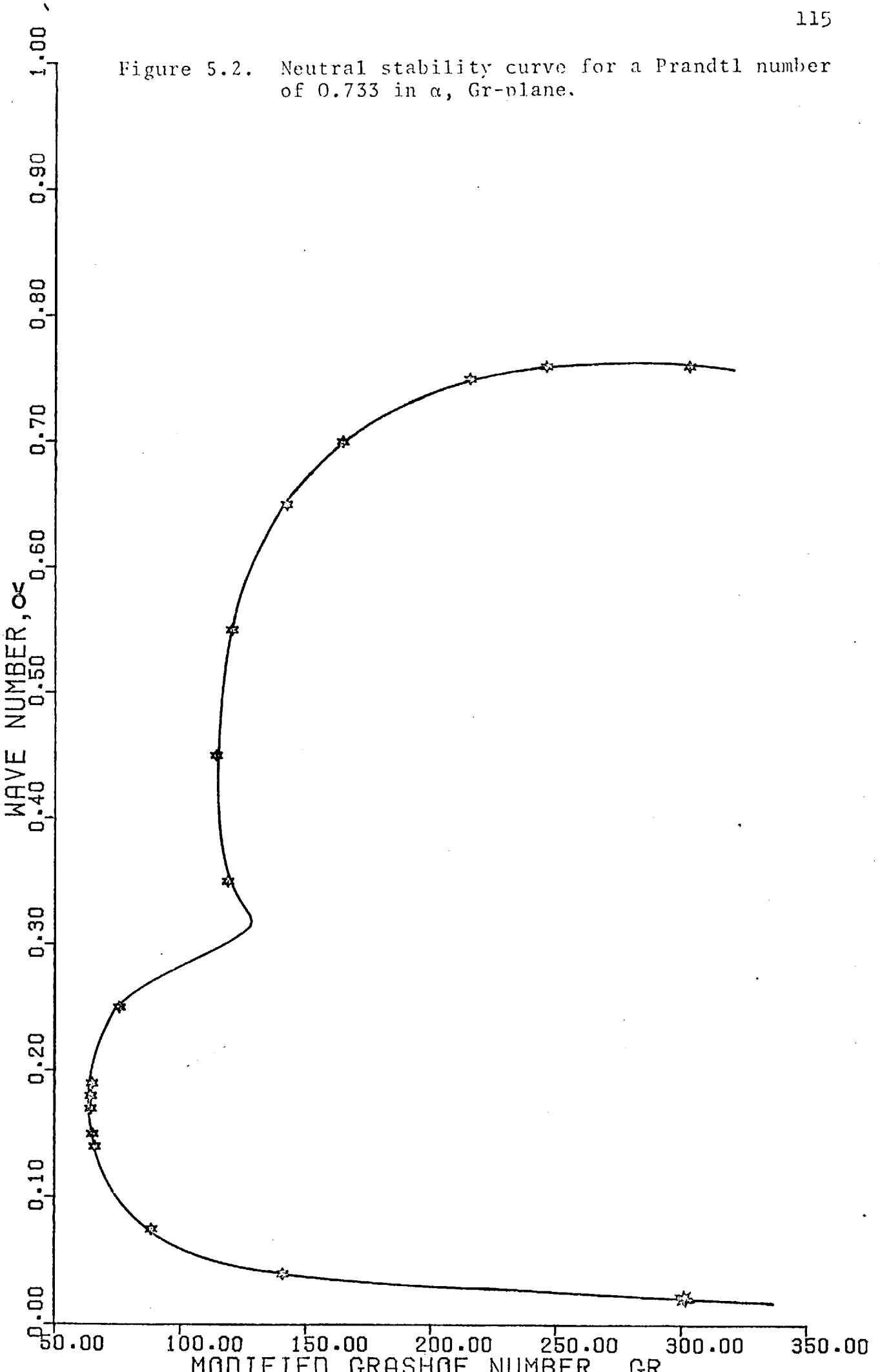

minimum critical value of the Grashof number is 64.5. The detailed solutions for the neutral stability curve for a Prandtl number of 0.733 are presented in Table F.4.(a). The table shows that the closest calculated point to the minimum critical Grashof number is at a Grashof number of 64.470, and at a wave number of 0.17 with a phase velocity of 0.25856.

Figure 5.3 shows the neutral stability curve for a Prandtl number of 0.733 in the phase velocity, Grashof number-plane (c_r, Gr-plane). A comparison of this figure with figure 5.4 reveals that for values of the wave number, α, less than 0.14, the phase velocity of the disturbance, c_r, is greater than the maximum velocity of the basic flow so that, consequently, there are no critical layers. This result is in contrast to the results which have been obtained by the use of the Orr-Sommerfeld equation for forced-convection boundary layer flows [63].

The solutions of the disturbance equations (3.2.41) and (3.2.42) for a Prandtl number of 0.733 and for the neutral stability curve are presented in figures 5.5 to 5.36. The computer program which was used for solving the disturbance equations, calculated and printed out the real and imaginary parts of the eigenfunctions (ψ,ξ) and their derivatives as well as the corresponding eigenvalues. Examination of these figures shows that as the value of wave number, α, increases, the plots of the eigenfunctions and their derivatives change shape and the oscillatory behaviour of the curves becomes more pronounced. Reference to these figures shows that for smaller

Figure 5.3 - Neutral stability curve for air, Prandtl number of 0.733, in c_r, Gr-plane.

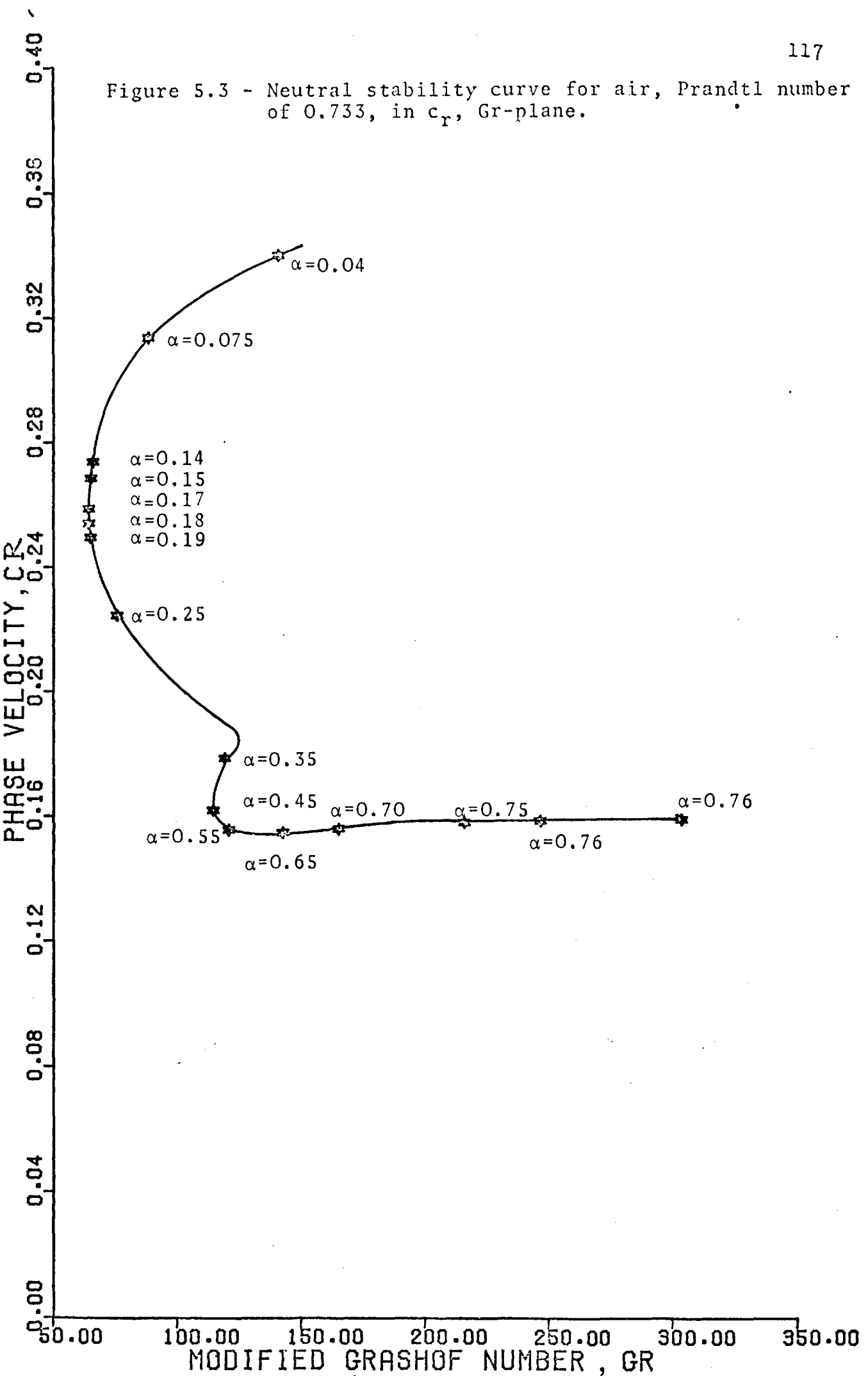

Figure 5.4. Velocity profile for a Prandtl number of 0.733 from Schmidt and Beckmann equations.

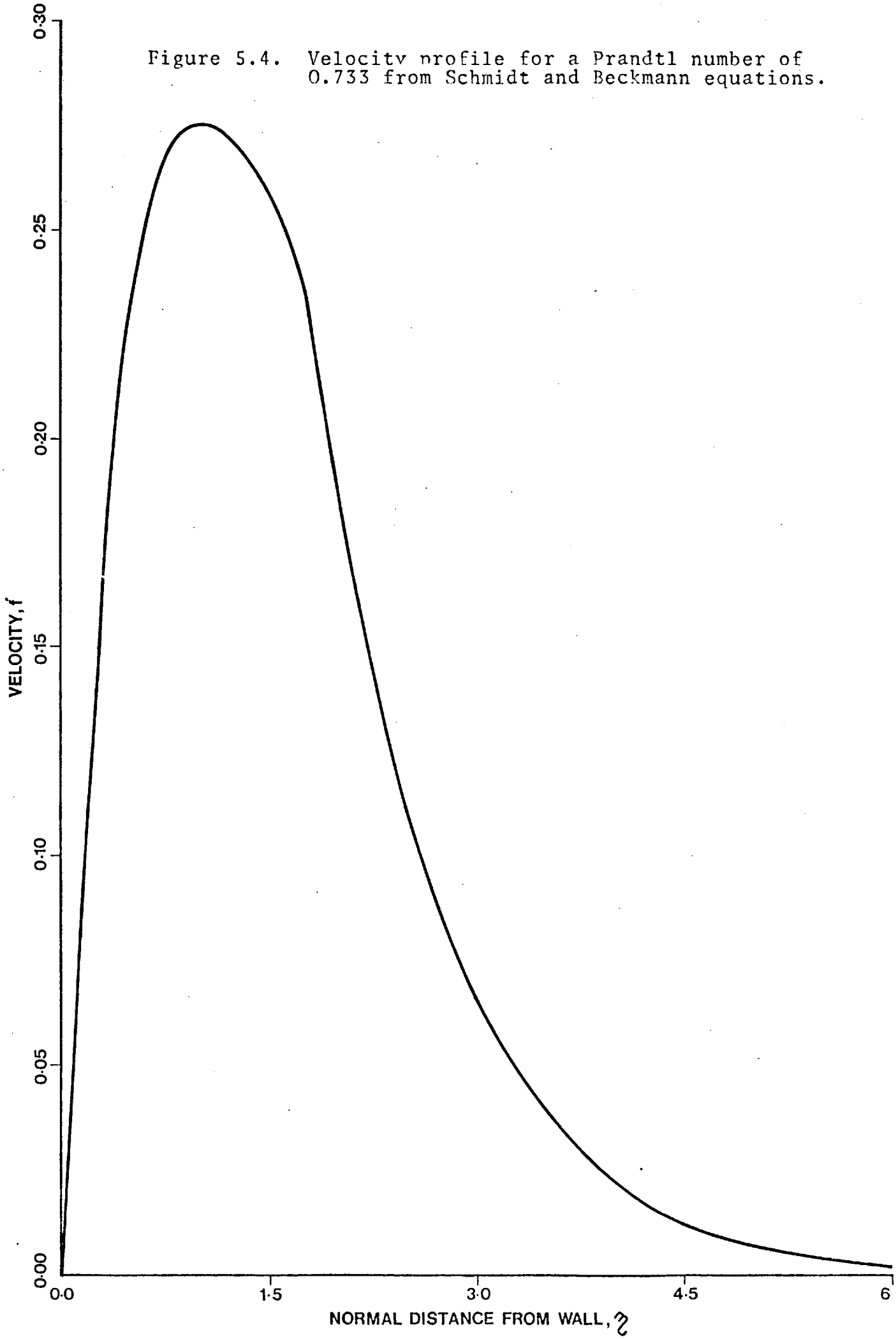

Eigenfunctions for air, Prandtl number of 0.733

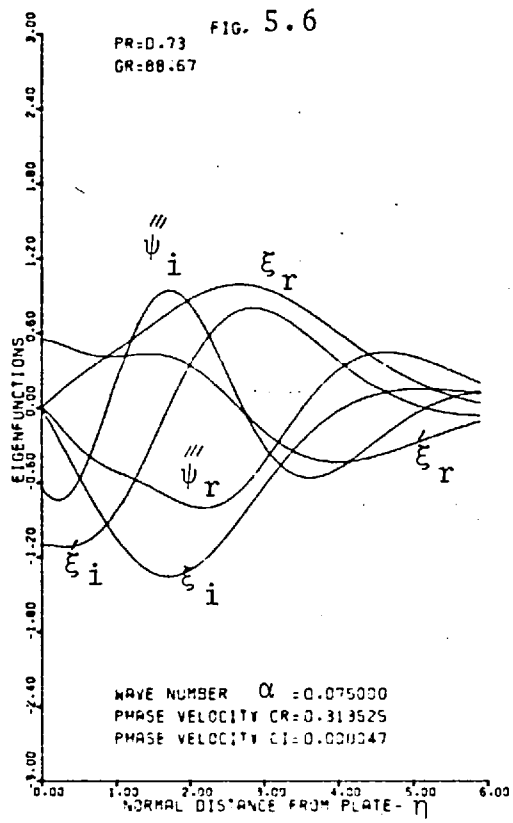

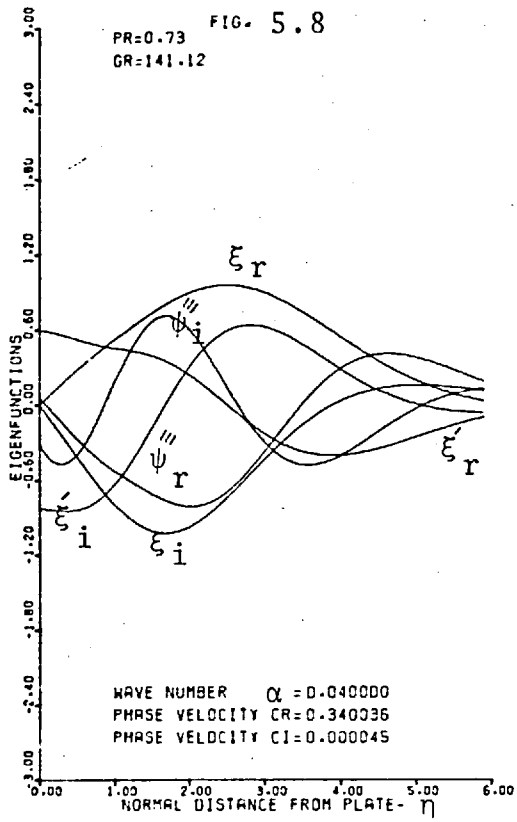

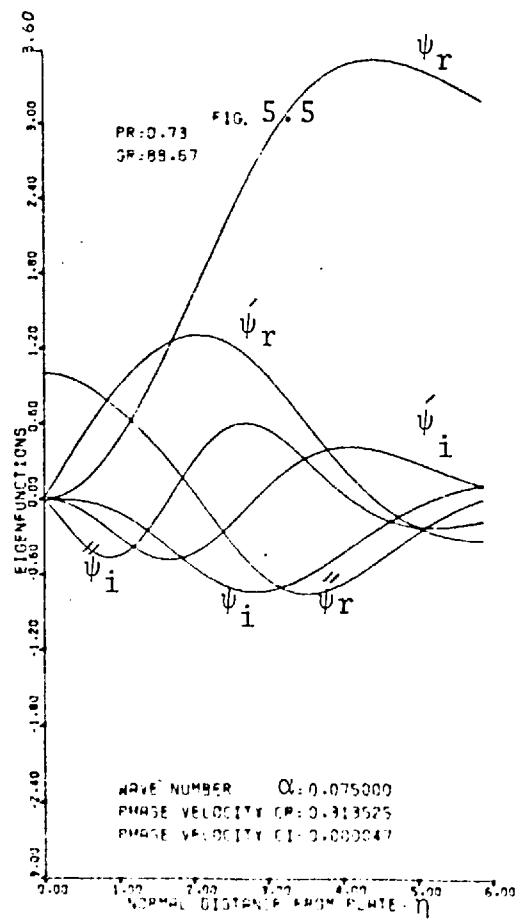

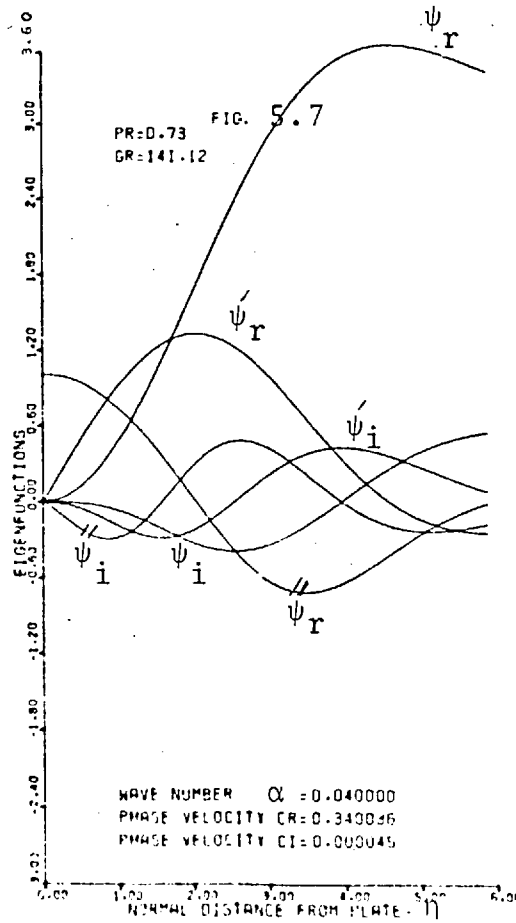

Eigenfunctions for air, Prandtl number of 0.733.

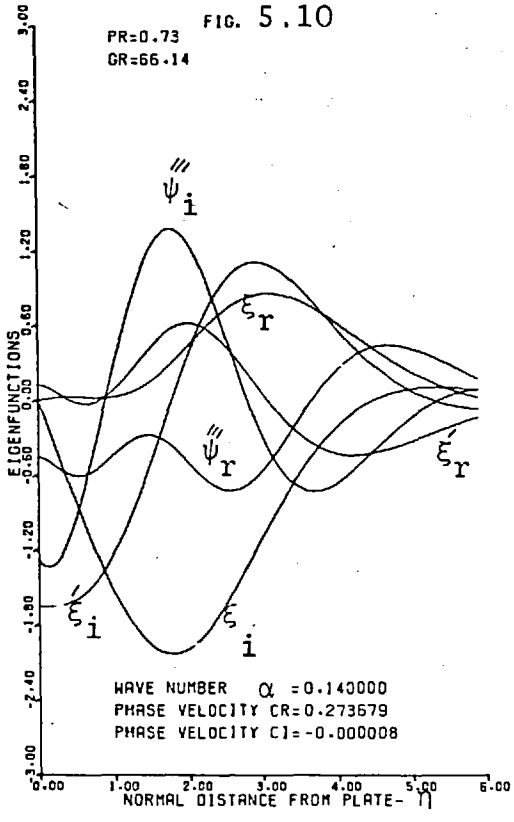

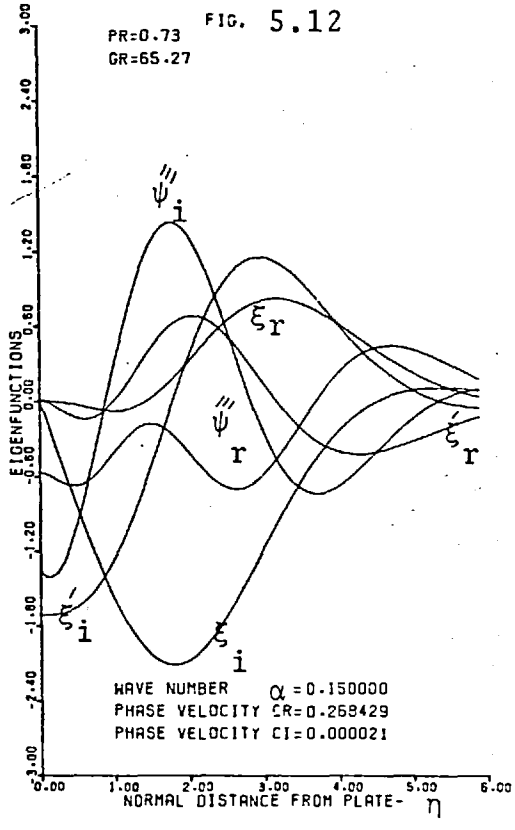

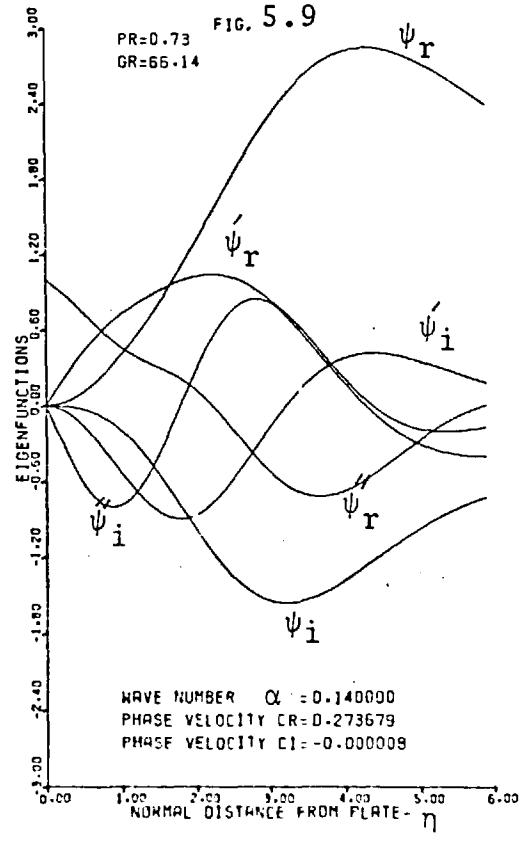

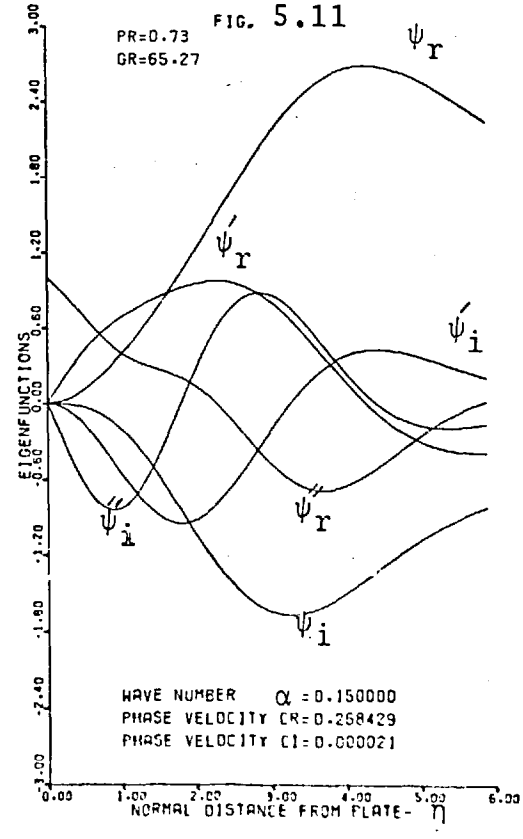

Eigenfunctions for air, Prandtl number of 0.733.

FIG. 5.14

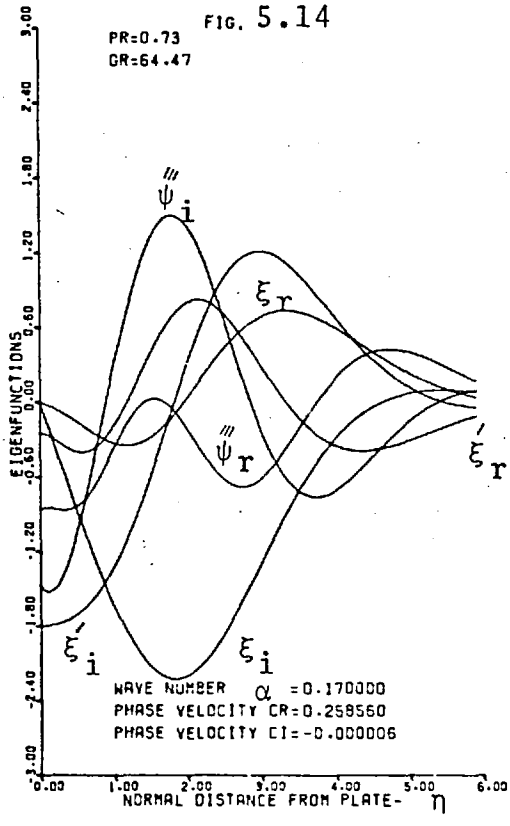

FIG. 5.16

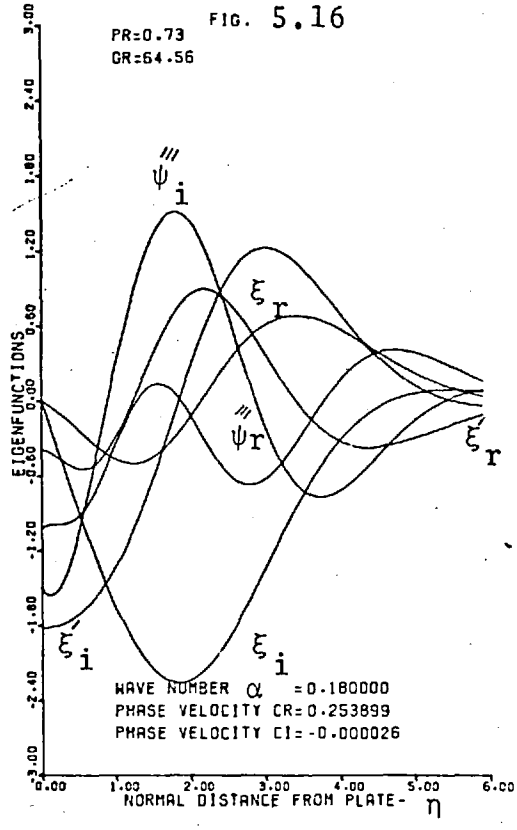

FIG. 5.13

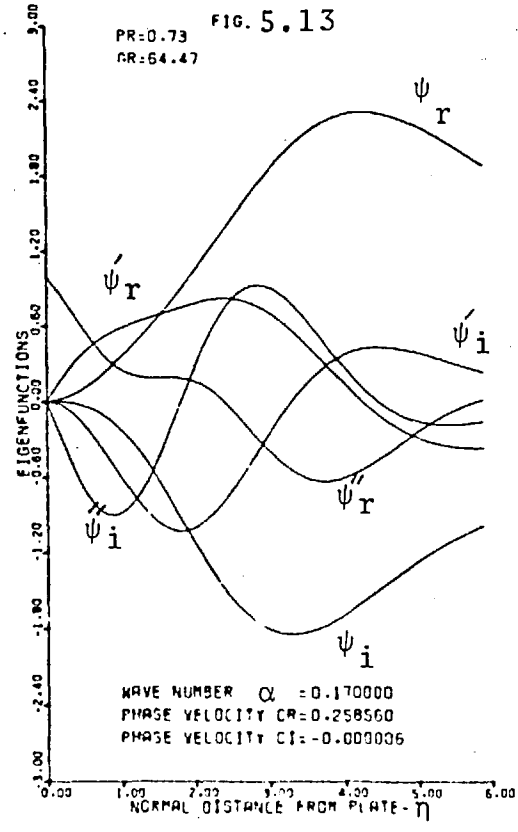

FIG. 5.15

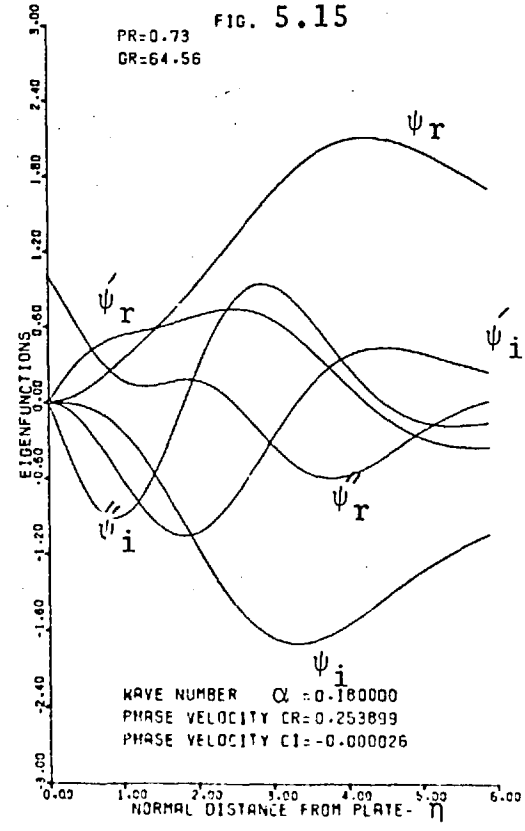

Eigenfunctions for air, Prandtl number of 0.733.

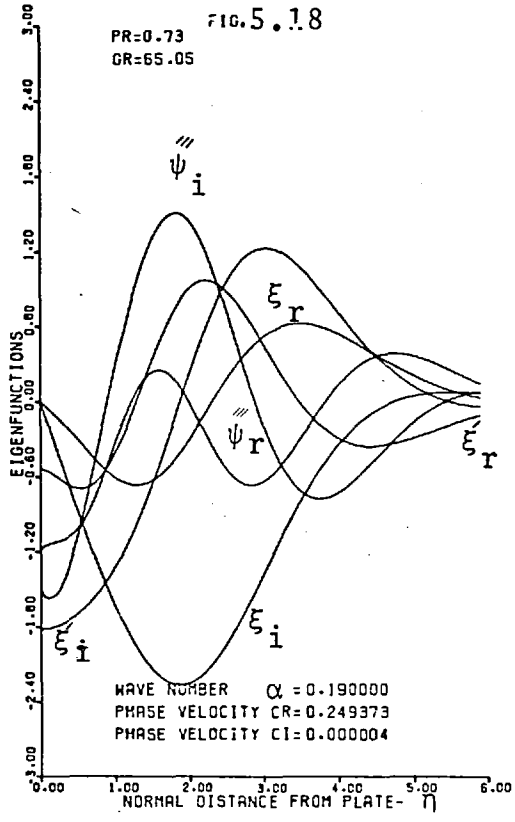

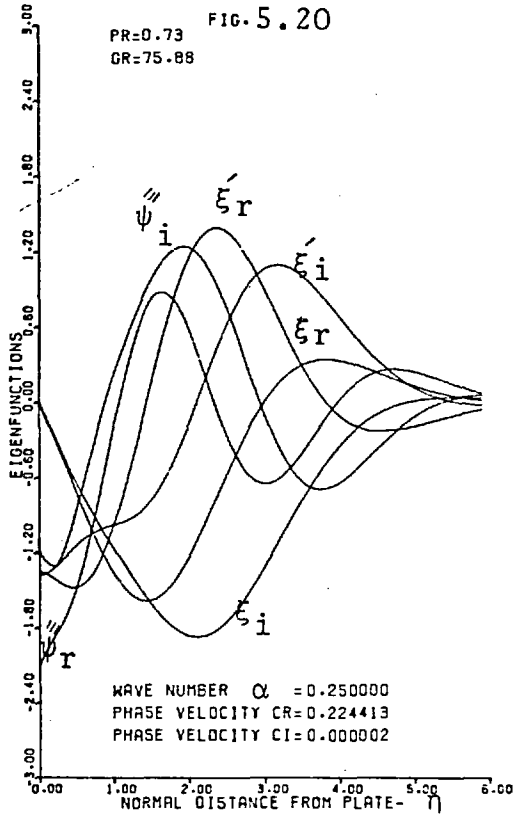

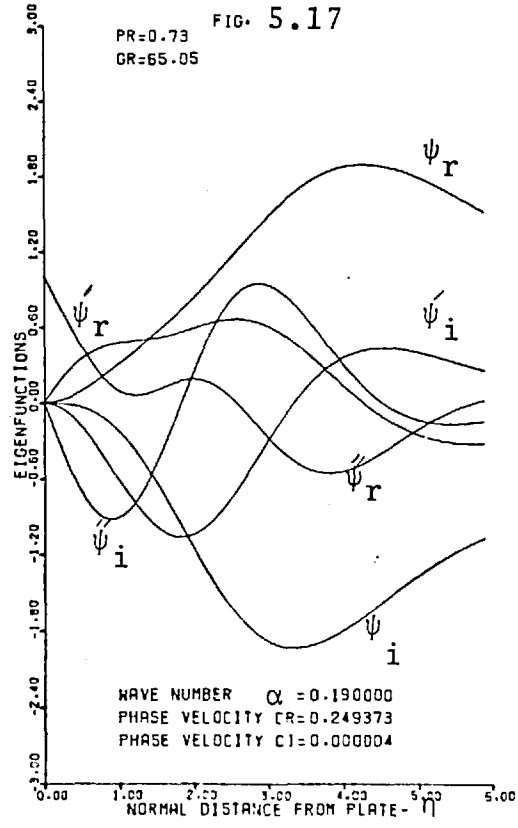

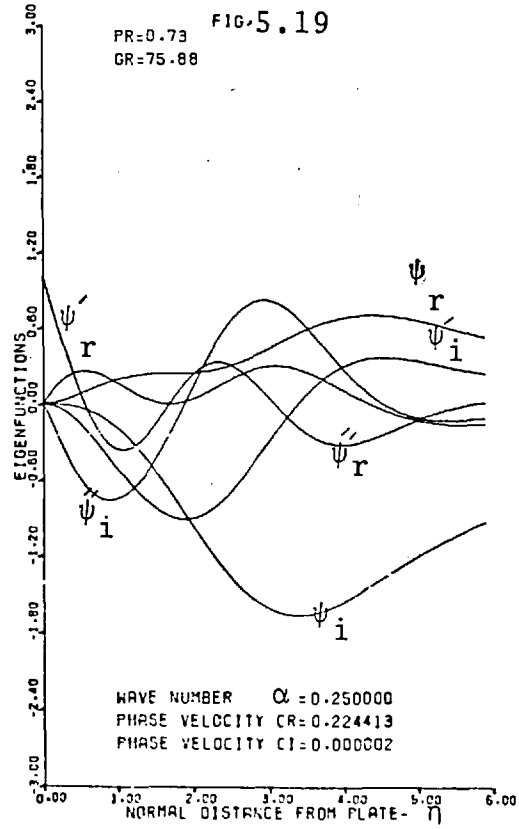

Eigenfunctions for air, Prandtl number of 0.733.

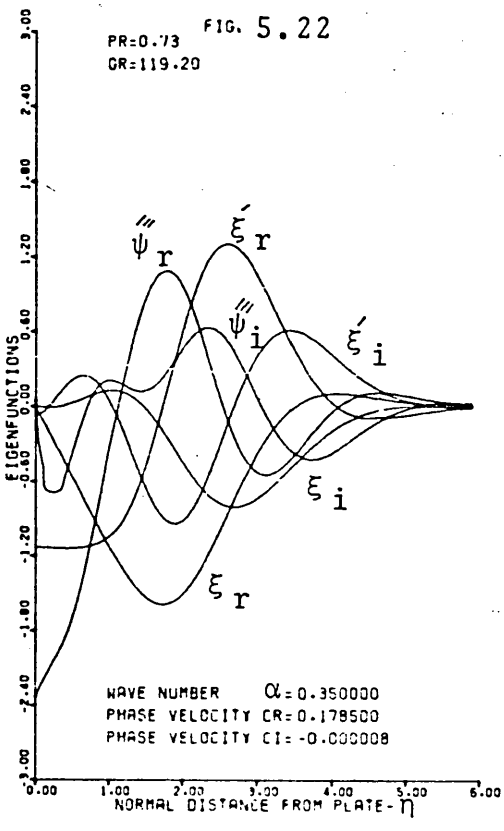

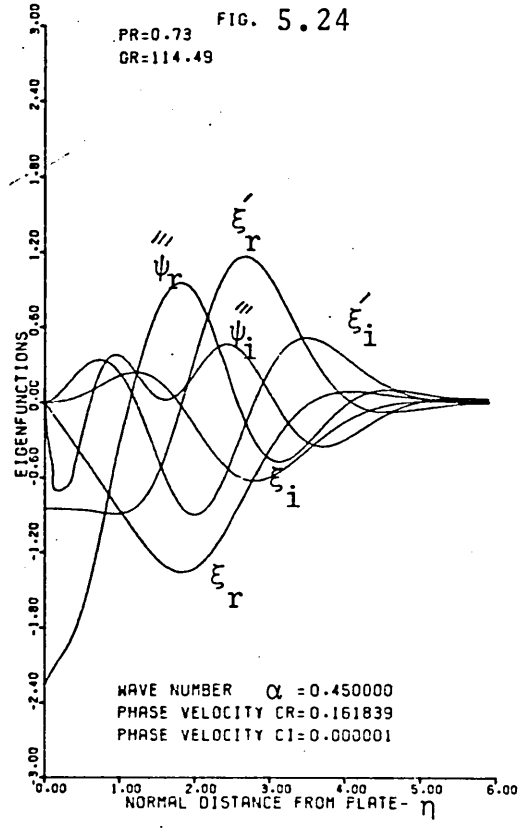

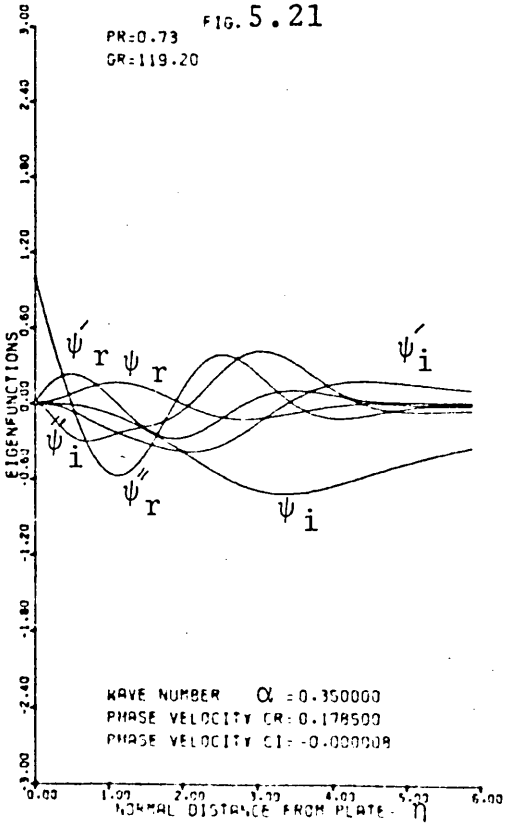

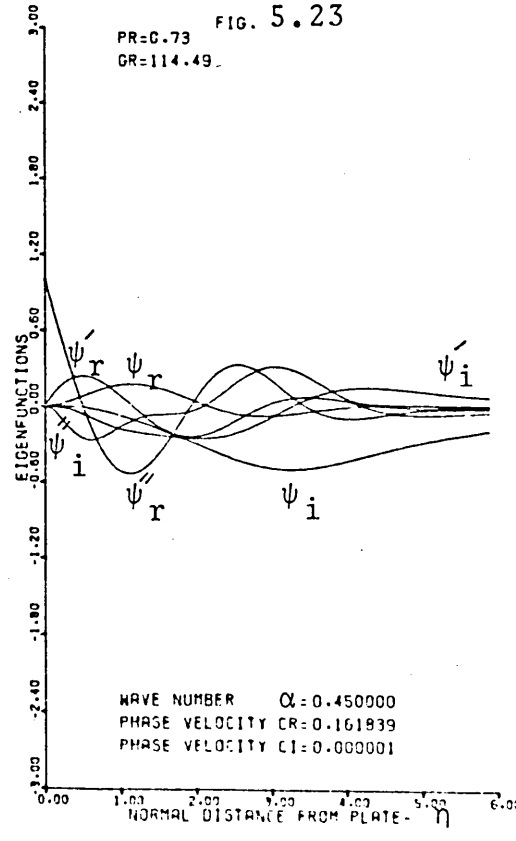

Eigenfunctions for air, Prandtl number of 0.733.

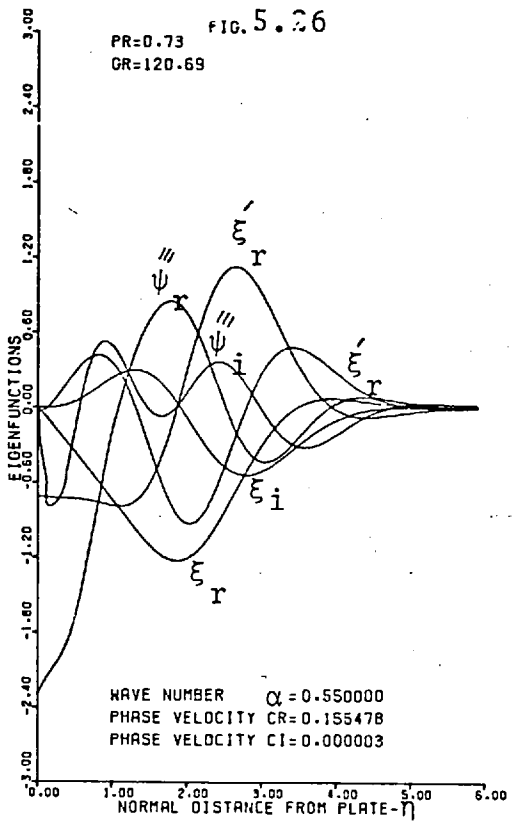

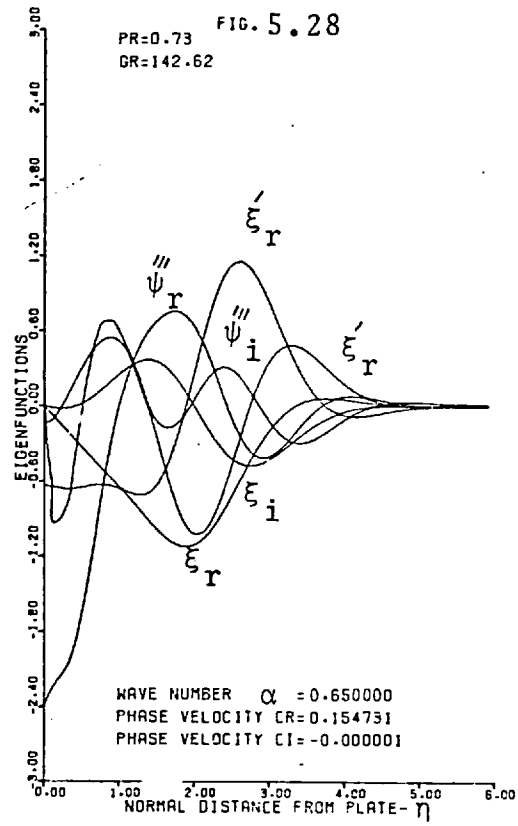

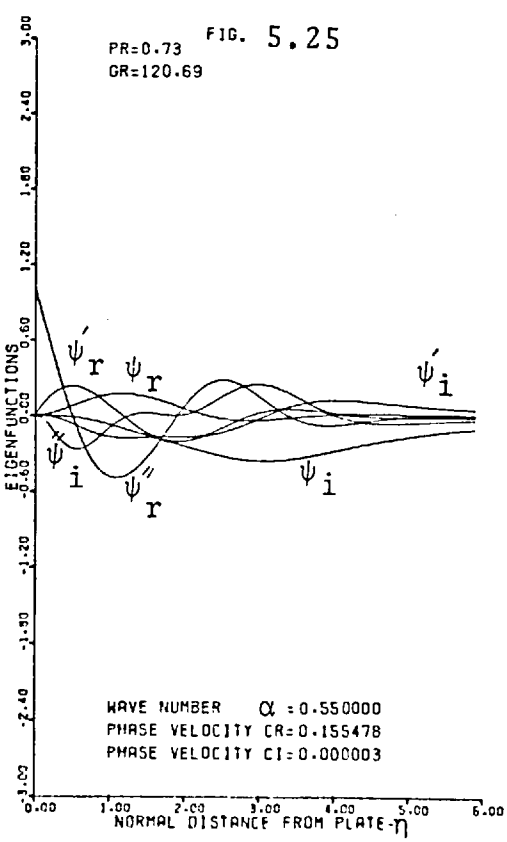

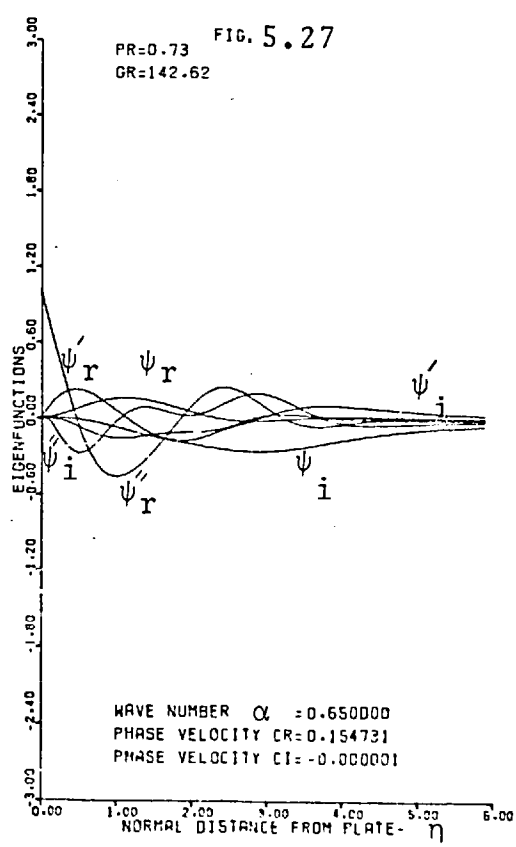

Eigenfunctions for air, Prandtl number of 0.733.

FIG. 5.30

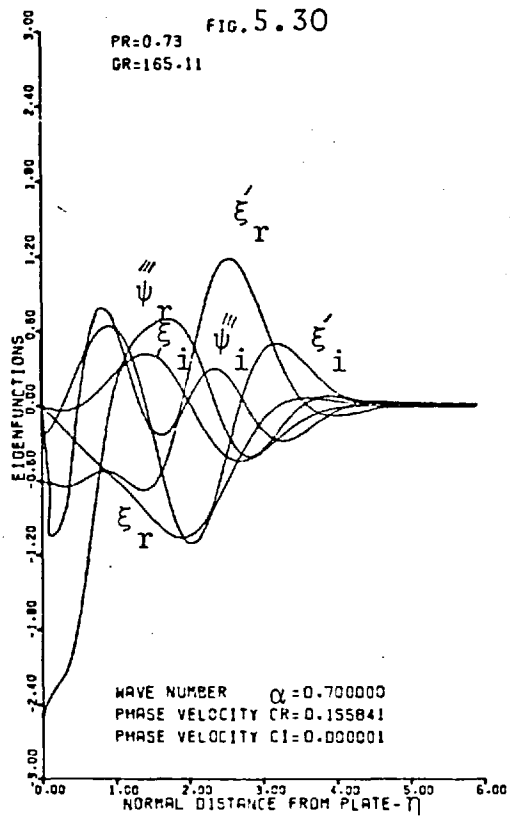

FIG. 5.32

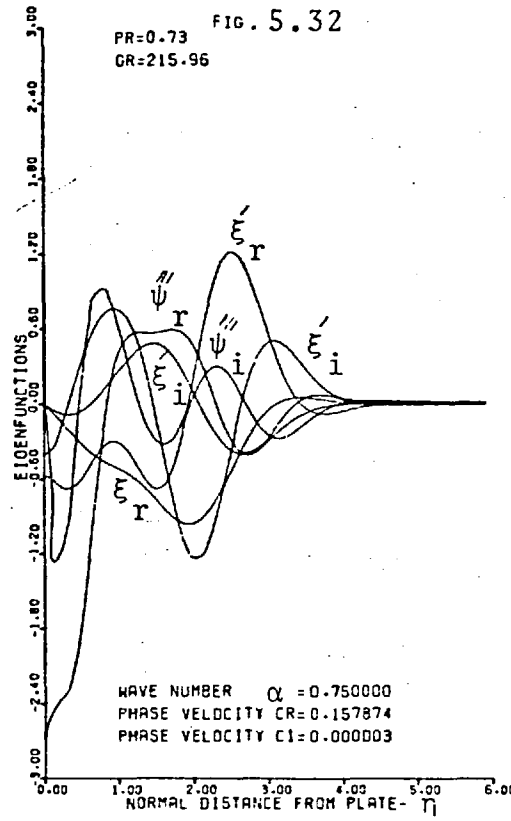

FIG. 5.29

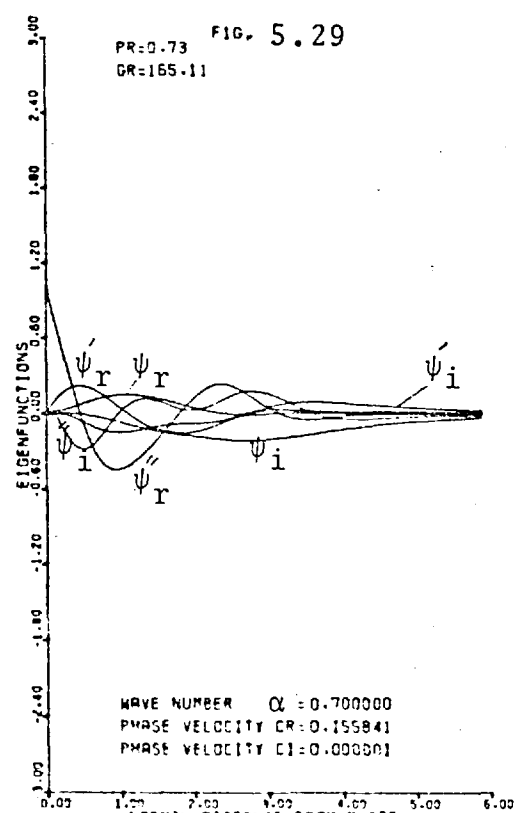

FIG. 5.31

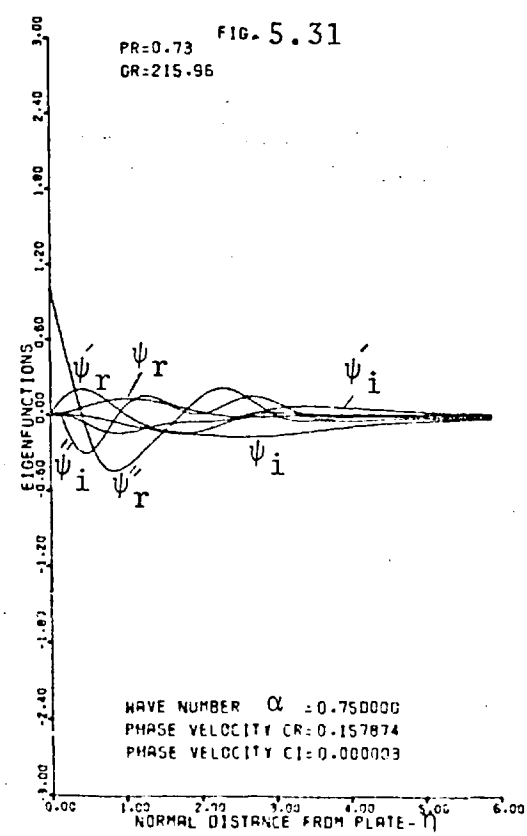

Eigenfunctions for air, Prandtl number of 0.733.

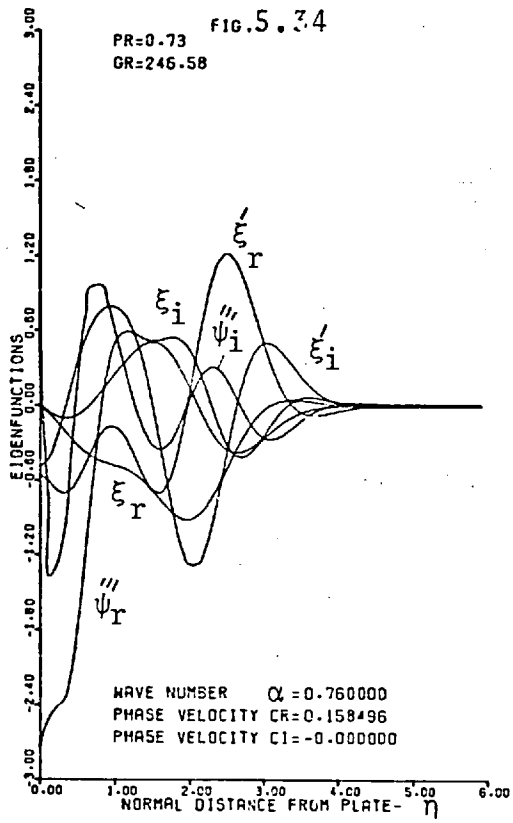

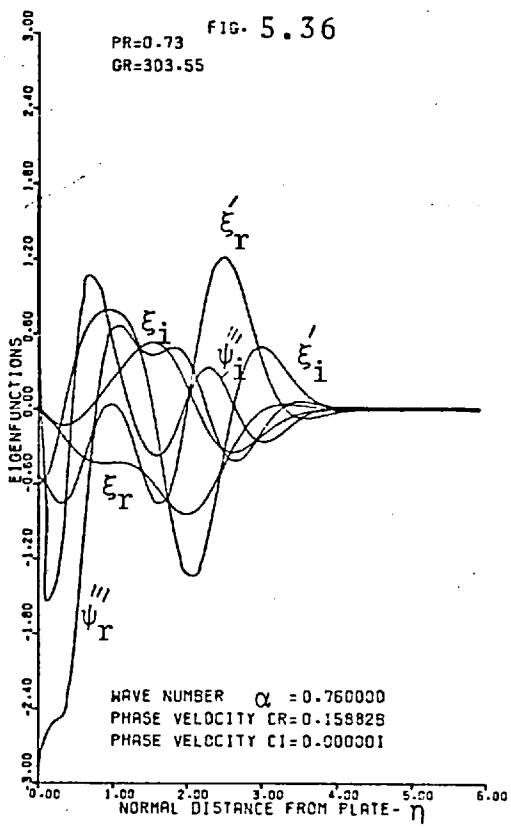

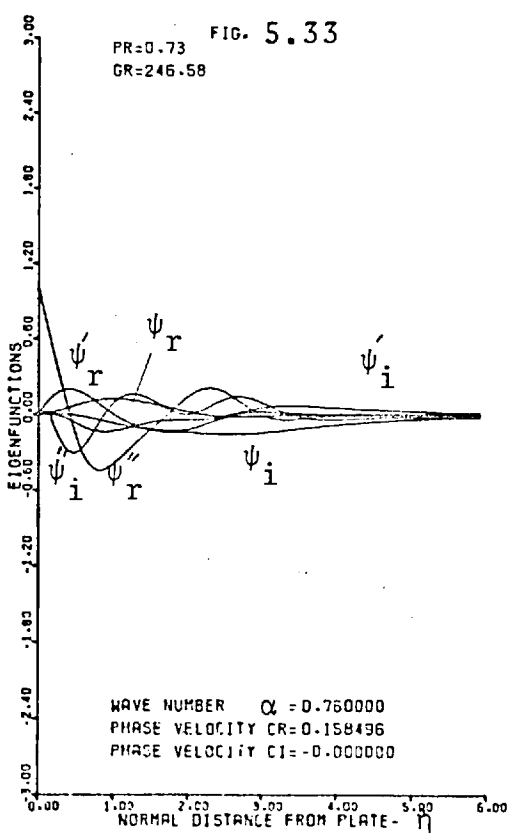

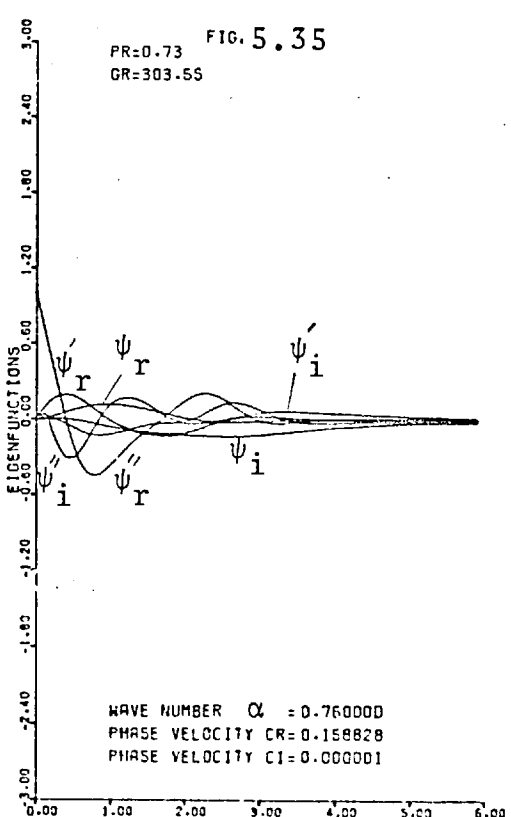

values of the wave number, α, the wave caused by the imposition of perturbations is not confined to the boundary layer, $\eta<\eta_{edg}$, but extends into the stationary region with a slow exponential decrease in amplitude with distance. As the wave number, α, becomes larger, the wave becomes confined to the boundary layer. It is of interest to note that for $\alpha>0.35$ the plots of the eigenfunctions are similar to those which were obtained by Nachtsheim [11] for the case when the effect of temperature fluctuations was not included. For a justification of these results the energy distribution curves will be examined. Before this examination is made, it should be recalled that two basically different kinds of instability arise in free-convection boundary layer flows. One kind results from the tendency for motion to occur in a stratified medium when a heavier fluid overlays a lighter fluid [6]. This type of instability is called "thermal instability". The other kind of instability is related to the shearing motion of the basic laminar flow and to the existence of a mechanism for transferring energy from the basic laminar flow to the disturbed motion via the Reynolds stress [11]. This is called "hydrodynamic instability".

Figures 5.37 to 5.52 show the energy distributions [see section (4.6)] for a Prandtl number of 0.733 for the neutral stability curve. Examination of the energy distributions for a small wave number of 0.04, figure 5.38, shows that the buoyancy term in the energy balance of the disturbed motion is very important because it is the only term which gives a positive contribution to the energy of the disturbed motion

Energy distributions for air, Prandtl number of 0.733.
e_{Re} = Reynolds stress e_D = Dissipation e_B = Buoyancy

FIG. 5.38

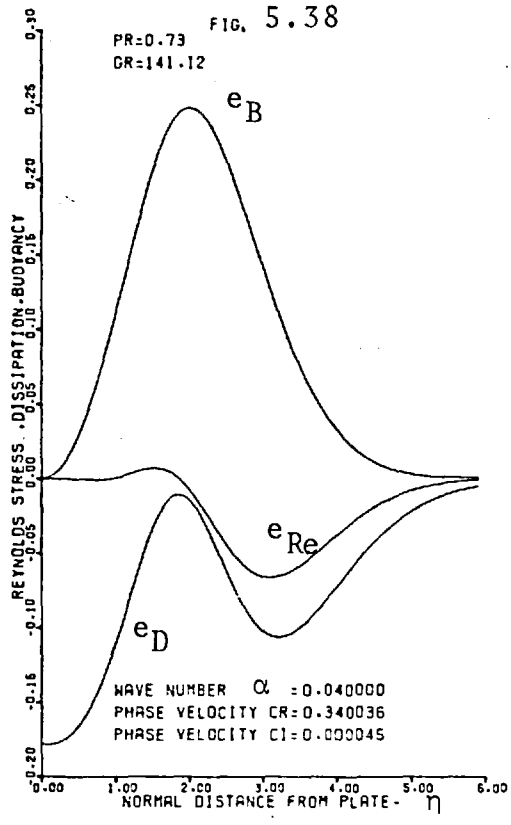

FIG. 5.40

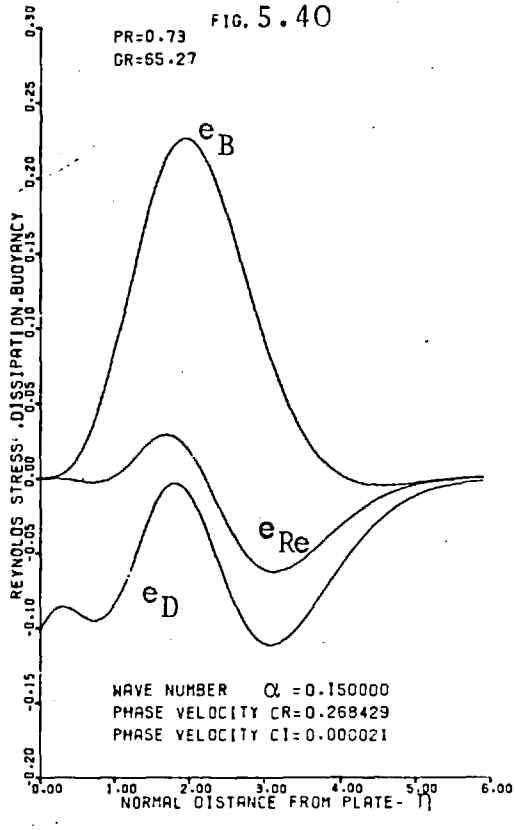

FIG. 5.37

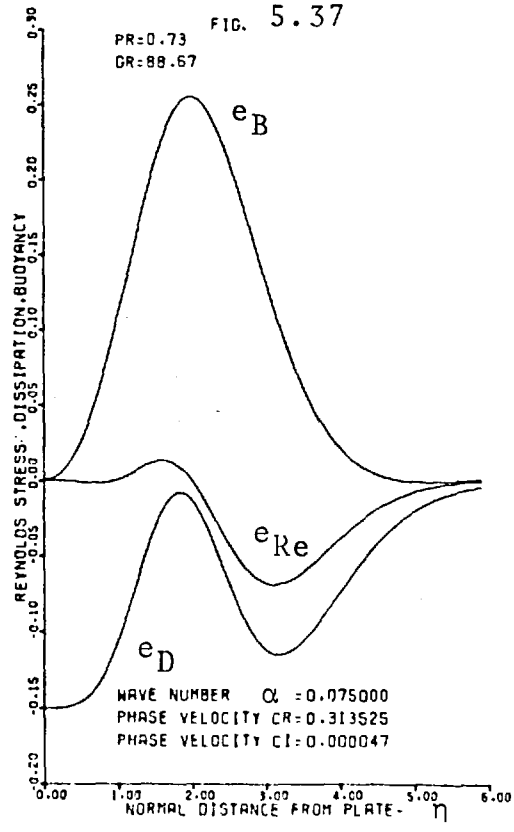

FIG. 5.39

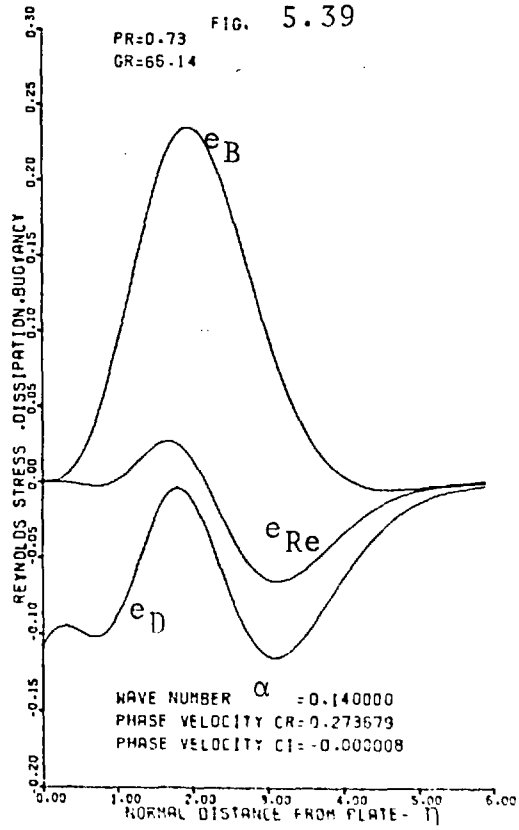

Energy distributions for air, Prandtl number of 0.733.
e_{Re}= Reynolds stress e_D = Dissipation e_B = Buoyancy

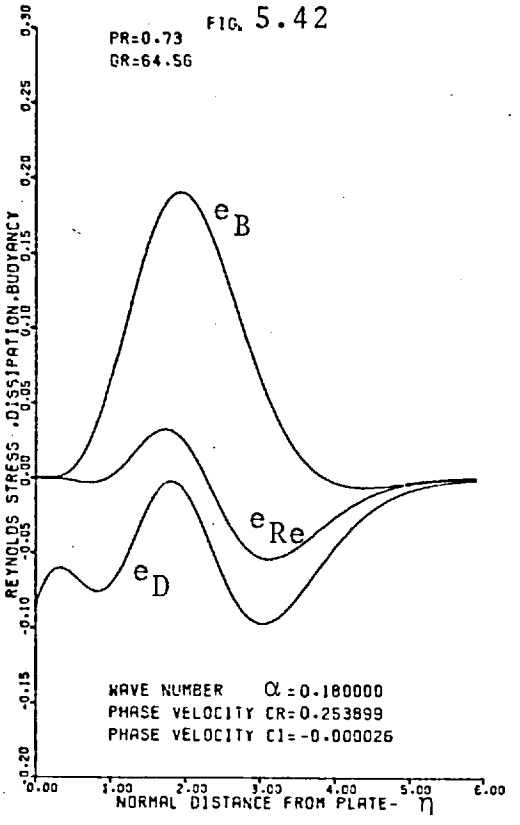

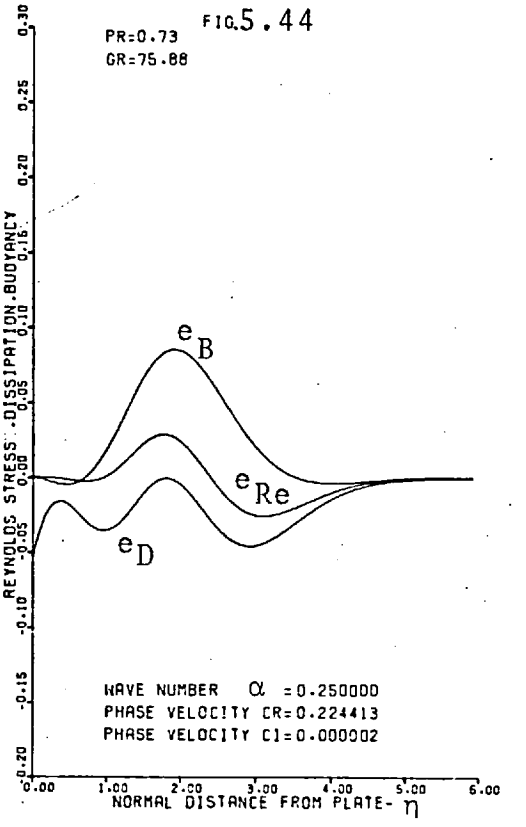

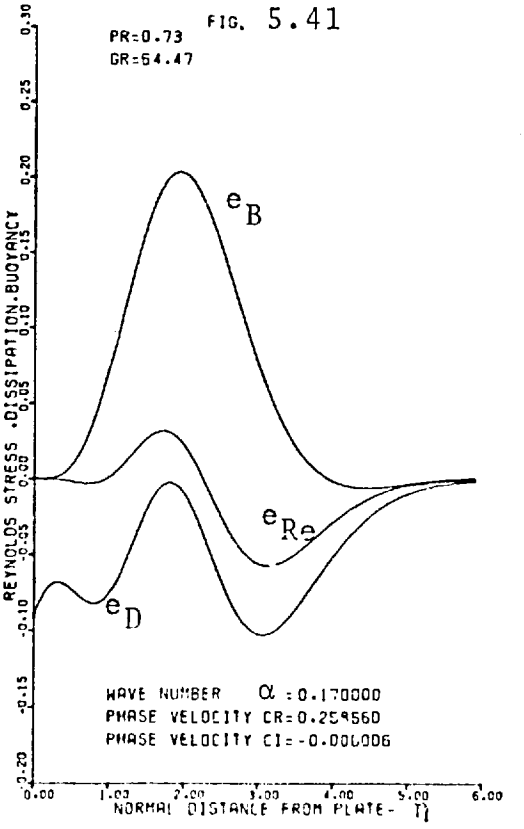

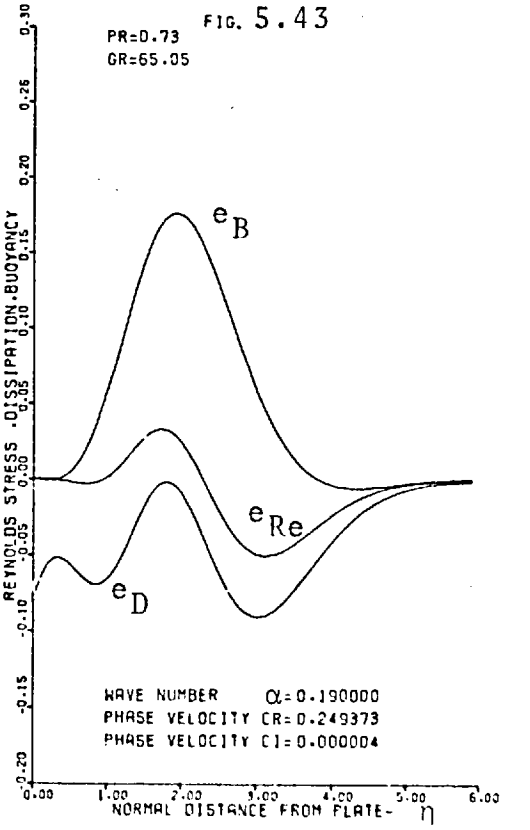

Energy distributions for air, Prandtl number of 0.733.
e_{Re} = Reynolds stress e_D = Dissipation e_B = Buoyancy

FIG. 5.46

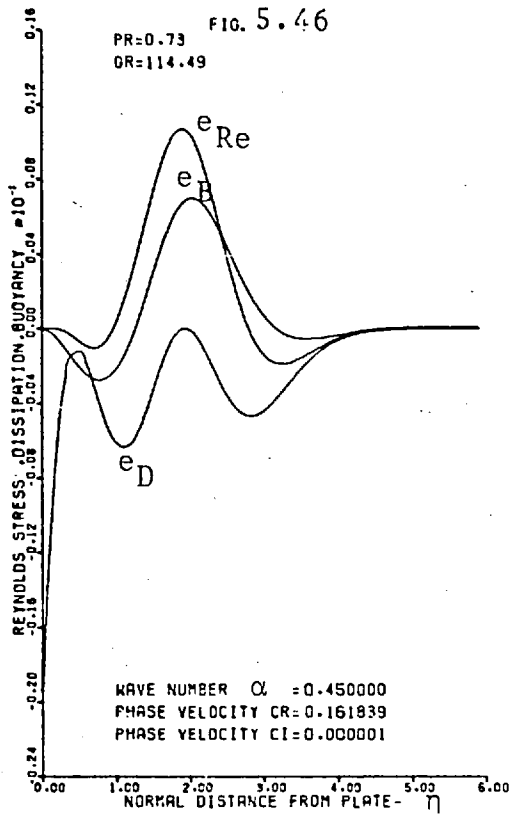

FIG. 5.48

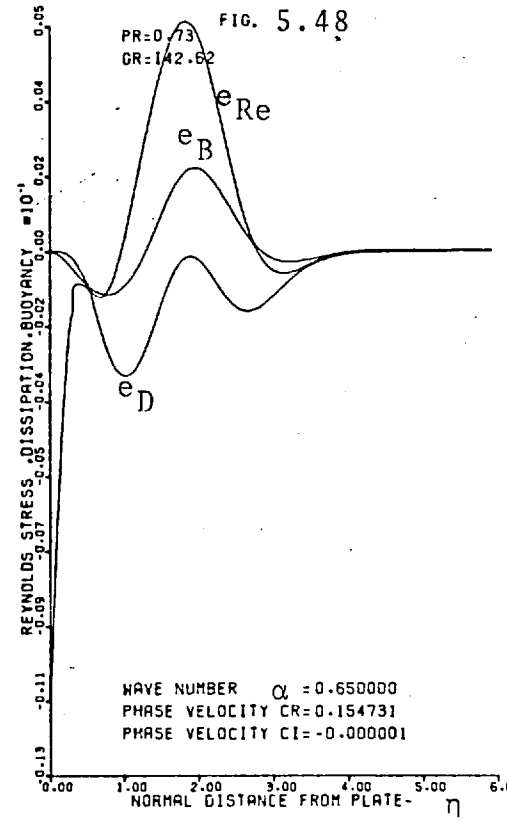

FIG. 5.45

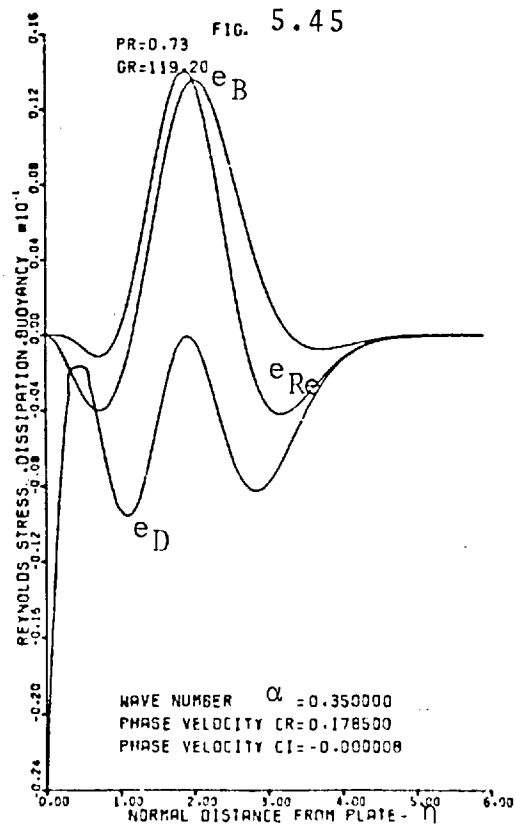

FIG. 5.47

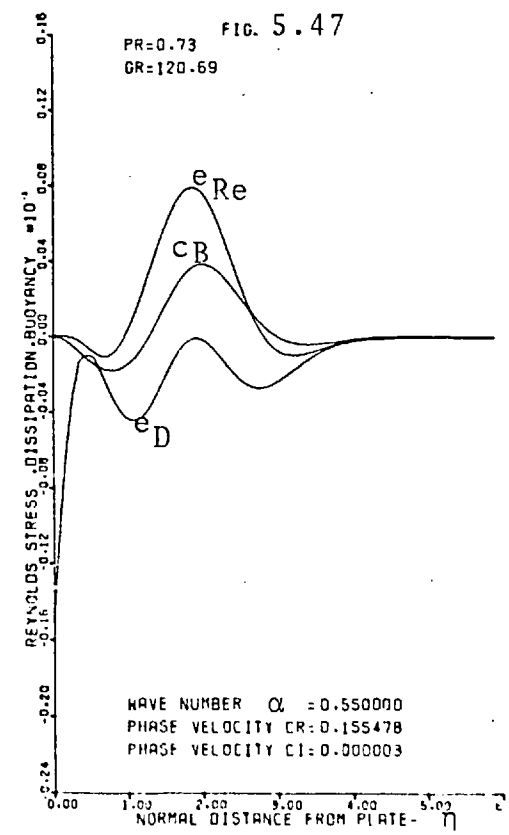

Energy distribution for air, Prandtl number of 0.733.
e_{Re} = Reynolds stress e_D = Dissipation e_B = Buoyancy

FIG. 5.50

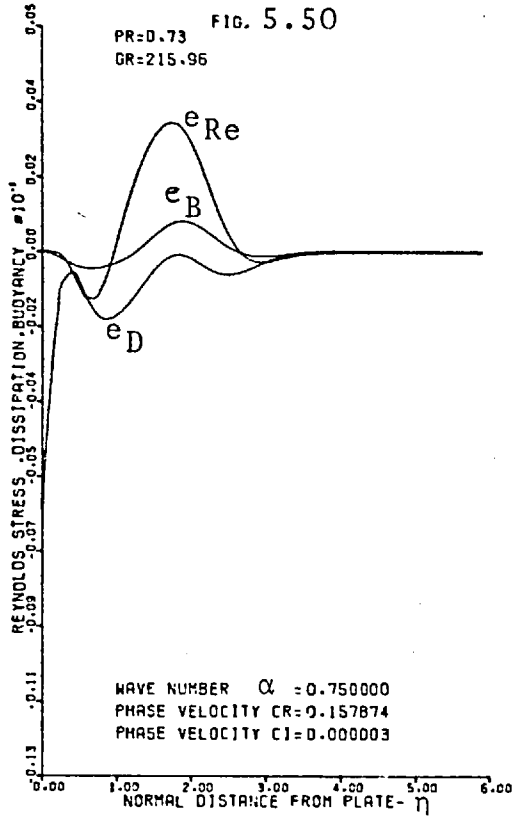

FIG. 5.52

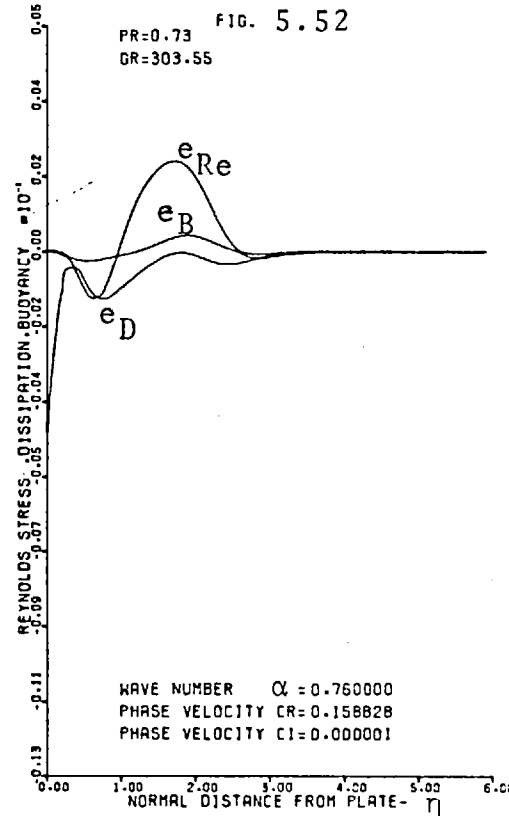

FIG. 5.49

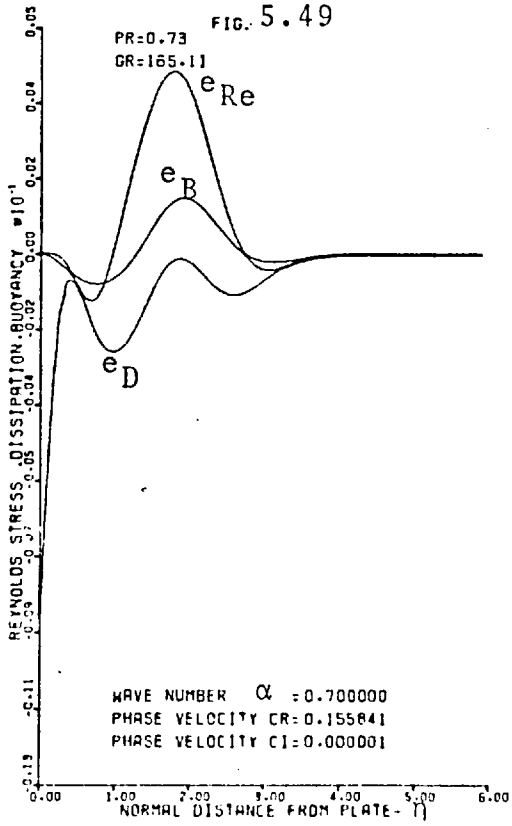

FIG. 5.51

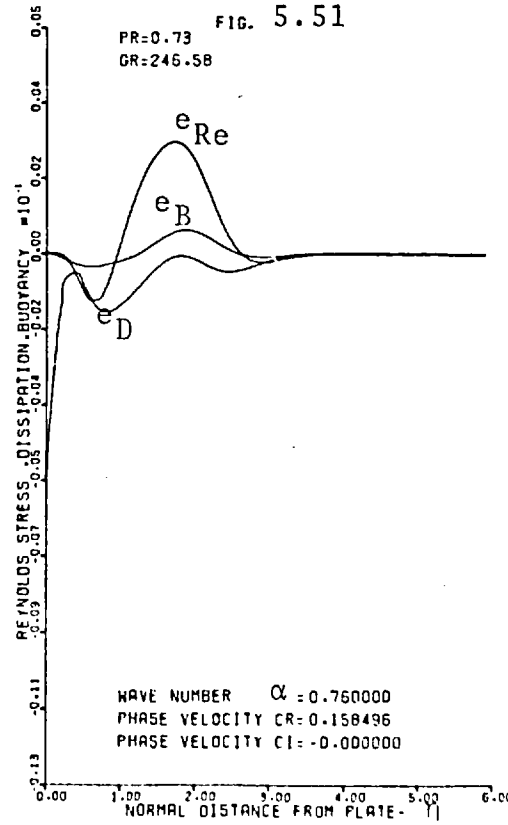

whereas the Reynolds stress term is actually subtracting energy. Figure 5.45 shows that at an increased wave number of 0.35 both the buoyancy term and the Reynolds stress term give positive contributions to the energy of the disturbed motion and only the dissipation term subtracts energy from it. From figures 5.51 and 5.52, it can be seen that for a large wave number of 0.76, the positive energy is contributed mostly by the Reynolds stress term. It can be concluded that since the buoyancy term becomes unimportant at large wave numbers the neglect of the temperature fluctuations for the purpose of solving the disturbance equations could be a good assumption for values of the wave number, α, greater than 0.7. For moderate values of the wave number, $0.35<\alpha<0.70$, figures 5.45 to 5.49 show that the neglect of the temperature fluctuations may be justified. However, for values of the wave number less than 0.35 the temperature fluctuations introduce instability and the buoyancy force plays a dominant role in the instability of the flow.

The above mentioned conclusion is also supported by an examination of the neutral stability curves obtained with and without the inclusion of the effects of temperature fluctuations. Figure 5.53 shows a comparison of the neutral stability curve obtained when temperature fluctuations are included, as in the present study for a Prandtl number of 0.733, with the neutral stability curves obtained when temperature fluctuations are not included. It can be seen that at low wave numbers, $\alpha<0.35$, the results with temperature fluctuations are distinctively different from the results without temperature fluctuations. At higher wave numbers,

Figure 5.53. A comparison between the neutral stability curve of the present work with that without temperature fluctuations for a Prandtl number of 0.733.

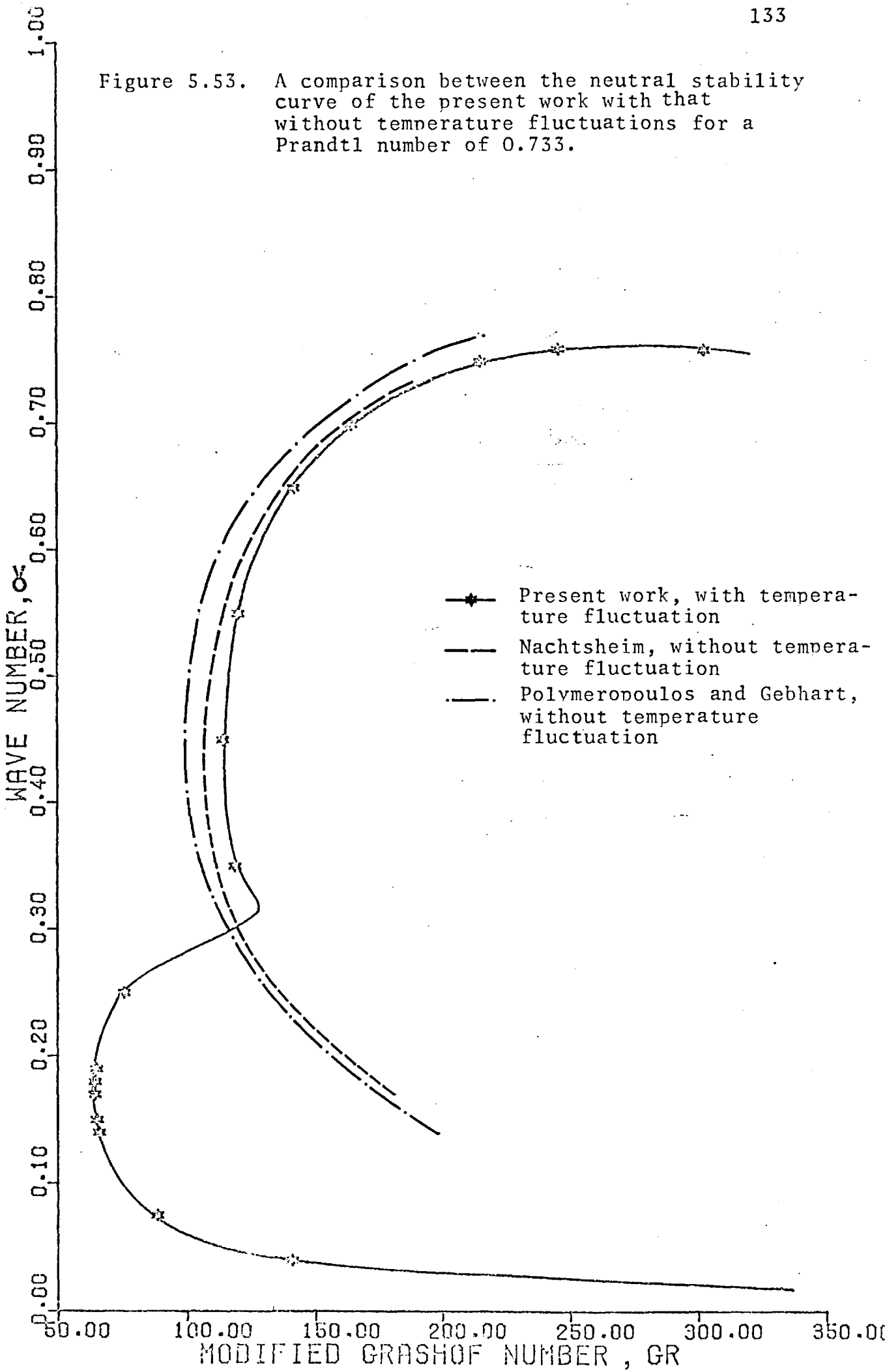

$\alpha>0.35$, the curve with temperature fluctuation resembles the curve without temperature fluctuations.

Figure 5.54 shows the neutral stability curve for a Prandtl number of 1.0 drawn in the wave number, Grashof number-plane (α, Gr-plane). The minimum critical value of the Grashof number is located at a Grashof number of 61.0. The detailed solutions for the neutral curve for a Prandtl number of 1.0 are tabulated in Table F.4.(b). It can be seen that the closest calculated point to the minimum critical Grashof number is at a Grashof number of 61.35, and at a wave number of 0.14 with a phase velocity of 0.26661.

Figure 5.55 shows the neutral stability curve for a Prandtl number of 1.0 in the phase velocity, Grashof number-plane (c_r, Gr-plane). A comparison of this figure with figure 5.56 reveals that for values of α less than 0.16, the phase velocity of disturbance wave, c_r, is greater than the maximum velocity of the basic flow, hence, there are no critical layers.

Figures 5.57 to 5.76 and 5.77 to 5.86 show the solutions of the disturbance equations and the energy distributions, respectively, for a Prandtl number of 1.0. The discussion of these figures is exactly similar to that for a Prandtl number of 0.733. Examination of the energy distributions for values of the wave number less than 0.35, figures 5.77 to 5.80, shows that the buoyancy term in the energy balance of the disturbed motion is the only term which gives a positive contribution to the energy of the disturbed motion. Figure 5.81 shows that for a wave number of 0.35 both the buoyancy term and the Reynolds stress give positive contributions to

Figure 5.54. Neutral stability curve for a Prandtl number of 1.0 in α, Gr-plane

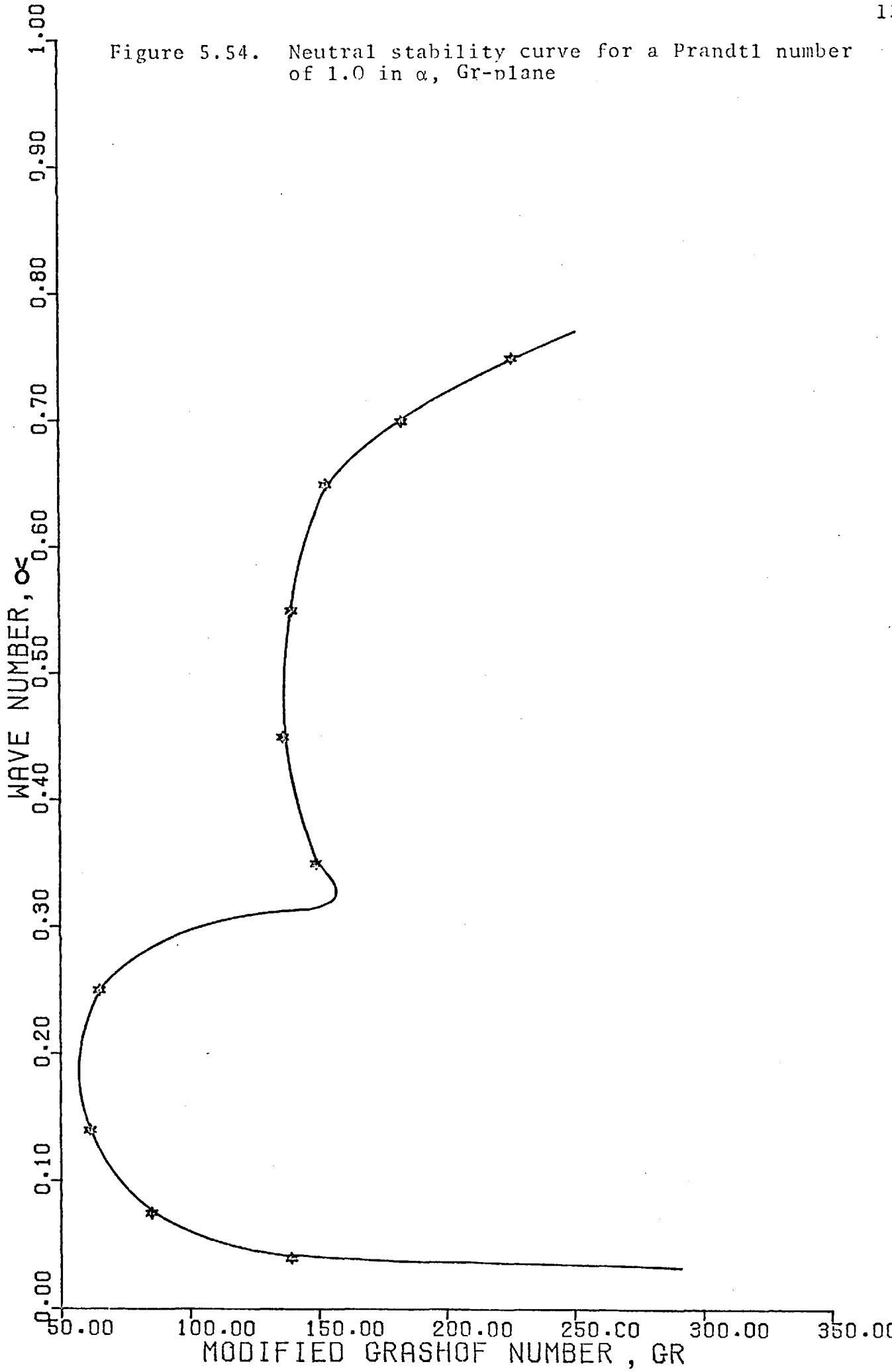

Figure 5.55 - Neutral stability curve for a Prandtl number of 1.0 in c_r, Gr-plane.

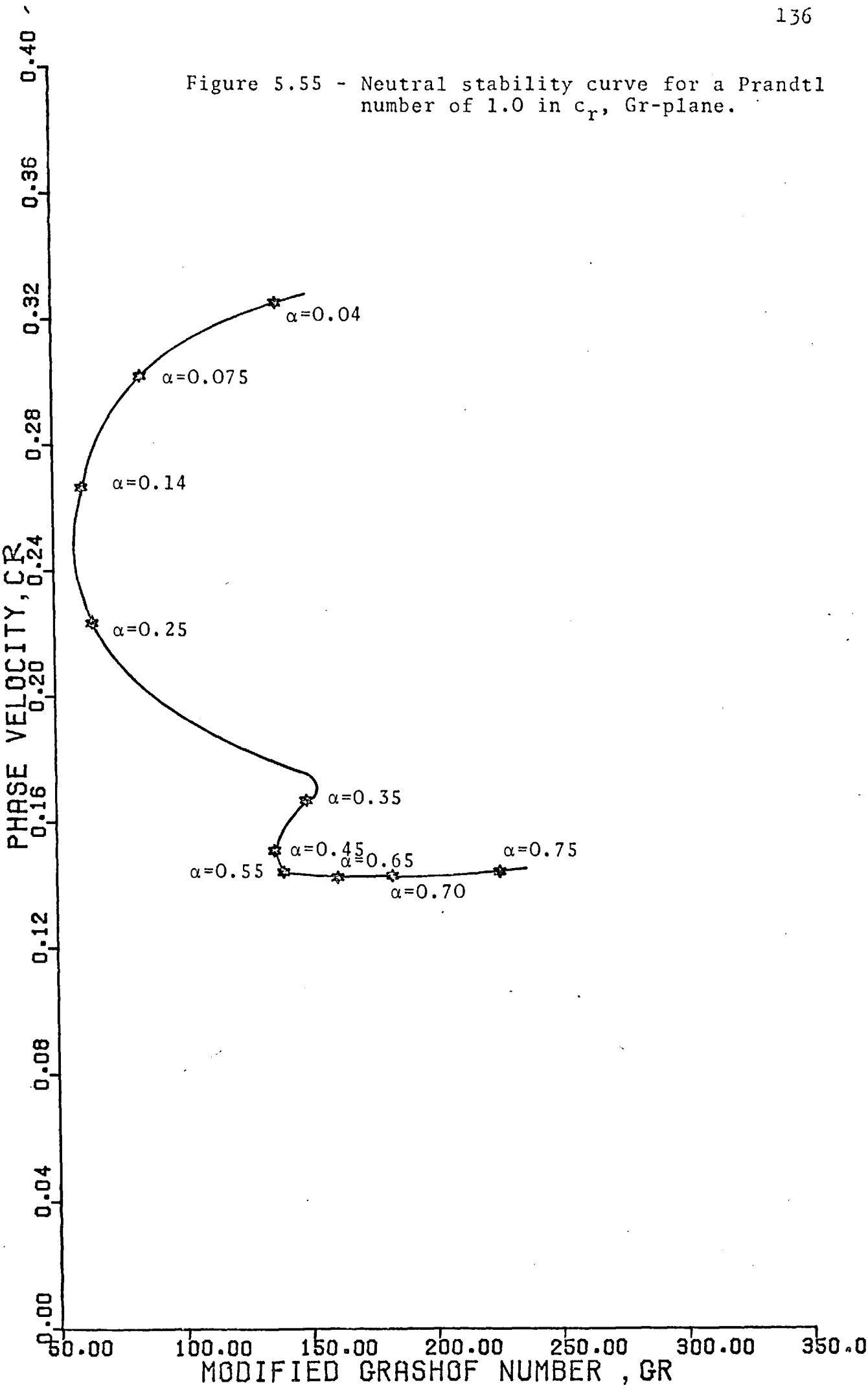

Figure 5.56. Velocity profile for a Prandtl number of 1.0 from Schmidt and Beckmann equations.

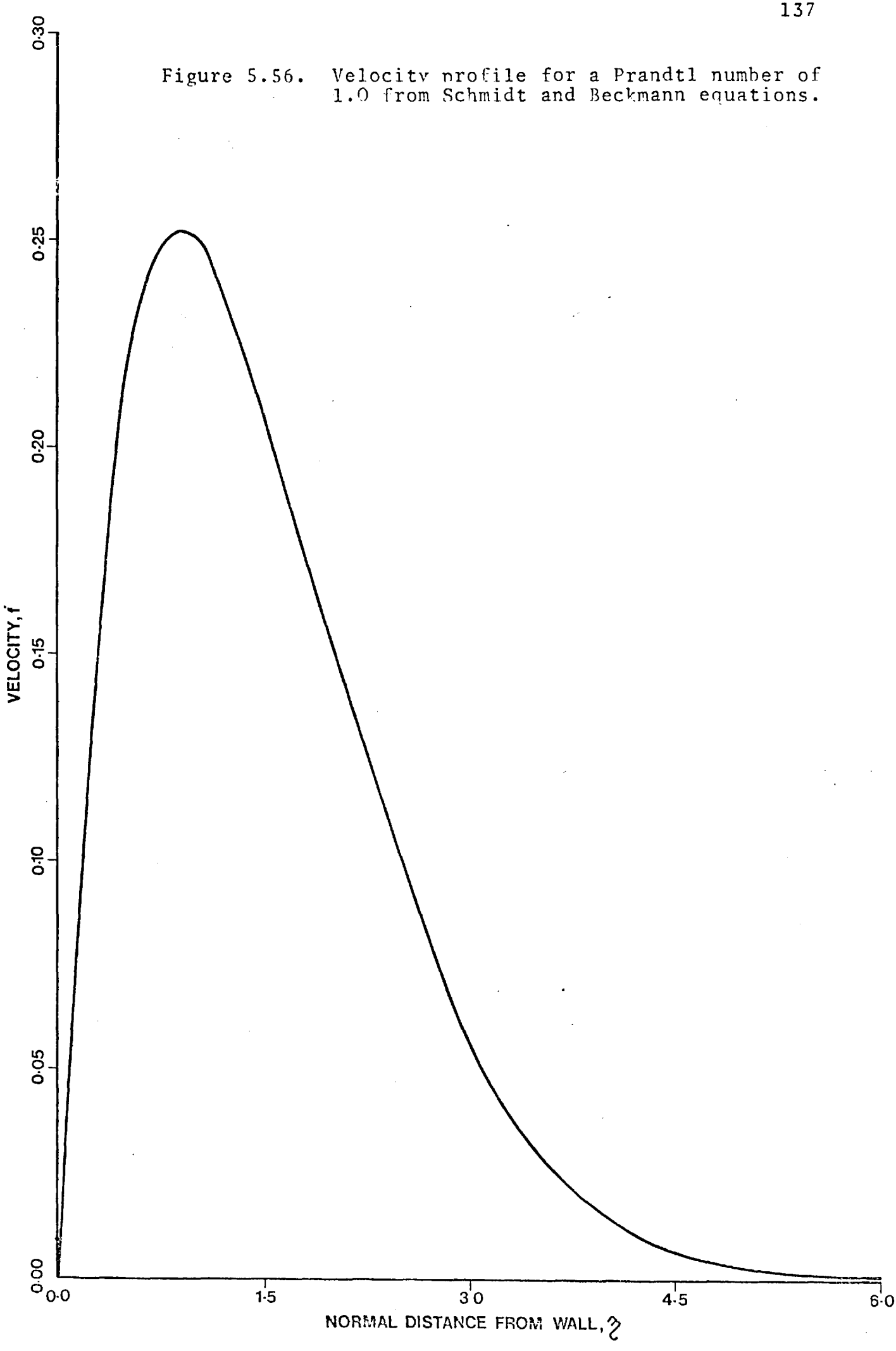

Eigenfunctions for a Prandtl number of 1.0.

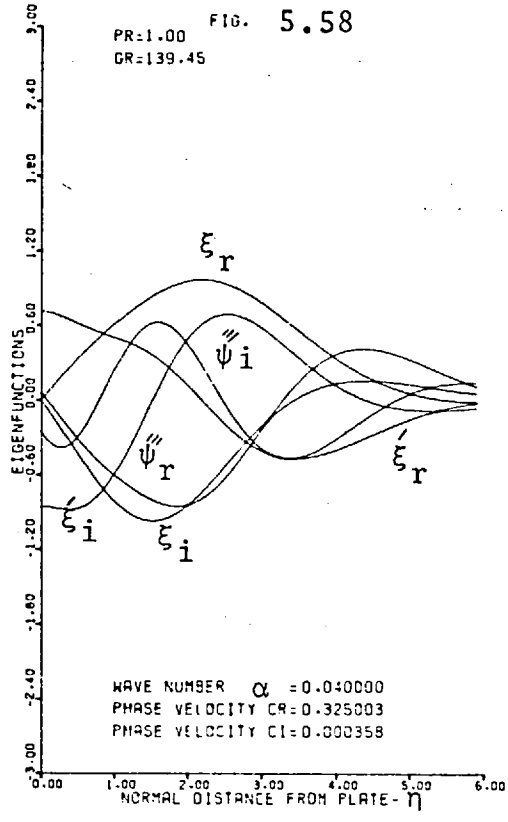

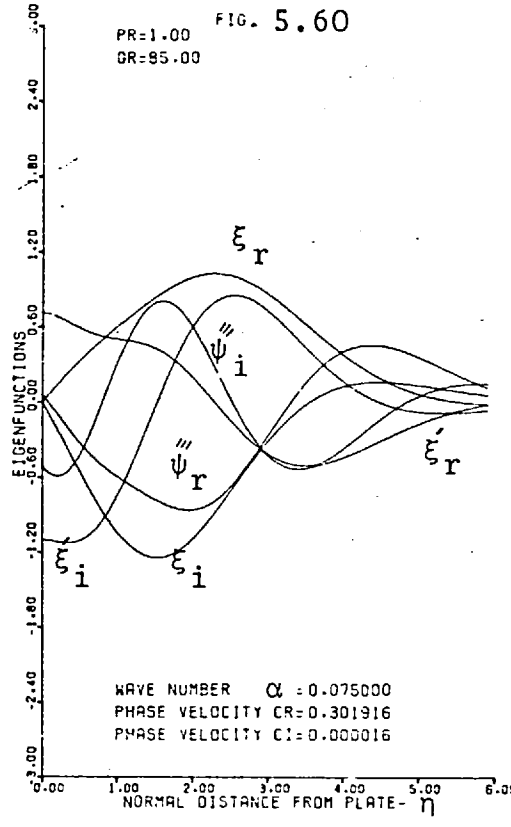

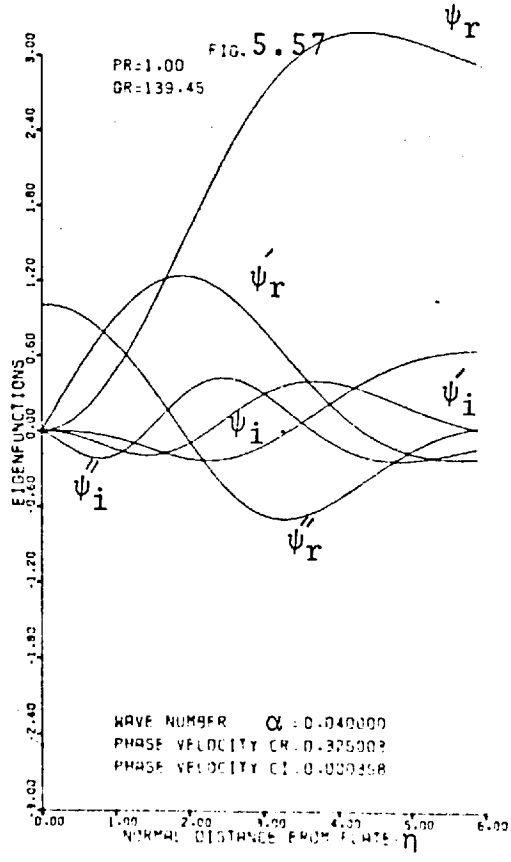

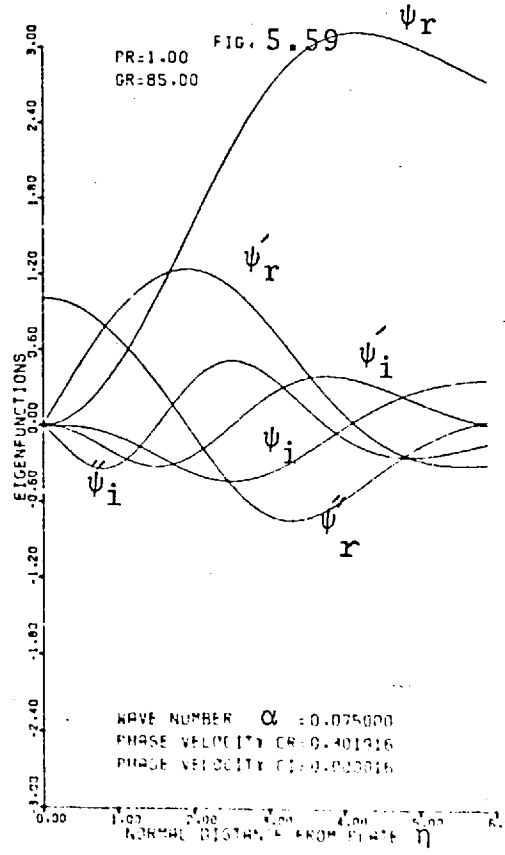

Eigenfunction for a Prandtl number of 1.0.

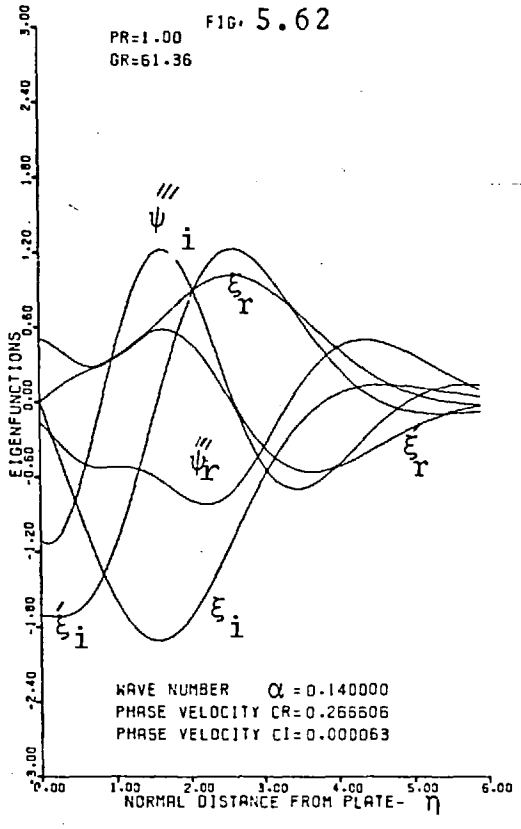

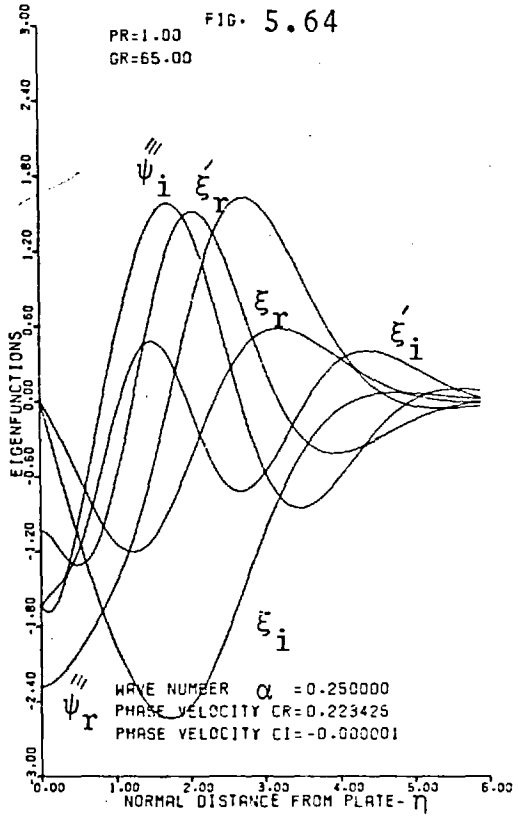

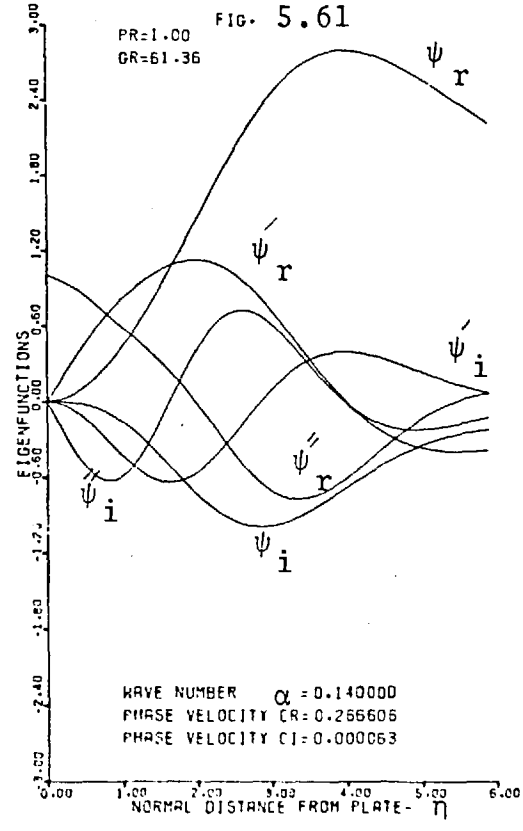

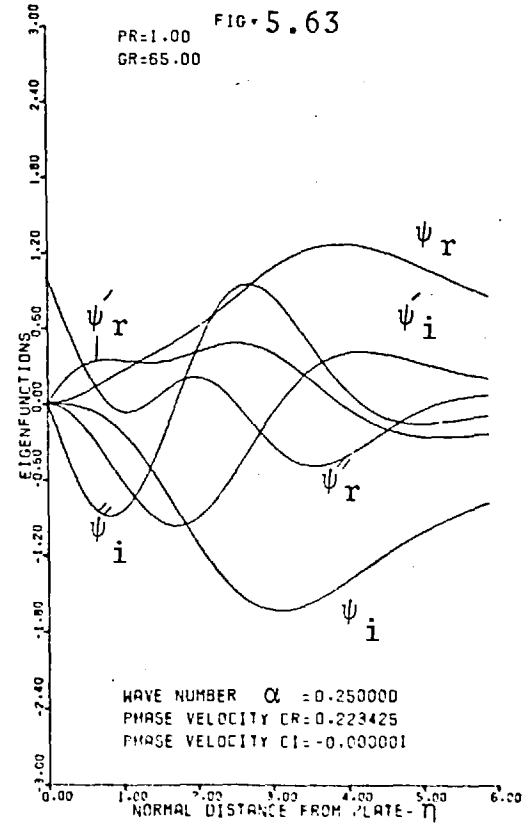

Eigenfunctions for a Prandtl number of 1.0.

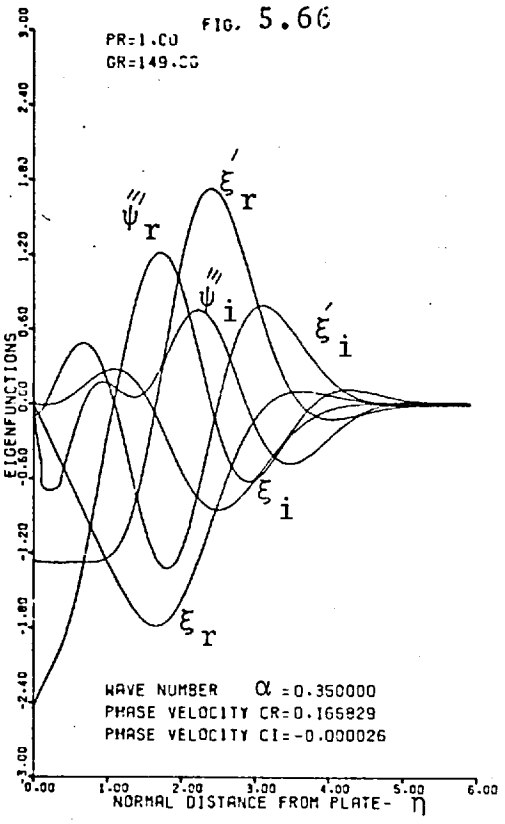

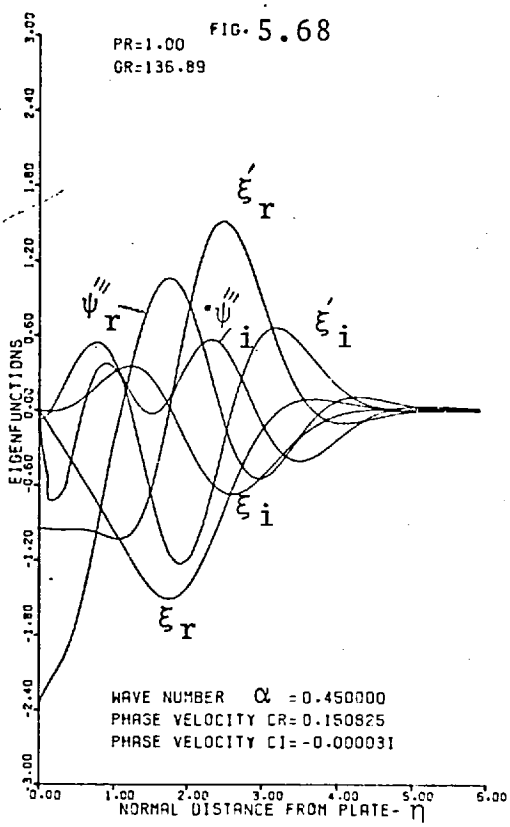

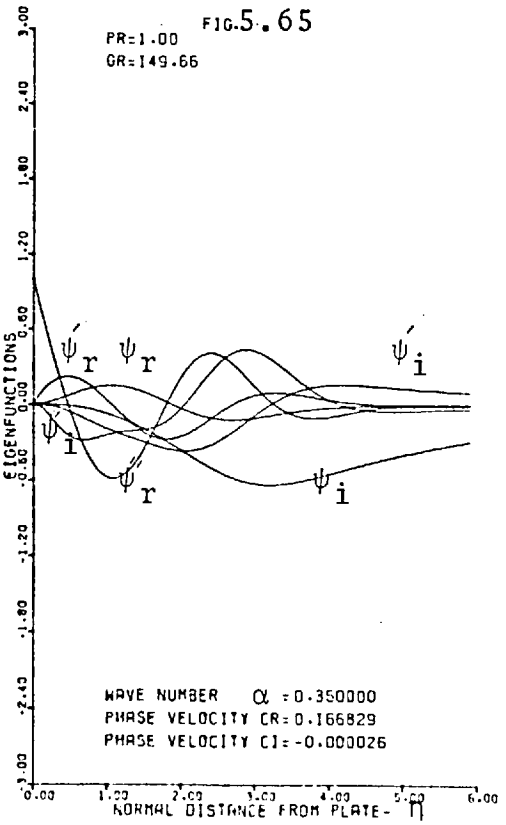

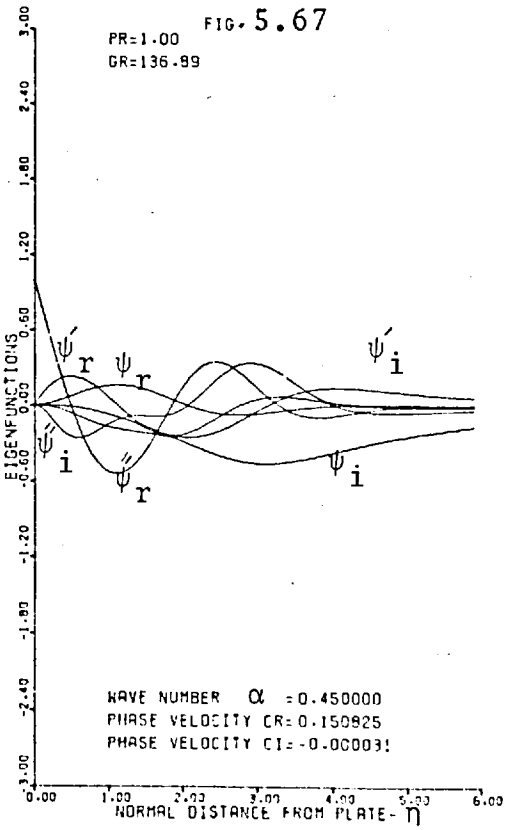

Eigenfunctions for a Prandtl number of 1.0.

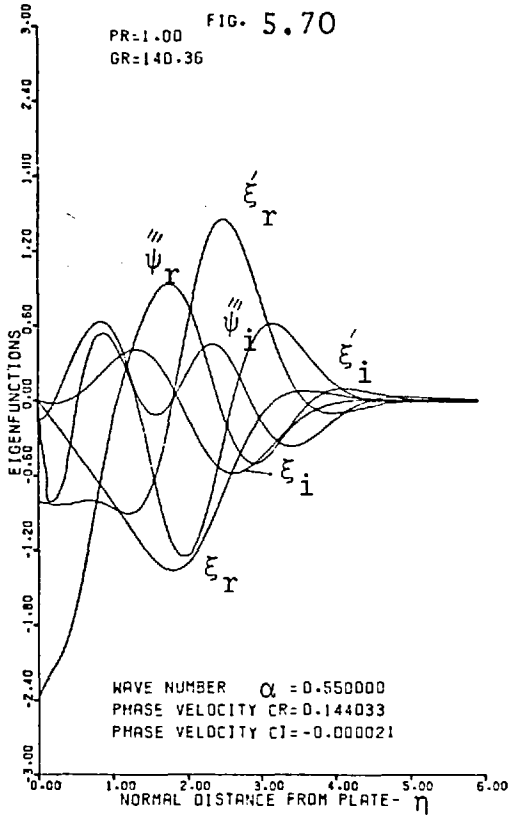

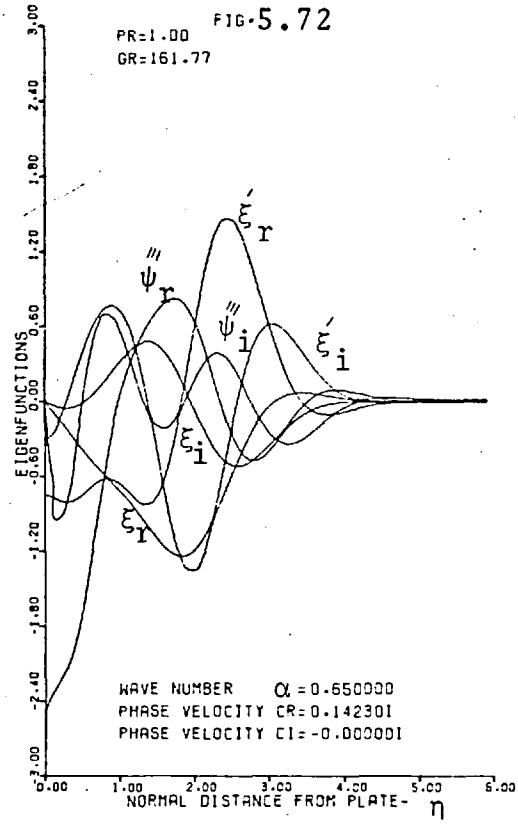

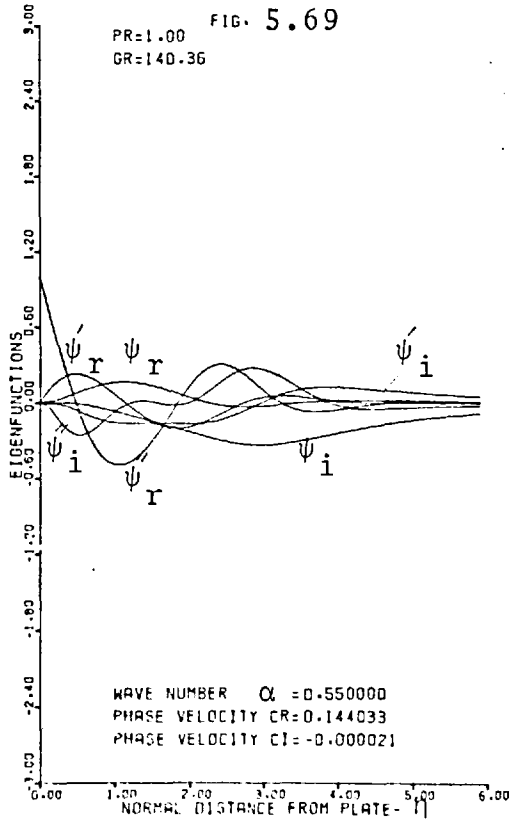

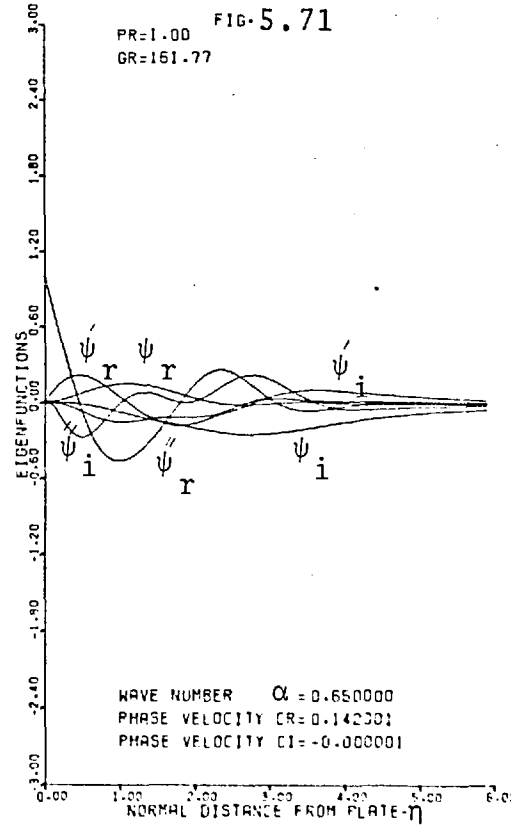

Eigenfunctions for a Prandtl number of 1.0.

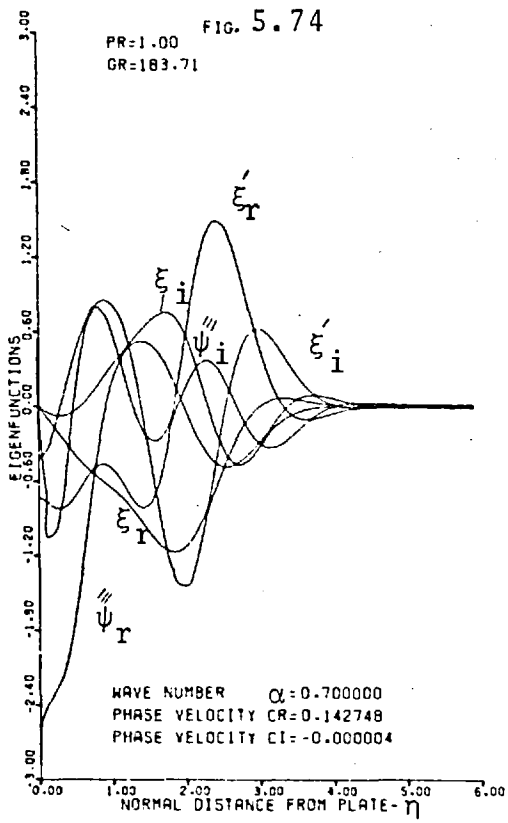

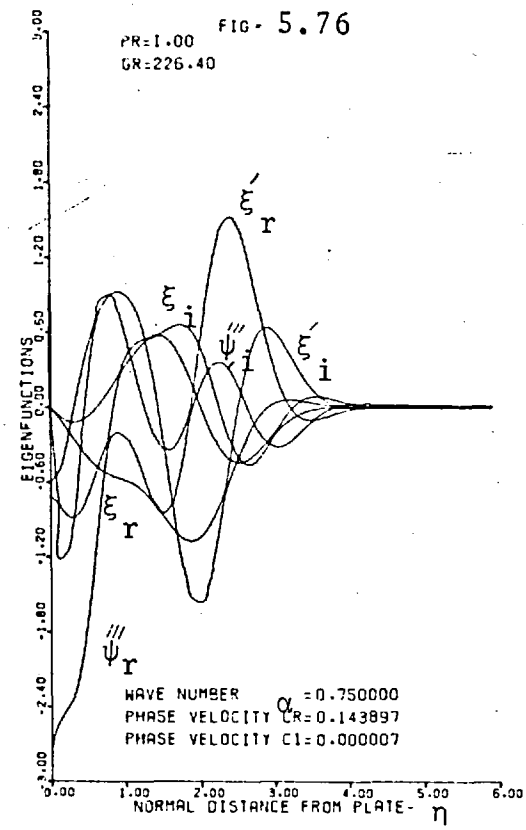

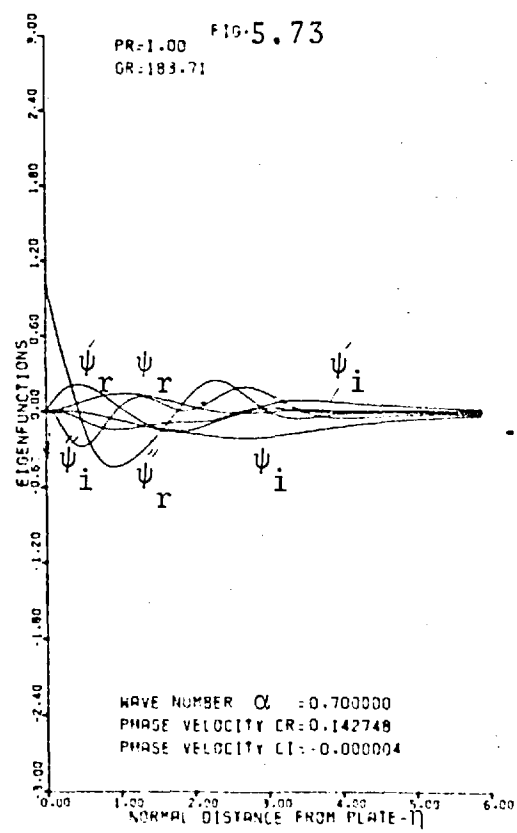

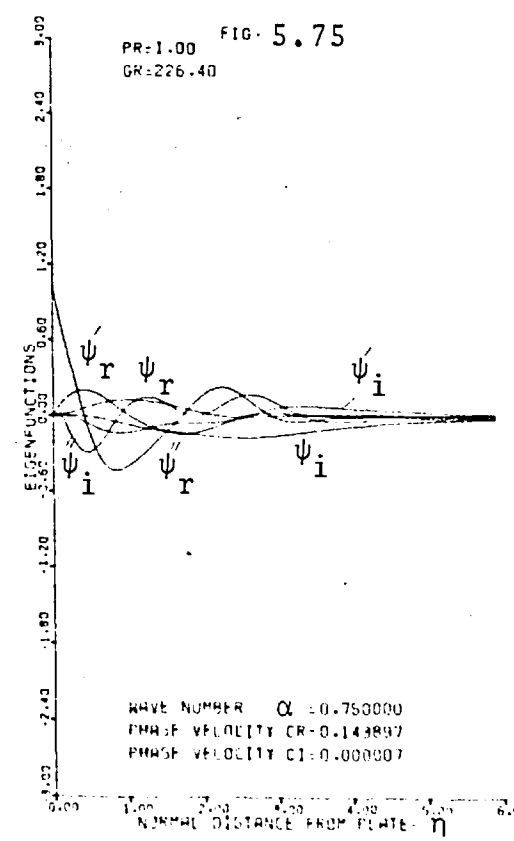

Energy distributions for a Prandtl number of 1.0.
e_{Re} = Reynolds stress e_D = Dissipation e_B = Buoyancy

FIG. 5.78

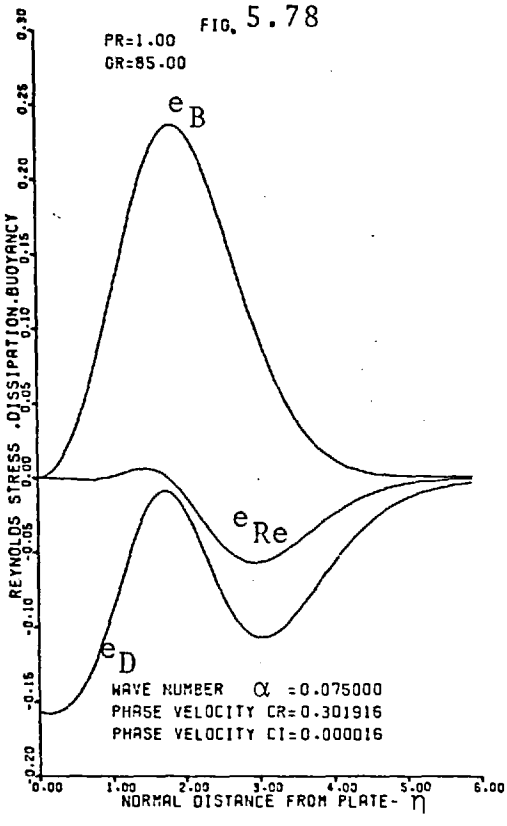

FIG. 5.80

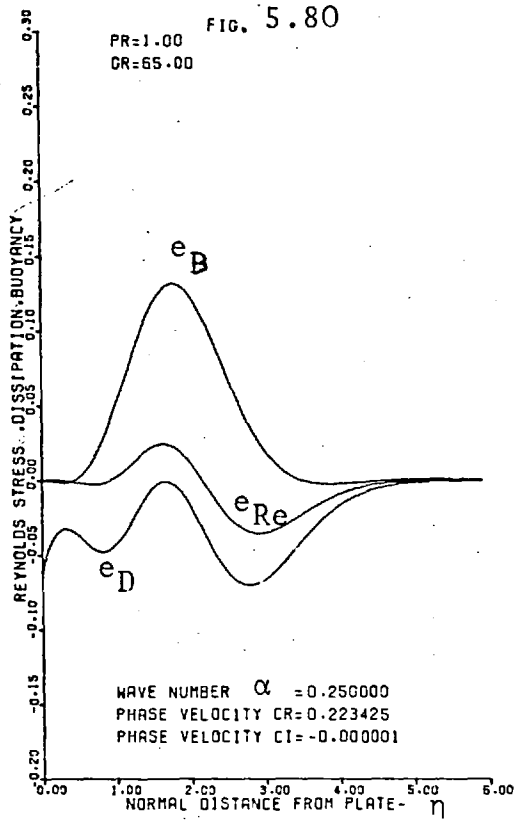

FIG. 5.77

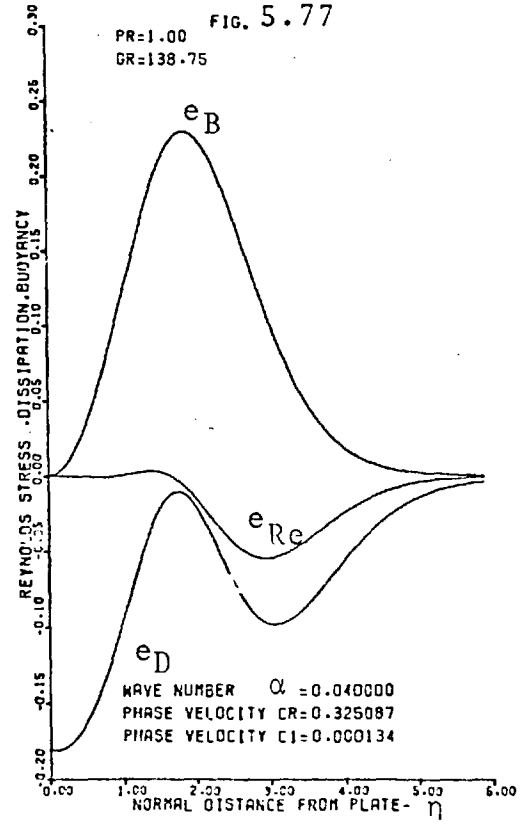

FIG. 5.79

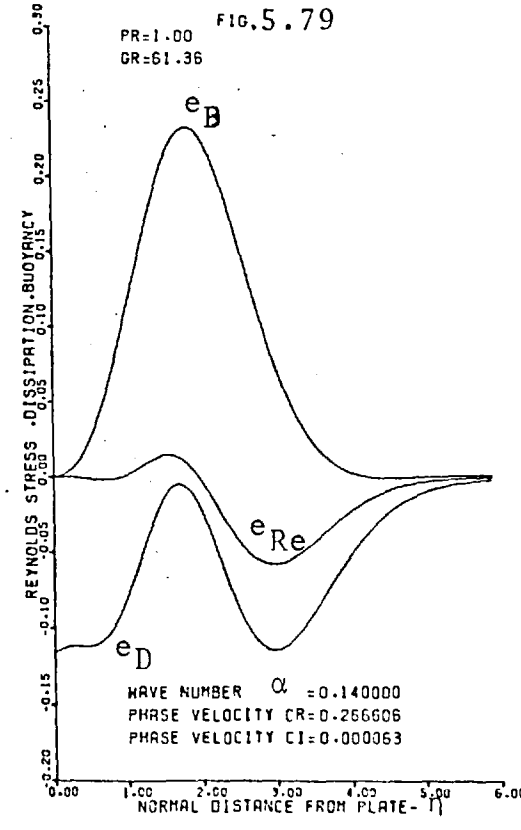

Energy distributions for a Prandtl number of 1.0.

e_{Re} = Reynolds stress e_D = Dissipation e_B = Buoyancy

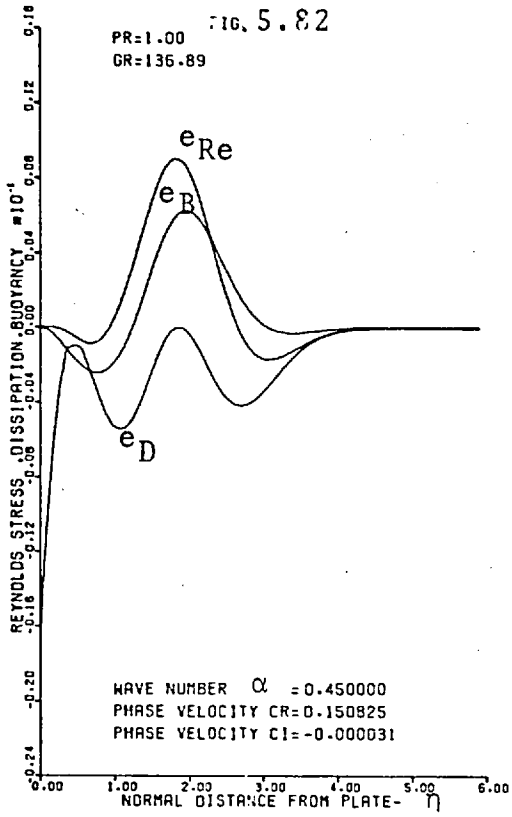

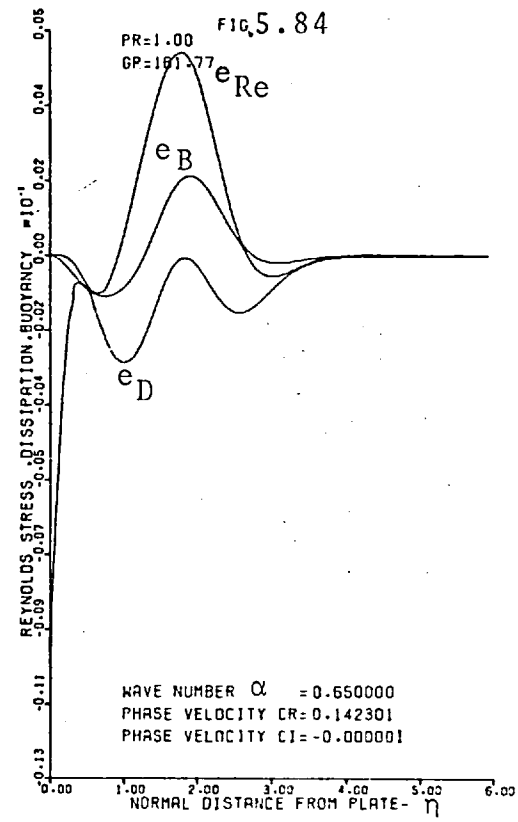

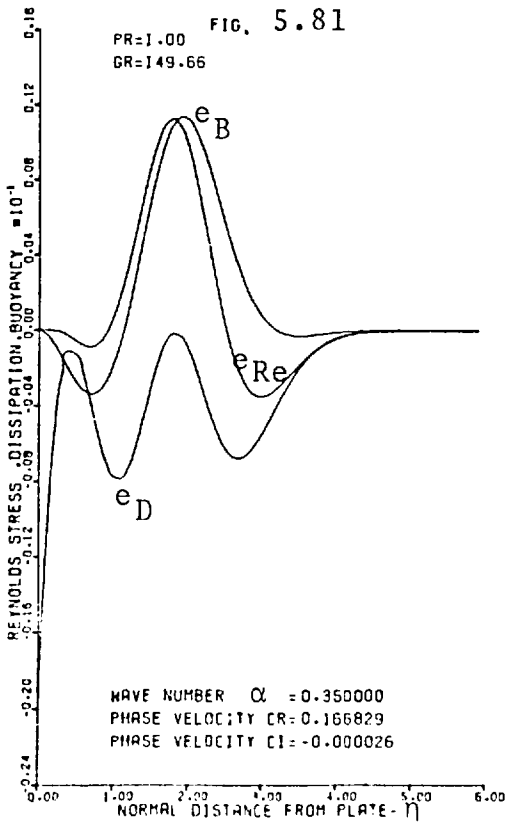

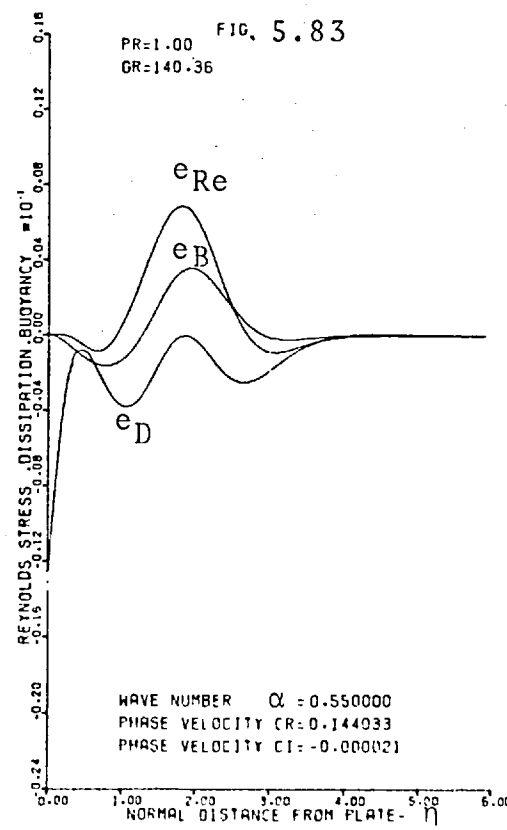

Energy distributions for a Prandtl number of 1.0.
e_{Re} = Reynolds stress e_D = dissipation e_B = Buoyancy

FIG. 5.86

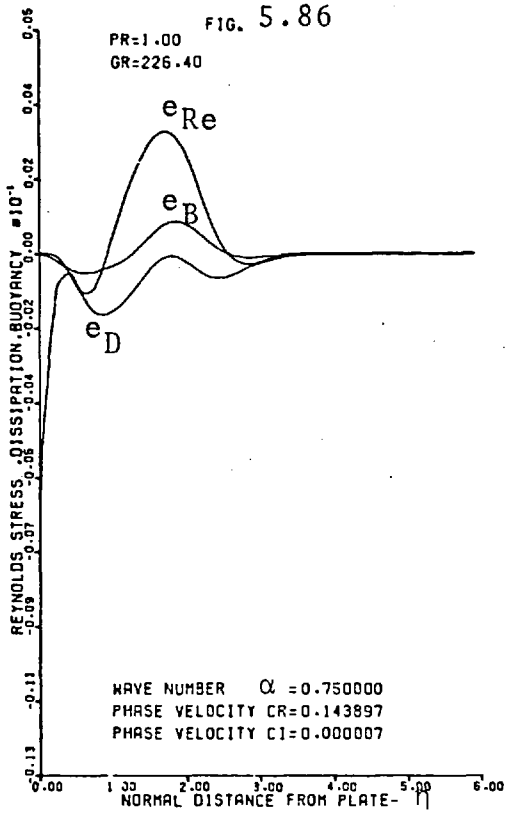

FIG. 5.85

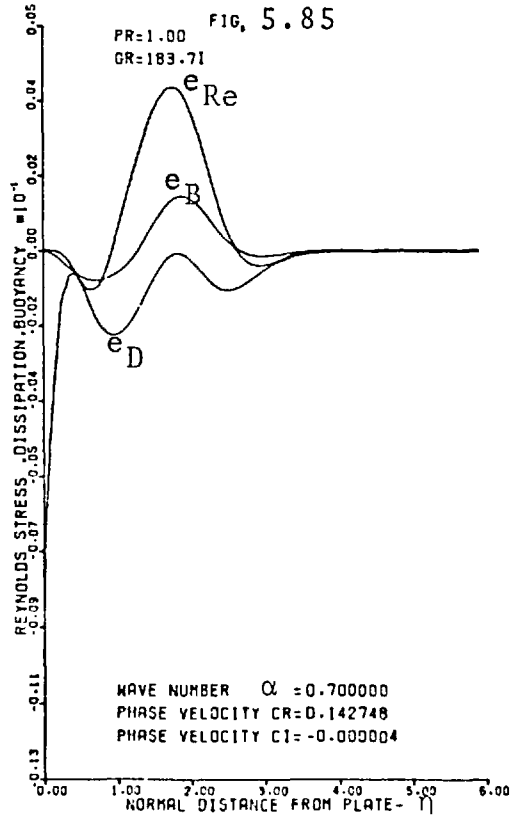

the energy of the disturbed motion. Figures 5.84 to 5.86 reveal that for values of the wave number greater than 0.65 the positive energy is contributed mostly by the Reynolds stress term.

5.3. Stability Results for Water, Prandtl Number of 6.7

The neutral stability curve in the wave number, Grashof number-plane (α, Gr-plane) for the case of a Prandtl number of 6.7 is shown in figure 5.87. It can be seen that the minimum critical value of the Grashof number is 43.0. The detailed solutions for the neutral stability curve for a Prandtl number of 6.7 are given in Table F.4.(c). The closest calculated point to the minimum critical Grashof number is at a Grashof number of 45.0, at a wave number of 0.45, and at a phase velocity of 0.15465.

Figure 5.88 shows the neutral stability curve for Prandtl number of 6.7 in the phase velocity, Grashof number-plane (c_r, Gr-plane). A comparison of this figure with figure 5.89 shows that all the points on figure 5.88 represent eigenvalues which possess the property that the phase velocity of the disturbance wave is greater than the maximum velocity of the basic flow.

The real and imaginary parts of the eigenfunctions and their derivatives and the corresponding eigenvalues are presented in figures 5.90 to 5.107. These figures show that in a manner similar to that when the Prandtl number has a value of 0.733 for low values of the wave number the disturbance wave is not confined to the boundary layer and extends into the stationary region with a slow exponential decrease

Figure 5.87. Neutral stability curve for a Prandtl number of 6.7 in α, Gr-plane.

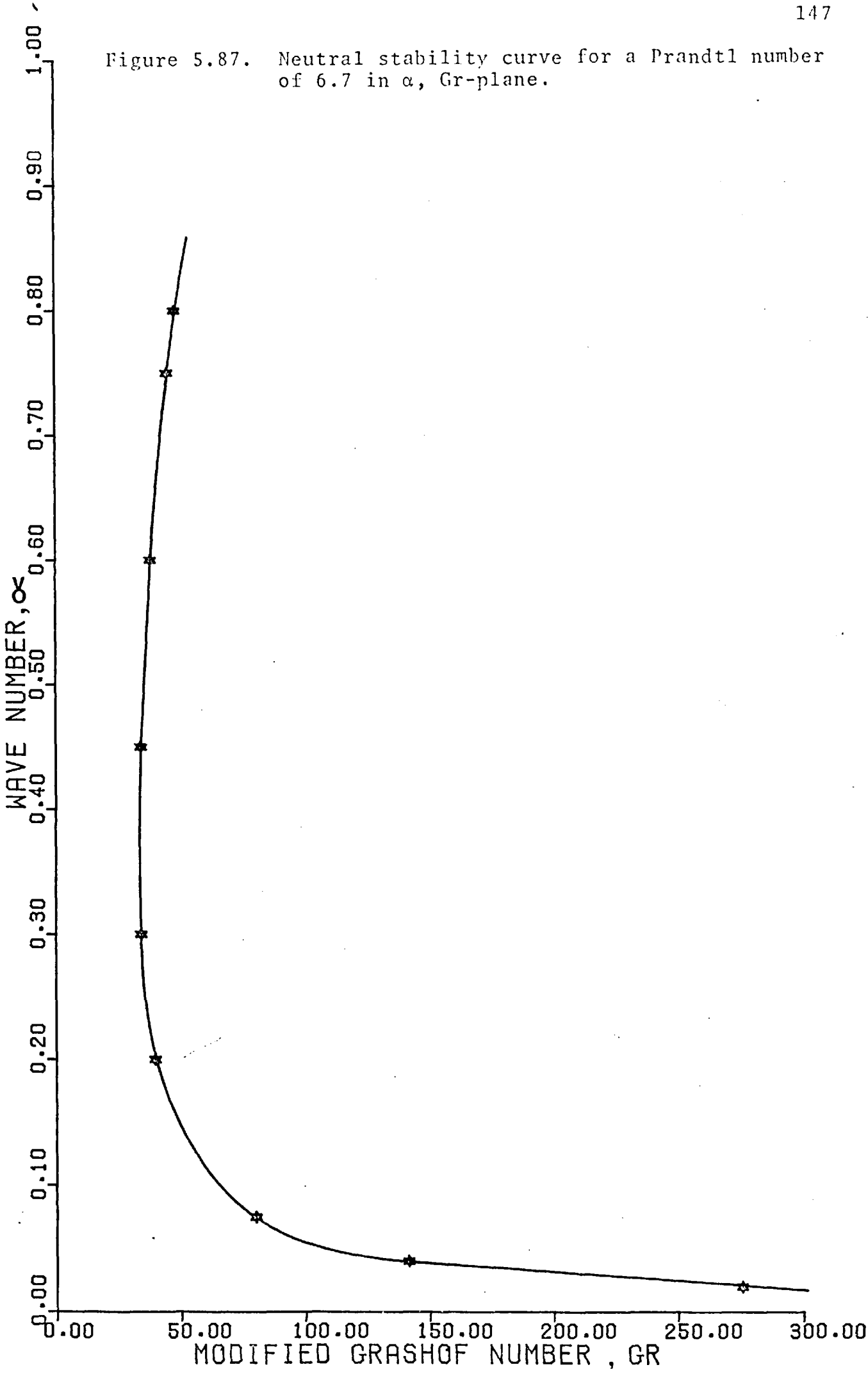

Figure 5.88 - Neutral stability curve for water, Prandtl number of 6.7, in c_r, Gr-plane.

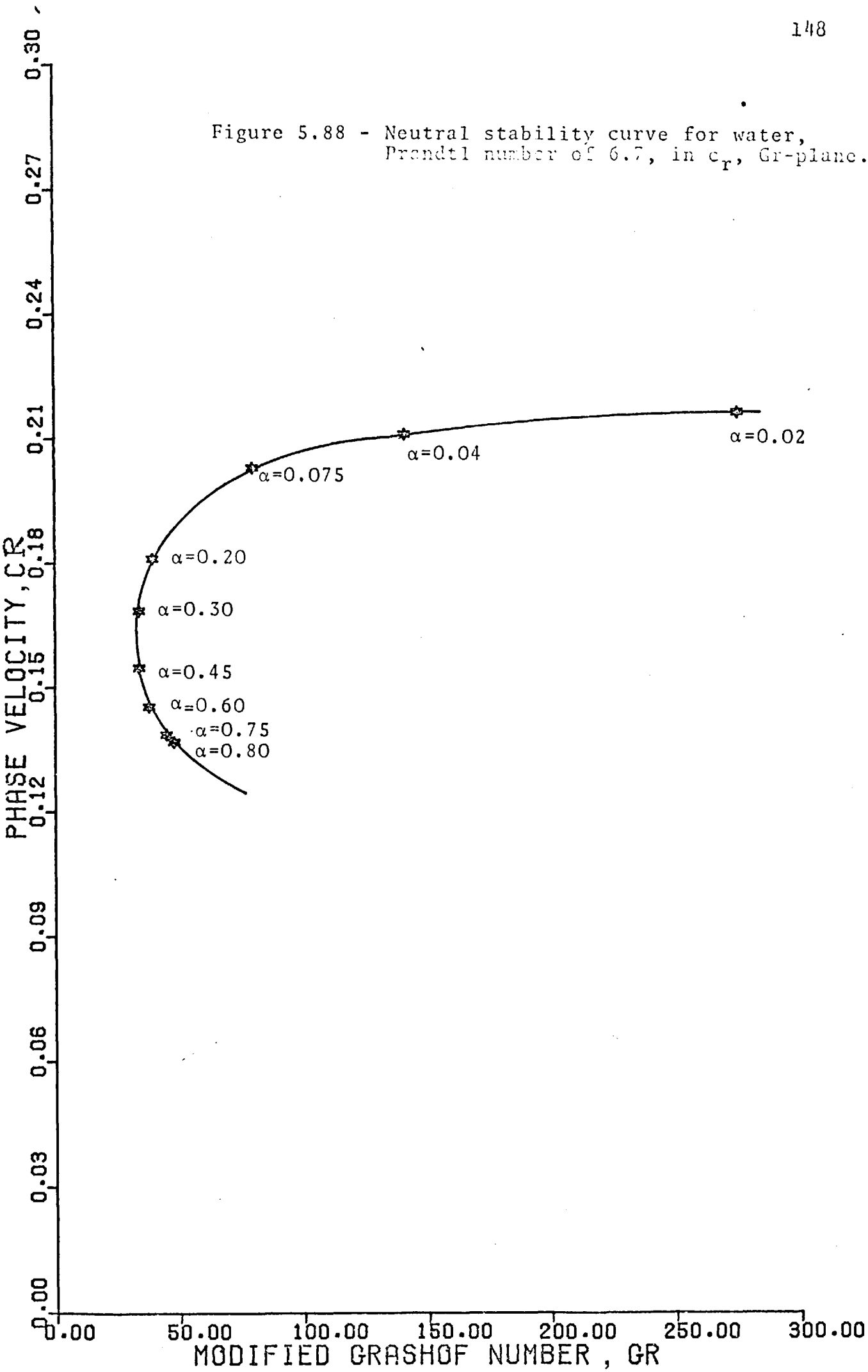

Figure 5.89. Velocity profile for a Prandtl number of 6.7 from Schmidt and Beckmann equations.

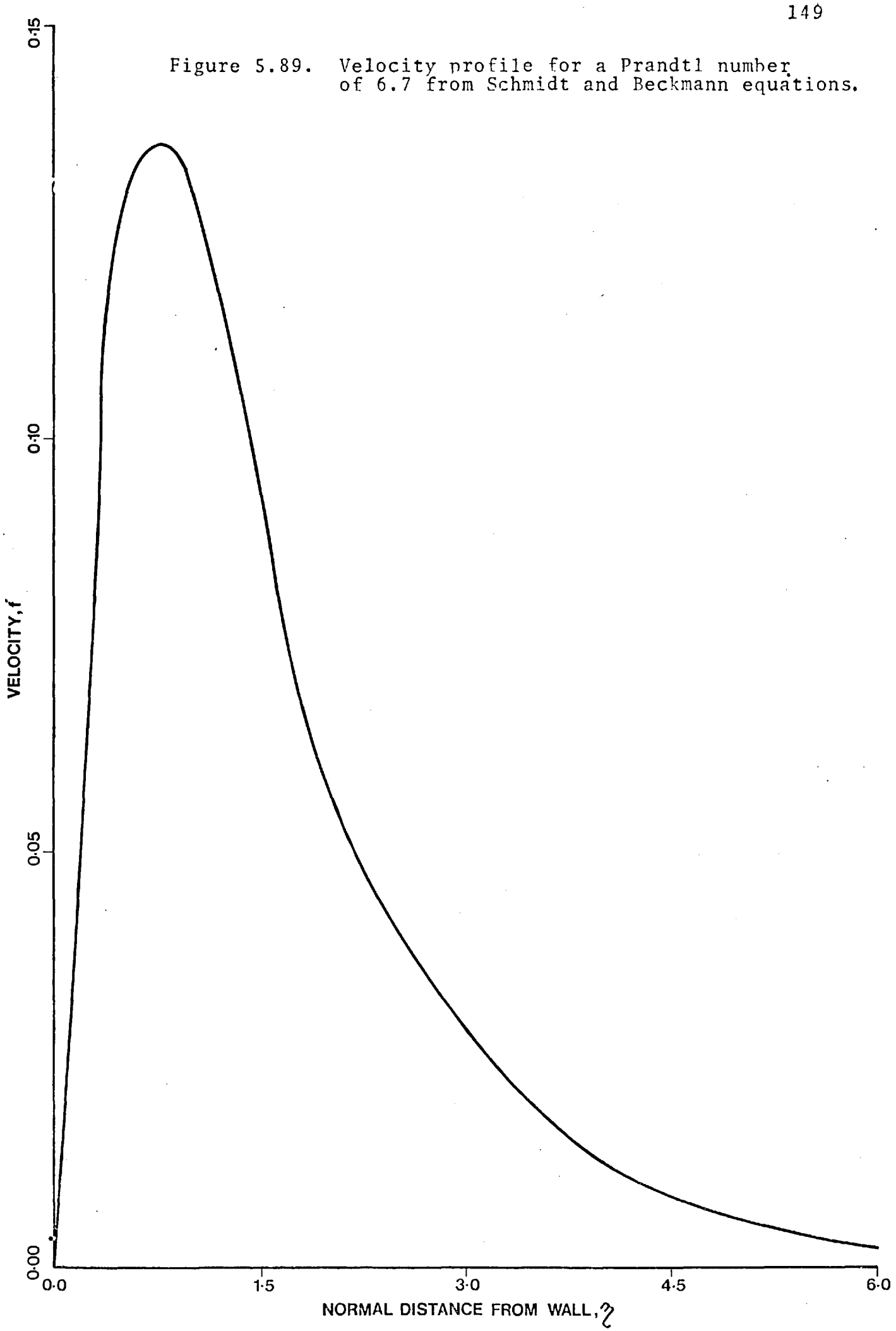

Eigenfunctions for water, Prandtl number of 6.7.

FIG. 5.91

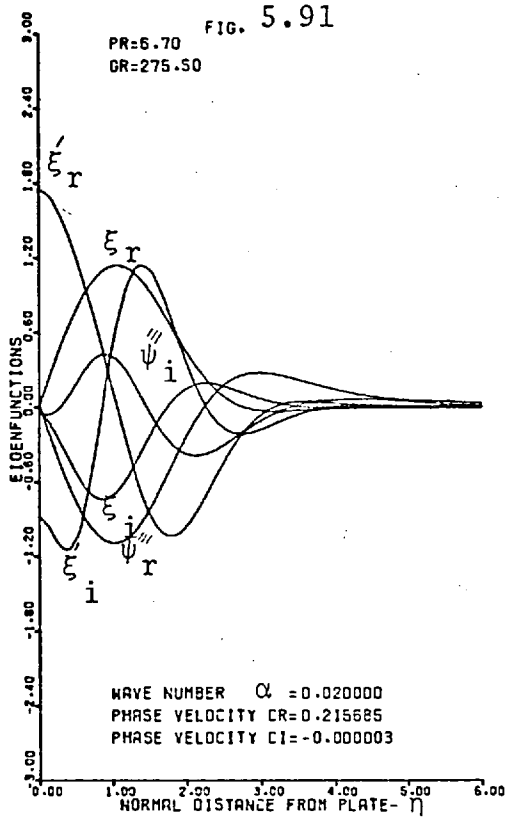

FIG. 5.93

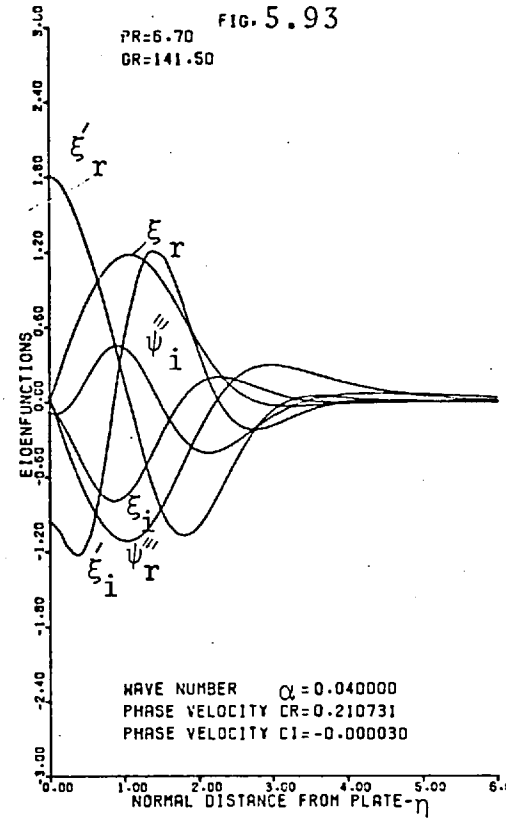

FIG. 5.90

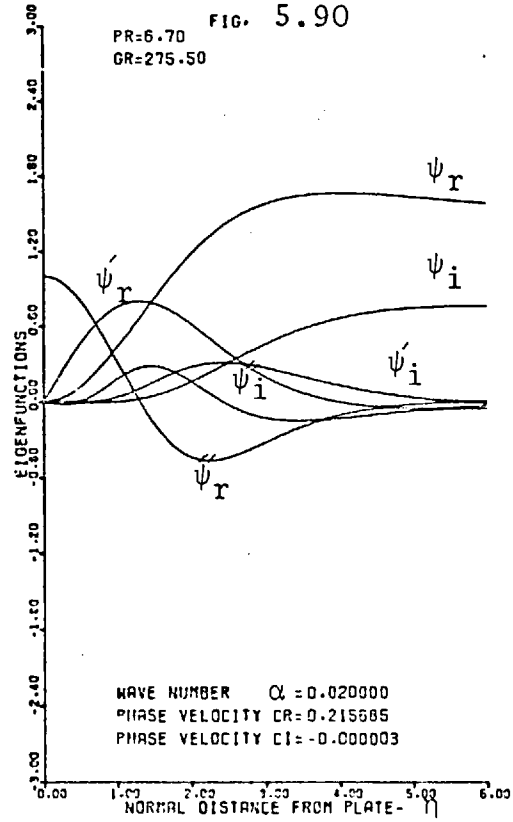

FIG. 5.92

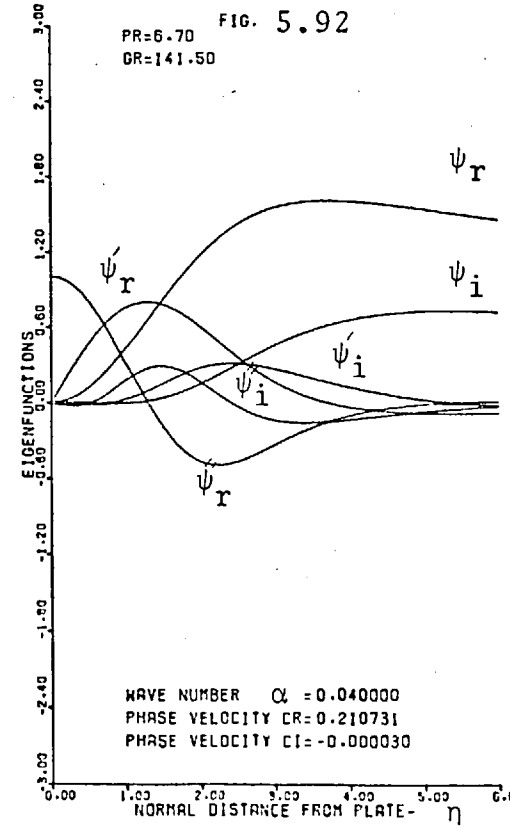

Eigenfunctions for water, Prandtl number of 6.7.

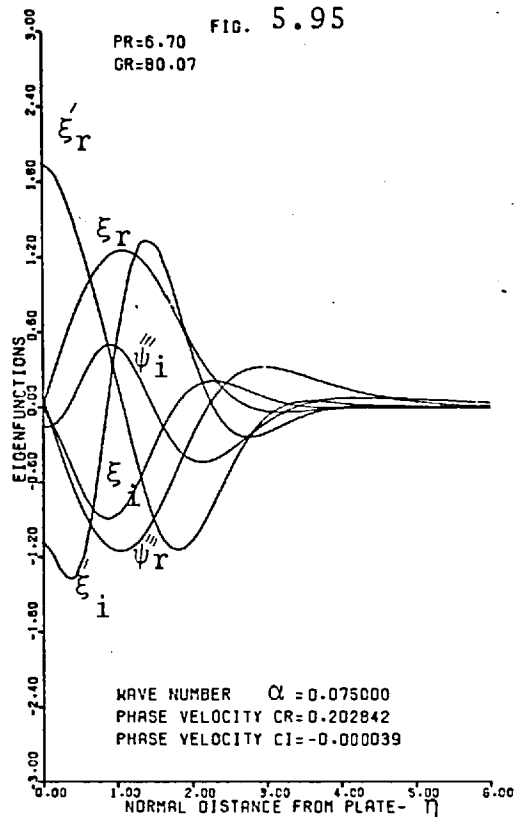

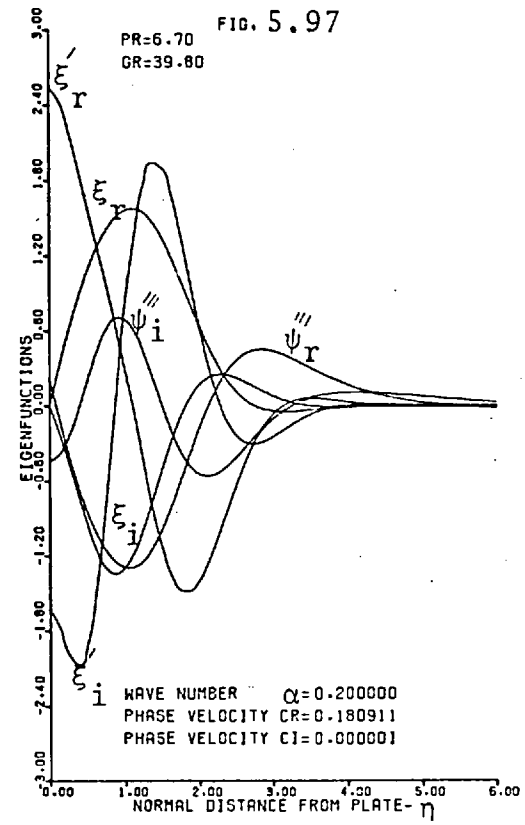

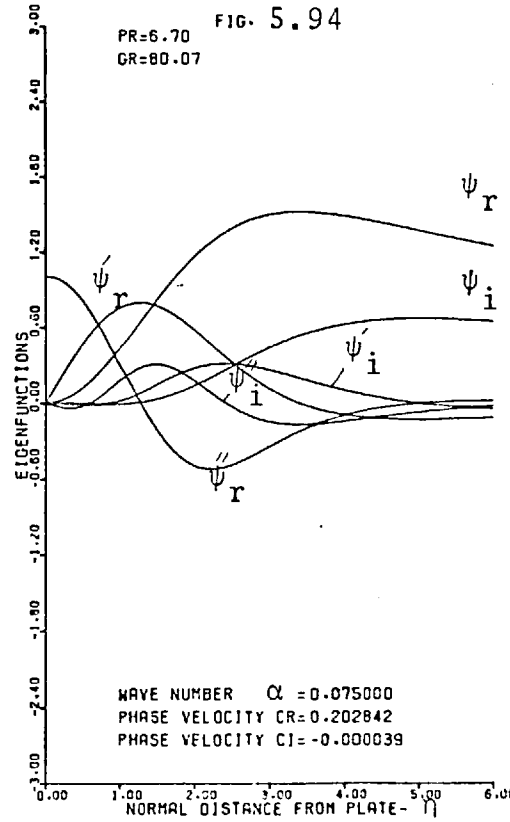

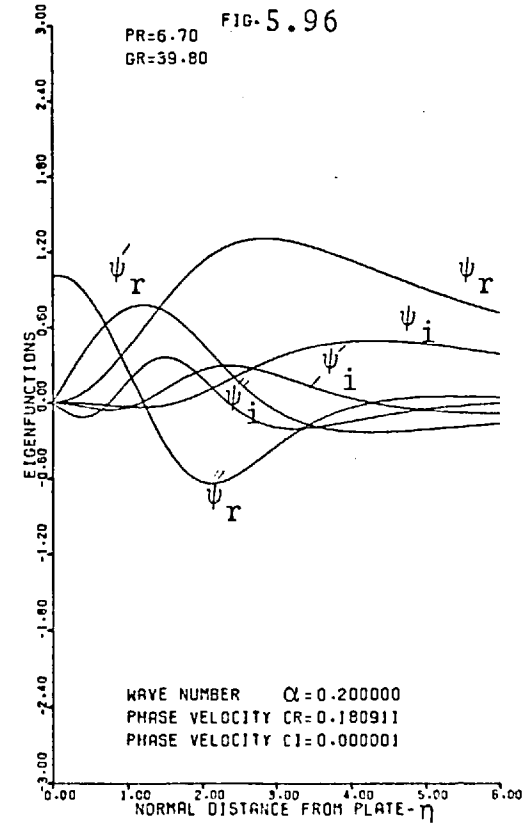

Eigenfunction for water, Prandtl number of 6.70.

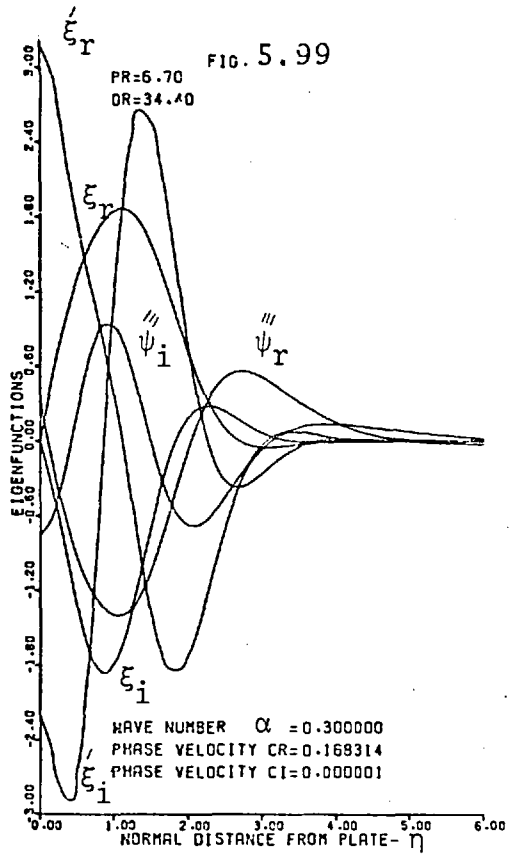

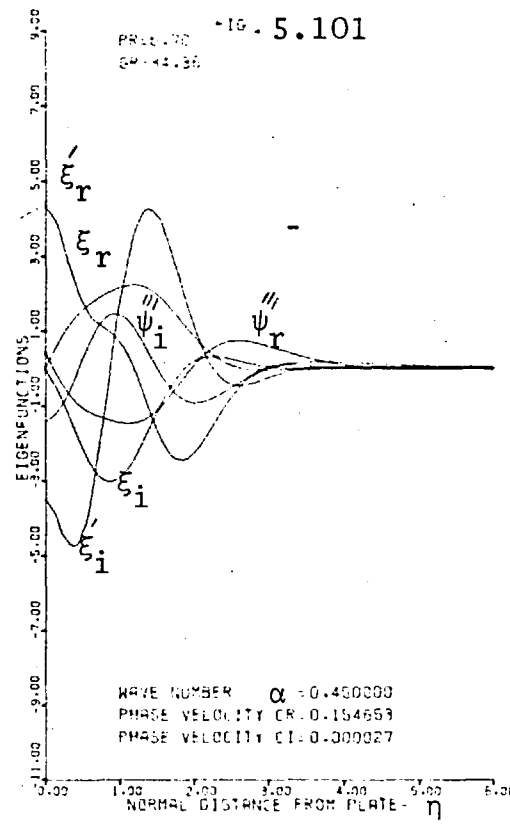

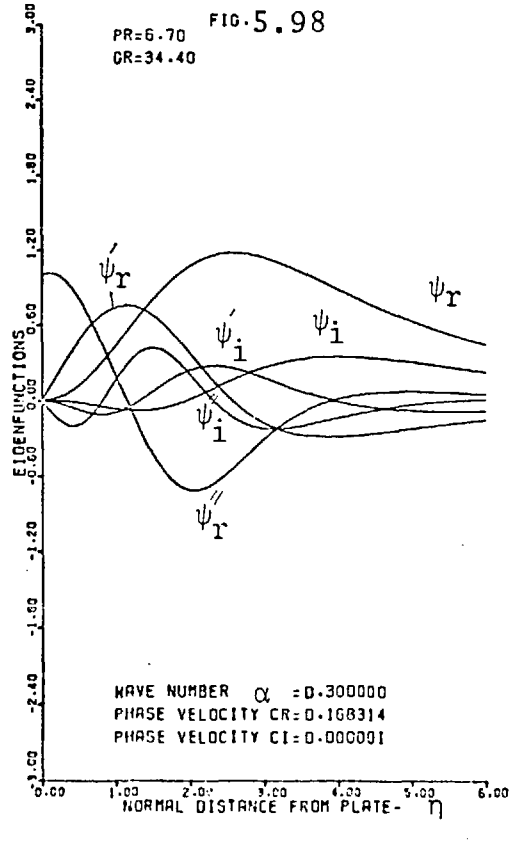

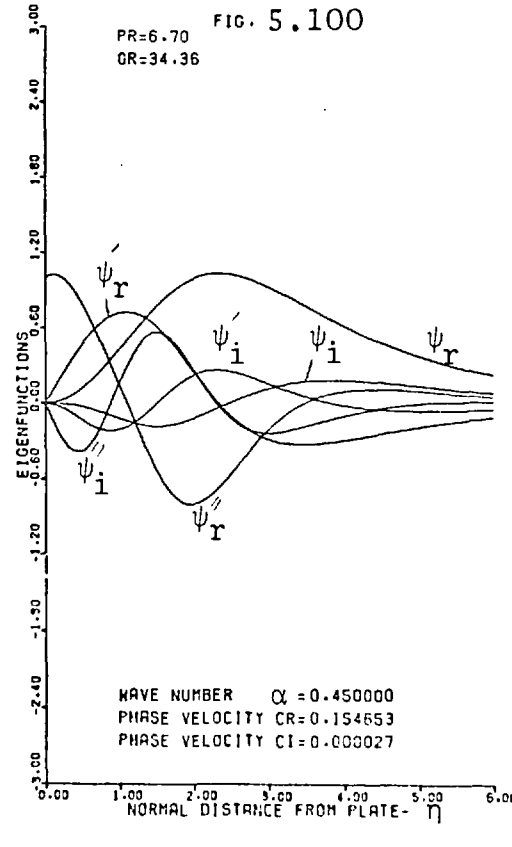

Eigenfunction for water, Prandtl number of 6.70.

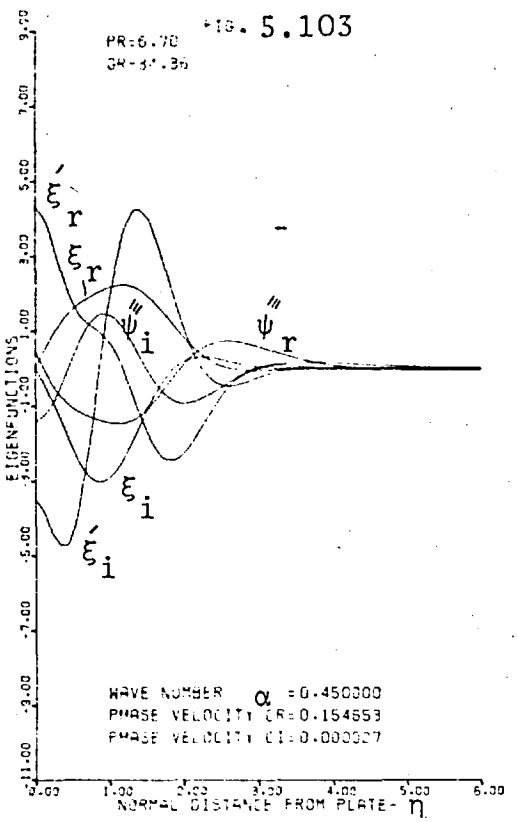

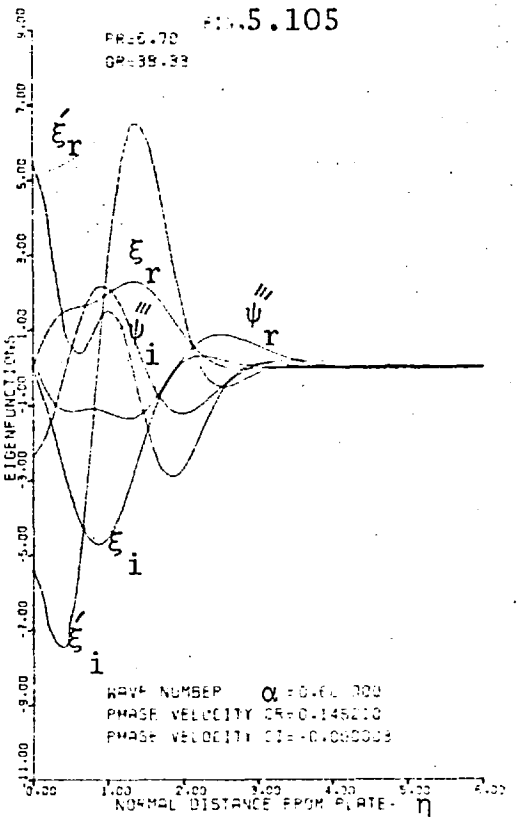

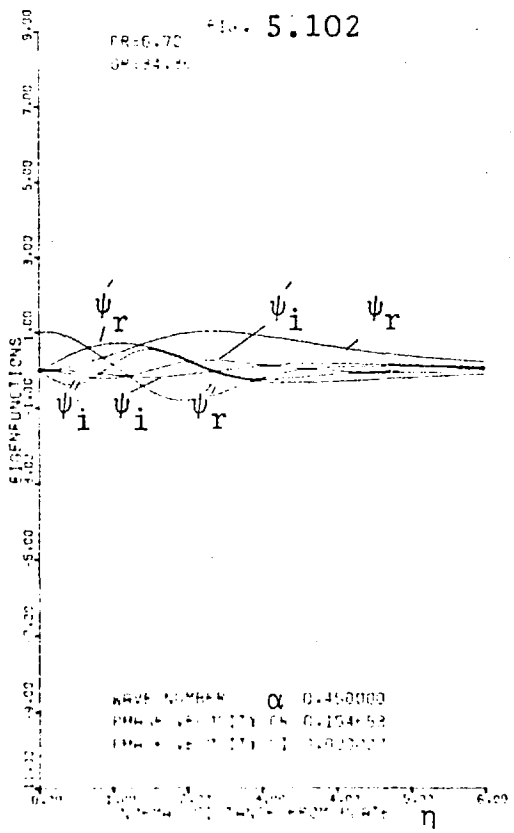

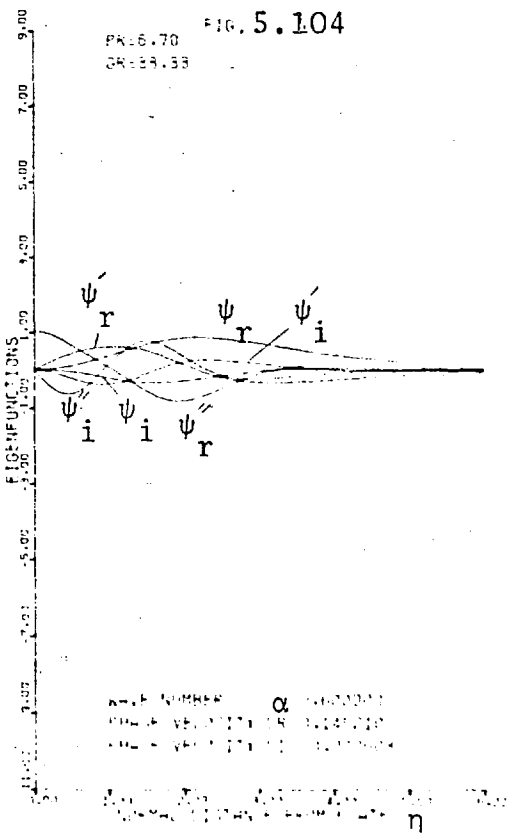

Eigenfunction for water, Prandtl number of 6.70.

FIG. 5.107

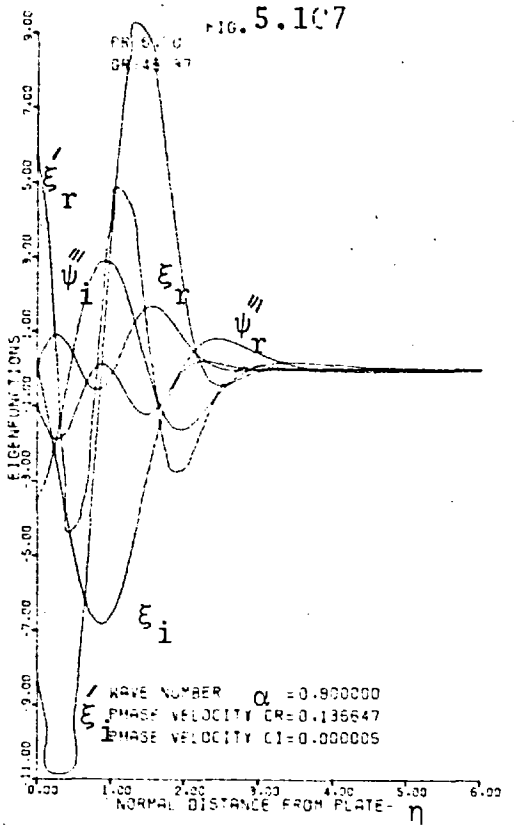

FIG. 5.106

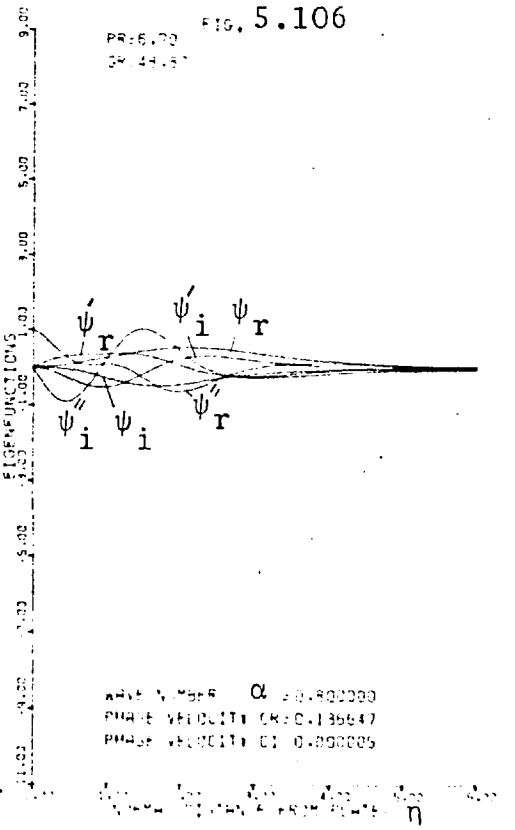

magnitude. As the wave number increases, the wave becomes confined to the boundary layer and the eigenfunctions start to oscillate. An examination of these figures shows that the results of the present work are considerably different from those when the effects of temperature fluctuations are ignored. For a clarification of the reason for this difference the energy distribution curves 5.108 to 5.115 will be studied. These figures show that the buoyancy term in the energy balance is the only term which gives a positive contribution to the energy of the disturbed motion and that the Reynolds stress term does not play an important role in the energy balance. Thus, it can be concluded that the buoyancy term provides most of the energy input into the disturbed motion, so that the omission of the temperature fluctuations cannot be justified. The neutral stability curves with and without temperature fluctuations are compared in figure 5.116. It can be seen that the present work gives a minimum critical Grashof number which is much lower than that obtained without temperature fluctuations.

5.4. Stability Results for Prandtl Numbers of 100.0 and 1000.0

Figures 5.117 and 5.118 show the neutral stability curve for a Prandtl number of 100.0 in the wave number, Grashof number-plane (α, Gr-plane) and in the phase velocity, Grashof number-plane (c_r, Gr-plane), respectively. Table F.4.(d) presents the detailed solutions of the disturbance equations for the neutral stability curve for a Prandtl number of 100.0. This table shows that the closest solution to the minimum critical

Energy distribution for water, Prandtl number of 6.70.
e_{Re}= Reynolds stress e_D = Dissipation e_B = Buoyancy

FIG. 5.109

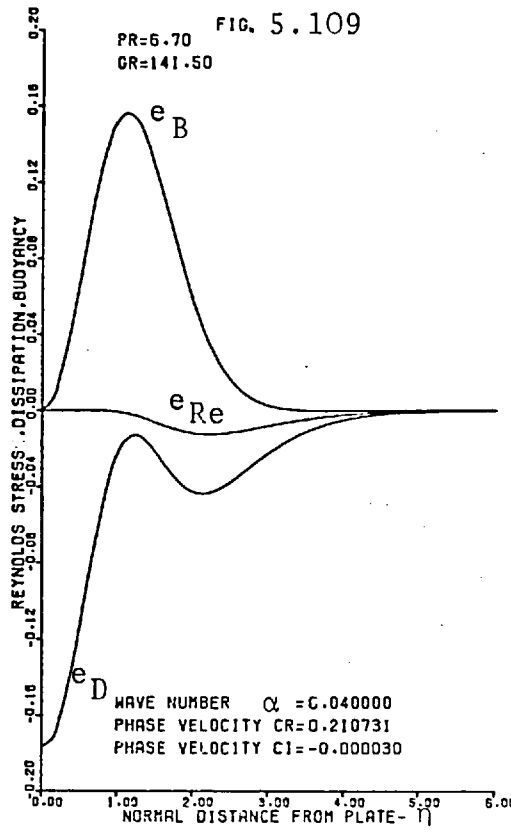

FIG. 5.111

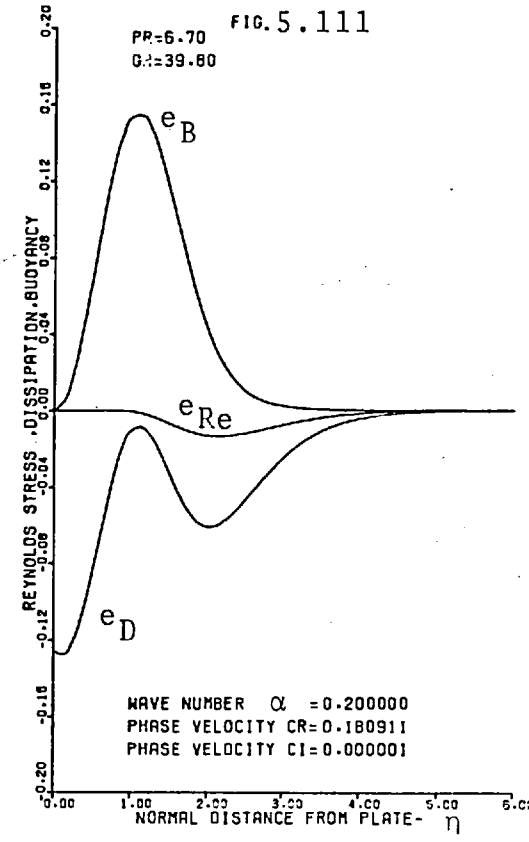

FIG. 5.108

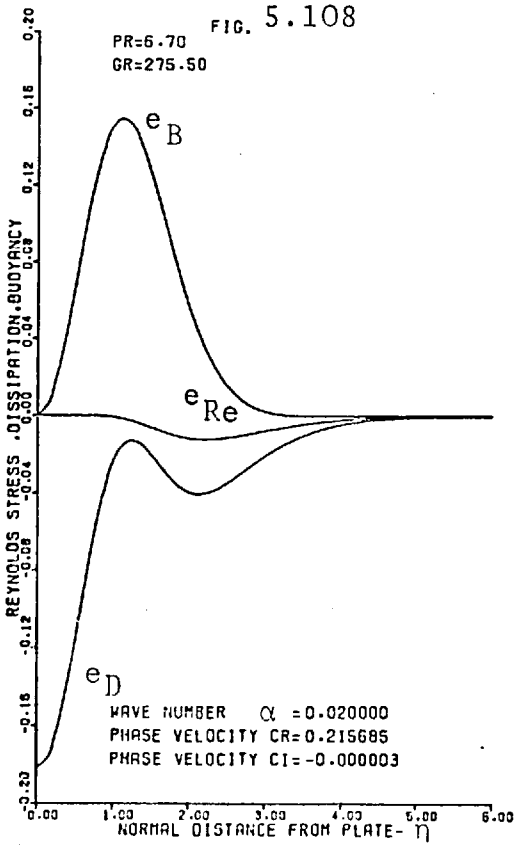

FIG. 5.110

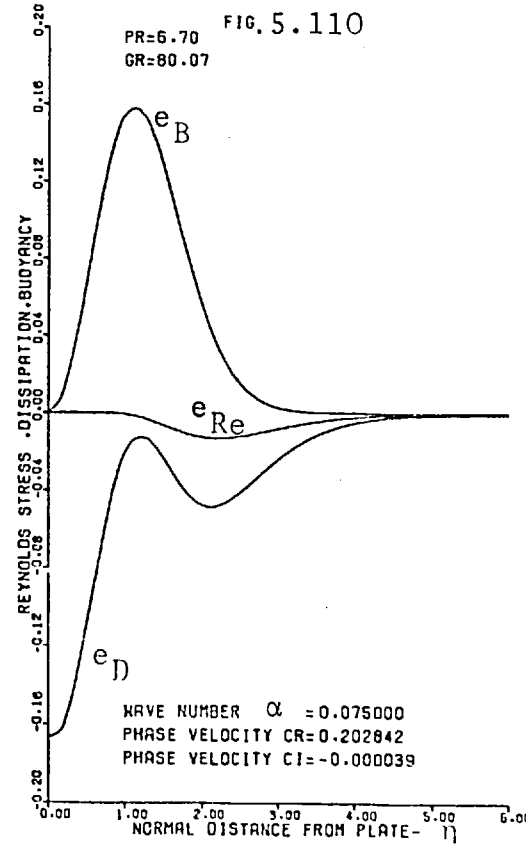

Energy distributions for water, Prandtl number of 6.70.
e_{Re} = Reynolds stress e_D = Dissipation e_B = Buoyancy

FIG. 5.113

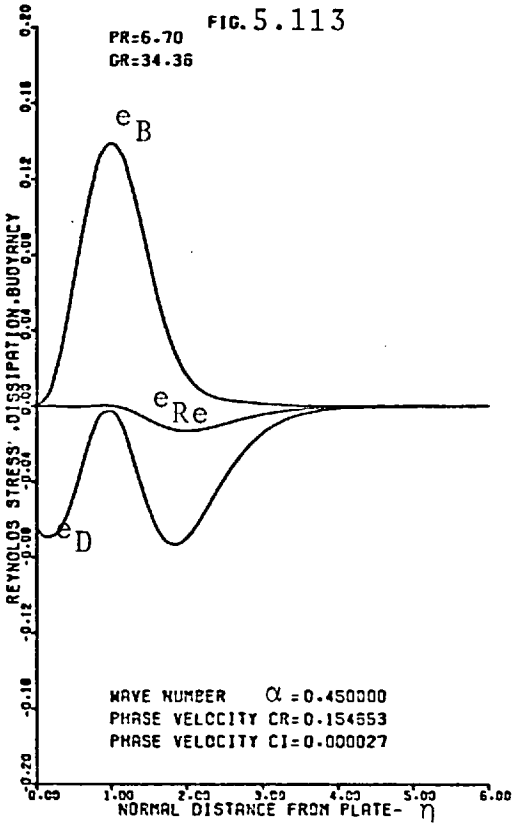

FIG. 5.115

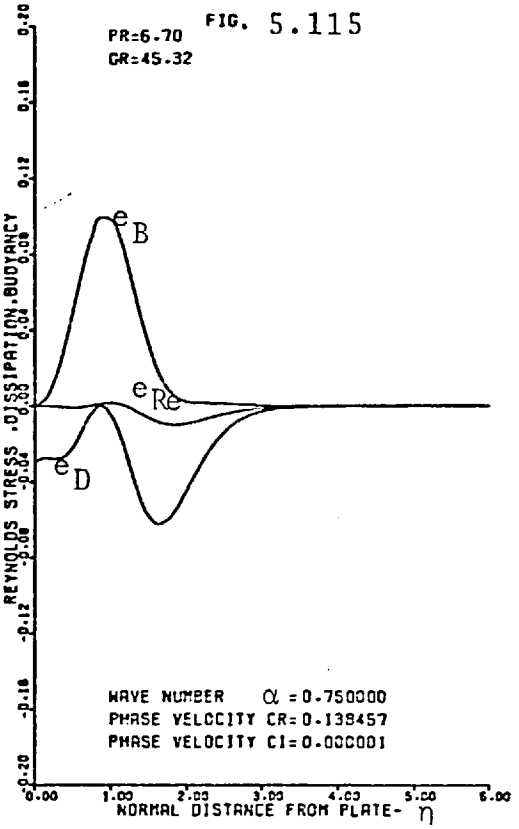

FIG. 5.112

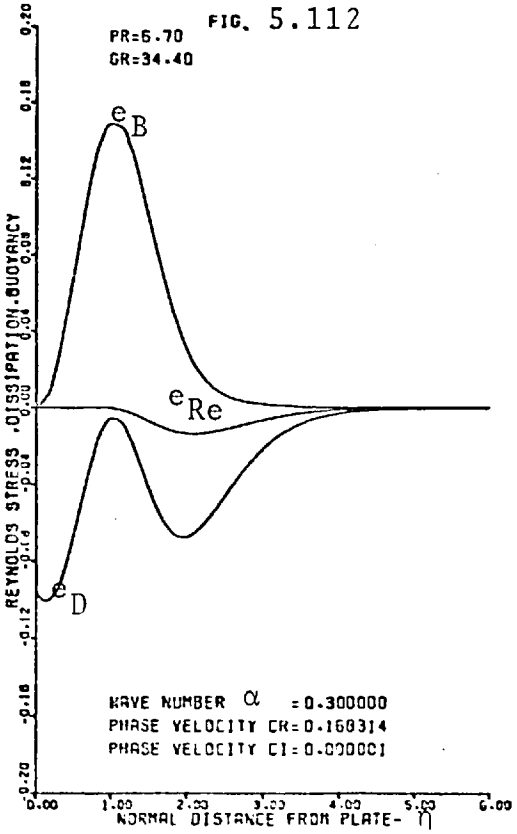

FIG. 5.114

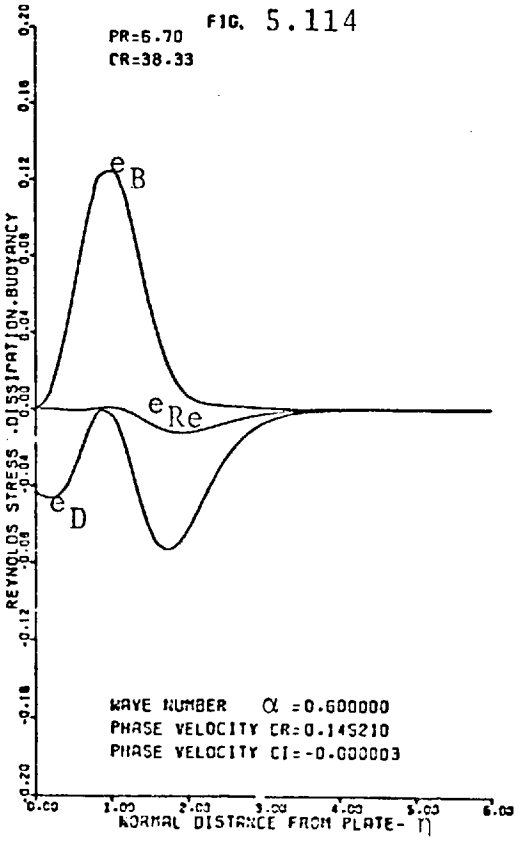

Figure 5.116. A comparison between the neutral stability curve of the present work with that without temperature fluctuations for a Prandtl number of 6.7

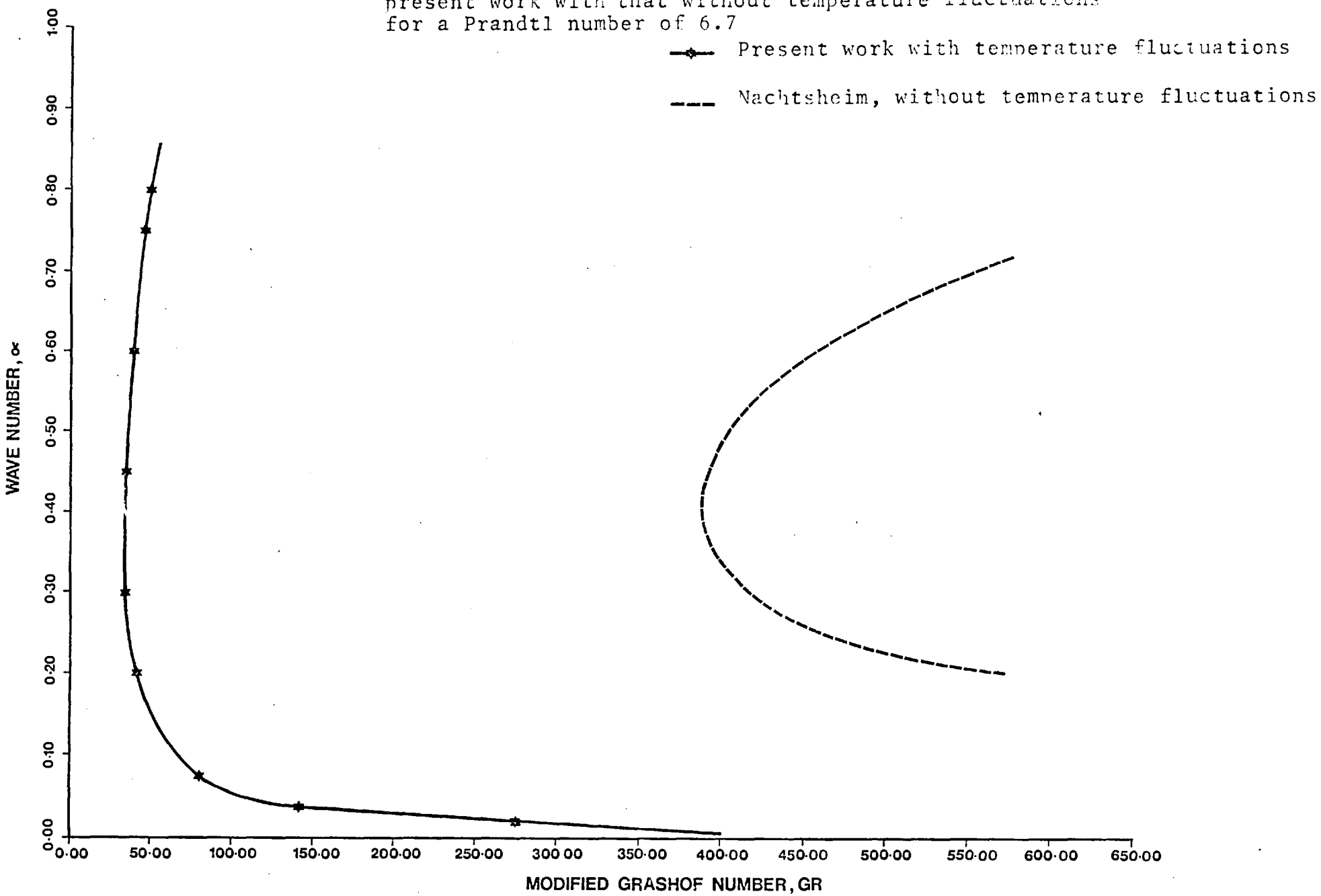

Figure 5.117. Neutral stability curve for a Prandtl number of 100.0 in α, Gr-plane.

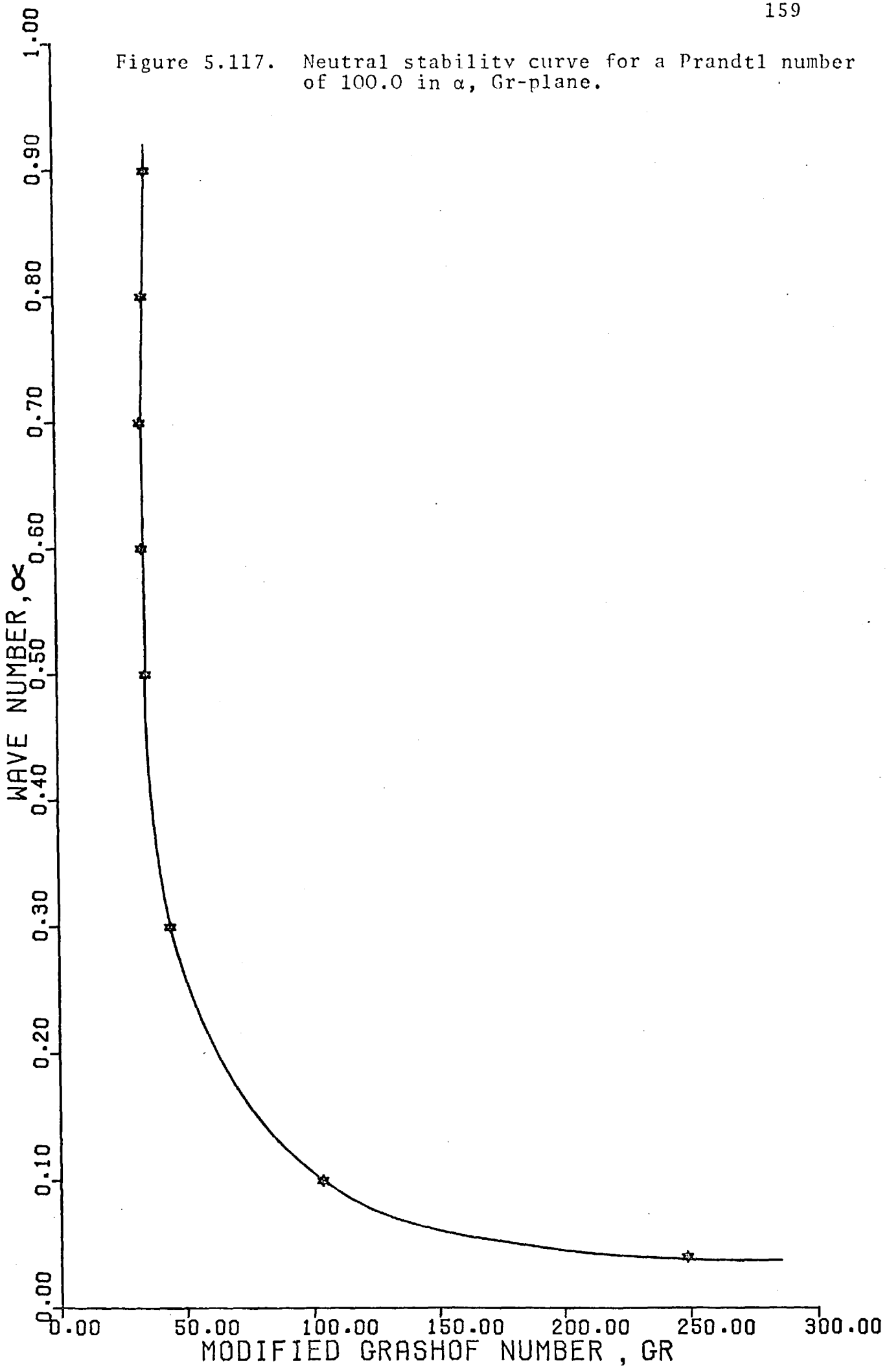

Figure 5.118 - Neutral stability curve for a Prandtl number of 100.0 in c_r, Gr-plane.

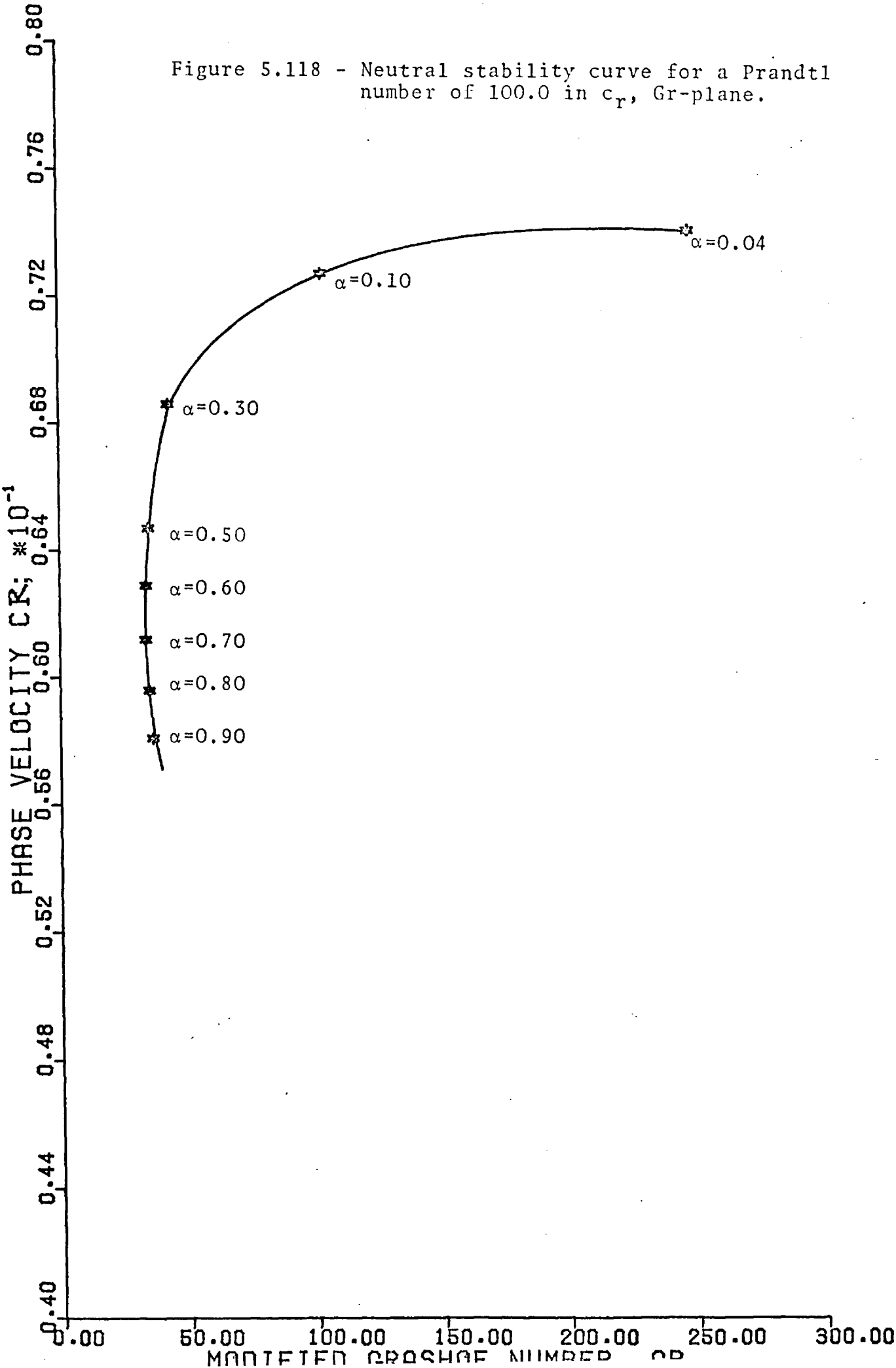

value of the Grashof number is at a Grashof number of 33.71, and at a wave number of 0.70 with a phase velocity of 0.06123.

A comparison of figure 5.118 with figure 5.119 shows that all the points on figure 5.118 possess the property that the phase velocity of the disturbance wave is greater than the maximum velocity of the basic flow.

Figures 5.120 to 5.135 show the real and imaginary parts of the eigenfunctions and of their derivatives and the corresponding eigenvalues for a Prandtl number of 100.0.

The energy distributions of the disturbed motion for a Prandtl number of 100.0 are shown by figures 5.136 to 5.143. It can be seen that, in a manner similar to the case when the Prandtl number is 6.7, the buoyancy term in the energy balance of the disturbed motion is the only term which gives a positive contribution to the energy of the disturbance motion, hence, the effect of temperature fluctuations cannot be ignored when the Prandtl number is 100.0.

Figures 5.144 and 5.145 show the neutral stability curve for a Prandtl number of 1000.0 in the wave number, Grashof number-plane (α, Gr-plane) and in the phase velocity, Grashof number-plane (c_r, Gr-plane), respectively. The detailed solutions for the neutral stability curve for a Prandtl number of 1000.0 are tabulated in Table F.4.(e). The table shows that the closest calculated point to the minimum critical value of the Grashof number is at a Grashof number of 33.0, and at a wave number of 0.6 with a phase velocity of 0.0410.

Once again, a comparison of figure 5.145 with figure 5.146 shows that all the points on figure 5.145 possess the property that the phase velocity of the disturbance wave is

Figure 5.119. Velocity profile for a Prandtl number of 100.0 from Schmidt and Beckmann equations.

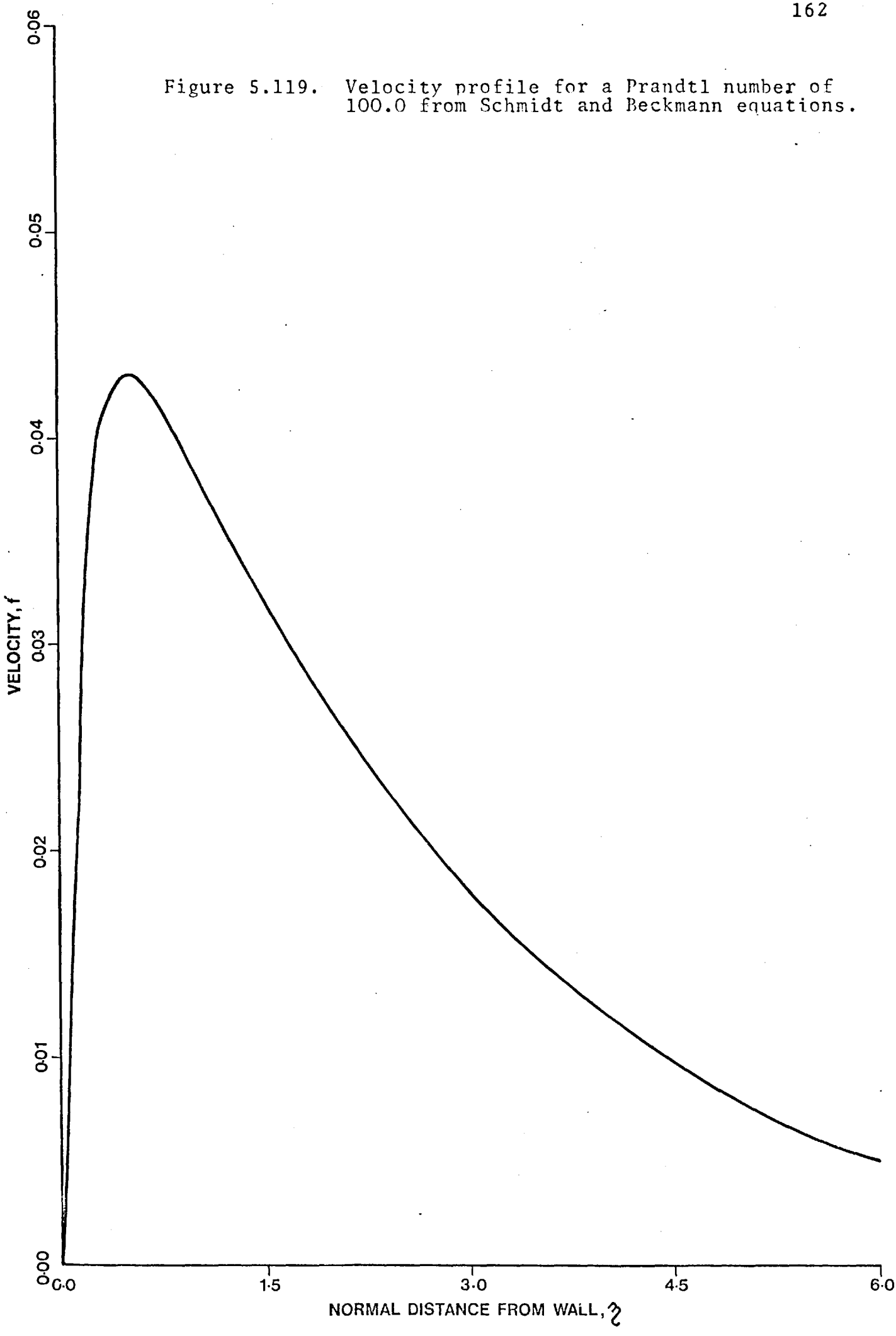

Eigenfunctions for a Prandtl number of 100.0

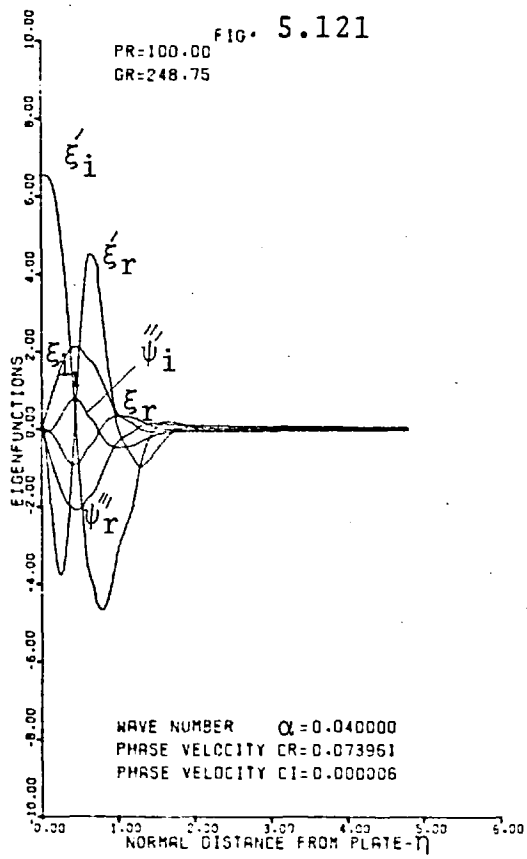

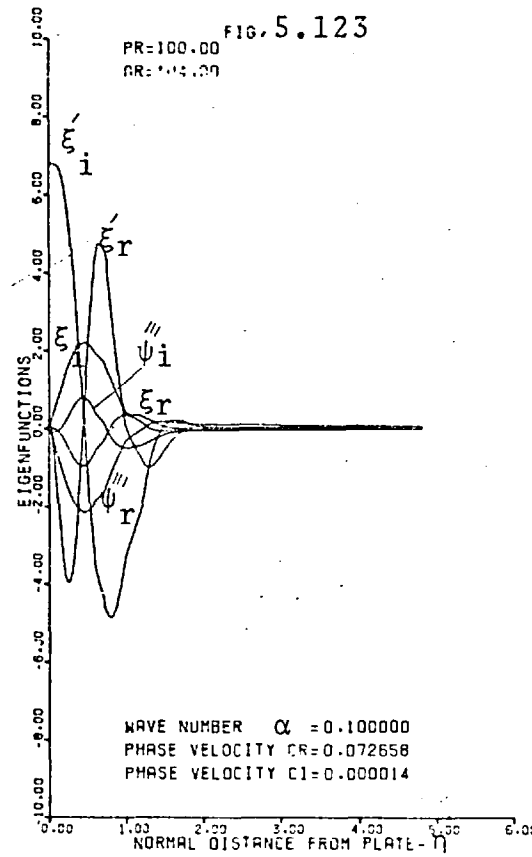

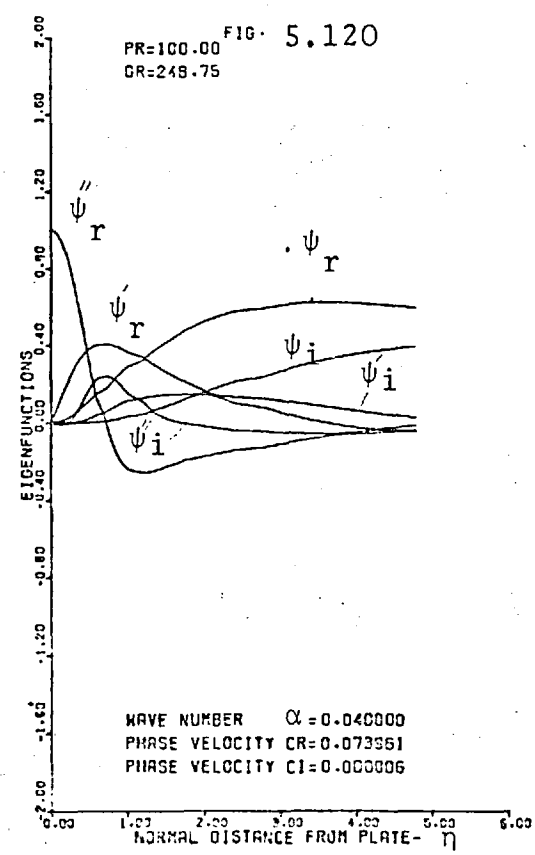

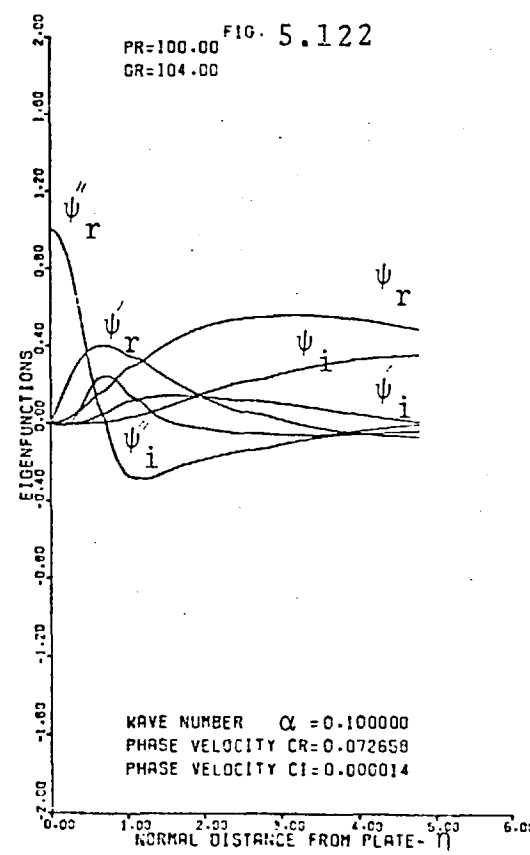

Eigenfunctions for a Prandtl number of 100.0.

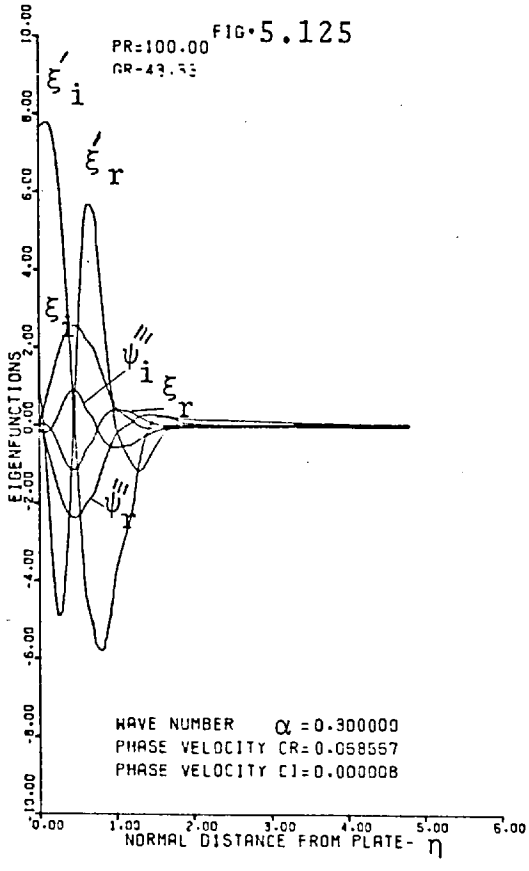

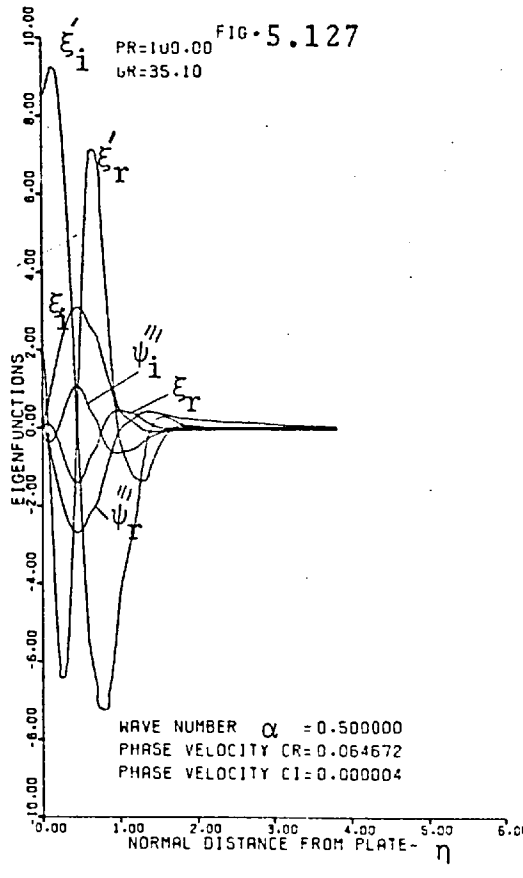

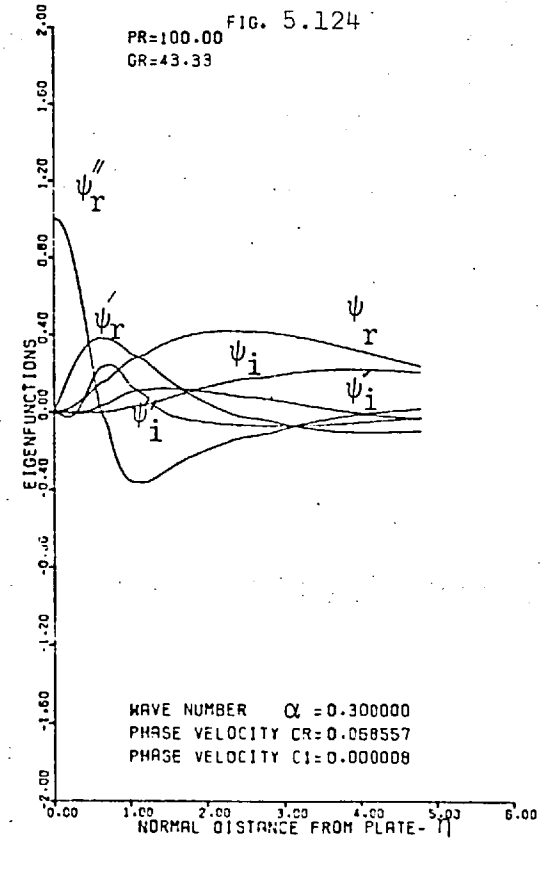

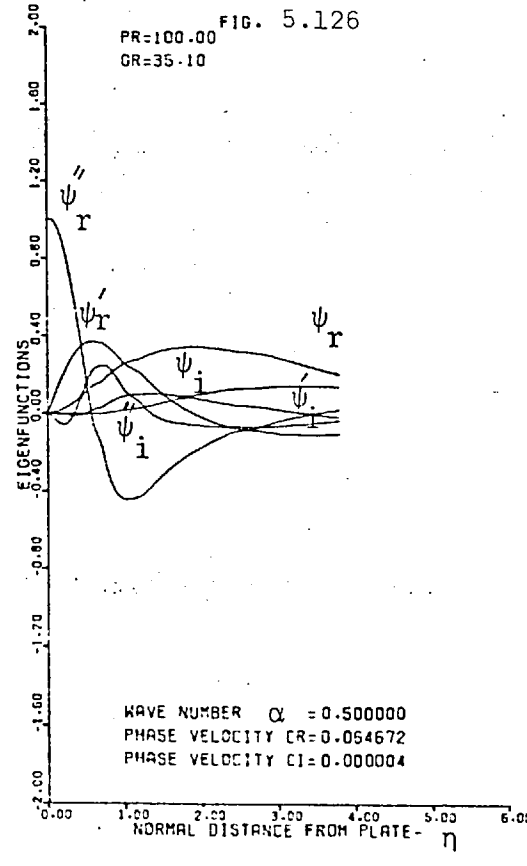

Eigenfunctions for a Prandtl number of 100.0.

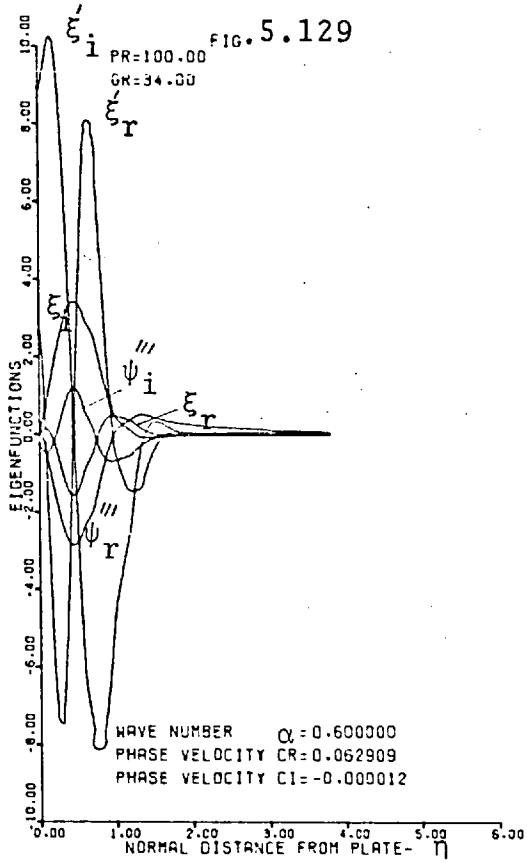

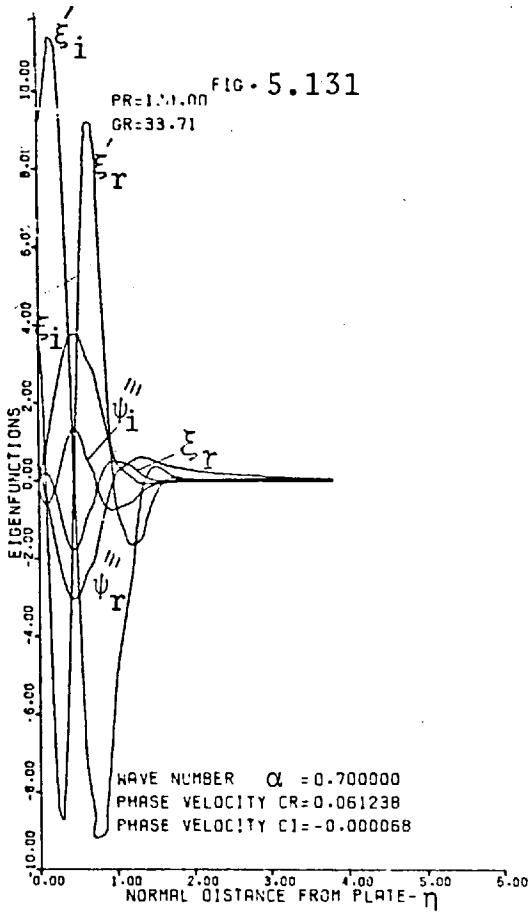

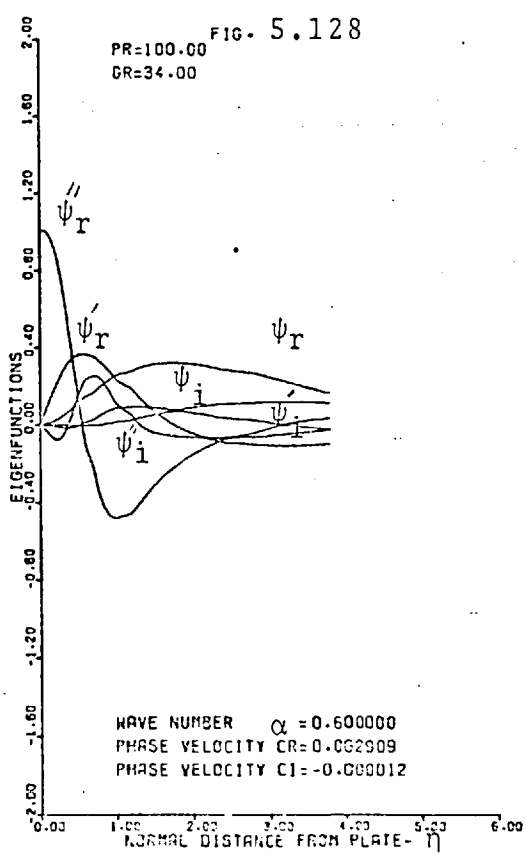

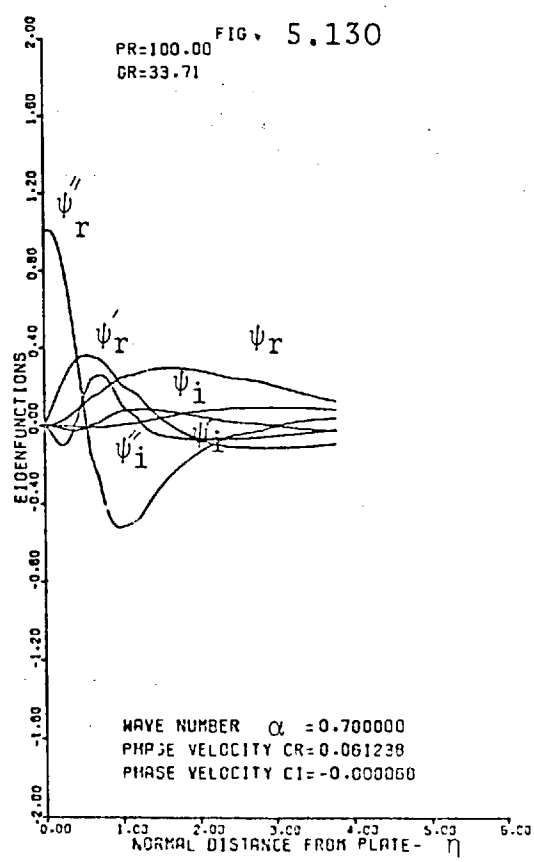

Eigenfunctions for a Prandtl number of 100.0

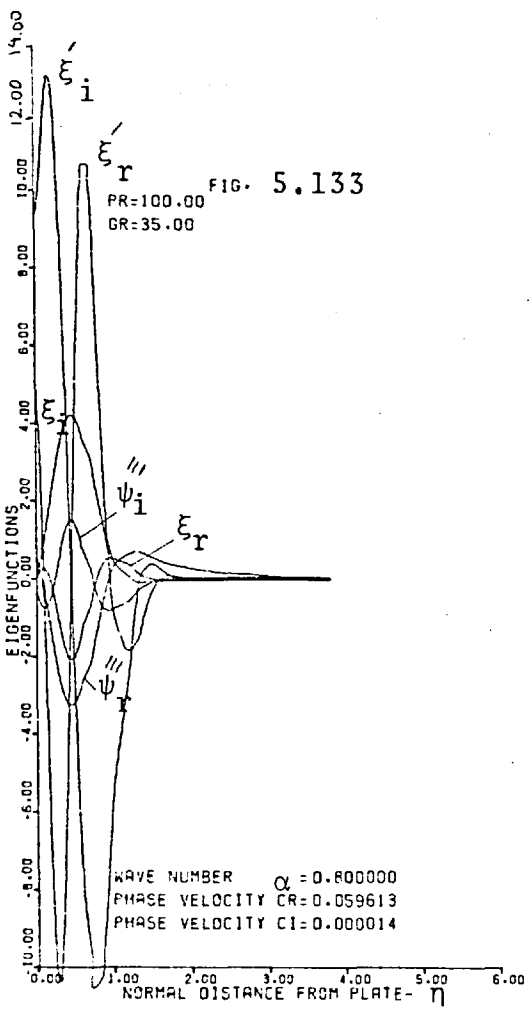

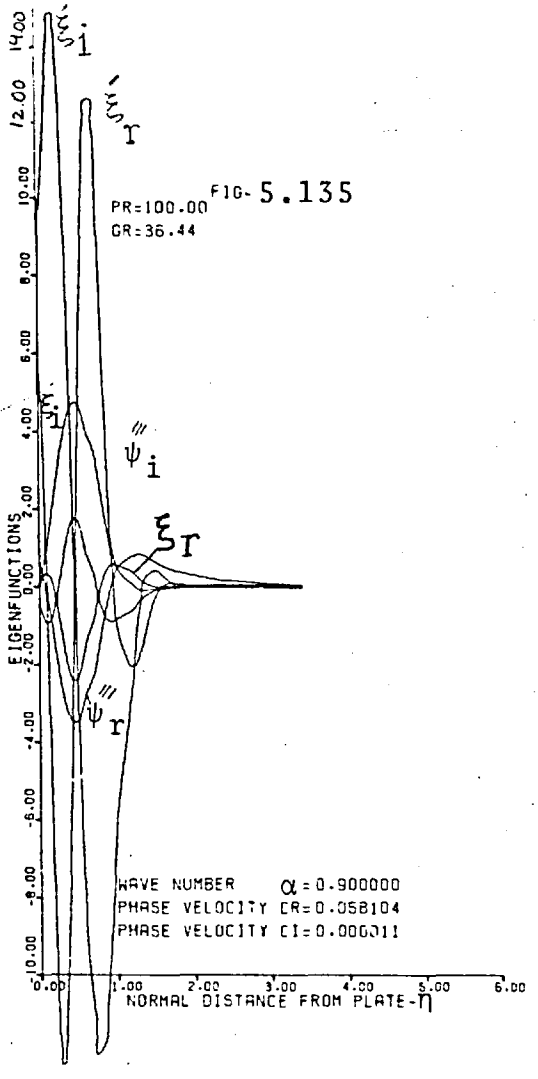

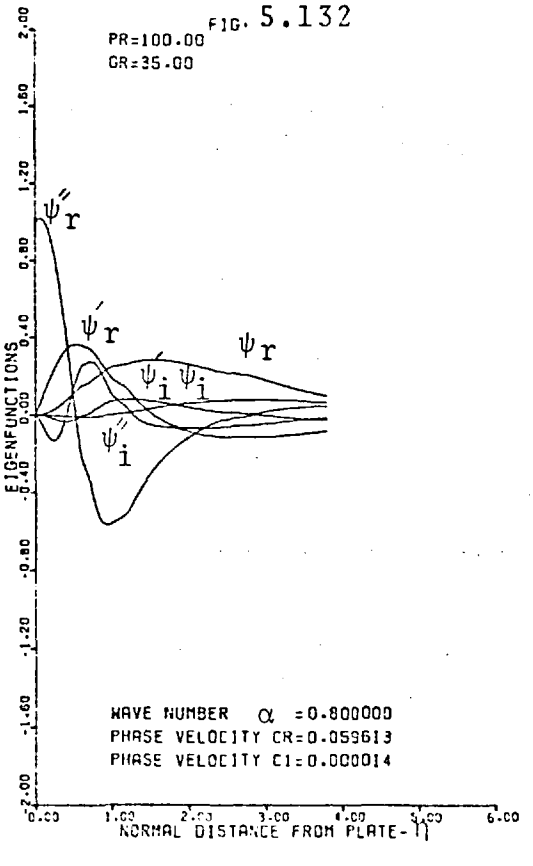

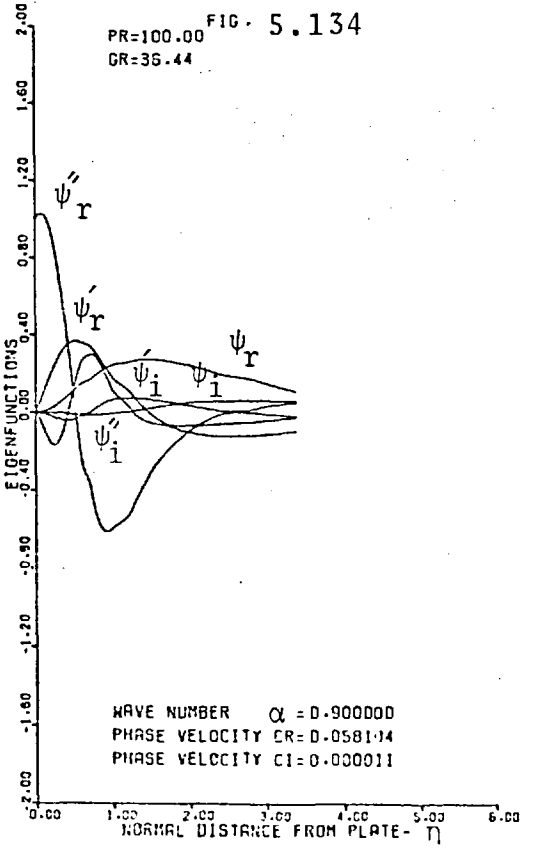

Energy distributions for a Prandtl number of 100.0.

e_{Re} = Reynolds stress e_D = Dissipation e_B = Buoyancy

FIG. 5.137

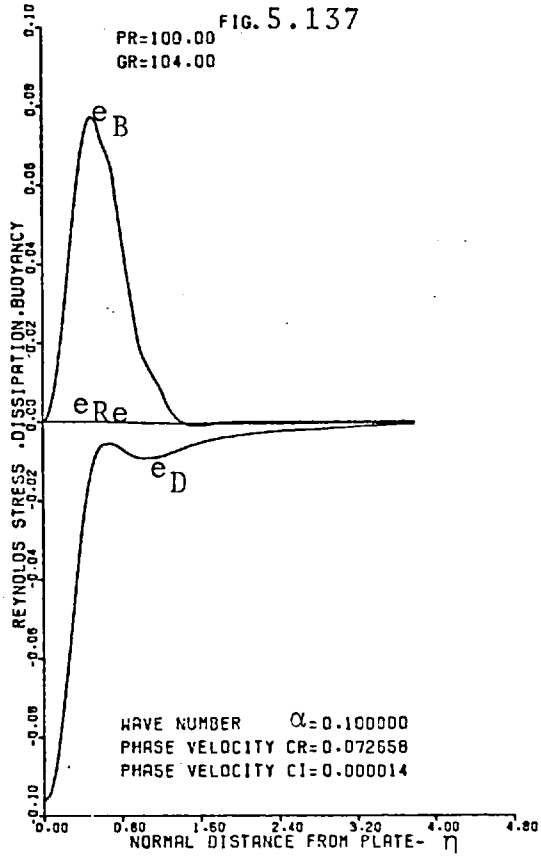

FIG. 5.139

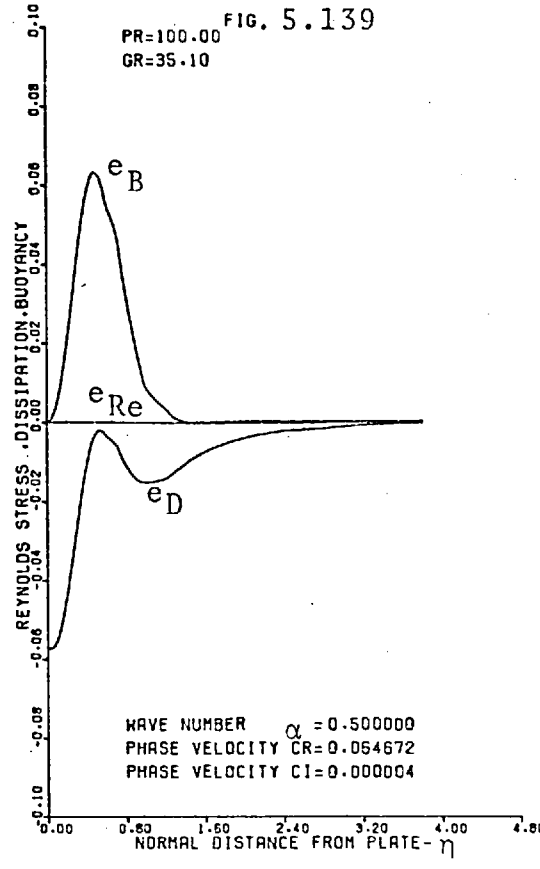

FIG. 5.136

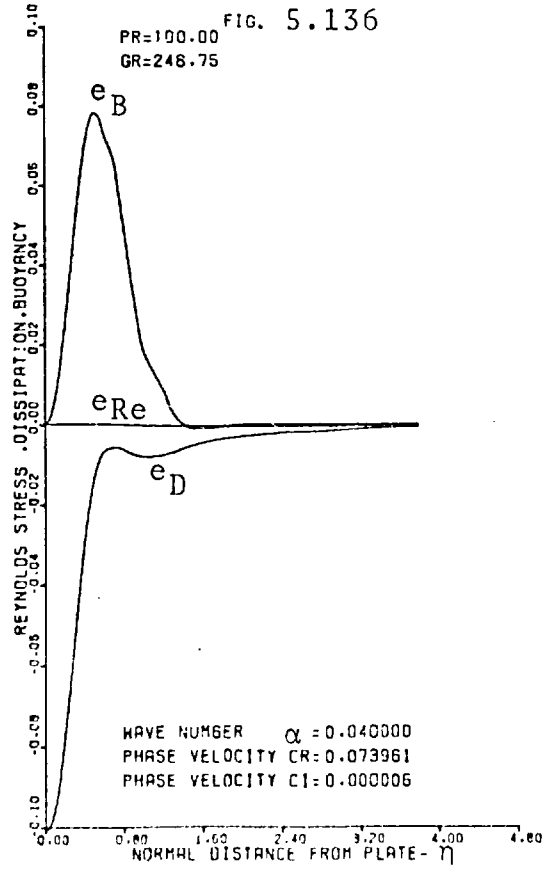

FIG. 5.138

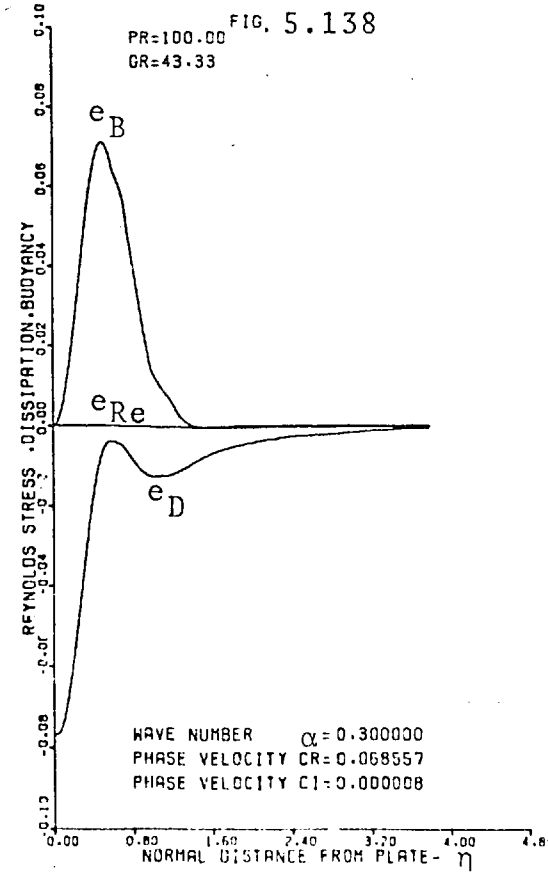

Energy distributions for a Prandtl number of 100.0.
e_{Re} = Reynolds stress e_D = Dissipation e_B = Buoyancy

FIG. 5.141

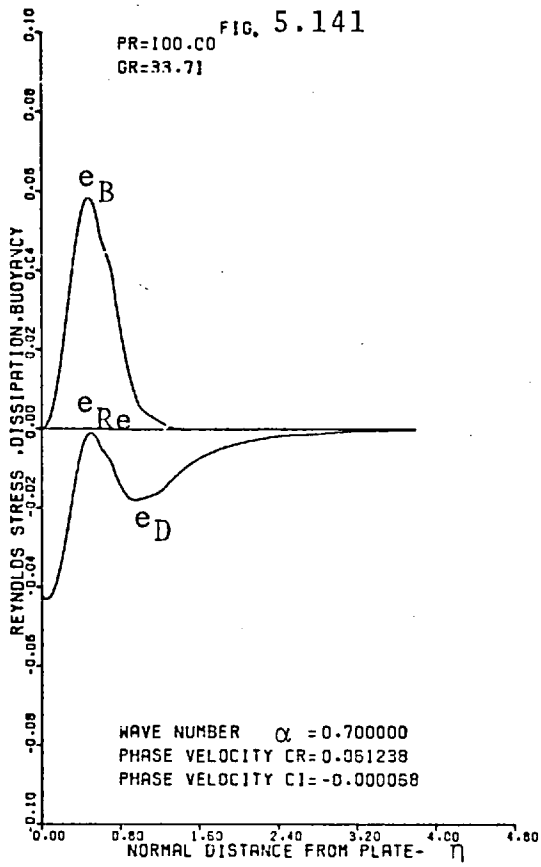

FIG. 5.143

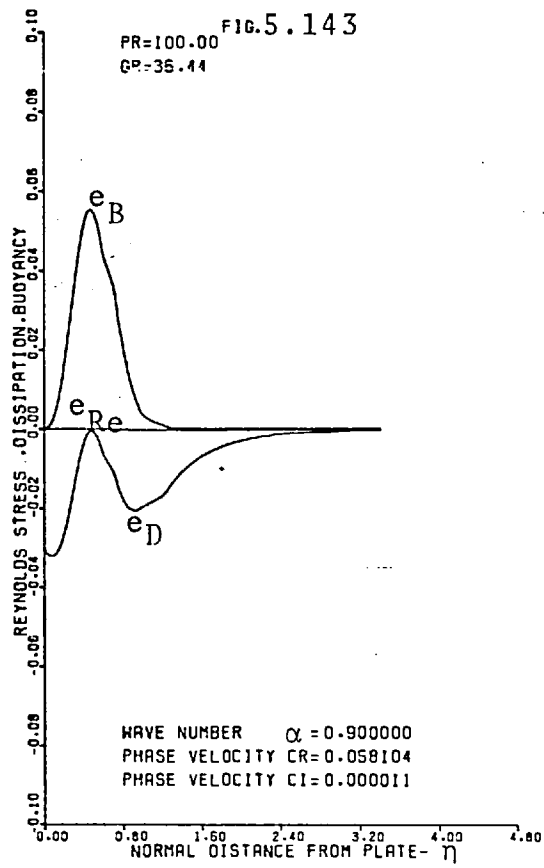

FIG. 5.140

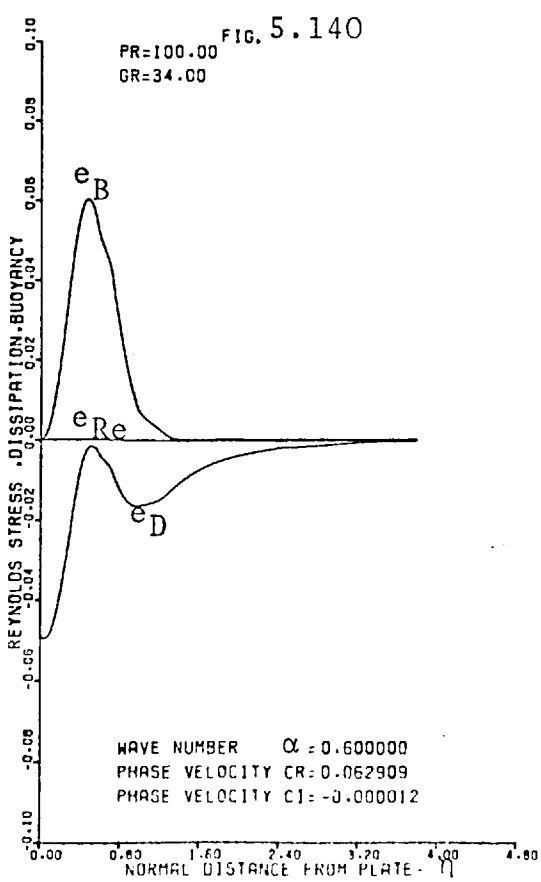

FIG. 5.142

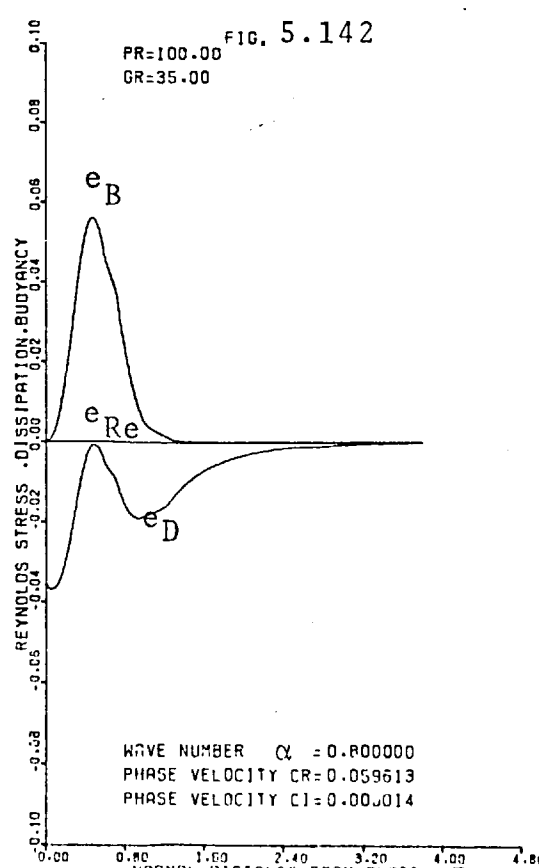

Figure 5.144 - Neutral stability curve for a Prandtl number of 1000.0 in α, Gr-plane.

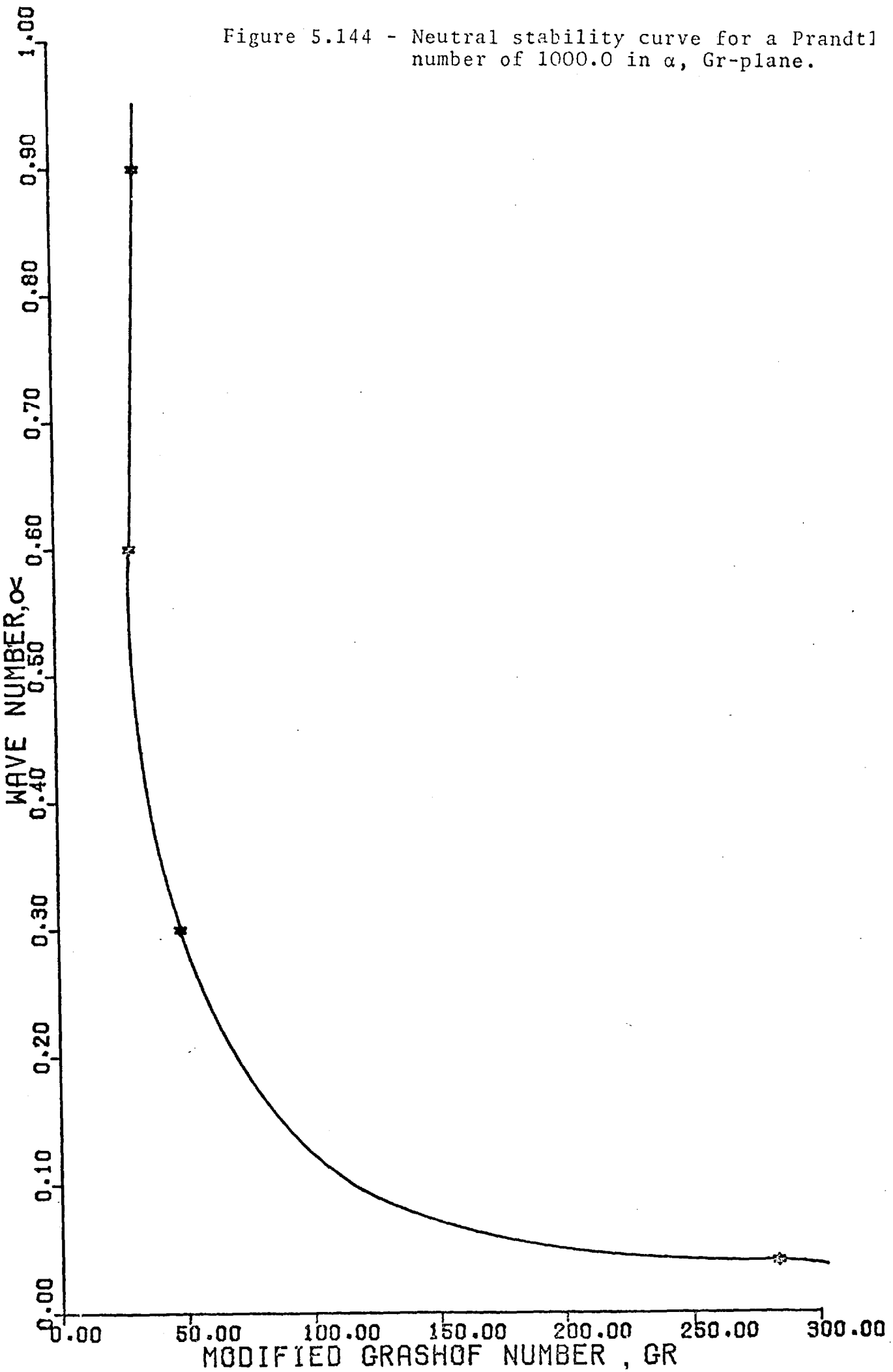

Figure 5.145 - Neutral stability curve for a Prandtl number of 1000.0 in c_r, Gr-plane.

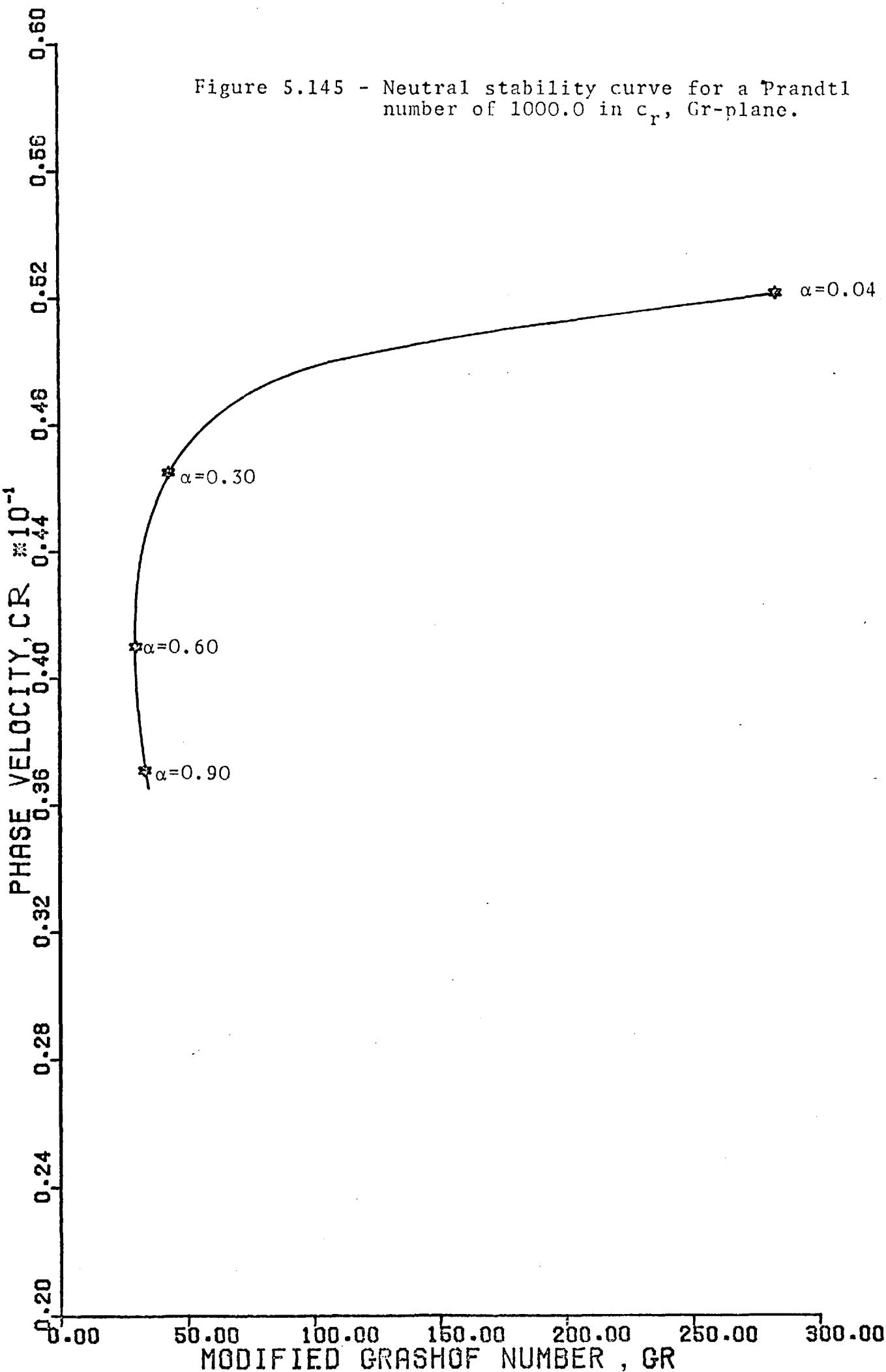

Figure 5.146. Velocity profile for a Prandtl number of 1000.0 from Schmidt and Beckmann equations.

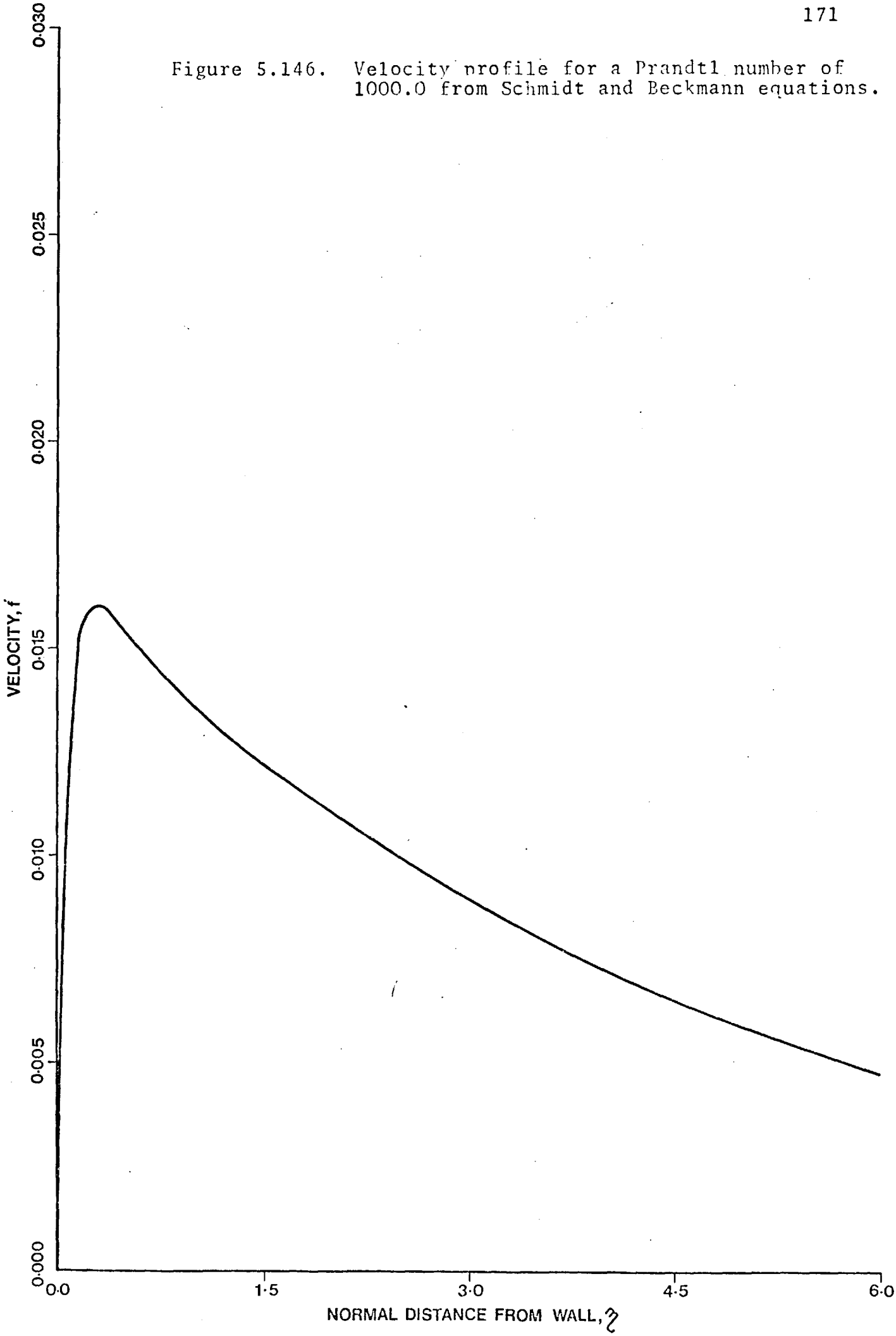

greater than the maximum velocity of the basic flow.

The real and imaginary parts of the eigenfunctions and of their derivatives and the corresponding eigenvalues for a Prandtl number of 1000.0 are presented by figures 5.147 to 5.154.

The energy distributions of the disturbed motion for a Prandtl number of 1000.0 are shown by figures 5.155 to 5.158. An examination of these figures shows that, in a manner similar to the case when the Prandtl number is 100.0, the buoyancy term in the energy balance of the disturbed motion is the only term which gives a positive contribution to the energy of the disturbed motion.

5.5. The Influence of the Prandtl Number on the Neutral Stability Curves

The neutral stability curves for Prandtl numbers of 0.733, 1.0, 6.7, 100.0 and 1000.0 in the wave number, Grashof number-plane (α, Gr-plane) are compared in figure 5.159. This figure shows that the shape of the neutral stability curves for Prandtl numbers of 0.733 and 1.0 are different from those obtained for the larger values of the Prandtl number of 6.7, 100.0 and 1000.0. There is a development of a nose-shaped piece on the neutral stability curves at Prandtl numbers of 0.733 and 1.0. The presence of the nose-shaped piece can be attributed to the changing roles of the buoyancy and Reynolds stress terms in the energy balance equation as the wave number changes. As discussed in section 5.2 for Prandtl number of 0.733 and 1.0 and for wave numbers less than 0.25 the buoyancy term in the energy balance of the disturbed motion is important

Eigenfunctions for a Prandtl number of 1000.0.

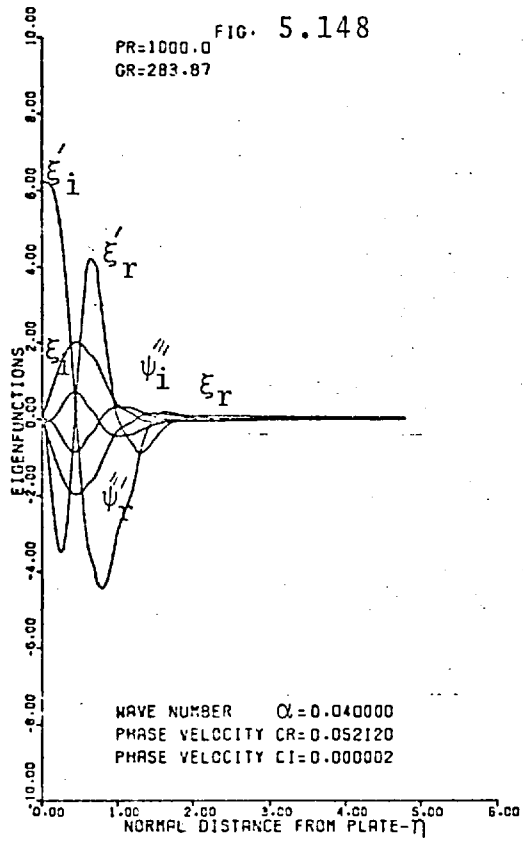

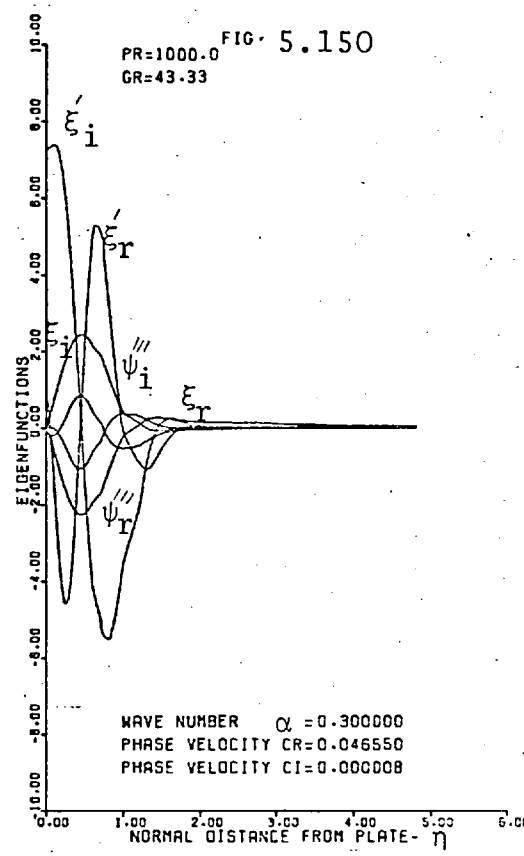

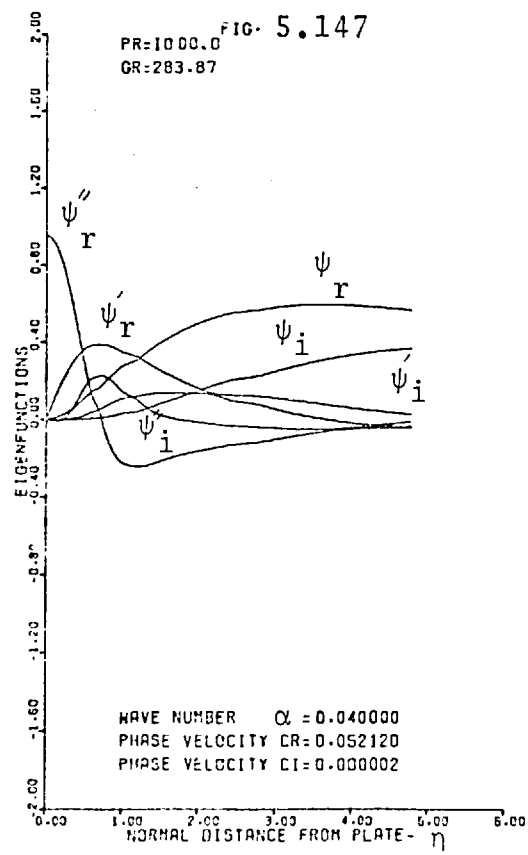

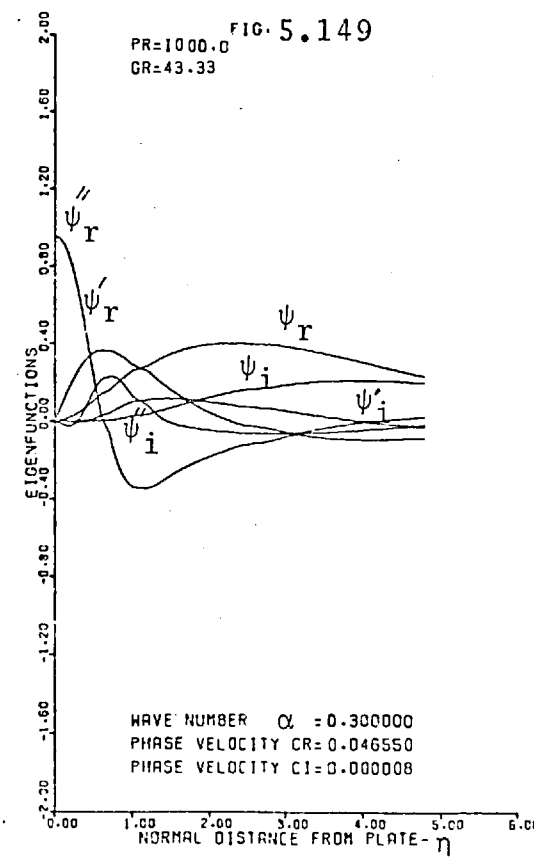

Eigenfunctions for a Prandtl number of 1000.0.

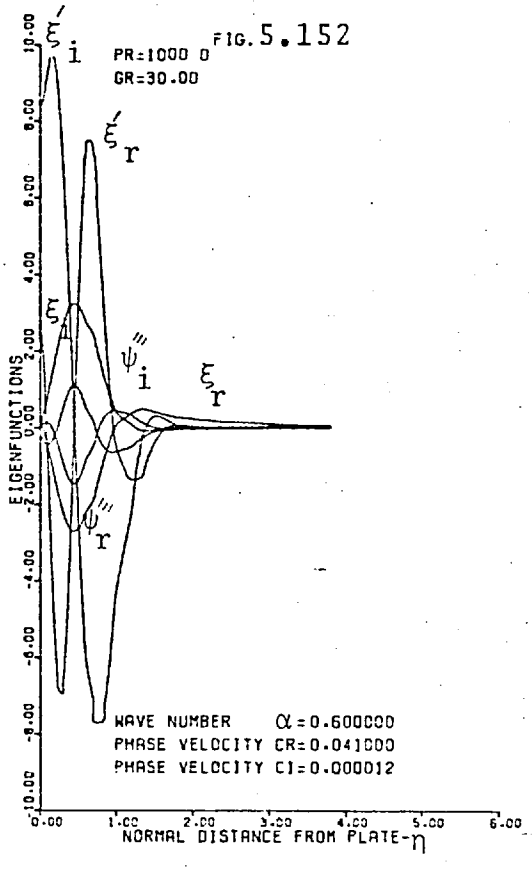

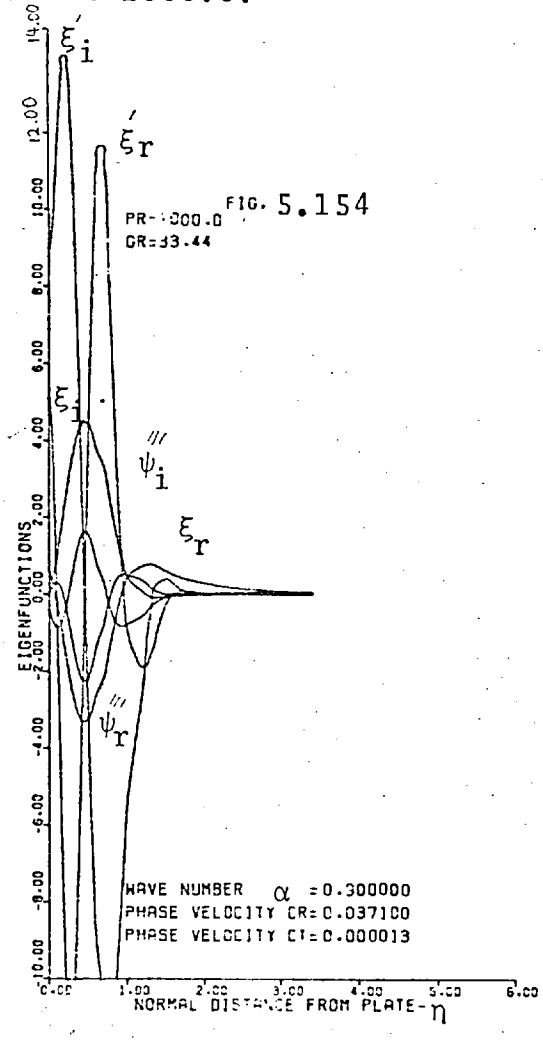

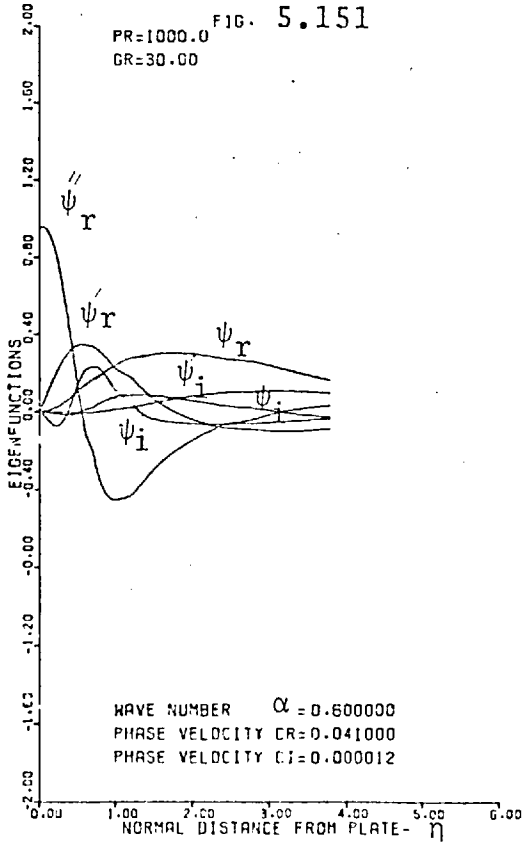

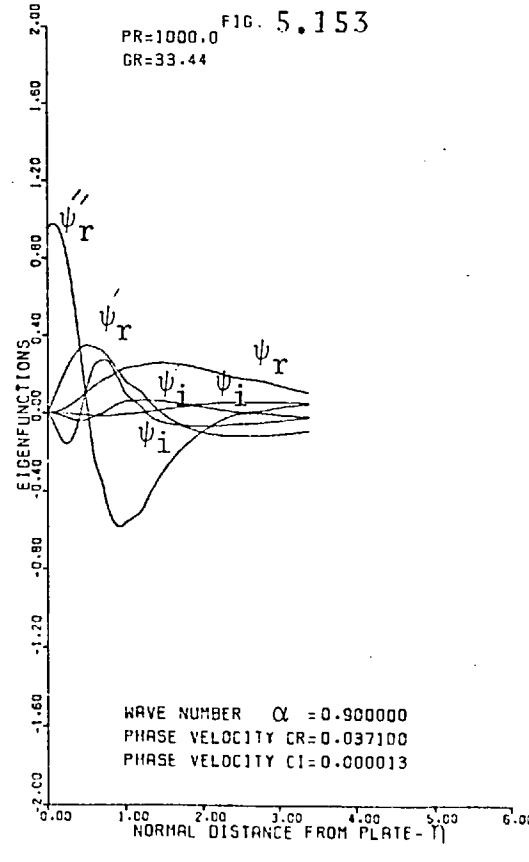

Energy distributions for a Prandtl number of 1000.0.

e_{Re} = Reynolds stress e_D = Dissipation e_B = Buoyancy

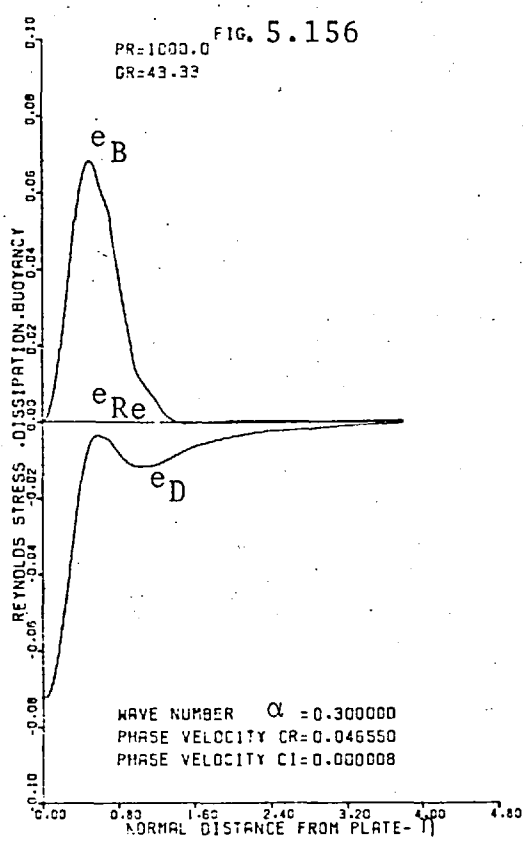

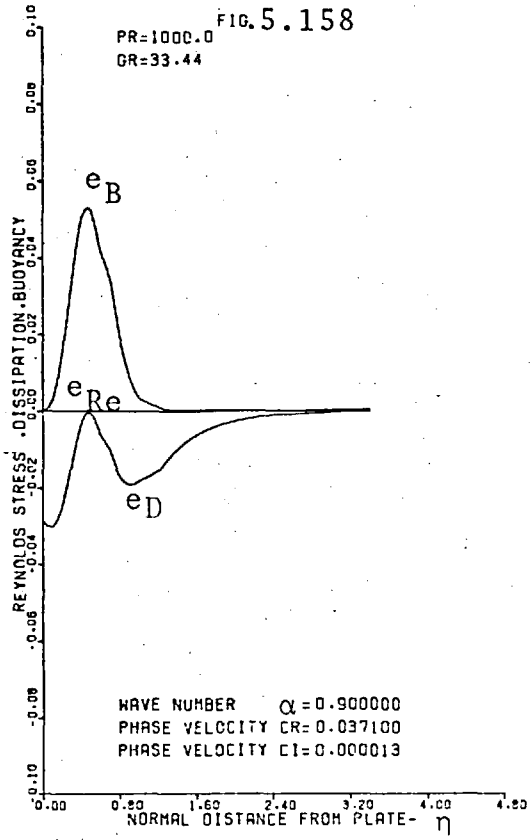

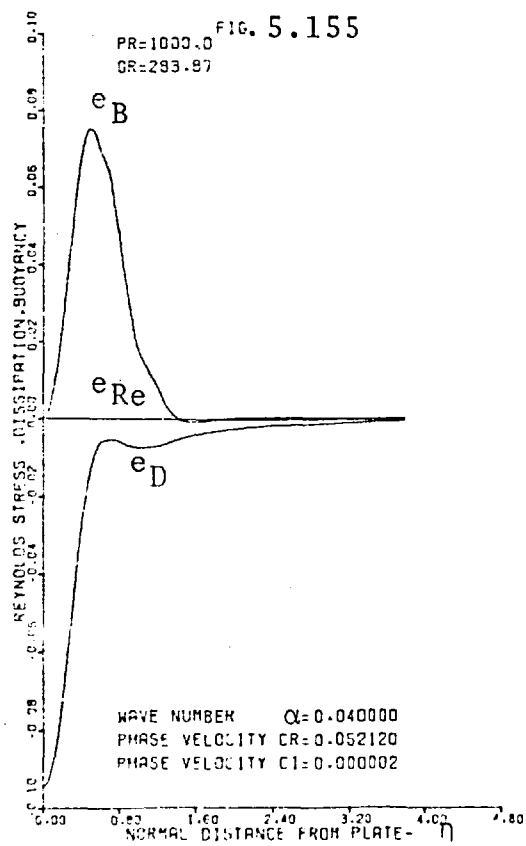

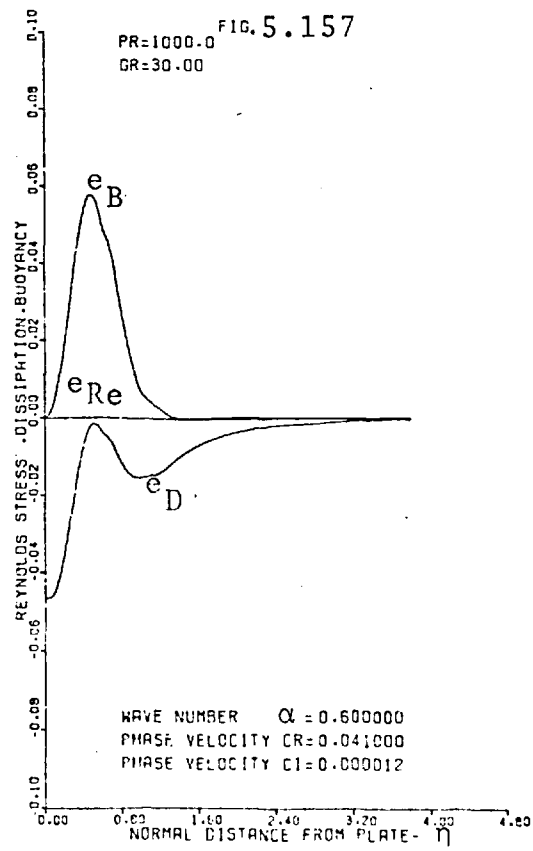

Figure 5.159 - Neutral stability curves for Prandtl numbers of 0.733, 1.0, 6.7, 100.0 and 1000.0 in α, Gr-plane.

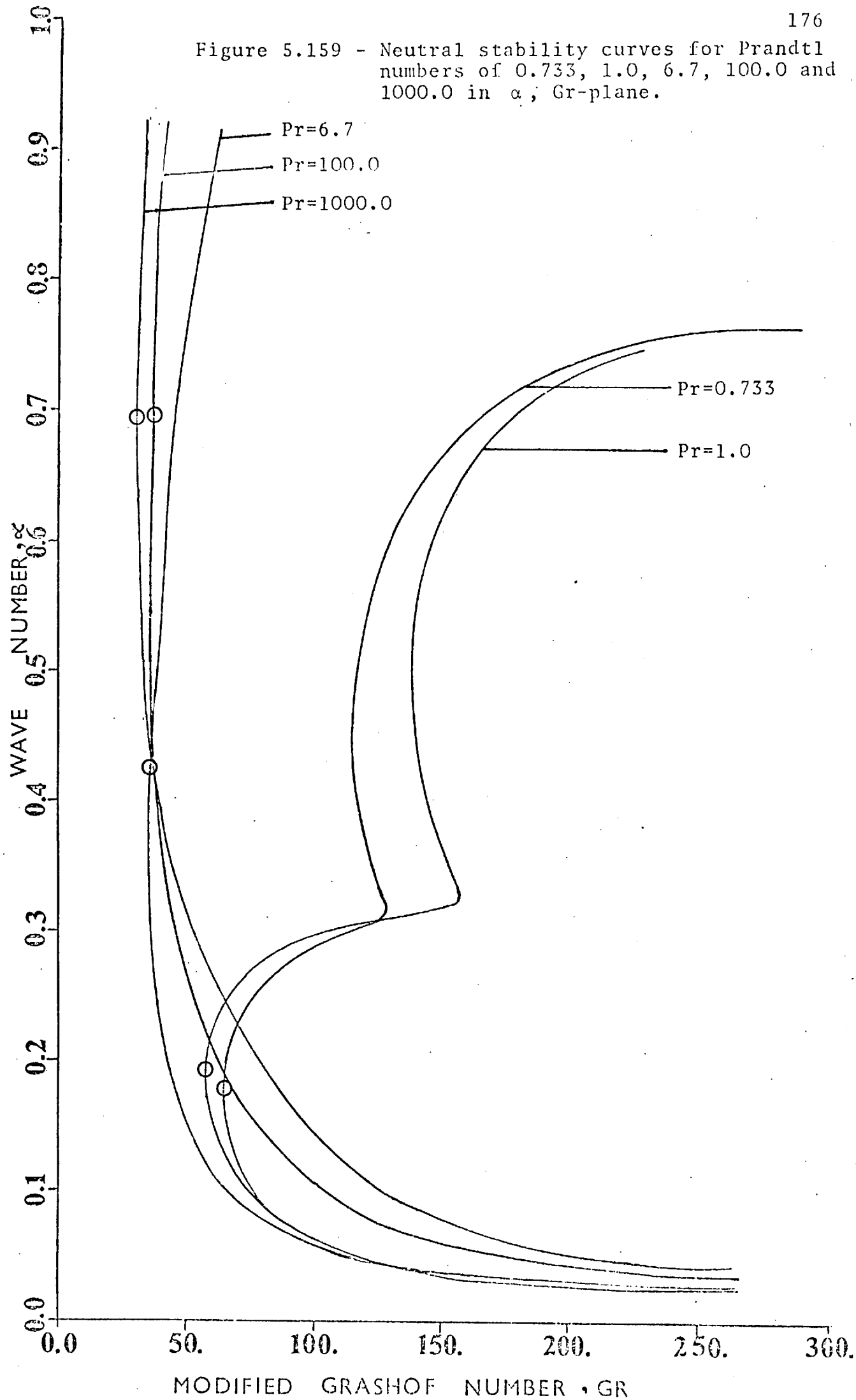

because it is the only term that gives a positive contribution to the energy of the disturbed motion whereas the Reynolds stress term subtracts energy. For wave numbers greater than about 0.25 the sign of the Reynolds stress term is reversed and at wave numbers greater than 0.35 the energy contributed by the Reynolds stress term is much larger than that contributed by buoyancy terms. Thus, the change in the shape of the neutral stability curves for Prandtl numbers of 0.733 and 1.0 at wave numbers around 0.35 is caused by the changing magnitudes of the buoyancy and Reynolds stress terms in the energy balance of the disturbed motion. For values of the Prandtl number of 6.7, 100.0 and 1000.0, the buoyancy term in the energy balance of the disturbed motion is the only term which gives a positive contribution at all ranges of the wave number and the Reynolds stress term does not make a positive contribution. Consequently a nose-shaped piece is not present on the neutral stability curves for Prandtl numbers of 6.7, 100.0 and 1000.0.

Another interesting feature of the behaviour of the neutral stability curves is that at low values of the wave number the increase in the Prandtl number is accompanied by an increase in the critical value of the Grashof number while for high values of the wave number this effect is reversed. This may be because at low values of the wave number the Reynolds stress term subtracts energy from the disturbed motion and has a stabilizing effect, secondly as the Prandtl number is increased the stabilizing effect of the Reynolds stress term increases. Thus, at low values of the wave number as the Prandtl number is increased the critical value of the Grashof number increases but at high values of wave number this effect is reversed.

5.6. The Influence of the Prandtl Number on the Minimum Critical Value of the Grashof Number

The neutral stability curves for Prandtl numbers of 0.733, 1.0, 6.7, 100.0 and 1000.0 in α, Gr-plane are shown in figure 5.159. The minimum critical value of the Grashof number are marked on the individual curves. An examination of this figure shows that as the Prandtl number is increased, the minimum critical value of the Grashof number decreases. This effect is more pronounced for Prandtl numbers in the range 0.733 to 6.7 than for the range 6.7 to 1000.0.

Figure 5.159 also shows that as the Prandtl number is increased, the value of the wave number corresponding to the minimum critical Grashof number increases. This increase is more noticeable for low values of the Prandtl number.

Figure 5.160 shows the neutral stability curves for Prandtl numbers of 0.733, 1.0, 6.7, 100.0 and 1000.0 in Cr, Gr-plane. A comparison between the neutral stability curves shows that as Prandtl number is increased the value of the phase velocity corresponding to the minimum critical Grashof number decreases. This effect is more pronounced for Prandtl numbers in the range 0.733 to 100.0 than for the range 100.0 to 1000.0.

Figure 5.160 - Neutral stability curves for Prandtl numbers of 0.733, 1.0, 6.7, 100.0 and 1000.0 in c_r, Gr-plane.

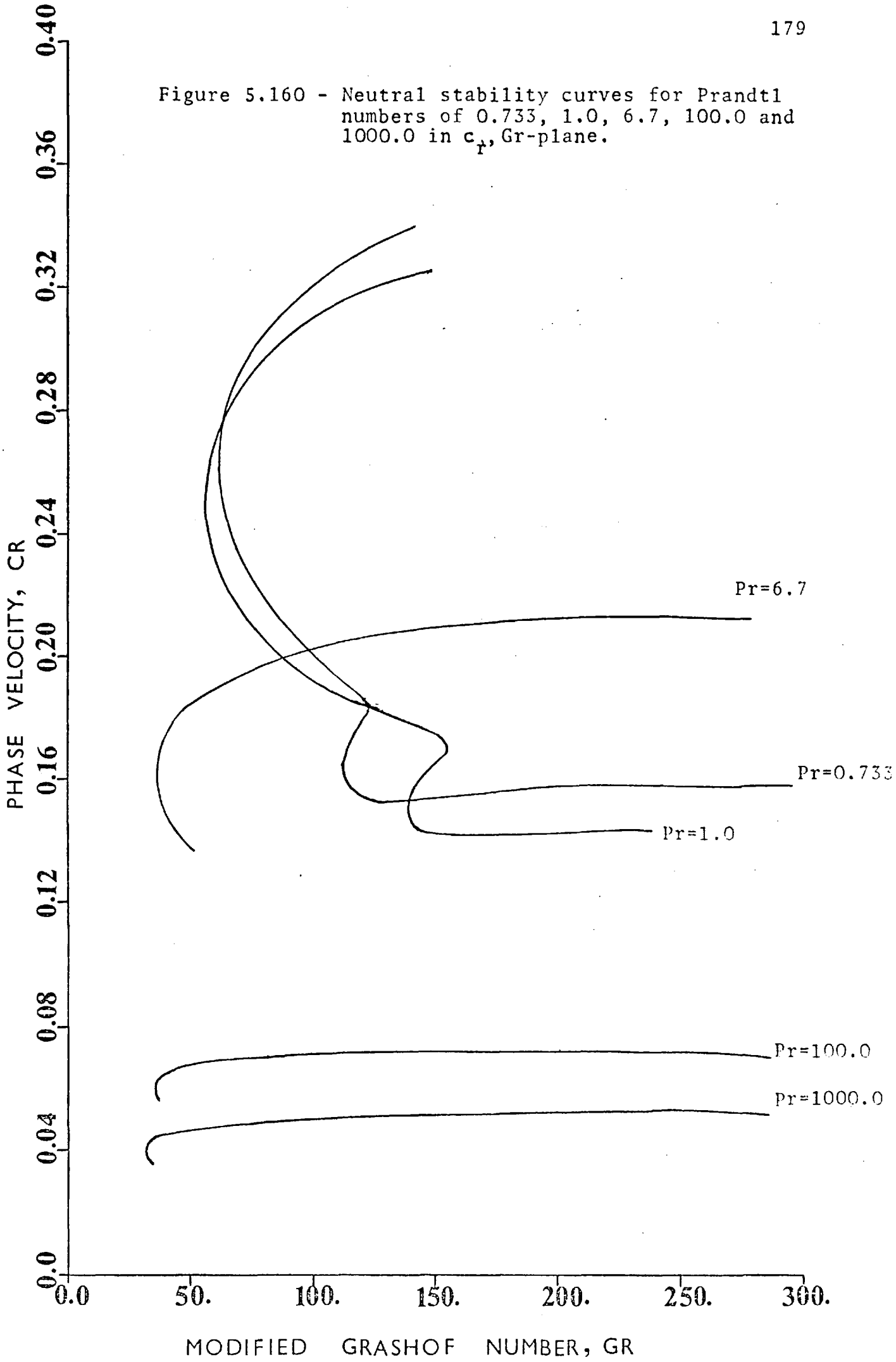

5.7. Comparison of the Present Results with the Existing Experimental Results

In order to assess the reliability of the present work, the neutral stability curves for Prandtl numbers of 0.733 and 6.7 are compared with the experimental results of the other workers. There have been no experimental results for neutral stability curves for Prandtl numbers of 1.0, 100.0 and 1000.0 with which the present results can be compared.

Figure 5.161 shows a comparison of the neutral stability curve for Prandtl numbers of 0.733 with the experimental results which have been obtained by other workers. Before examining figure 5.161, it is worth considering that the experimental investigations of the stability of the free-convection boundary layer flows over a vertical plate [see Chapter 2]. These investigations have involved the observation of natural and artificial oscillations. Figure 5.161 shows that the experimental results of Polymeropoulos and Gebhart [5] based on the observation of artificial oscillations are in agreement with the present theoretical results. The experimental results of Eckert and Soehghen [21], Lock et al. [64] and Polymeropoulos [65] based on the observations of the natural oscillations, are also shown in figure 5.161 which reveals a considerable disagreement with present results. The explanation of this disagreement is outlined as follows: First , natural oscillations are too small to be detected during their initial stages of amplifications [5], consequently the observation of natural oscillation alone does not give any definite information either on the location of the neutral stability curve, or on the question of the applicability of

Figure 5.161 - A comparison between the neutral stability curve of present work with experimental data for air, Prandtl number of 0.733.

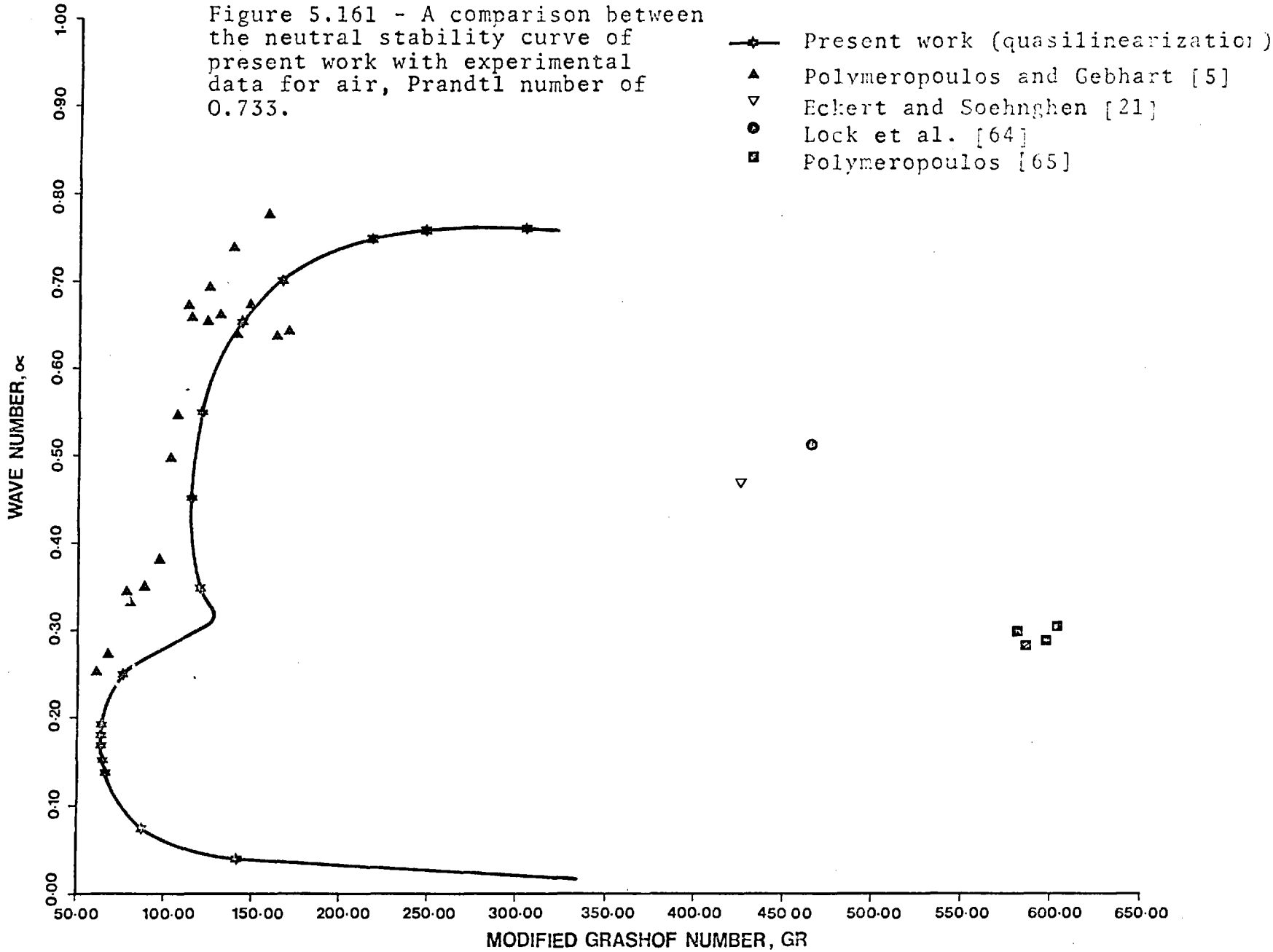

Figure 5.162 - A comparison between the neutral stability curve of present work with experimental data for water, Prandtl number of 6.7.

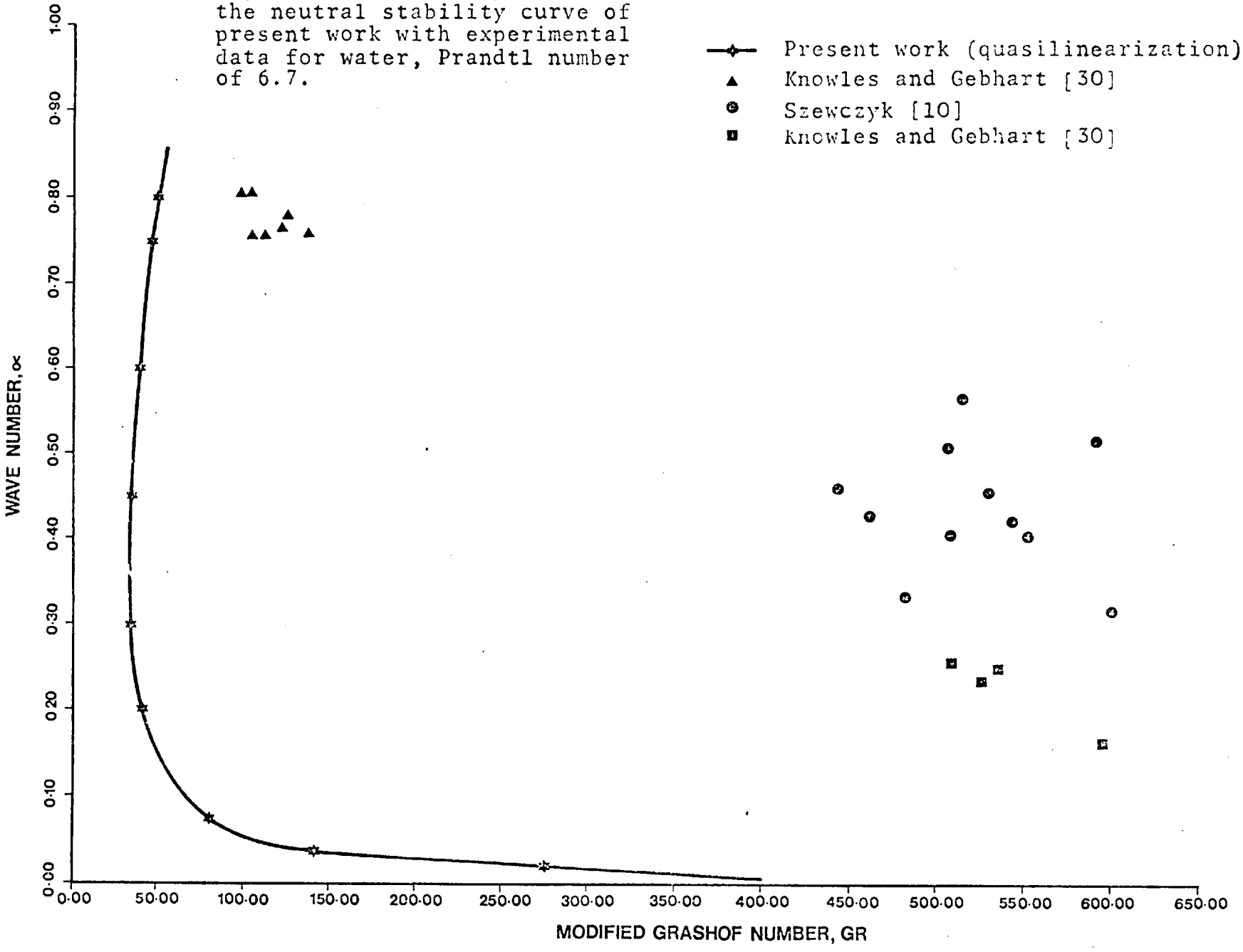

linear stability theory to free-convection boundary layer flows. Secondly, natural disturbances arise out of disturbances at the most amplified frequencies, rather than from a disturbance at the frequency which first begins to amplify [29], consequently all of the points which have been obtained for natural instability [see figure 5.161] lie in the unstable part of the stability plane and, in particular, in the regions which would be reached by disturbances of frequencies which amplify at a high rate.

The experimental results for Prandtl number of 6.7 are compared with the results of the present work in figure 5.162. It can again be concluded that the experimental results of Knowles and Gebhart [30] based on the observation of the artificial oscillations are in agreement with the present results but the other workers' results based on the natural oscillations are not in agreement.

Figures 5.163 and 5.164 show a comparison of the neutral stability curves for Prandtl numbers of 0.733, 1.0, 6.7, 100.0 and 1000.0 using the quasilinearization and the trial-and-error techniques which reveal that the results of the trial-and-error technique are in good agreement with the quasilinearization technique within one per cent accuracy.

Figure 5.163 - A comparison between the neutral stability curves of present work using the quasi-linearization technique with those using trial-and-error technique.

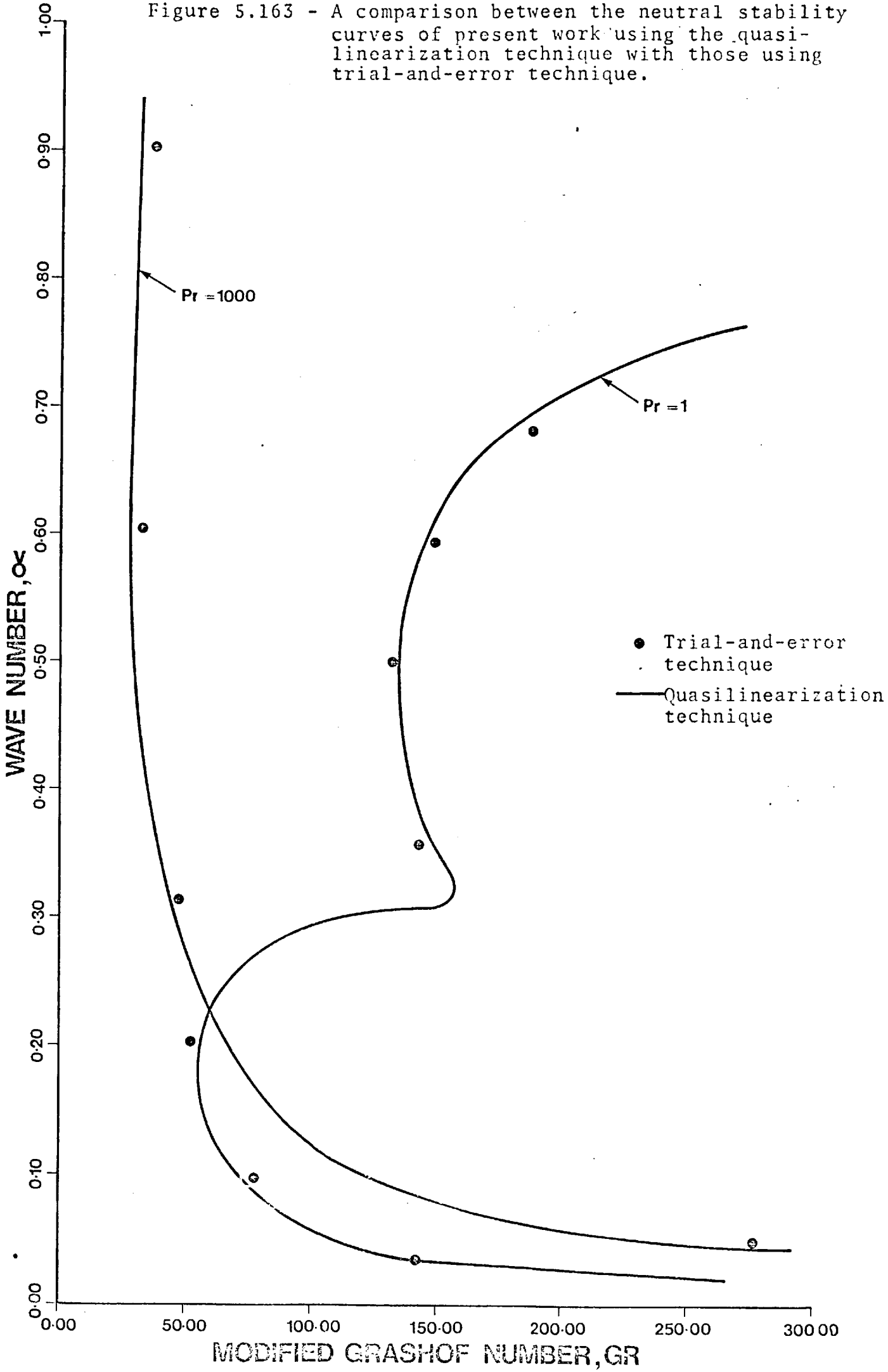

Figure 5.164 - A comparison between the neutral stability curves of present work using the quasi-linearization technique with those using trial-and-error technique.

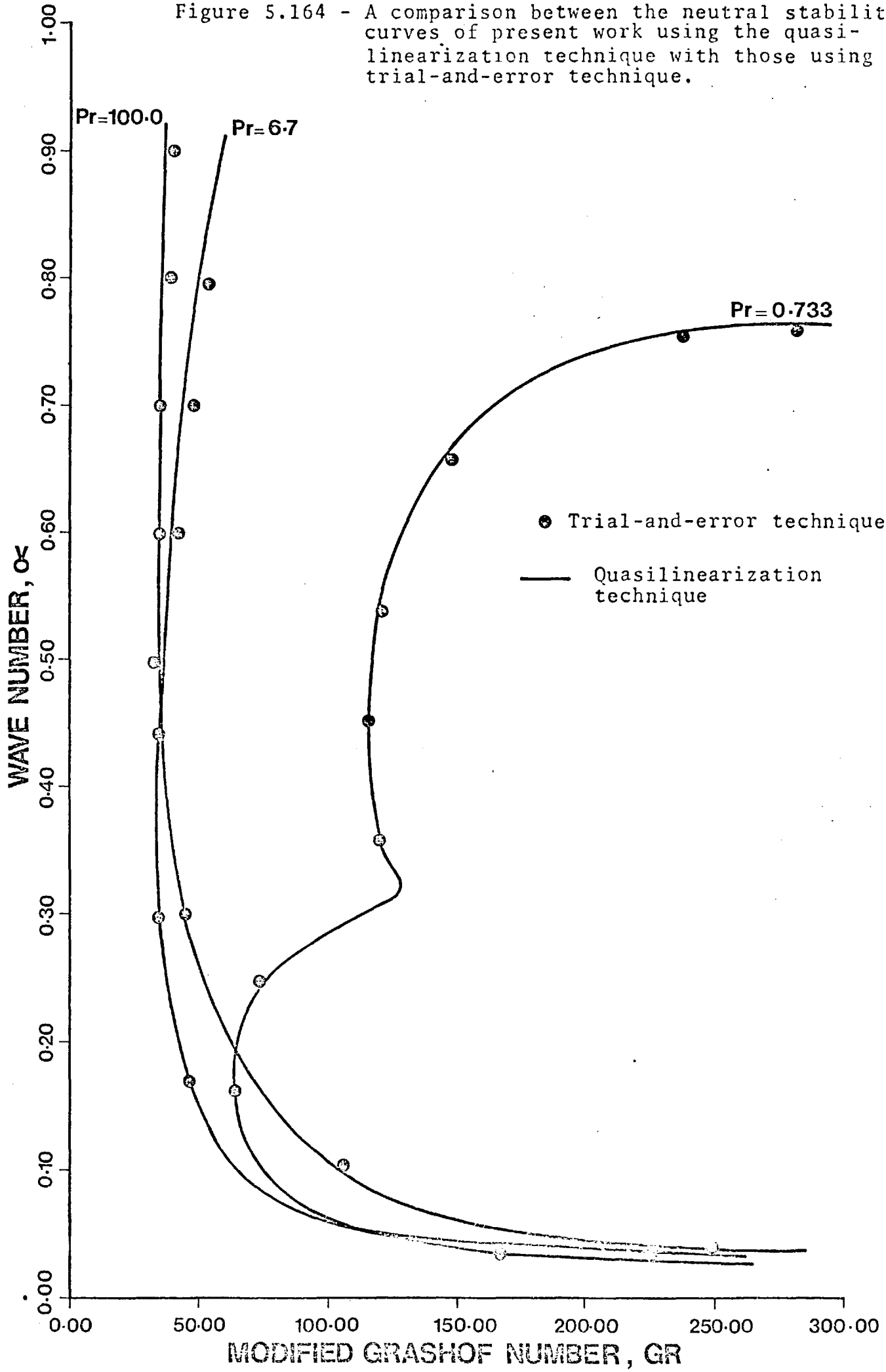

CHAPTER 6

CONCLUSIONS

The results of the present study may be summarized as follows:

1) The disturbance differential equations which govern the instability of free-convection boundary layer flows along an isothermal vertical plate have been derived. The derivation was based upon linear stability theory and on the introduction of a perturbation stream function and perturbation temperature function. These equations were rewritten in dimensionless form by the introduction of dimensionless variables.

2) The disturbance differential equations were solved by two different techniques:

i) A quasilinearization technique was used to solve the boundary value problem associated with solution of the two ordinary disturbance differential equations. The disturbance differential equations were solved for a range of Prandtl numbers 0.733 to 1000.0 and for a range of Grashof numbers 2×10^4 to 10^8.

ii) A trial-and-error technique was developed by the use of Cauchy-Riemann relations. This technique was employed for solving the disturbance differential equations for the ranges of Prandtl number and Grashof number stated above. For the trial-and-error technique very accurate estimates of the unknown parameters were needed in order to obtain a solution, while in the application of the quasilinearization technique only crude initial guesses were required. It was found that when accurate initial guesses were provided the trial-and-error technique required less computation time than the quasilinearization technique for the same accuracy.

Therefore, the quasilinearization technique may be used to supply initial guesses which can then be used in the trial-and-error thus saving computation time.

3) A computer program was written to solve the boundary value problems associated with the disturbance differential equations. This program was written in a general form and may be adapted to solve boundary value problems not necessarily associated with the problem of the instability of the free-convection boundary layer flows along a vertical plate.

4) The unknown boundary conditions and eigenvalues were determined with an accuracy of four decimal places. Within this accuracy the size of the integration step length, the value of the convergence criterion and the effective boundary layer thickness were optimized.

5) Neutral stability curves were obtained in the wave number, Grashof number-plane (α, Gr-plane) and in the phase velocity, Grashof number-plane (Cr, Gr-plane) for Prandtl numbers of 0.733, 1.0, 6.7, 100.0 and 1000.0.

6) A comparison of the neutral stability curves for different Prandtl numbers showed that the value of the Prandtl number influences the minimum critical value of the Grashof number. As the Prandtl number was increased, it was observed that the minimum critical value of the Grashof number decreased. This effect was more pronounced for Prandtl numbers in the range 0.733 to 6.7 than for the range 6.7 to 1000.0.

7) It was found that as the Prandtl number was increased, the value of the wave number, α, corresponding to the minimum critical Grashof number, increased. The increase was more noticeable for low values of Prandtl number.

8) A comparison of the neutral stability curves in the phase velocity, Grashof number-plane for different Prandtl numbers revealed that as the Prandtl number was increased, the value of the phase velocity corresponding to the minimum critical Grashof number decreased. This effect was more pronounced for Prandtl numbers in the range 0.733 to 100.0 than for the range 100.0 to 1000.0.

9) A kinetic energy balance equation for disturbed motion was solved in order to find the importance of the buoyancy term in the disturbance differential equations. It was found that neglect of the temperature fluctuations for the purpose of solving the disturbance equations for Prandtl numbers of 0.733 and 1.0 may only be justified for wave numbers greater than 0.35. However, for Prandtl numbers of 6.7 and greater it was found that the temperature fluctuations introduce instability at all values of the wave numbers.

10) The minimum critical Grashof numbers were found to correspond to values of the wave number at which the phase velocity of the disturbance wave was greater than the maximum velocity of the basic laminar flow, consequently no critical layers were found to exist. Therefore, asymptotic methods in the form of expansions about the critical layers cannot provide a reliable value of the minimum Grashof number.

11) The neutral stability curves for Prandtl numbers of 0.733 and 6.7 were compared with the experimental results obtained by other workers based on artificial oscillations. The comparison showed that the experimental results were in good agreement with predicted curves. Thus it may be concluded that linear stability theory can be used for the prediction of

the instability of free-convection boundary layer flows.

12) It is to be hoped that some future work will be directed towards:-

i) obtaining the neutral stability curves for the range of the Prandtl numbers of 1.0 to 6.7 which can be useful in an interpretation of the influence of the Prandtl number on the neutral curves.

ii) a study of the instability of free-convection boundary layer flows along curved surfaces.

APPENDIX A

CONDITIONS TO BE SATISFIED AT THE EDGE OF BOUNDARY LAYER

Conditions to be satisfied at edge of boundary layer

The technique used by Brown in reference [66] is used to eliminate the arbitrary constants in equations (3.2.47) and (3.2.48) in order to obtain a set of linear and homogeneous relations in the dependent variables of equations (3.2.41) and (3.2.42) and their derivatives, which are to be satisfied at the edge of the boundary layer.

In order to satisfy the boundary conditions (3.2.44), it is necessary that $c_1 = c_3 = c_5 = 0$. Further, in order that the solutions (3.2.47) and (3.2.48) agree with the numerical solution of equations (3.2.41) and (3.2.42) is obtained by numerical integration when $\eta = \eta_{edg}$, it is necessary that

$$\psi = c_1\exp(\alpha\eta_{edg}) + c_2\exp(-\alpha\eta_{edg}) + c_3\exp(\beta\eta_{edg}) + c_4\exp(-\beta\eta_{edg}) + c_5\exp(\gamma\eta_{edg}) + c_6\exp(-\gamma\eta_{edg}) \quad \text{(A-1)}$$

Thus:

$$\psi' = c_1\alpha\exp(\alpha\eta_{edg}) - c_2\alpha\exp(-\alpha\eta_{edg}) + c_3\beta\exp(\beta\eta_{edg}) - c_4\beta\exp(-\beta\eta_{edg}) + c_5\gamma\exp(\gamma\eta_{edg}) - c_6\gamma\exp(-\gamma\eta_{edg}) \quad \text{(A-2)}$$

$$\psi'' = c_1\alpha^2\exp(\alpha\eta_{edg}) + c_2\alpha^2\exp(-\alpha\eta_{edg}) + c_3\beta^2\exp(\beta\eta_{edg}) + c_4\beta^2\exp(-\beta\eta_{edg}) + c_5\gamma^2\exp(\gamma\eta_{edg}) + c_6\gamma^2\exp(-\gamma\eta_{edg}) \quad \text{(A-3)}$$

$$\psi''' = c_1\alpha^3\exp(\alpha\eta_{edg}) - c_2\alpha^3\exp(-\alpha\eta_{edg}) + c_3\beta^3\exp(\beta\eta_{edg}) - c_4\beta^3\exp(-\beta\eta_{edg}) + c_5\gamma^3\exp(\gamma\eta_{edg}) - c_6\gamma^3\exp(-\gamma\eta_{edg}) \quad \text{(A-4)}$$

$$\xi = -c_5\frac{(\gamma^2-\alpha^2)(\gamma^2-\beta^2)\exp(\gamma\eta_{edg})}{\gamma} + c_6\frac{(\gamma^2-\alpha^2)(\gamma^2-\beta^2)\exp(-\gamma\eta_{edg})}{\gamma} \quad \text{(A-5)}$$

$$\xi' = -c_5(\gamma^2-\alpha^2)(\gamma^2-\beta^2)\exp(\gamma\eta_{edg}) - c_6(\gamma^2-\alpha^2)(\gamma^2-\beta^2)\exp(-\gamma\eta_{edg}) \quad \text{(A-6)}$$

The left hand sides of equations (A-1) to (A-6) are obtained from numerical integration of equations (3.2.41) and (3.2.42) from $\eta = 0$ to $\eta = \eta_{edg}$. The solution of equations (A-1) to (A-6) gives the arbitrary constants $(c_1, c_2, \ldots, c_5)$. Since $c_1 = c_2 = c_5 = 0$, the three determinants that give c_1, c_3, and c_5 must be vanish. Hence,

$$\begin{vmatrix} \psi & 1 & 1 & 1 & 1 & 1 \\ \psi' & -\alpha & \beta & -\beta & \gamma & -\gamma \\ \psi'' & \alpha^2 & \beta^2 & \beta^2 & \gamma^2 & \gamma^2 \\ \psi''' & -\alpha^3 & \beta^3 & -\beta^3 & \gamma^3 & -\gamma^3 \\ \xi & 0 & 0 & 0 & -\frac{(\gamma^2-\alpha^2)(\gamma^2-\beta^2)}{\gamma} & \frac{(\gamma^2-\alpha^2)(\gamma^2-\beta^2)}{\gamma} \\ \xi' & 0 & 0 & 0 & -(\gamma^2-\alpha^2)(\gamma^2-\beta^2) & -(\gamma^2-\alpha^2)(\gamma^2-\beta^2) \end{vmatrix} = 0 \quad \text{(A-7)}$$

$$\begin{bmatrix} 1 & 1 & \psi & 1 & 1 & 1 \\ \alpha & -\alpha & \psi' & -\beta & \gamma & -\gamma \\ \alpha^2 & \alpha^2 & \psi'' & \beta^2 & \gamma^2 & \gamma^2 \\ \alpha^3 & -\alpha^3 & \psi''' & -\beta^3 & \gamma^3 & -\gamma^3 \\ 0 & 0 & \xi & 0 & -\frac{(\gamma^2-\alpha^2)(\gamma^2-\beta^2)}{\gamma} & \frac{(\gamma^2-\alpha^2)(\gamma^2-\beta^2)}{\gamma} \\ 0 & 0 & \xi' & 0 & -(\gamma^2-\alpha^2)(\gamma^2-\beta^2) & -(\gamma^2-\alpha^2)(\gamma^2-\beta^2) \end{bmatrix} = 0$$

(A-8)

$$\begin{bmatrix} 1 & 1 & 1 & 1 & \psi & 1 \\ \alpha & -\alpha & \beta & -\beta & \psi' & -\gamma \\ \alpha^2 & \alpha^2 & \beta^2 & \beta^2 & \psi'' & \gamma \\ \alpha^3 & -\alpha^3 & \beta^3 & -\beta^3 & \psi''' & -\gamma^3 \\ 0 & 0 & 0 & 0 & \xi & \frac{(\gamma^2-\alpha^2)(\gamma^2-\beta^2)}{\gamma} \\ 0 & 0 & 0 & 0 & \xi' & -(\gamma^2-\alpha^2)(\gamma^2-\beta^2) \end{bmatrix} = 0$$

(A-9)

Equation (A-7) to (A-9) can be reduced to:

$$\psi'''^* - \alpha^{*2}\psi'^* + \beta(\psi''^* - \alpha^{*2}\psi) + \frac{\gamma^*}{\gamma^*+\beta^*}\xi^* = 0$$

$$\psi'''^* + \alpha^*\psi''^* - \beta^{*2}(\psi'^* + \alpha^*\psi^*) + \frac{\gamma^*}{\gamma^*+\beta^*}\xi^* = 0$$

$$\xi'^* + \gamma\xi^* = 0$$

APPENDIX B

NEWTON-RAPHSON METHOD

Newton-Raphson Method

Let X^o be an approximate root of the single algebraic equation:

$$f(X) = 0 \qquad \text{(B-1)}$$

Suppose that the exact root is:

$$X = X^o + h \qquad \text{(B-2)}$$

where h is a small quantity. By substitution of equation (B-2) into (B-1),

$$f(X^o + h) = 0 \qquad \text{(B-3)}$$

Consider the following assumptions:

i) f(X) is convex function

ii) The root X is simple

iii) $f'(X) < 0$

Function f(X) can then be represented by figure (B-1). The equation (B-3) can be expanded by Taylor's Theorem,

$$f(X^o+h) = f(X^o) + hf'(X^o) + 1/2h^2f''(X^o) + \ldots = 0. \qquad \text{(B-4)}$$

If h is small, the terms in $h^2, h^3, \ldots$ can be neglected, so that

$$f(X^o) + hf'(X^o) = 0. \qquad \text{(B-5)}$$

This yields the second approximation:

$$X^1 = X^o - \frac{f(X^o)}{\acute{f}(X^o)} \qquad \text{(B-6)}$$

The process is repeated at X^1 leading to a new value X^2 and so on, then the general relation can be written as:

$$X^{K+1} = X^K - \frac{f(X^K)}{\acute{f}(X^K)} \qquad \text{(B-7)}$$

Now some of the important properties of the Newton-Raphson method will be discussed as follows:

i) There is no solution to equation (B-7) if $\acute{f}(X^K) = 0$

ii) It is clear from figure (B-1) that

$$X^o < X^1 < X^2 < \ldots\ldots < X \qquad \text{(B-8)}$$

This property of equation (B-8) is known as monotonic convergence, and analytically follows from the inequalities:

$$f(X^K) > 0 \qquad \acute{f}(X^K) < 0 \qquad \text{(B-9)}$$

If $f(X^K)<0$, thus the initial approximation X^o is not part of the monotonic sequence, but the sequence $X^1, X^2, \ldots\ldots X^K$ is still monotonic convergence. It can easily be shown that this monotonicity also exists for a concave function, i.e. $\acute{f}(X)>0$, which is an important property computationally.

iii) Another property of the Newton-Raphson method, which is even more important computationally is the quadratic convergence of this method. This can be demonstrated as follows:

Equation (B-7) can be written as:

$$X^{K+1} - X = X^K - \frac{f(X^K)}{f'(X^K)} - X$$

thus,

$$X^{K+1} - X = X^K - \frac{f(X^K)}{f'(X^K)} - \left(X - \frac{f(X)}{f'(X)}\right)$$

Hence,

$$X^{K+1} - X = \phi(X^K) - \phi(X) \qquad \text{(B-10)}$$

The Taylor's series expansion of equation (B-10) is:

$$X^{K+1} - X = (X^{K+1}-X)\phi'(X) + \frac{(X^K-X)^2}{2}\phi''(\theta) \qquad \text{(B-11)}$$

where $X_o \leq X^K \leq \theta \leq X$

Since $\phi'(X)$ can be expressed as:

$$\phi'(X) = \frac{f(X)f''(X)}{f'(X)^2} \qquad \text{(B-12)}$$

Therefore,

$$\phi'(X) = 0$$

Hence,

$$|X^{K+1} - X| \leq R|X^K - X|^2 \qquad \text{(B-13)}$$

where $R = \max.|\phi''(\theta)|/2$ is a bound dependence on $f'''(X)$.

Furthermore,

$$X^{K+1} - X^K = \phi(X^K) - \phi(X^{K-1})$$

$$= (X^K-X^{K-1})\phi'(X^{K-1}) + \frac{(X^K-X^{K-1})^2}{2}\phi''(\theta) \qquad \text{(B-14)}$$

where $X^{K-1} \leq \theta < X^{K}$, which leads to

$$(X^{K+1}-X^{K}) = (X^{K}-X^{K-1})\frac{f(X^{K-1})f''(X^{K-1})}{f'(X^{K-1})^2} + \frac{(X^{K}-X^{K-1})^2\psi''(\theta)}{2} \tag{B-15}$$

Equation (B-14) yields:

$$\frac{f(X^{K-1})}{f'(X^{K-1})} = X^{K} - X^{K-1}$$

Hence,

$$(X^{K+1}-X^{K}) = (X^{K}-X^{K-1})^2\left[\frac{f''(X^{K-1}}{f'(X^{K-1})} + \frac{\phi''(\theta)}{2}\right] \tag{B.16}$$

Thus,

$$|X^{K+1}-X^{K}| \leq R_1|X^{K}-X^{K-1}|^2 \tag{B-17}$$

where

$$R_1 = \max_{X_o \leq \theta \leq x}\left[\frac{|f''(\theta)|}{|f(\theta)|} + \frac{|\psi''(\theta)|}{2}\right] \tag{B-18}$$

This quadratic convergence is not only important because of the computing time, but also because of round-off error which is likely to increase as the number of iterations increases.

The above mentioned method can be easily generalized to the higher dimensions, Bellman and Kalaha [47], as follows: Considering a system of simultaneous equations

$$f_i(X_1,X_2,....x_N) = 0. \qquad i = 1,2,....N \tag{B-19}$$

or in a vector form

$$\underline{F}(\underline{X}) = 0. \tag{B-20}$$

Taking $\underline{X}^o$ as a initial approximation

$$\underline{F}(\underline{X}) = \underline{F}(\underline{X}^o) + J(\underline{X}^o)(\underline{X}-\underline{X}^o) \tag{B-21}$$

where $J(\underline{X}^o)$ is a Jacobian matrix:

$$J(\underline{X}^o) = (\frac{\partial f_i}{\partial x_j})_{X=Xo} \tag{B-22}$$

From equation (B-21) the new approximation can be expressed as:

$$\underline{X}^1 = \underline{X}^o - J(\underline{X}^o)^{-1} \underline{F}(\underline{X}^o) \tag{B-23}$$

This can be written in general form as:

$$\underline{X}^K = \underline{X}^{K-1} - J(\underline{X}^{K-1})^{-1}\underline{F}(\underline{X}^{K-1}) \tag{B-24}$$

Figure B.1

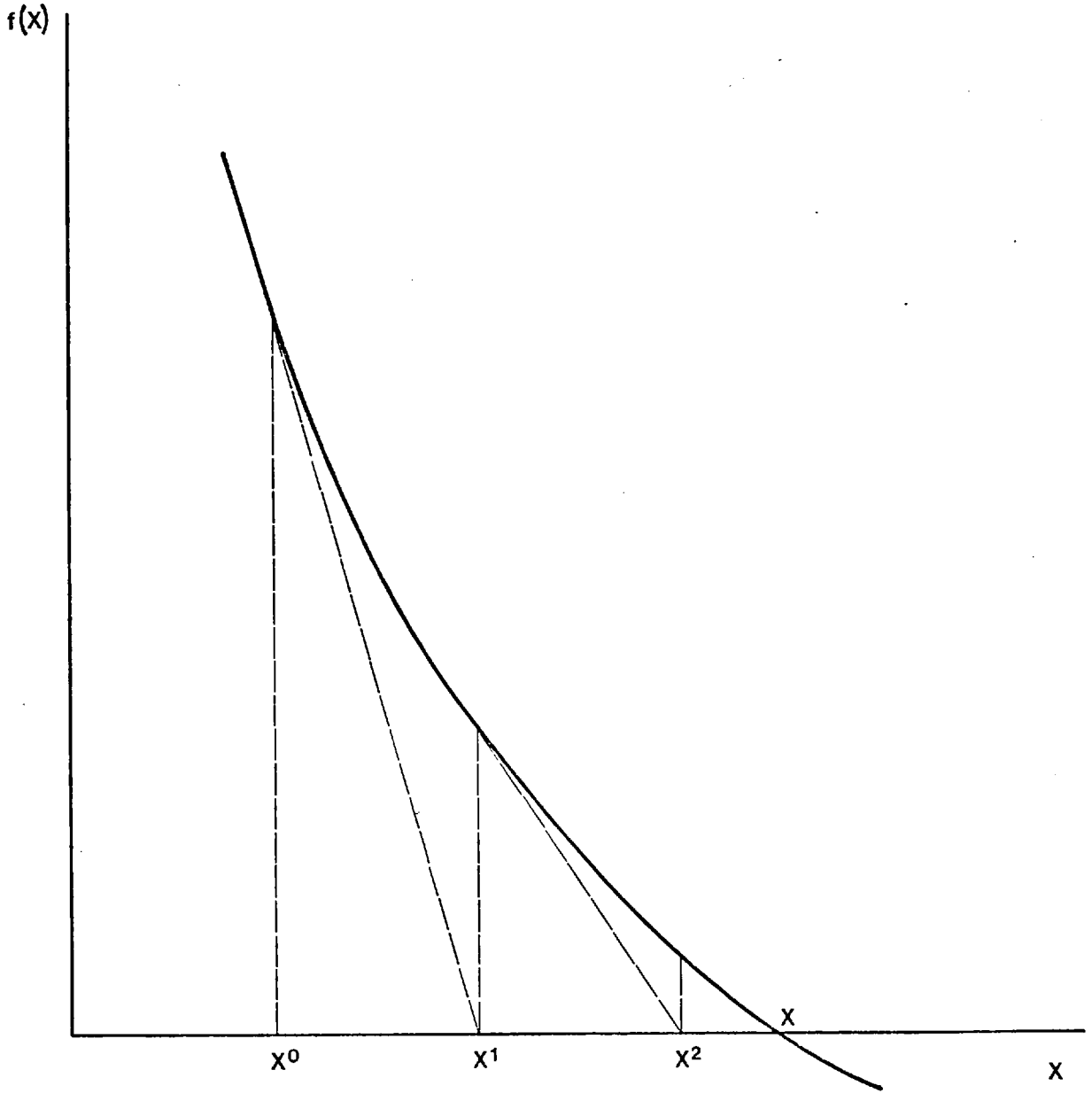

Newton-Raphson method.

APPENDIX C

THE SUPERPOSITION PRINCIPLE

The Superposition Principle

The superposition principle supposes that one particular solution and several non-trivial homogeneous solutions are obtainable. The complete solution is the weighted sum of these solutions.

Consider the following linearized ordinary differential equations with variable coefficients:

$$\frac{d\underline{X}^{K+1}}{dt} = \underline{f}(\underline{X}^{K},t) + \underline{J}(\underline{X}^{K}).(\underline{X}^{K+1} - \underline{X}^{K}) \qquad \text{(C-1)}$$

with the boundary conditions:

$$\begin{aligned} X_i^{K+1}(0) &= X_{i0} \qquad i = 1,m \\ X_q^{K+1}(t_f) &= X_{qf} \qquad q = m+1,n \end{aligned} \qquad \text{(C-2)}$$

Any solution of these equations constitutes the particular solution

$$X_{1p}^{K+1}(t),\ X_{2p}^{K+1}(t),\ \ldots\ldots\ X_{np}^{K+1}(t) \qquad \text{(C-3)}$$

By removing from the particular equations anything not containing X_i^{K+1}, i = 1,n a set of homogeneous equations is obtained.

Now let $X_{1Hj}^{K+1}(t),\ X_{2Hj}^{K+1}(t),\ldots\ldots X_{nHj}^{K+1}(t)$,

j = 1,n be any set of n non-trivial and distinct solutions of the homogeneous equations. Then the solution of equation (C-1) is represented by:

$$X_i^{K+1}(t) = X_{ip}^{K+1}(t) + \sum_{j=1}^{n} a_j^{K+1}\, X_{iHj}^{K+1}(t) \qquad i = 1,n \qquad \text{(C-4)}$$

where the unknown constants a_j^{K+1} will be determined using the boundary conditions, the subscript i represents the ith variable and subscript j represents j^{th} homogeneous solution. If initial conditions used in obtaining the above particular and homogeneous solutions, satisfy the given initial conditions of the problem, then the number of distinct and non-trivial homogeneous solutions required is reduced by the number of initial conditions satisfied. This leads to a considerable saving of computation time. By means of the initial conditions in (C-2), equations (C-4) are reduced to:

$$X_i^{K+1}(t) = X_{ip}^{K+1}(t) + \sum_{j=1}^{n-m} a_j^{K+1} X_{iHj}^{K+1}(t) \qquad i = 1,n \tag{C-5}$$

APPENDIX D

ORTHOGONALIZATION OF VECTOR SETS

Orthogonalization of Vector Sets [67]

It is often desirable to form an orthogonal set of S linear combinations of original vectors from a set of S linearly independent vectors $u_1, u_2, \ldots . u_s$. It is also convenient to normalize the vectors in such a way that each is a unit vector. The following procedure is a simple one and it can be extended to other similar problems.

First select any one of the original vectors, say $v_1 = u_1$ and divide it by its length, then the first member of desired set can be obtained

$$e_1 = \frac{u_1}{\ell(u_1)} \qquad \text{(D-1)}$$

next choose a second vector, say u_2, from the original set and write $v_2 = u_2 - ce_1$. The requirement that v_2 be orthogonal to e_1 leads to determination of

$$(e_1, v_2) = (e_1, u_2) - c(e_1 - e_1) = 0$$

or

$$c = (e_1, u_2)$$

so that

$$v_2 = u_2 - (e_1, u_2)e_1 \qquad \text{(D-2)}$$

Since e_1 is a unit vector, the familiar geometrical interpretation of the scalar product in two or three dimensions leads to the statement that (e_1, u_2) is "the scalar component of u_2 in the direction of e_1" and hence that in equation (D-2)

we have "subtracted off e_1 component from u_2".

The second member, e_2, of the desired set of orthogonal unit vector is obtained by dividing v_2 by its length

$$e_2 = \frac{v_2}{\ell(v_2)} \tag{D-3}$$

in third step write $v_3 = u_3 - c_1e_1 - c_2e_2$. The requirement that v_3 be simultaneously orthogonal to e_1 and e_2, then determines value of c_1 and c_2 which are in accordance with the geometrical interpretation described above, and there follows

$$v_3 = u_3 - (e_1,u_3)e_1 - (e_2,u_3)e_2 \tag{D-4}$$

so that the "e_1 and e_2 components" of u_3, are subtracted off. The third required vector e_3 is then given by

$$e_3 = \frac{v_3}{\ell(v_3)} \tag{D-5}$$

A continuation of this process finally determines the s^{th} member of the required set in the form of

$$e_s = \frac{v_s}{\ell(v_s)} \tag{D-6}$$

where

$$v_2 = u_s - \sum_{K=1}^{s-1} (e_K,u_s)e_K \tag{D-7}$$

This method which is often called the Gram-Schmidt orthogonalization procedure, would fail if and only if at some stage $v_r = 0$. But this would mean that u_r is a linear combination of

$e_1, e_2, \ldots . e_{r-1}$ and hence a linear combination of $u_1, u_2, \ldots$ u_{r-1}, in contradiction with the hypothesis that the set of u's is linearly independent.

It is seen that this procedure permits the determination of an orthonormal basis (a basis comprising mutually of the orthogonal unit vectors) for a vector space when any set of the spanning vector is known.

When the vectors $u_1, \ldots . u_s$ are complex, the same procedure clearly applies if the Hermitlien products and the lengths are used throughout.

APPENDIX E

CAUCHY-RIEMANN EQUATIONS

Cauchy-Riemann Equations

Let f(z) be a function of the complex variable $z = x + iy$. Then write

$$f(z) = u(x,y) + iv(x,y) \tag{E-1}$$

where u and v are real functions of the two real variables x and y.

Suppose that equation (E-1) is differentiable. Then it can be shown that if u,v satisfy the equations

$$\frac{\partial u}{\partial x} = \frac{\partial v}{\partial y} \tag{E-2}$$

$$\frac{\partial u}{\partial y} = - \frac{\partial v}{\partial x} \tag{E-3}$$

we have

$$f(z) - f(z_o) = u(x,y) - u(x_o y_o) + i(v(x,y) - v(x_o,y_o)$$

where $z_o = x_o + iy_o$.

Since f(z) is differentiable, $[f(z) - f(z_o)]/(z-z_o)$, it must approach a unique limiting value when $z \to z_o$ from any direction. First the case when z approaches z_o along a line parallel to the real axis is considered, i.e. $z = x + y_o$. Hence

$$\frac{f(z) - f(z_o)}{z - z_o} = \frac{u(x,y_o) - u(x_o,y_o)}{x - x_o} + i \frac{v(x,y_o) - v(x_o,y_o)}{x - x_o}$$

and taking the limit as $z \to z_o$ gives

$$f'(z_o) = \frac{\partial u}{\partial x} + i \frac{\partial v}{\partial x} \qquad \text{(E-4)}$$

The same result must be obtained when z approaches z_o along a line parallel to the imaginary axis, i.e. when $z = x_o + iy$. In this case

$$\frac{f(z) - f(z_o)}{z - z_o} = \frac{u(x_o,y) - u(x_o,y_o)}{i(y - y_o)} + \frac{i[v(x_o,y) - v(x_o,y_o)]}{i(y - y_o)}$$

Thus

$$f'(z_o) = - i \frac{\partial u}{\partial y} + \frac{\partial v}{\partial y} \qquad \text{(E-5)}$$

Equating real and imaginary parts of equations (E-4), (E-5) gives the Cauchy-Riemann equations (E-2) and (E-3). The above proof shows that when a function of a complex variable is differentiable, its real and imaginary parts satisfy the Cauchy-Riemann equations.

APPENDIX F

TABLES OF RESULTS

TABLE F.1. The effect of the integration step length on the predicted values of $\overset{\prime\prime\prime}{\psi}(0)_r$, $\overset{\prime\prime\prime}{\psi}(0)_i$, $\acute{\xi}(0)_r$, $\acute{\xi}(0)_i$, c_r and c_i

Table F.1.(a)

Pr = 1.0 $\quad \alpha Gr = 8.0 \quad \alpha = 0.02 \quad \eta_{edg} = 8.0$ Convergence criterion 1×10^{-4}

$\eta(0) \rightarrow \eta(1)$	H $\eta(1) \rightarrow \eta_{edg}$	$\overset{\prime\prime\prime}{\psi}(0)_r$	$\overset{\prime\prime\prime}{\psi}(0)_i$	$\acute{\xi}(0)_r$	$\acute{\xi}(0)_i$	c_r	c_i
0.1	0.200	-.10677	-1.02778	0.54968	-1.64521	0.26673	-.00212
0.05	0.100	-.10771	-1.03562	0.54493	-1.63868	0.26723	-.00256
0.02	0.040	-.10986	-1.05309	0.53601	-1.64411	0.26767	-.00270
0.01	0.020	-.11107	-1.05749	0.53341	-1.64446	0.26774	-.00275
0.008	0.016	-.11109	-1.05751	0.53339	-1.64452	0.26776	-.00277

Table F.1.(b)

Pr = 1.0 $\quad \alpha Gr = 75.0 \quad \alpha = 0.65 \quad \eta_{edg} = 8.0$ Convergence criterion 1×10^{-4}

H		$\overset{\prime\prime\prime}{\psi}(0)_r$	$\overset{\prime\prime\prime}{\psi}(0)_i$	$\overset{\prime}{\xi}(0)_r$	$\overset{\prime}{\xi}(0)_i$	c_r	c_i
$\eta(0)\rightarrow\eta(1)$	$\eta(1)\rightarrow\eta_{edg}$						
0.100	0.200	-2.22815	0.35228	-.83155	-.18614	0.13927	-.00809
0.050	0.100	-2.29247	0.25424	-.82891	-.12480	0.14009	-.00781
0.020	0.040	-2.29927	0.18605	-.82335	-.09022	0.14041	-.00765
0.010	0.020	-2.30177	0.16143	-.82071	-.07920	0.14047	-.00758
0.008	0.016	-2.30292	0.15541	-.81961	-.08412	0.14050	-.00754
0.006	0.012	-2.30309	0.15521	-.81942	-.08372	0.14052	-.00753

Table F.1.(c)

Pr = 6.7 $\quad \alpha Gr = 7.0 \quad \alpha = 0.02 \quad \eta_{edg} = 8.0$ Convergence criterion 1×10^{-4}

H		$\overset{\prime\prime\prime}{\psi}(0)_r$	$\overset{\prime\prime\prime}{\psi}(0)_i$	$\xi'(0)_r$	$\xi'(0)_i$	c_r	c_i
$\eta(0)\to\eta(1)$	$\eta(1)\to\eta_{edg}$						
0.1250	0.250	0.04183	-.10695	1.99911	-.90799	0.21038	-.00932
0.0625	0.125	0.04211	-.09935	1.97653	-.93220	0.20899	-.00732
0.0250	0.050	0.04222	-.09947	1.95956	-.94682	0.20830	-.00659
0.0125	0.025	0.04226	-.09950	1.95418	-.95130	0.20807	-.00634
0.0100	0.020	0.04227	-.09953	1.95391	-.95152	0.20800	-.00630

Table F.1.(d)

Pr = 6.7 $\quad \alpha Gr = 21.5 \quad \alpha = 0.6 \quad \eta_{edg} = 8.0$ Convergence criterion 1×10^{-4}

H		$\overset{'''}{\psi}(0)_r$	$\overset{'''}{\psi}(0)_i$	$\overset{'}{\xi}(0)_r$	$\overset{'}{\xi}(0)_i$	c_r	c_i
$\eta(0)\to\eta(1)$	$\eta(1)\to\eta_{edg}$						
0.1250	0.250	0.21453	-2.24919	5.40006	-4.76311	0.14584	-.00013
0.0625	0.125	0.31930	-2.23391	5.45128	-4.99837	0.14606	-.00091
0.0250	0.050	0.36695	-2.24162	5.44766	-5.16330	0.14611	-.00143
0.0125	0.025	0.38250	-2.24384	5.44575	-5.21530	0.14614	-.00161
0.0100	0.020	0.38202	-2.24462	5.44521	-5.21912	0.14615	-.00169
0.0080	0.016	0.38200	-2.24469	5.44519	-5.21919	0.14615	-.00170

Table F.1.(e)

Pr = 100.0 αGr = 11.70 α = 0.04 η_{edg} = 14.0 Convergence criterion 1×10^{-3}

H		$\overset{\prime\prime\prime}{\psi}(0)_r$	$\overset{\prime\prime\prime}{\psi}(0)_i$	$\xi'(0)_r$	$\xi'(0)_i$	c_r	c_i
$\eta(0)\rightarrow\eta(1)$	$\eta(1)\rightarrow\eta_{edg}$						
0.1250	0.250	0.03468	-.04212	6.50301	0.60131	0.08358	0.00297
0.0625	0.125	0.03498	-.04907	6.48010	0.57682	0.07420	0.00190
0.0250	0.050	0.03509	-.04920	6.46838	0.56183	0.07360	0.00113
0.0125	0.025	0.03511	-.04923	6.46311	0.55682	0.07337	0.00091
0.0100	0.020	0.03512	-.04925	6.46287	0.55641	0.07307	0.00086

Table F.1.(f)

Pr = 10000 αGr = 27.0 α = 0.80 η_{edg} = 14.0 Convergence criterion 1×10^{-3}

H		$\overset{'''}{\psi}(0)_r$	$\overset{'''}{\psi}(0)_i$	$\xi'(0)_r$	$\xi'(0)_i$	c_r	c_i
$\eta(0)\rightarrow\eta(1)$	$\eta(1)\rightarrow\eta_{edg}$						
0.1250	0.250	.35117	-.35919	9.48107	4.73457	.05927	.00101
0.0625	0.125	.45213	-.34413	9.53210	4.51116	.05951	.00032
0.0250	0.050	.52017	-.35264	9.52612	4.37667	.05967	-.00018
0.0125	0.025	.53692	-.35611	9.52417	4.32123	.05971	-.00036
0.0100	0.020	.53611	-.35701	9.52390	4.31812	.05972	-.00041
0.0080	0.160	.53609	-.35709	9.52386	4.31808	.05972	-.00042

Table F.2. The effect of the value of η_{edg} on the predicted values of $\overset{\prime\prime\prime}{\psi}(0)_r$, $\overset{\prime\prime\prime}{\psi}(0)_i$, $\overset{\prime}{\xi}(0)_r$, $\overset{\prime}{\xi}(0)_i$, c_r and c_i

Table F.2.(a)

Pr = 0.733 αGr = 51.3 α = 0.45 H = 0.008 ($0<\eta<1$), 0.016 ($1<\eta<8$)

Convergence criterion 1 x 10^{-4}

η_{edg}	$\overset{\prime\prime\prime}{\psi}(0)_r$	$\overset{\prime\prime\prime}{\psi}(0)_i$	$\overset{\prime}{\xi}(0)_r$	$\overset{\prime}{\xi}(0)_i$	c_r	c_r
5.0	-2.25936	0.10317	-.84869	0.00303	0.16152	-.00036
5.5	-2.26154	0.10421	-.85040	0.00074	0.16176	-.00021
6.0	-2.26231	0.10460	-.85103	-.00004	0.16185	-.00015
6.5	-2.26259	0.10472	-.85122	-.00035	0.16188	-.00014
7.0	-2.26269	0.10480	-.85134	-.00044	0.16189	-.00013
7.5	-2.26271	0.10482	-.85137	-.00047	0.16189	-.00013

Table F.2.(b)

Pr = 0.733 $\quad \alpha Gr = 6.6 \quad \alpha = 0.075 \quad H = 0.01\ (0<\eta<1),\ 0.02\ (1<\eta<8)$

Convergence criterion 1×10^{-4}

η_{edg}	$\overset{///}{\psi}(0)_r$	$\overset{///}{\psi}(0)_i$	$\xi'(0)_r$	$\xi'(0)_i$	c_r	c_i
5.0	0.00100	-.72460	o.51937	-1.16319	0.30632	-.00313
5.5	0.00785	-.66095	0.53822	-1.11759	0.31121	-.00121
6.0	0.01008	-.63005	0.54648	-1.09560	0.31365	-.00027
6.5	0.01104	-.61434	0.55056	-1.08447	0.31490	0.00019
7.0	0.01155	-.60625	0.55266	-1.07877	0.31556	0.00043
7.5	0.01181	-.60257	0.55365	-1.07617	0.31586	0.00053
8.0	0.01192	-.60201	0.55391	-1.07530	0.31592	0.00055

Table F.2.(c)

Pr = 6.7 $\quad \alpha Gr = 21.0 \quad \alpha = 0.6 \quad H = 0.01\ (0<\eta<1),\ 0.02\ (1<\eta<8)$

Convergence criteron 1×10^{-4}

η_{edg}	$\overset{///}{\psi}(0)_r$	$\overset{///}{\psi}(0)_i$	$\overset{/}{\xi}(0)_r$	$\overset{/}{\xi}(0)_i$	c_r	c_i
5.0	0.38294	-2.24426	5.44747	-5.21613	0.14613	-.00161
5.5	0.38264	-2.24402	5.44633	-5.21569	0.14614	-.00161
6.0	0.38256	-2.24391	5.44596	-5.21546	0.14614	-.00161
6.5	0.38251	-2.24386	5.44582	-5.21536	0.14614	-.00161
7.0	0.38250	-2.24388	5.44577	-5.21531	0.14614	-.00161
7.5	0.38250	-2.24384	5.44575	-5.21530	0.14614	-.00161
8.0	0.38250	-2.24384	5.44575	-5.21530	0.14614	-.00161

Table F.2.(d)

Pr = 6.7 $\quad \alpha Gr = 4.8 \quad \alpha = 0.04 \quad H = 0.0125\ (0<\eta<1),\ 0.025\ (1<\eta<8)$

Convergence criterion 1×10^{-4}

η_{edg}	$\overset{'''}{\psi}(0)_r$	$\overset{'''}{\psi}(0)_i$	$\overset{'}{\xi}(0)_r$	$\overset{'}{\xi}(0)_i$	c_r	c_i
5.0	0.05530	-.09555	1.74370	-.99023	0.20919	-.00673
5.5	0.04862	-.08689	1.72813	-.97211	0.21049	-.00627
6.0	0.04447	-.08127	1.71843	-.96065	0.21131	-.00599
6.5	0.04191	-.07703	1.71251	-.95347	0.21183	-.00581
7.0	0.04033	-.07542	1.70886	-.94893	0.21215	-.00571
7.5	0.03936	-.07397	1.70662	-.94605	0.21236	-.00565
8.0	0.03936	-.07397	1.70662	-.94605	0.21236	-.00565

Table F.2.(e)

Pr = 100 $\quad \alpha Gr = 23.60 \quad \alpha = 0.70 \quad H = 0.01\ (0<\eta<1),\ 0.02\ (1<\eta<14)$

Convergence criterion 1×10^{-4}

η_{edg}	$\overset{\prime\prime\prime}{\psi}(0)_r$	$\overset{\prime\prime\prime}{\psi}(0)_i$	$\overset{\prime}{\xi}(0)_r$	$\overset{\prime}{\xi}(0)_i$	c_r	c_i
8.0	0.40621	-.29772	9.22461	3.49482	0.05963	-.00091
9.0	0.40610	-.29685	9.21403	3.49344	0.06042	-.00054
10.0	0.40570	-.29649	9.21370	3.49205	0.06091	-.00028
11.0	0.40550	-.29627	9.21357	3.49187	0.06112	-.00016
12.0	0.40540	-.29613	9.21345	3.49177	0.06120	-.00010
13.0	0.40535	-.29609	9.21340	3.49171	0.06123	-.00006
14.0	0.40535	-.29609	9.21340	3.49171	0.06123	-.00006

Table F.2.(f)

Pr = 100.0 $\quad \alpha Gr = 9.95 \quad \alpha = 0.04 \quad H = 0.0125\ (0<\eta<1),\ 0.025\ (1<\eta<14)$

Convergence criterion 1×10^{-4}

η_{edg}	$\overset{'''}{\psi}(0)_r$	$\overset{'''}{\psi}(0)_i$	$\overset{'}{\xi}(0)_r$	$\overset{'}{\xi}(0)_i$	c_r	c_i
8.0	0.03160	-.04510	6.53173	0.17049	0.07208	-.00198
9.0	0.03240	-.04437	6.53089	0.16962	0.07304	-.00102
10.0	0.03288	-.04392	6.53004	0.16914	0.07353	-.00049
11.0	0.03312	-.04368	6.52980	0.16890	0.07378	-.00021
12.0	0.03324	-.04356	6.52967	0.16878	0.07390	-.00007
13.0	0.03330	-.04350	6.52961	0.16872	0.07395	-.00001
14.0	0.03333	-.04347	6.52959	0.16870	0.07396	0.000005

Table F.2.(g)

Pr = 1000.0 $\quad \alpha Gr = 30.07 \quad \alpha = 0.90 \quad H = 0.01\ (0<\eta<1),\ 0.02\ (1\leq\eta<15)$

Convergence criterion 1×10^{-4}

η_{edg}	$\dddot{\psi}(0)_r$	$\dddot{\psi}(0)_i$	$\dot{\xi}(0)_r$	$\dot{\xi}(0)_i$	c_r	c_i
9.0	0.70032	-0.42322	9.59372	5.97472	0.03595	-.000105
10.0	0.69970	-0.42254	9.59280	5.97387	0.03655	-.000045
11.0	0.69938	-0.42218	9.59243	5.97349	0.03685	-0.00015
12.0	0.69922	-0.42202	9.59225	5.97332	0.03700	-.00005
13.0	0.69914	-0.42194	9.59216	5.97324	0.03707	-.00001
14.0	0.69910	-0.42191	9.59213	5.97321	0.03710	0.000014
15.0	0.69910	-0.42191	9.59213	5.97321	0.03710	0.000014

Table F.2.(h)

Pr = 1000.0 $\quad \alpha Gr = 11.35 \quad \alpha = 0.04 \quad H = 0.0125\ (0<\eta<1),\ 0.025\ (1<\eta<15)$

Convergence criterion 1×10^{-4}

η_{edg}	$\overset{\prime\prime\prime}{\psi}(0)_r$	$\overset{\prime\prime\prime}{\psi}(0)_i$	$\xi'(0)_r$	$\xi'(0)_i$	c_r	c_i
9.0	0.04419	-.04402	6.91621	0.18472	0.04432	-.00011
10.0	0.04327	-.04319	6.91571	0.18346	0.04545	-.00063
11.0	0.04269	-.04264	6.91492	0.18273	0.04595	-.00031
12.0	0.04239	-.04236	6.91457	0.18236	0.04624	-.00015
13.0	0.04224	-.04222	6.91436	0.18222	0.04641	-.00008
14.0	0.04216	-.04215	6.91426	0.18214	0.04650	-.00002
15.0	0.04213	-.04211	6.91421	0.18210	0.04655	0.000008

Table F.3. The effect of variation of the convergence criterion on the predicted values of $\overset{'''}{\psi}(0)_r$, $\overset{'''}{\psi}(0)_i$, $\xi'(0)_r$ and $\xi'(0)_i$

Table F.3.(a)

Pr = 1.0 αGr = 10.0 H = 0.01 ($0<\eta<1$), 0.02 ($1<\eta<8$)

η_{edg} = 8.0

Convergence criterion	$\overset{'''}{\psi}(0)_r$	$\overset{'''}{\psi}(0)_i$	$\xi'(0)_r$	$\xi'(0)_i$
1×10^{-1}	-.295696	-1.192017	0.422965	-1.837846
1×10^{-2}	-.296023	-1.191222	0.422642	-1.836232
1×10^{-3}	-.296499	-1.190246	0.422559	-1.835627
1×10^{-4}	-.296498	-1.190243	0.422560	-1.835625
1×10^{-10}	-.296496	-1.190242	0.422562	-1.835624

Table F.3.(b)

Pr = 1.0 αGr = 20.0 H = 0.01 ($0<\eta<1$), 0.02 ($1<\eta<8$)

η_{edg} = 8.0

Convergence criterion	$\overset{'''}{\psi}(0)_r$	$\overset{'''}{\psi}(0)_i$	$\xi'(0)_r$	$\xi'(0)_i$
1×10^{-2}	-1.242515	-1.315850	-.252807	-2.182972
1×10^{-3}	-1.243294	-1.315408	-.253664	-2.182238
1×10^{-4}	-1.243296	-1.315408	-.253667	-2.182237
1×10^{-8}	-1.243296	-1.315408	-.253667	-2.182237

Table F.3.(c)

Pr = 0.733 αGr = 43.3 H = 0.01 (0<η<1), 0.02 (1<η<8)

η_{edg} = 8.0

Convergence criterion	$\overset{'''}{\psi}(0)_r$	$\overset{'''}{\psi}(0)_i$	$\xi'(0)_r$	$\xi'(0)_i$
1×10^{-2}	-2.334374	-.076053	-1.087878	-.078892
1×10^{-3}	-2.334374	-.076054	-1.087879	-.078891
1×10^{-4}	-2.334374	-.076054	-1.087879	-.078891

Table F.3.(d)

Pr = 0.733 αGr = 92.6 H = 0.008 (0<η<1), 0.016 (1<η<8)

η_{edg} = 8.0

Convergence criterion	$\overset{'''}{\psi}(0)_r$	$\overset{'''}{\psi}(0)_i$	$\xi'(0)_r$	$\xi'(0)_i$
1×10^{-2}	-2.407675	0.396336	-.636164	-.143490
1×10^{-3}	-2.407675	0.396334	-.636163	-.143490
1×10^{-4}	-2.407675	0.396334	-.636163	-.143490

Table F.3.(e)

Pr = 0.733 αGr = 116.8 H = 0.008 (0<η<1), 0.016 (1<η<8)

η_{edg} = 8.0

Convergence criterion	$\overset{'''}{\psi}(0)_r$	$\overset{'''}{\psi}(0)_i$	$\xi'(0)_r$	$\xi'(0)_i$
1×10^{-1}	-2.505072	0.620371	-.603466	-.241194
1×10^{-2}	-2.504070	0.620371	-.603467	-.241194
1×10^{-3}	-2.504070	0.620371	-.603467	-.241194

Table F.3.(f)

Pr = 0.733 αGr = 194.0 H = 0.008 ($0<\eta<1$), 0.016 ($1<\eta<8$)

η_{edg} = 8.0

Convergence criterion	$\overset{'''}{\psi}(0)_r$	$\overset{'''}{\psi}(0)_i$	$\overset{'}{\xi}(0)_r$	$\overset{'}{\xi}(0)_i$
1×10^{-1}	-2.765087	1.379021	-.556569	-.511254
1×10^{-2}	-2.765087	1.379018	-.556569	-.511254
1×10^{-3}	-2.765087	1.379018	-.556569	-.511254

Table F.3.(g)

Pr = 0.733 αGr = 238.0 H = 0.008 ($0<\eta<1$), 0.016 ($1<\eta<8$)

η_{edg} = 8.0

Convergence criterion	$\overset{'''}{\psi}(0)_r$	$\overset{'''}{\psi}(0)_i$	$\overset{'}{\xi}(0)_r$	$\overset{'}{\xi}(0)_i$
1×10^{-1}	-2.896378	1.806945	-.535212	-.630194
1×10^{-2}	-2.896375	1.806944	-.535213	-.630195
1×10^{-3}	-2.896375	1.866944	-.535213	-.630195

Table F.3.(h)

Pr = 6.7 αGr = 5.4 H = 0.0125 ($0<\eta<1$), 0.025 ($1<\eta<8$)

η_{edg} = 8.0

Convergence criterion	$\overset{'''}{\psi}(0)_r$	$\overset{'''}{\psi}(0)_i$	$\overset{'}{\xi}(0)_r$	$\overset{'}{\xi}(0)_i$
1×10^{-2}	0.040476	-.081070	1.783867	-.949303
1×10^{-3}	0.040439	-.081051	1.783780	-.949280
1×10^{-4}	0.040439	-.081052	1.783781	-.949281
1×10^{-5}	0.040439	-.081052	1.783781	-.949281

Table F.3.(i)

Pr = 6.7 αGr = 7.625 H = 0.0125 ($0<\eta<1$), 0.025 ($1<\eta<8$)

η_{edg} = 8.0

Convergence criterion	$\overset{'''}{\psi}(0)_r$	$\overset{'''}{\psi}(0)_i$	$\overset{'}{\xi}(0)_r$	$\overset{'}{\xi}(0)_i$
1×10^{-2}	0.077757	-.186064	2.110014	1.102342
1×10^{-3}	0.077766	-.186070	2.110042	1.102351
1×10^{-4}	0.077766	-.186071	2.110041	1.102350
1×10^{-5}	0.077766	-.186071	2.1100041	1.102350

Table F.3. (j)

Pr = 6.7 αGr = 10.8 H = 0.0125 ($0<\eta<1$), 0.025 ($1<\eta<8$)

η_{edg} = 8.0

Convergence criterion	$\overset{'''}{\psi}(0)_r$	$\overset{'''}{\psi}(0)_i$	$\overset{'}{\xi}(0)_r$	$\overset{'}{\xi}(0)_i$
1×10^{-2}	0.316604	-.782690	3.207060	-2.254298
1×10^{-3}	0.316604	-.782692	3.207061	-2.254299
1×10^{-4}	0.316604	-.782693	3.207061	-2.254300
1×10^{-5}	0.316604	-.782693	3.207061	-2.254300

Table F.3. (k)

Pr = 6.7 αGr = 16.0 H = 0.01 ($0<\eta<1$), 0.02 ($1<\eta<8$)

η_{edg} = 8.0

Convergence criterion	$\overset{'''}{\psi}(0)_r$	$\overset{'''}{\psi}(0)_i$	$\overset{'}{\xi}(0)_r$	$\overset{'}{\xi}(0)_i$
1×10^{-2}	0.409160	-1.461158	4.324022	-3.555262
1×10^{-3}	0.409158	-1.461160	4.324020	-3.555271
1×10^{-4}	0.409158	-1.461160	4.324020	-3.555271

Table F.3. (l)

Pr = 6.7 αGr = 23.0 H = 0.01 ($0<\eta<1$), 0.02 ($1<\eta<8$)

η_{edg} = 8.0

Convergence criterion	$\overset{'''}{\psi}(0)_r$	$\overset{'''}{\psi}(0)_i$	$\overset{'}{\xi}(0)_r$	$\overset{'}{\xi}(0)_i$
1×10^{-1}	0.252920	-2.362100	5.396645	-5.413396
1×10^{-2}	0.252927	-2.362101	5.396670	-5.413400
1×10^{-3}	0.252926	-2.362101	5.396671	-5.413400

Table F.3. (m)

Pr = 6.7 αGr = 34.0 H = 0.01 ($0<\eta<1$), 0.02 ($1<\eta<8$)

η_{edg} = 8.0

Convergence criterion	$\overset{'''}{\psi}(0)_r$	$\overset{'''}{\psi}(0)_i$	$\overset{'}{\xi}(0)_r$	$\overset{'}{\xi}(0)_i$
1×10^{-0}	-.539119	-3.313967	5.817129	-7.710943
1×10^{-1}	-.539122	-3.313995	5.817172	-7.711062
1×10^{-2}	-.539123	-3.314001	5.817182	-7.711083
1×10^{-3}	-.539123	-3.314002	5.817182	-7.711084

Table F.3. (n)

Pr = 100.0 αGr = 6.0 H = 0.0125 ($0<\eta<1$), 0.025 ($1<\eta<8$)

η_{edg} = 14.0

Convergence criterion	$\overset{'''}{\psi}(0)_r$	$\overset{'''}{\psi}(0)_i$	$\overset{'}{\xi}(0)_r$	$\overset{'}{\xi}(0)_i$
1×10^{-1}	0.025479	-.028459	6.216778	-1.082179
1×10^{-2}	0.026561	-.028463	6.229509	-1.090698
1×10^{-3}	0.026564	-.028464	6.229510	-1.090702

Table F.3. (o)

Pr = 100.0 αGr = 17.55 H = 0.01 ($0<\eta<1$), 0.02 ($1<\eta<8$)

η_{edg} = 14.0

Convergence criterion	$\overset{'''}{\psi}(0)_r$	$\overset{'''}{\psi}(0)_i$	$\overset{'}{\xi}(0)_r$	$\overset{'}{\xi}(0)_i$
1×10^{-1}	0.236559	-.201614	8.517355	1.958726
1×10^{-2}	0.236421	-.201166	8.515257	1.961794
1×10^{-3}	0.236418	-.201169	8.515260	1.961796

Table F.3. (p)

Pr = 100.0 αGr = 32.8 H = 0.01 ($0<\eta<1$), 0.02 ($1<\eta<8$)

η_{edg} = 14.0

Convergence criterion	$\overset{'''}{\psi}(0)_r$	$\overset{'''}{\psi}(0)_i$	$\overset{'}{\xi}(0)_r$	$\overset{'}{\xi}(0)_i$
1×10^{-1}	0.669027	-.450309	9.456580	5.514023
1×10^{-2}	0.668993	-.450230	9.456098	5.514251
1×10^{-3}	0.668995	-.450227	9.456101	5.514253

Table F.4. The values of α and its corresponding values of Gr, αGr, c_r, c_i and the missing boundary conditions $\ddot{\psi}(0)_r$, $\ddot{\psi}(0)_i$, $\dot{\xi}(0)_r$, $\dot{\xi}(0)_i$ on the neutral stability curve.

Table F.4.(a) Prandtl number of 0.733

α	Gr	αGr	c_r	c_i	$\ddot{\psi}(0)_r$	$\ddot{\psi}(0)_i$	$\dot{\xi}(0)_r$	$\dot{\xi}(0)_i$
.040	141.125	5.645	0.34003	0.44×10^{-4}	0.05020	-.31500	0.59182	-0.83089
.075	88.666	6.65	0.31352	0.46×10^{-4}	0.00756	-.63364	0.54621	-1.11005
.140	66.142	9.26	0.27368	$-.78 \times 10^{-5}$	-.44931	-1.27640	0.12693	-1.64606
.150	65.266	9.79	0.26842	0.21×10^{-4}	-.57568	-1.35392	0.01264	-1.71059
.170	64.470	10.96	0.25856	$-.55 \times 10^{-5}$	-.86327	-1.46396	-.24763	-1.79793
.180	64.555	11.62	0.25390	$-.25 \times 10^{-4}$	-1.02086	-1.49201	-.39008	-1.81681
.190	65.053	12.36	0.24937	0.35×10^{-5}	-1.11863	-1.49912	-.53898	-1.81651
.250	75.880	18.97	0.22441	0.23×10^{-5}	-2.10759	-1.08707	-1.35261	-1.38222
.350	119.200	41.72	0.17850	$-.78 \times 10^{-5}$	-2.33602	0.05979	-1.12884	--.07255
.450	114.489	51.52	0.16183	0.83×10^{-6}	-2.26368	0.10623	-.84868	-.00185
.550	120.690	66.38	0.15547	0.33×10^{-6}	-2.30026	0.18623	-.71633	-.04073
.650	142.615	92.70	0.15473	$-.14 \times 10^{-5}$	-2.40826	0.39723	-.63591	-.14401
.700	165.114	115.58	0.15584	0.89×10^{-6}	-2.24980	0.60895	-.60527	-.23579
.750	215.960	161.97	0.15787	0.31×10^{-5}	-2.26610	1.06318	-.57282	-.40814
.760	246.579	187.40	0.15849	$-.64 \times 10^{-9}$	-2.74314	1.31460	-.56014	-.49125
.760	303.552	230.70	0.15883	$-.90 \times 10^{-6}$	-2.87625	1.73623	-.53862	-.61198

Table F.4. (b) Prandtl number of 1.0

α	Gr	αGr	c_r	c_i	$\psi'''(0)_r$	$\psi'''(0)_i$	$\xi'(0)_r$	$\xi'(0)_i$
0.040	139.45	5.578	0.32500	0.35×10^{-3}	0.05393	-.25303	0.71182	-.853195
0.075	85.00	6.375	0.30192	0.16×10^{-4}	0.05522	-.50855	0.71315	-1.10085
0.140	61.35	8.590	0.26661	0.62×10^{-4}	-.16410	-1.10306	0.50296	-1.70636
0.250	65.00	16.250	0.22343	0.10×10^{-5}	-1.64860	-1.16233	-1.03011	-2.28143
0.350	149.65	52.380	0.16683	$-.26 \times 10^{-4}$	-2.45105	0.16335	-1.26524	-.11022
0.450	136.89	61.600	0.15082	0.31×10^{-4}	-2.35023	0.14978	-.94501	-.08955
0.550	140.36	77.200	0.14403	$-.20 \times 10^{-4}$	-2.37091	0.19456	-.81351	-.16280
0.650	161.76	105.150	0.14230	$-.96 \times 10^{-6}$	-2.48829	0.36596	-.74972	-.30995
0.700	183.71	128.600	0.14275	$-.39 \times 10^{-5}$	-2.57827	0.54328	-.73162	-.42423
0.750	226.40	169.800	0.14390	0.73×10^{-5}	-2.72093	0.88314	-.71248	-.60271

Table F.4. (c)

Prandtl number of 6.7

α	Gr	αGr	c_r	c_i	$\psi'''(0)_r$	$\psi'''(0)_i$	$\xi'(0)_r$	$\xi'(0)_i$
0.020	275.50	5.51	0.21568	$-.31 \times 10^{-5}$	0.02208	-.04562	1.75120	-.87873
0.040	141.50	5.66	0.21073	$-.29 \times 10^{-4}$	0.04129	-.08490	1.81157	-.95174
0.075	80.06	6.005	0.20284	$-.38 \times 10^{-4}$	0.07582	-.15477	1.94307	-1.08273
0.200	39.80	7.96	0.18091	0.99×10^{-6}	0.20964	-.44468	2.53945	-1.63052
0.300	34.40	10.32	0.16831	0.64×10^{-6}	0.32063	-.75554	3.16746	-2.21866
0.450	34.35	20.25	0.15465	0.27×10^{-4}	0.42660	-1.42515	4.30431	-3.50228
0.600	38.33	23.00	0.14521	$-.26 \times 10^{-5}$	0.25293	-2.36211	5.39668	-5.41340
0.750	45.32	33.99	0.13846	0.14×10^{-5}	-.53827	-3.33139	5.81803	-7.71081
0.800	48.37	38.70	0.13667	0.50×10^{-5}	-.95744	-3.51928	5.71936	-8.37739

Table F.4. (d)

Prandtl number of 100.0

α	Gr	αGr	c_r	c_i	$\psi'''(0)_r$	$\psi'''(0)_i$	$\xi'(0)_r$	$\xi'(0)_i$
0.04	248.75	9.95	0.07396	0.56×10^{-5}	0.03333	-0.04347	6.52959	.16870
0.10	104.00	10.40	0.07265	0.14×10^{-4}	0.05078	-0.06209	6.77400	.22371
0.30	43.33	13.00	0.06857	0.83×10^{-5}	0.12266	-0.12611	7.65007	.79772
0.50	35.10	17.55	0.06467	0.35×10^{-5}	0.23641	-0.20117	8.51526	1.96180
0.60	34.00	20.40	0.06291	$-.11 \times 10^{-4}$	0.31183	-.24554	8.88203	2.68264
0.70	33.71	23.60	0.06123	$-.67 \times 10^{-4}$	0.40535	-.29609	9.21340	3.49171
0.80	35.00	28.00	0.05961	0.13×10^{-4}	0.52335	-.36662	9.36696	4.46903
0.90	36.44	32.80	0.05810	0.11×10^{-4}	0.66900	-.45023	9.45610	5.55143

Table F.4. (e)

Prandtl number of 1000

α	Gr	αGr	c_r	c_i	$\overset{\prime\prime\prime}{\psi}(0)_r$	$\overset{\prime\prime}{\psi}(0)_i$	$\overset{\prime}{\xi}(0)_r$	$\overset{\prime}{\xi}(0)_i$
0.04	283.82	11.35	0.05212	0.23×10^{-5}	0.04213	-0.04211	6.91421	0.18210
0.30	43.33	13.15	0.04655	0.81×10^{-5}	0.14568	-0.11757	7.92132	0.81210
0.60	30.00	18.10	0.04100	0.12×10^{-4}	0.33148	-0.23231	9.11210	2.89121
0.90	33.44	30.07	0.03710	0.13×10^{-4}	0.69910	-0.42191	9.59213	5.97321

F.5. Functions f and H and derivatives for various Prandtl numbers from Schmidt and Beckmann equations

F.5.(a) Prandtl number of 0.733

η	f	f'	f''	H	H'
0.0	0.0000	0.0000	0.6741	1.0000	-.5080
0.5	0.0649	0.2238	0.2465	0.7477	-.4953
1.0	0.1949	0.2745	-.0149	0.5139	-.4303
1.5	0.3244	0.2348	-.1222	0.3246	-.3228
2.0	0.4254	0.1685	-.1324	0.1913	-.2130
2.5	0.4941	0.1088	-.1035	0.1073	-.1281
3.0	0.5370	0.0657	-.0695	0.0583	-.0725
3.6	0.5660	0.0339	-.0386	0.0273	-.0350
4.2	0.5807	0.0169	-.0200	0.0126	-.0164
4.8	0.5879	0.0082	-.0099	0.0057	-.0076
5.4	0.5914	0.0040	-.0047	0.0025	-.0035
6.0	0.5932	0.0021	-.0022	0.0011	-.0016
6.8	0.5943	0.0010	-.0008	0.0003	-.0006
7.6	0.5949	0.0006	-.0002	0.0000	-.0002
8.0	0.5951	0.0005	-.0001	0.0000	-.0001

F.5.(b) Prandtl number of 1.0

η	f	f'	f''	H	H'
0.0	0.0000	0.0000	0.6421	1.0000	-0.5671
0.5	0.0610	0.2089	0.2208	0.7189	-.5488
1.0	0.1809	0.2502	-.0263	0.4638	-.4589
1.5	0.2975	0.2083	-.1203	0.2684	-.3197
2.0	0.3859	0.1450	-.1233	0.1422	-.1907
2.5	0.4441	0.0904	-.0928	0.0708	-.1020
3.0	0.4791	0.0524	-.0602	0.0339	-.0509
3.6	0.5016	0.0254	-.0321	0.0136	-.0210
4.2	0.5122	0.0116	-.0158	0.0053	-.0084
4.8	0.5169	0.0049	-.0075	0.0020	-.0034
5.4	0.5187	0.0018	-.0034	0.0008	-.0013
6.0	0.5194	0.0004	-.0014	0.0002	-.0005
6.8	0.5194	0.0000	-.0010	0.0000	-.0004
7.4	0.5193	0.0000	-.0005	0.0000	-.0003
8.0	0.5193	0.0000	-.0001	0.0000	-.0002

F.5.(c) Prandtl number of 6.7

η	f	f'	f''	H	H'
0.0	0.0000	0.0000	0.4547	1.0000	-1.0408
0.5	0.0388	0.1244	0.0866	0.4986	-.9016
1.0	0.1041	0.1259	-.0500	0.1588	-.4397
1.5	0.1595	0.0943	-.0658	0.0319	-.1154
2.0	0.1989	0.0648	-.0508	0.0044	-.0188
2.5	0.2257	0.0435	-.0352	0.0005	-.0022
3.0	0.2436	0.0289	-.0237	0.0000	-.0002
3.5	0.2554	0.0192	-.0159	0.0000	0.0000
4.0	0.2633	0.0127	-.0105	0.0000	0.0000
4.5	0.2684	0.0083	-.0070	0.0000	0.0000
5.0	0.2718	0.0055	-.0046	0.0000	0.0000
5.5	0.2741	0.0036	-.0031	0.0000	0.0000
6.0	0.2755	0.0023	-.0020	0.0000	0.0000
6.5	0.2765	0.0015	-.0013	0.0000	0.0000
7.0	0.2771	0.0010	-.0009	0.0000	0.0000
7.5	0.2775	0.0006	-.0006	0.0000	0.0000
8.0	0.2777	0.0004	-.0004	0.0000	0.0000

F.5.(d) Prandtl number of 100.0

η	f	f'	f''	H	H'
0.00	0.0000	0.0000	0.2517	1.0000	-2.191
0.10	0.0011	0.0205	0.1626	0.7815	-2.166
0.20	0.0039	0.0332	0.0952	0.5709	-2.018
0.30	0.0076	0.0402	0.0749	0.3836	-1.704
0.40	0.0118	0.0434	0.0176	0.2341	-1.276
0.50	0.0162	0.0442	0.0002	0.1287	-.8393
0.60	0.0206	0.0437	-.0087	0.0634	-.4837
0.70	0.0249	0.0426	-.0126	0.0280	-.2440
0.80	0.0291	0.0413	-.0413	0.0111	-.1088
0.90	0.0331	0.0399	-.0142	0.0039	-.0428
1.00	0.0371	0.0385	-.0140	0.0012	-.0149
1.50	0.0546	0.0320	-.0119	0.0000	0.0000
2.00	0.0692	0.0265	-.0101	0.0000	0.0000
3.00	0.0912	0.0180	-.0071	0.0000	0.0000
4.00	0.1061	0.0121	-.0049	0.0000	0.0000
5.00	0.1160	0.0081	-.0033	0.0000	0.0000
6.00	0.1226	0.0053	-.0022	0.0000	0.0000
8.00	0.1297	0.0022	-.0010	0.0000	0.0000
10.00	0.1326	0.0008	-.0005	0.0000	0.0000
12.00	0.1335	0.0002	-.0002	0.0000	0.0000
14.00	0.1336	0.0000	-.0001	0.0000	0.0000

F.5.(e) Prandtl number of 1000.0

η	f	f'	f''	H	H'
0.00	0.0000	0.0000	0.1450	1.0000	-3.9660
0.10	0.0006	0.0102	0.0647	0.6096	-3.7310
0.20	0.0018	0.0142	0.0209	0.2847	-2.6280
0.30	0.0033	0.0152	0.0032	0.0944	-1.2200
0.40	0.0048	0.0152	-.0019	0.0213	-.3596
0.50	0.0063	0.0150	-.0028	0.0032	-.0672
0.60	0.0078	0.0147	-.0029	0.0003	-.0080
0.80	0.0107	0.0141	-.0028	0.0000	0.0000
1.00	0.0135	0.0136	-.0027	0.0000	0.0000
1.40	0.0187	0.0125	-.0025	0.0000	0.0000
1.80	0.0235	0.0115	-.0023	0.0000	0.0000
2.20	0.0279	0.0106	-.0022	0.0000	0.0000
2.60	0.0320	0.0098	-.0020	0.0000	0.0000
3.00	0.0358	0.0090	-.0019	0.0000	0.0000
3.60	0.0409	0.0080	-.0017	0.0000	0.0000
4.20	0.0454	0.0070	-.0015	0.0000	0.0000
5.00	0.0505	0.0060	-.0012	0.0000	0.0000
7.00	0.0603	0.0039	-.0008	0.0000	0.0000
10.00	0.0691	0.0022	-.0004	0.0000	0.0000
14.00	0.0752	0.0011	-.0002	0.0000	0.0000
18.00	0.0786	0.0007	0.0000	0.0000	0.0000
22.00	0.0809	0.0005	0.0000	0.0000	0.0000

APPENDIX G

COMPUTER PROGRAMMES

G.1. The User's Guide to the Computer Programmes

The numerical techniques which have been employed to solve the disturbance differential equations have been presented in chapter 4. The numerical solutions of a number of problems have been calculated with the aid of a digital computer.

Two computer programmes have been developed. The programme 1 and the programme 2 solve the disturbance differential equations by the quasilinearization and trial-and-error techniques respectively.

The programmes are written in FORTRAN IV language, and in their present form may be run on CDC 6600 and CDC 6400 computers which work with fifteen significant figures on single precision. In order to run them on other machines some modifications may be necessary. Both programmes have been written so that the only changes required from run to run are in the data input. All of the data are read in from data cards.

Section G.2 presents a list of the FORTRAN symbols which are used in programmes together with their meanings. The flow charts are presented for main programmes in section G.3. The complete programme listings are presented in section G.4. The function of each subroutine in the programmes is described in the listing. Therefore the user should not find difficulty in understanding and using the programmes.

G.2. List of Symbols Used in the Computer Programmes

FORTRAN Symbol	Meaning
A	$a_1^K - a_1^{K+1}$
ABETA	β^2
AGAMA	γ^2
ALFAG	$i\alpha Gr$
ALFAS	α^2
B	$a_2^K - a_1^{K+1}$
C	$a_3^K - a_3^{K+1}$
C_1	a_1^K
C_2	a_2^K
C_3	a_3^K
C_4	a_4^K
C_5	a_5^K
CØNST(5)	a_1^{K+1}, a_2^{K+1}, a_3^{K+1}, a_4^{K+1}, a_5^{K+1}
CS	Phase velocity, c.
D	$a_4^K - a_5^K$
DELMAX	Stepwise increase of the effective infinity
E	$a_5^K - a_5^{K+1}$
ERMINA	Prescribed accuracy for A.
ERMINB	Prescribed accuracy for B.
ERMINC	Prescribed accuracy for C.
ERMIND	Prescribed accuracy for D.
ERMINE	Prescribed accuracy for E.

FORTRAN Symbol	Meaning
F	f
FF	f'
FFF	f''
FFFF	f'''
GR	Grashof number, Gr.
GUESS(8)	Original guesses to solution if no approximation is available.
H	Current integration step length.
HS(10)	Array which contains the variable integration steps.
IEXTEND	Set to 1 if the effective infinity is to be increased at any time.
IPRINT	If a print out of the solution is required every iteration.
IX	The number of step changes specified for the numerical integration.
JWRITE(10)	Print out control; the results are printed every JWRITE(I) steps at a step length HS(I).
MM	The number of separate problems to be solved for the current run.
MMAX(5)	Current maximum number of integration steps.
N	Number of first order equations to be solved.
NC	Iteration counter.

FORTRAN Symbol	Meaning
NCMAX	Maximum number of iterations allowed.
NHMG	Number of homogeneous sets to be solved.
NMAX(10)	The total number of iterations allowed.
PR	Prandtl number, Pr.
T	H
TT	H'
X	η
XMAX	η_{edg}
XXMAX	$\eta_{edg\ max}$
Y(6)	Y(I), I = 1,6
YD(6)	Dummy array in subroutine RKINT
YG(6)	$Y'(I)$, I,6
YH(6)	Dummy array in subroutine RKINT
YHϕ(3,6,1000)	$Y(I)_h^{K+1}(\eta)$ I = 1,6; h = 1,NHMG; η = 1,XMAX
YI(6,6)	Initial conditions for homogeneous sets of equation
YK(6,1000)	$Y(I)^K(\eta)$
YL(6)	$Y(I)^K$ at the point where the function is evaluated
YP(3,1000)	$Y(I)_p^{K+1}(\eta)$, I = 1,5; η = 1, XMAX
ZMAX(10)	The value of X at which the change of integration step length is to be made.

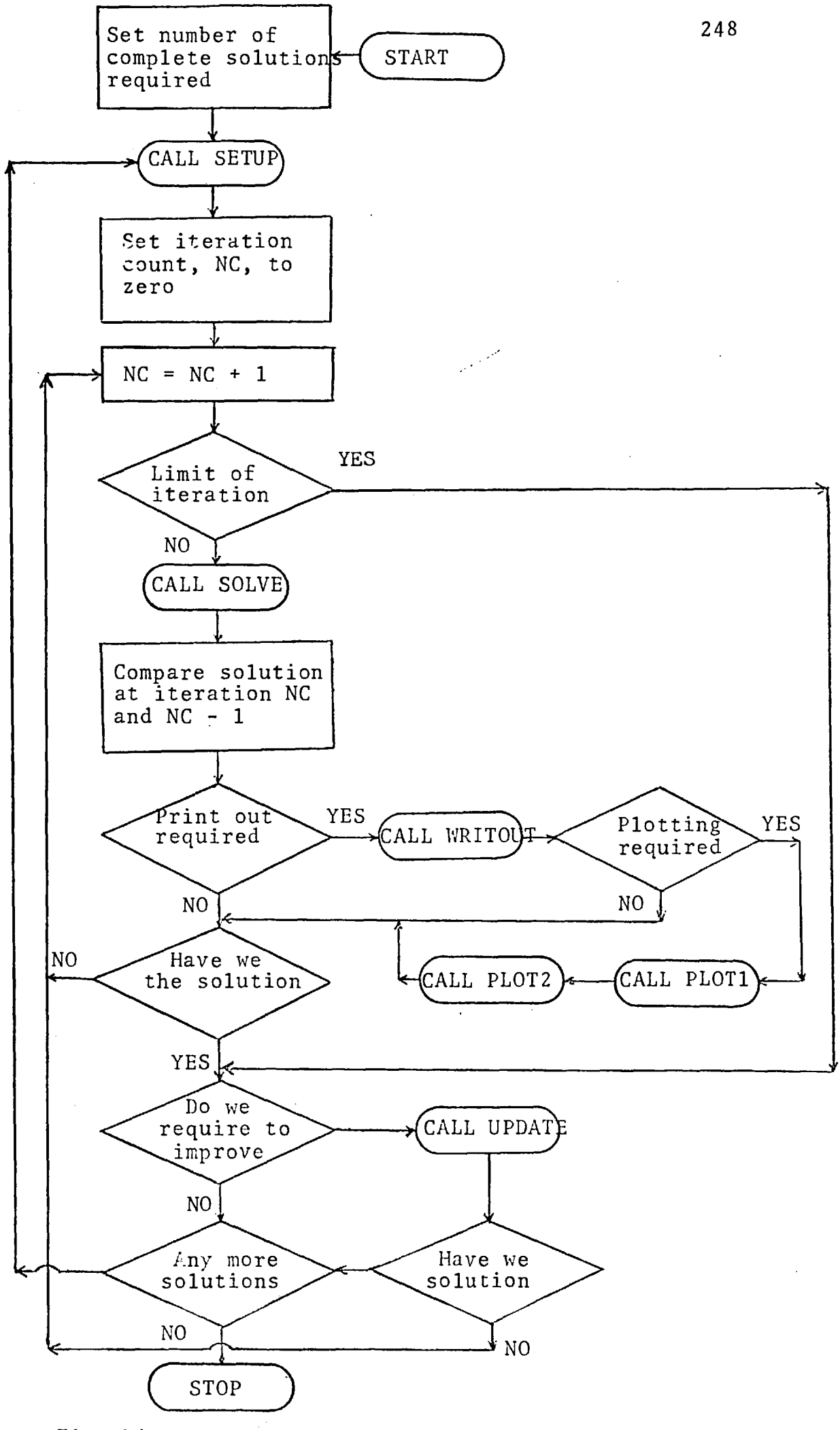

Flow Diagram G.3.1. Subroutine MAIN for Programme 1.

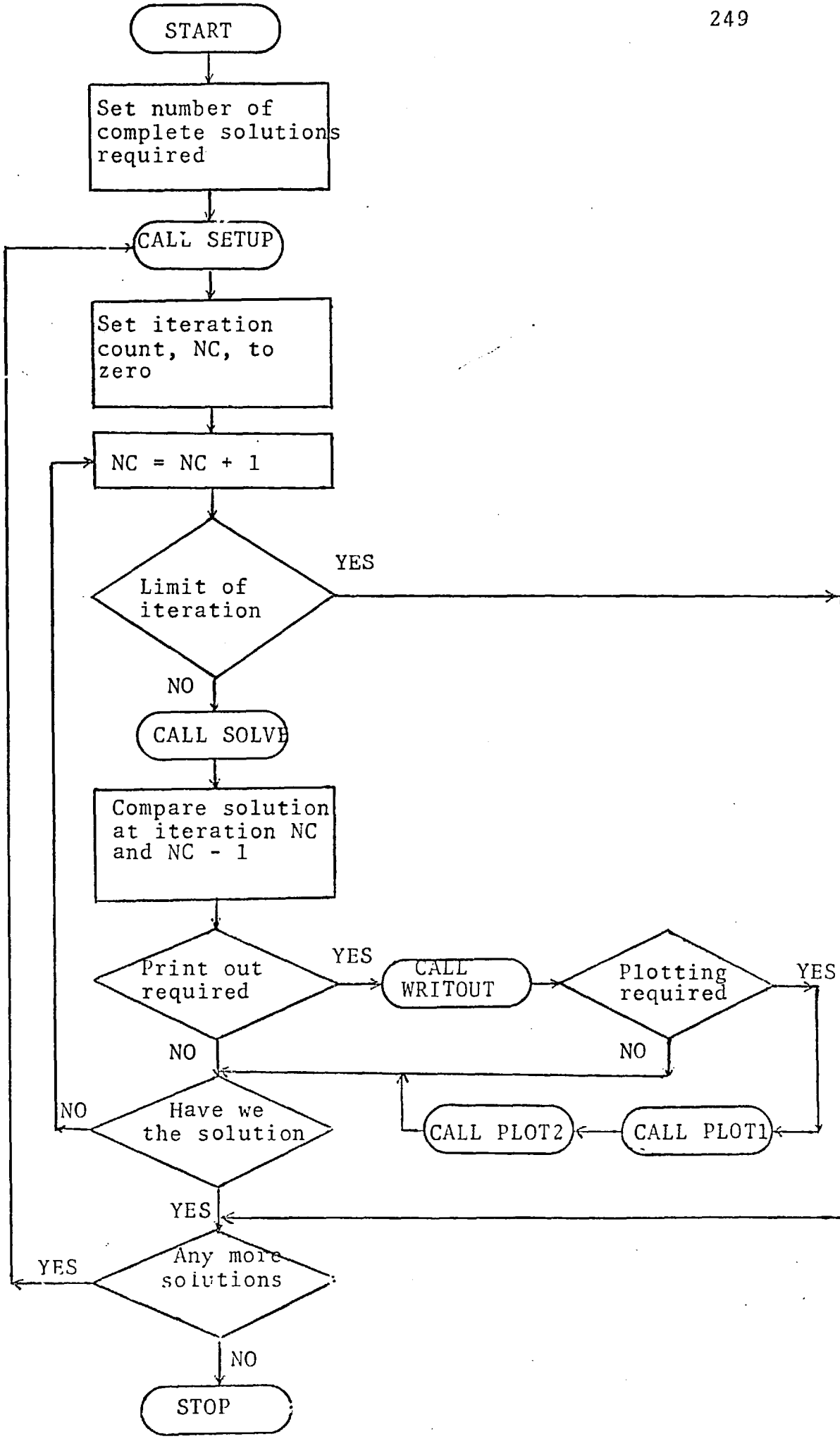

Flow Diagram G.3.2. Subroutine MAIN for Programme 2.

```
C**** C.4.1. LISTING OF THE COMPUTER PROGRAMME1.
C**** QUASILINEARIZATION TECHNIQUE.
      PROGRAM MAIN (INPUT=1001,OUTPUT=1001,TAPE5=INPUT,TAPE6=OUTPUT,
     1TAPE62)
      DIMENSION HS(10),NMAX(10)
      DIMENSION FF(500),FFF(500),TT(500),EE(100),EEE(100),PP(100)
      COMPLEX   YK(8,500 ),YH(8),Y(8),YG(8),YD(8),YL(8)
      COMPLEX A,B,C,D,E,C1,C2,C3,C4,C5,CONST(10),YI(8,8)
      COMPLEX  ACO,BCO,CCO,DCO,ECO,GR,PR,CS,  ALFAG,ALFAS,AGAMA,ABETA
      COMMON /ST1/A,B,C,D,E,ERMINA,ERMINB,ERMINC,ERMIND,ERMINE,NC,NCMAX
      COMMON/ST2/DELMAX,IEXTEND,IPRINT,ISTEUP,
     1XXMAX,XMAX,JWRITE(10),ZMAX(10)
      COMMON/ST3/CONST,HS,NMAX,YI,IX
      COMMON/ST4/YK,YH,Y,YG,YD,YL
      COMMON/ST6/X,NHMG,M,N
      COMMON/ST7/ACO,BCO,CCO,DCO,ECO
      COMMON/ST8/FF,FFF,TT,EE,EEE,PP
      COMMON/ST9/ALFAG,ALFAS,AGAMA,ABETA,GR,PR,CS
      COMMON/ST10/NB,ND,DND
      EXTERNAL  YGRD1
      NB=0
      PR=(.733,.0)
      READ (5,100) XXMAX,DELMAX,IPRINT ,IEXTEND,NCMAX
      READ(5,1234)(EE(I),EEE(I),PP(I),I=1,80 )
      READ(5,1235) EE(81),EEE(81),PP(81)
      CALL START(0)
      DND=1.
   12 CONTINUE
      ND=0
      NB=NB+1
      N=8
      NHMG=5
      MM=1
C**** MM IS THE NUMBER OF COMPLETE SOLUTIONS TO BE SOLVED DURING THE
C**** PRESENT COPUTER RUN.
      DO 4 NUMB=1,MM
      CALL SETUP
C**** SETUP DEFINES A NUMBER OF CONTROL VARIABLES  AND PHYSICAL PARAMETER
C**** WHICH DESCRIBE THE SESTEM.
    1 NC=NC+1
C**** UPDATING OF THE ITERATION COUNT FOR THE CURRENT SOLUTION.
      WRITE(6,4444)NC,NCMAX
      CALL SOLVE
C**** SOLVE CALCULATES A NEW APPROXIMATION TO THE SOLUTION USING THE
C**** QUASILINEARIZATION TECHNIQUE.
      IF(NC.EQ.1) GO TO 2
      C1=(0.,0.)
      C2=(0.,0.)
      C3=(0.,0.)
      C4=(0.,0.)
      C5=(0.,0.)
      A= CONST(1)-C1
      IF(A.LT.0.) A=-A
      B= CONST(2)-C2
      IF (B.LT.0.) B=-B
      C= CONST(3)-C3
      IF (C.LT.0.) C=-C
      D= CONST(4)-C4
      IF(D.LT.0.)D=-D
```

```
      F= CONST(5)-C5
      IF (F.LT.0.) E=-F
      IF(A.LE.ERMINA.AND.B.LE.ERMINB) IPRINT=0
      IF(C.LE.ERMINC.AND.D.LE.ERMIND) IPRINT=0
      IF(F.LE.ERMINE)                 IPRINT=0
C**** CONVERGENCE CHECK AND PRINTOUT CONTROL.
    2 C1=CONST(1)
      C2=CONST(2)
      C3=CONST(3)
      C4=CONST(4)
      C5=CONST(5)
      X=0.
      YK(1,1)=(0.,0.)
      YK(2,1)=(0.,0.)
      YK(3,1)=CONST(1)
      YK(4,1)=CONST(2)
      YK(5,1)=(0.,0.)
      YK(6,1)=CONST(3)
      YK(7,1)=CONST(4)
      YK(8,1)=CONST(5)
      IF(IPRINT.EQ.0) CALL WRITOUT
C**** WRITOUT CALLED IF REQUIRED TO PRINT OUT THE TABLE OF RESULT.
      IF(IPRINT.EQ.0) CALL PLOT1
C**** PLOT1 CALLED IF REQUIRED TO PLOT THE IGENFUNCTIONS.
      IF(IPRINT.EQ.0) CALL PLOT2
C**** PLOT2 CALLED IF REQUIRED TO PLOT THE ENERGY DISTRIBUTION.
       CALL UPDATE
C**** UPDATE IS CALLED IF THE SOLUTION REQUIRES UPDATING
      GO TO 12
      CALL FNPLOT
      STOP
  100 FORMAT(2F10.5,2I1,I2)
 1234 FORMAT(8F10.5)
 1235 FORMAT(3F10.5)
 4444 FORMAT(1X,2I5)
      END
```

```
C**** G.4.2. LISTING OF THE COMPUTER PROGRAMME2.
C**** TRIAL-AND-ERROR TECHNIQUE.
      PROGRAM MAIN (INPUT=1001,OUTPUT=1001,TAPE5=INPUT,TAPE6=OUTPUT,
     1TAPE62)
      DIMENSION FO(100),YKR(6,360) ,YKI(6,360),YREY(360),YDIS(360),YBOU(
     1360)
      DIMENSION HS(10),NMAX(10)
      DIMENSION EE(500),EEE(500),TT(500),FF(100),EEE(100),PP(100)
      COMPLEX   YK(6,500 ),YH(6),Y(6),YG(6),YD(6),YL(6)
      COMPLEX A,B,C1,C2,CONST(10),YI(6,6)
      COMPLEX  ACO,BCO,CCO,DCO,ECO,GR,PR,CS, ALFAG,ALFAS,AGAMA,ABETA
      COMMON/ST1/A,ERMINA,ERMINB,NC,NCMAX,B
      COMMON/ST2/DELMAX,IEXTEND,IPRINT,ISTEUP,
     1XXMAX,XMAX,JWRITE(10),ZMAX(10)
      COMMON/ST3/CONST,HS,NMAX,YI,IX
      COMMON/ST4/YK,YH,Y,YG,YD,YL
      COMMON/ST6/X,NHMG,M,N
      COMMON/ST7/ACO,BCO,CCO,DCO,ECO
      COMMON/ST8/FF,FFF,TT,EE,EEE,PP
      COMMON/ST9/ALFAG,ALFAS,AGAMA,ABETA,GR,PR,CS
      COMMON/ST10/NB,ND,DND
      COMMON/ST11/FO
      COMMON/ST12/YREY,YDIS,YBOU
      EXTERNAL  YGRD1
      NB=0
       PR=(.733,.0)
      READ (5,100) XXMAX,DELMAX,IPRINT ,IEXTEND,NCMAX
      READ(5,1234)(EE(I),EEE(I),PP(I),I=1,80 )
      READ(5,1235) EE(81),EEE(81),PP(81)
      CALL START(0)
      DND=1.
   12 CONTINUE
      ND=0
      NB=NB+1
      N=6
      NHMG=3
      MM=1
C**** MM IS THE NUMBER OF COMPLETE SOLUTIONS TO BE SOLVED DURING THE
C**** PRESENT COPUTER RUN.
       IF(NB.EQ.1 )  GO TO 70
       IF(NB.EQ.2 )  GO TO 71
       IF(NB.EQ.3 )  GO TO 72
       IF(NB.EQ.4 )  GO TO 73
       IF(NB.EQ.5 )  GO TO 74
       IF(NB.EQ.6 )  GO TO 75
       IF(NB.EQ.7 )  GO TO 76
       IF(NB.EQ.8 )  GO TO 77
       IF(NB.EQ.9 )  GO TO 78
       IF(NB.EQ.10)  GO TO 79
       IF(NB.EQ.11)  GO TO 80
       IF(NB.EQ.12)  GO TO 81
       IF(NB.EQ.13)  GO TO 82
       IF(NB.EQ.14)  GO TO 83
      IF(NB.EQ.15) GO TO 84
       IF(NB.EQ.16) GO TO  85
      IF (NB.EQ.17) GO TO 4
   70 CONTINUE
      CS=(.31253 ,.0)
      ALFAG=(.0,6.65   )
```

```
      ALFAS=(.005625,.0)
      GO TO 90
   71 CONTINUE
      CS=(.34003 ,.0)
      ALFAG=(.0,5.6450)
      ALFAS=(.0016,.0)
      GO TO 90
   72 CONTINUE
      CS=(.27368 ,.0)
      ALFAG=(.0,9.2600)
      ALFAS=(.0196,.0)
      GO TO 90
   73 CONTINUE
      CS=(.26843 ,.0)
      ALFAG=(.0,9.7900)
      ALFAS=(.0225,.0)
      GO TO 90
   74 CONTINUE
      CS=(.25855 ,.0)
      ALFAG=(.0,10.96)
      ALFAS=(.0289,.0)
      GO TO 90
   75 CONTINUE
      CS=(.25390,.0)
      ALFAG=(.0,11.62)
      ALFAS=(.0324,.0)
      GO TO 90
   76 CONTINUE
      CS=(.24937,.0)
      ALFAG=(.0,12.36)
      ALFAS=(.0361,.0)
      GO TO 90
   77 CONTINUE
      CS=(.22440,.0)
      ALFAG=(.0,18.97)
      ALFAS=(.0625,.0)
      GO TO 90
   78 CONTINUE
      CS=(.17850,.0)
      ALFAG=(.0,41.72)
      ALFAS=(.1225,.0)
      GO TO 90
   79 CONTINUE
      CS=(.161839,.0)
      ALFAG=(.0,51.52)
      ALFAS=(.2025,.0)
      GO TO 90
   80 CONTINUE
      CS=(.155478,.0)
      ALFAG=(.0,66.38)
      ALFAS=(.3025,.0)
      GO TO 90
   81 CONTINUE
      CS=(.154731,.0)
      ALFAG=(.0,92.70)
      ALFAS=(.4225,.0)
      GO TO 90
   82 CONTINUE
      CS=(.155841,.0)
```

```
      ALFAG=(.0,115.58)
      ALFAS=(.4900,.0)
      GO TO 90
   83 CONTINUE
      CS=(.157874,.0)
      ALFAG=(.0,161.97)
      ALFAS=(.5625,.0)
      GO TO 90
   84 CONTINUE
      CS=(.158505,.0)
      ALFAS=(.5776,.0)
      ALFAG=(.0,187.4)
      GO TO 90
   85 CONTINUE
      ALFAS=(.5776,.0)
      ALFAG=(.0,230.7)
      CS=(.158828,.0)
   90 CONTINUE
      ND=ND+1
      DO 4 NUMB=1,MM
      CALL SETUP
C**** SETUP DEFINES A NUMBER OF CONTROL VARIABLES  AND PHYSICAL PARAMETER
C**** WHICH DESCRIBE THE SESTEM.
    1 NC=NC+1
C**** UPDATING OF THE ITERATION COUNT FOR THE CURRENT SOLUTION.
      WRITE(6,4444)NC,NCMAX
      CALL SOLVE
C**** SOLVE CALCULATES A NEW APPROXIMATION TO THE SOLUTION USING THE
C**** TRIAL-AND-ERROR TECHNIQUE .
      IF(NC.EQ.1) GO TO 2
      C1=(0.,0.)
       C2=(0.,0.)
      A= CONST(1)-C1
      IF(A.LT.0.) A=-A
      B= CONST(2)-C2
      IF (B.LT.0.) B=-B
      IF(A.LE.ERMINA.AND.B.LE.ERMINB) IPRINT=0
C**** CONVERGENCE CHECK AND PRINTOUT CONTROL.
      WRITE(6,1006) A,B
    2 C1=CONST(1)
      C2=CONST(2)
      X=0.
      YK(1,1)=(0.,0.)
      YK(2,1)=(0.,0.)
      YK(3,1)=(1.,0.)
      YK(4,1)=CONST(1)
      YK(5,1)=(0.,0.)
      YK(6,1)=CONST(2)
      IF (ND.EQ.4) CALL WRITOUT
C**** WRITOUT CALLED IF REQUIRED TO PRINT OUT THE TABLE OF RESULT.
      IF (ND.EQ.4) CALL PLOT1
C**** PLOT1 CALLED IF REQUIRED TO PLOT THE IGENFUNCTIONS.
      IF (ND.EQ.4) CALL PLOT2
C**** PLOT2 CALLED IF REQUIRED TO PLOT THE ENERGY DISTRIBUTION.
       IF(ND.LE.3) GO TO 90
      GO TO 12
      CALL ENPLOT
      STOP
  100 FORMAT(2E10.5,2I1,I2)
```

```
1234 FORMAT(8F10.5)
1235 FORMAT(3F10.5)
4444 FORMAT(1X,215)
1006 FORMAT (6X,*A          =*,E17.10,5X,*B          =*,E17.10/)
     END
```

```
      SUBROUTINE SETUP
      DIMENSION FF(500),FFF(500),TT(500),EE(100),EEE(100),PP(100)
      DIMENSION HS(10),NMAX(10)
      COMPLEX   YK(6,500 ),YH(6),Y(6),YG(6),YD(6),YL(6),YI(6,6),CONST(10
     1),GUESS(10),A,B
      COMPLEX  GR,PR,CS,ALFAS,ALFAG,AGAMA,ABETA
      COMMON/ST1/A,ERMINA,ERMINB,NC,NCMAX,B
      COMMON/ST2/DELMAX,IEXTEND,IPRINT,ISTEUP,
     1XXMAX,XMAX,JWRITE(10),ZMAX(10)
      COMMON/ST3/CONST,HS,NMAX,YI,IX
      COMMON/ST4/YK,YH,Y,YG,YD,YL
      COMMON/ST6/X,NHMG,M,N
      COMMON/ST8/FF,FFF,TT,EE,EEE,PP
      COMMON/ST9/ALFAG,ALFAS,AGAMA,ABETA,GR,PR,CS
      COMMON/ST10/NB,ND,DND
      AGAMA=ALFAS-CS*ALFAG*PR
      ABETA=ALFAS-CS*ALFAG
      HS(1)=.01$HS(2)=.02$HS(3)=0.02$HS(4)=HS(5)=.02
      ZMAX(1)=1.$ZMAX(2)=4.$ZMAX(3)=6.$ZMAX(4)=8.$ZMAX(5)=XXMAX
      JWRITE(1)=5$JWRITE(2)=JWRITE(3)=JWRITE(4)=JWRITE(5)=5
      NC=0
      DO 3 K=1,100,10
      K1=K+9
      NC=NC+1
      KK=-1
      DO 3 L=K,K1
      IF(NC.GT.10)GO TO 16
      ABA=(FF(NC+1)-FF(NC))/10.
      ABB=(FFF(NC+1)-FFF(NC))/10.
      ABC=(PP(NC+1)-PP(NC))/10.
      KK=KK+1
      FF(L)=FF(NC)+ABA*KK
      FFF(L)=FFF(NC)+ABB*KK
      TT(L)=PP(NC)+ABC*KK
    3 CONTINUE
      K=0
   16 DO 4 K=1,345,5
      K1=K+4
      NC=NC+1
      KK=-1
      DO 4 L=K,K1
      ABB=(FFF(NC+1)-FFF(NC))/5.
      ABA=(FF(NC+1)-FF(NC))/5.
      ABC=(PP(NC+1)-PP(NC))/5.
      KK=KK+1
      KO=L+100
      FF(KO)=FF(NC)+ABA*KK
      FFF(KO)=FFF(NC)+ABB*KK
      TT(KO)=PP(NC)+ABC*KK
    4 CONTINUE
      IX=5
      XMAX=ZMAX(4)
      A=(1.,1.)
      B=(1.,1.)
      NHMG=3
      GUESS(1)=(1.,.1)$GUESS(2)=(.5,-.1)$GUESS(3)=(.3,-.5)$GUESS(4)=(.1
     1,-1.)$GUESS(5)=(1.,-3.)$GUESS(6)=(1.,-2.)
C**** GUESSED VALUES TO BE SUPPLIED IF REQUIRED.
      ERMINA=1.E-6 $ ERMINB=1.E-6
```

```
C**** LIMITS FOR CONVERGENCE FOR ACCEPTABLE SOLUTION.
      NMAX(1)=((ZMAX(1)+1.E-5)/HS(1))+1.00001
C**** CALCULATIONS OF THE NUMBER OF STEPS TO BE MADE AT EACH STEPLENGTH.
      WRITE(6,1000)  PR
      WRITE(6,2000)     HS(1),ZMAX(1),NMAX(1)
C**** PRINT OUT OF STEP DATA FOR CHECK.
      DO 6 K=2,IX
      NMAX(K)=(((ZMAX(K)-ZMAX(K-1))+1.E-5)/HS(K))+NMAX(K-1)
    6 WRITE(6,2000) HS(K),ZMAX(K),NMAX(K)
      IF(IEXTEND.EQ.1.OR.ISETUP.EQ.1) IX=4
      YI(1,1)=(0.,0.)$YI(1,2)=(0.,0.)$YI(1,3)=(1.,0.)$YI(1,4)=(0.,0.)$YI
     1(1,5)=(0.,0.)$YI(1,6)=(0.,0.)
      YI(2,1)=(0.,0.)$YI(2,2)=(0.,0.)$YI(2,3)=(0.,0.)$YI(2,4)=(1.,0.)$YI
     1(2,5)=(0.,0.)$YI(2,6)=(0.,0.)
      YI(3,1)=(0.,0.)$YI(3,2)=(0.,0.)$YI(3,3)=(0.,0.)$YI(3,4)=(0.,0.)$YI
     1(3,5)=(0.,0.)$YI(3,6)=(1.,0.)
C**** INITIAL CONDITIONS FOR THE HOMOGENEOUS SETS.
      NC=0
C**** SET THE ITERATION COUNT.
      JK=NMAX(IX)
      WRITE(6,1002) JK
      DO 7 M=1,JK
      DO 7 I=1,6
    7 YK(I,M)=GUESS(I)
      RETURN
 1000 FORMAT(1X,* PR=  *,F11.5,F10.5)
 2000 FORMAT(1X,2(F10.5,5X),I5/)
 1002 FORMAT(1X,* JK = *,I5)
      END
```

```
      SUBROUTINE SOLVF
      DIMENSION FF(500),FFF(500),TT(500),FE(100),FEF(100),PP(100)
      DIMENSION HS(10),NMAX(10)
      COMPLEX YHO(3,6,370)
      COMPLEX ALFA
      COMPLEX DCSIA
      COMPLEX  BR
      COMPLEX  GR,PR,CS,ALFAS,ALFAG,AGAMA,ABETA,ALFAQ,ABETQ,AGAMQ
      COMPLEX  YK(6,500 ),YH(6),Y(6),YG(6),YD(6),YL(6),HY1IN(6),HY2IN(6)
     1 ,HY3IN(6), HY4IN(6),HY5IN(6),HY6IN(6),CONST(10),YI(6,6)
      COMPLEX MABO,MBBO,MCBO,MABOP,MBBOP,MCBOP
      COMMON/   /YHO
      COMMON/ST3/CONST,HS,NMAX,YI,IX
      COMMON/ST4/YK,YH,Y,YG,YD,YL
      COMMON/ST6/X,NHMG,M,N
      COMMON/ST8/FF,FFF,TT,FE,FEF,PP
      COMMON/ST9/ALFAG,ALFAS,AGAMA,ABETA,GR,PR,CS
      COMMON/ST10/NB,ND,DND
      EXTERNAL  YGRD1
      M=0
C**** M IS THE STEP CONUTER. M=1 AT SURFACE OF BODY.
      X=0.
      IX=4
      DO 8 L=1,IX
      H=HS(L)
      NMAX(4)=365
      MMAX=NMAX(L)
    3 M=M+1
      MORTH=0
      IF(MORTH.EQ.0) GO TO 55
      CALL ORTHO
   55 CONTINUE
      DO  9NH=1,NHMG
      IF(M.GT.1) GO TO 1
      DO 5 I=1,N
    5 Y(I)=YI(NH,I)
      GO TO 2
    1 CONTINUE
      DO 21 I=1,N
   21 Y(I)=YHO(NH,I,M)
    2 CALL RKINT (H,YGRD1)
C**** RKINT STEPS FROM X TO X+H.
      DO 7 I=1,N
      LO=M+1
    7 YHO(NH,I,LO)=Y(I)
    9 CONTINUE
      IF(M.LT.MMAX) GO TO 3
    8 CONTINUE
      MMAX=351
      DO 11NH=1,NHMG
      HY1IN(NH)=YHO(NH,1,MMAX)
      HY2IN(NH)=YHO(NH,2,MMAX)
      HY3IN(NH)=YHO(NH,3,MMAX)
      HY4IN(NH)=YHO(NH,4,MMAX)
      HY5IN(NH)=YHO(NH,5,MMAX)
      HY6IN(NH)=YHO(NH,6,MMAX)
   11 CONTINUE
      ALFAQ=CSQRT(ALFAS)
      ABETQ=CSQRT(ABETA)
```

```
      AGAMO=CSQRT(AGAMA)
      MABO=HY4IN(1)+ALFAQ*HY3IN(1)-ABETA*HY2IN(1)-ABETA*ALFAQ*HY1IN(1)
     1 +(AGAMA/(AGAMA-ALFAS))*HY5IN(1)+(ALFAQ/(AGAMA-ALFAS))*HY6IN(1)
      MABO=-MABO
      MBBO=HY4IN(2)+ALFAQ*HY3IN(2)-ABETA*HY2IN(2)-ABETA*ALFAQ*HY1IN(2)
     1+(AGAMA/(AGAMA-ALFAS))*HY5IN(2)+(ALFAQ/(AGAMA-ALFAS))*HY6IN(2)
      MCBO=HY4IN(3)+ALFAQ*HY3IN(3)-ABETA*HY2IN(3)-ABETA*ALFAQ*HY1IN(3)
     1+(AGAMA/(AGAMA-ALFAS))*HY5IN(3)+(ALFAQ/(AGAMA-ALFAS))*HY6IN(3)
      MABOP=HY4IN(1)+ABETQ*HY3IN(1)-ALFAS*HY2IN(1)-ALFAS*ABETQ*HY1IN(1
     1)+(AGAMA/(AGAMA-ABETA))*HY5IN(1)+(ABETQ/(AGAMA-ABETA))*HY6IN(1)
      MABOP=-MABOP
      MBBOP=HY4IN(2)+ABETQ*HY3IN(2)-ALFAS*HY2IN(2)-ALFAS*ABETQ*HY1IN(2
     1)+(AGAMA/(AGAMA-ABETA))*HY5IN(2)+(ABETQ/(AGAMA-ABETA))*HY6IN(2)
      MCBOP=HY4IN(3)+ABETQ*HY3IN(3)-ALFAS*HY2IN(3)-ALFAS*ABETQ*HY1IN(3
     1)+(AGAMA/(AGAMA-ABETA))*HY5IN(3)+(ABETQ/(AGAMA-ABETA))*HY6IN(3)
      CONST(2)=((MABO*MBBOP)-(MABOP*MBBO))/((MBBOP*MCBO)-(MBBO*MCBOP))
      CONST(1)=(MABO-(MCBO*CONST(2)))/MBBO
C**** CALCULATION OF THE CONSTANTS.
      WRITE(6,1003) CONST(1)
      WRITE(6,1004) CONST(2)
C**** PRINT OUT THE VALUES OF THE CONSTANTS.
      DO 10 M=2,MMAX
      DO 10 I=1,N
      YK(I,M)=YHO(1,I,M)+CONST(1)*YHO(2,I,M)+CONST(2)*YHO(3,I,M)
   10 CONTINUE
C**** CALCULATE THE NEW SOLUTION BY SUPERPOSITION.
      BR=AGAMO*YK(5,MMAX)+YK(6,MMAX)
      ALFA=CSQRT(ALFAS)
      GR=ALFAG/ALFA
      WRITE(6,44) ALFA,GR,CS
   44 FORMAT (1X,*ALFA*,2(E15.8),1X,*GR*,2(E15.8),1X,*CS*,2(E15.8))
      WRITE(6,1005)   BR
 1005 FORMAT(35X,*BR=*,2(E17.10))
      BRR=REAL(BR)
      BRI=AIMAG(BR)
      CSR=REAL(CS)
      CSI=AIMAG(CS)
      WRITE (6,12) NR,ND
   12 FORMAT (35X,*NR=*,I5,*ND=*,I5)
      IF(ND.EQ.1)  GO TO 30
      IF(ND.EQ.2)  GO TO 31
      IF(ND.EQ.3)  GO TO 32
      IF(ND.EQ.4) GO TO 33
   30 CONTINUE
      BRR1=BRR
      BRI1=BRI
      CSR1=CSR
      CSI1=CSI
      CS=CS+(.0000001,.0)
      GO TO 33
   31 CONTINUE
      BRR2=BRR
      BRI2=BRI
      CSR2=CSR
      CSI2=CSI
      CS=CS+(-.0000001,.0000001)
      GO TO 33
   32 CONTINUE
      BRR3=BRR
```

```
      BRI3=BRI
      CSR3=CSR
      CSI3=CSI
      BRRDR=BRR2-BRR1
      BRIDR=BRI2-BRI1
      BRRDI=BRR3-BRR1
      BRIDI=BRI3-BRI1
      CSRD1=CSR2-CSR1
      CSRD2=CSR3-CSR1
      CSID1=CSI2-CSI1
      CSID2=CSI3-CSI1
      BRR1=-BRR1
      BRI1=-BRI1
      DCSR=((BRR1*BRIDI)-(BRI1*BRRDI))/(BRRDR*BRIDI-BRIDR*BRRDI)
      DCSI=(BRR1-DCSR*BRRDR)/BRRDI
      DCSRZ=DCSR*CSRD1
      DCSIZ=DCSI*CSID2
      DCSIA=(.0,1.)*DCSIZ
      CS=CS+(.0,-.0000001)
      CS=CS+DCSRZ+DCSIA
   33 CONTINUE
C**** CAUCHY-RIEMANN EQUATION.
      RETURN
 1003 FORMAT(6X,*R-CONST(1)   =*,E17.10,5X,*I-CONST(1)   =*,E17.10)
 1004 FORMAT(6X,*R-CONST(2)   =*,E17.10,5X,*I-CONST(2)   =*,E17.10)
      END
```

```
      SUBROUTINE WRITOUT
      DIMENSION FO(100),YKR(6,360) ,YKI(6,360),YREY(360),YDIS(360),YBOU(
     1360)
      DIMENSION HS(10),NMAX(10)
      DIMENSION FF(500),FFF(500),TT(500),EE(100),EEE(100),PP(100)
      COMPLEX YHO(3,6,370)
      COMPLEX   YK(6,500 ),YH(6),Y(6),YG(6),YD(6),YL(6),YI(6,6),CONST(10
     1) ,A,B
      COMPLEX  GR,PR,CS,ALFAS,ALFAG,AGAMA,ABETA,ALFAQ,ABETQ,AGAMQ
      COMMON/   /YHO
      COMMON/ST1/A,ERMINA,ERMINB,NC,NCMAX,B
      COMMON/ST2/DELMAX,IEXTEND,IPRINT,ISTEUP,
     1XXMAX,XMAX,JWRITE(10),ZMAX(10)
      COMMON/ST3/CONST,HS,NMAX,YI,IX
      COMMON/ST4/YK,YH,Y,YG,YD,YL
      COMMON/ST6/X,NHMG,M,N
      COMMON/ST8/FF,FFF,TT,EE,EEE,PP
      COMMON/ST9/ALFAG,ALFAS,AGAMA,ABETA,GR,PR,CS
      COMMON/ST10/NB,ND,DND
      COMMON/ST11/FO
      COMMON/ST12/YREY,YDIS,YBOU
C**** WRITOUT,PRINTS OUT THE VALUES OF THE SOLUTION IF REQUIRED.
C**** KN IS THE NUMBER OF THE GRID LINE AT WICH THE PRINT OUT BEGINS.
C**** KM IS THE FINAL GRID NUMBER.
C**** KL IS THE STEPWISE INCREASE AT WHICH INTERMEDIATE VALUES ARE
C**** PRINTED.
      MP=0
      ALFGR=AIMAG(ALFAG)
      ALFAR=REAL(ALFAS)
      WRITE(6,1001)
      KN=1
      JWRITE(1)=10
      X=-HS(1)*JWRITE(1)
      IX=3
      DO 2 L=1,IX
      KL=NMAX(L)
      KM=JWRITE(L)
      IF(KM.EQ.0) IERROR=3
      IF(IERROR.NE.0) RETURN
      DO 1 M=KN,KL,KM
      X=X+HS(L)*KM
      WRITE(6,1002) X,(YK(I,M),I=1,3)
    1 CONTINUE
      KN=NMAX(L)+JWRITE(L+1)
    2 CONTINUE
      WRITE(6,1003)
      KN=1
      X=-HS(1)*JWRITE(1)
      DO 8 L=1,IX
      KL=NMAX(L)
      KM=JWRITE(L)
      DO 9 M=KN,KL,KM
      X=X+HS(L)*KM
      WRITE(6,1002) X,(YK(I,M),I=4,6)
    9 CONTINUE
    8 KN=NMAX(L)+JWRITE(L+1)
      WRITE(6,1004)
      KN=1
      X=-HS(1)*JWRITE(1)
```

```
      DO 3 L=1,IX
      KL=NMAX(L)
      KM=JWRITE(L)
      DO4 M=KN,KL,KM
      MP=MP+1
      DO 5 I=1,N
      YKR(I,M)=REAL(YK(I,M))
      YKI(I,M)=AIMAG(YK(I,M))
    5 CONTINUE
      YPEY(M)=-(YKR(2,M)*YKI(1,M)-YKI(2,M)*YKR(1,M))*FO(MP)
      YDIS(M)=-(1/ALFGR)*((ALFAR*YKR(1,M)-YKR(3,M))**2+(ALFAR*YKI(1,M)-
     1YKI(3,M))**2)
      YBOU(M)=(1/ALFGR)*(YKR(5,M)*YKR(2,M)+YKI(5,M)*YKI(2,M))
      X=X+HS(L)*KM
      WRITE(6,1005) X,YPEY(M),YDIS(M),YBOU(M)
    4 CONTINUE
      KN=NMAX(L)+JWRITE(L+1)
    3 CONTINUE
      RETURN
1001 FORMAT(5X,1HX,10X,6HR-Y(1),12X,6HI-Y(1),12X,6HR-Y(2),12X,6HI-Y(2),
     112X,6HR-Y(3),12X,6HI-Y(3))
1003 FORMAT(5X,1HX,10X,6HR-Y(4),12X,6HI-Y(4),12X,6HR-Y(5),12X,6HI-Y(5),
     112X,6HR-Y(6),12X,6HI-Y(6))
1002 FORMAT (2X,F8.5,6(1X,E17.10))
1004 FORMAT(5X,1HX,10X,16HREYNOLDS STRESSE,18X,11HDISSIPATION,18X,8HBUO
     1YANCY)
1005 FORMAT(2X,F8.5,3(10X,E17.10))
      END
```

```
      SUBROUTINE PLOT1
      DIMENSION XX(100),YYR(100), YYI(100)
      DIMENSION HS(10),NMAX(10)
      DIMENSION FF(500),FFF(500),TT(500),EE(100),EEE(100),PP(100)
      COMPLEX YHO(3,6,500)
      COMPLEX   YK(6,500 ),YH(6),Y(6),YG(6),YD(6),YL(6),YI(6,6),CONST(10
     1) ,A,B
      COMPLEX  GR,PR,CS,ALFAS,ALFAG,AGAMA,ABETA,ALFA
      COMMON/   /YHO
      COMMON/ST1/A,ERMINA,ERMINB,NC,NCMAX,B
      COMMON/ST2/DELMAX,IEXTEND,IPRINT,ISTEUP,
     1XXMAX,XMAX,JWRITE(10),ZMAX(10)
      COMMON/ST3/CONST,HS,NMAX,YI,IX
      COMMON/ST4/YK,YH,Y,YG,YD,YL
      COMMON/ST6/X,NHMG,M,N
      COMMON/ST8/FF,FFF,TT,EE,EEE,PP
      COMMON/ST9/ALFAG,ALFAS,AGAMA,ABETA,GR,PR,CS
      COMMON/ST10/NB,ND,DND
C**** EIGENFUNCTIONS.
      RR=AIMAG(GR)
      ALFA=CSQRT(ALFAS)
      ALF=REAL(ALFA)
      CSR=REAL(CS)
      CSI=AIMAG(CS)
      JWRITE(1)=10
      IX=3
      FX1=.0
      DX2=1.
      FY1=-3.
      DY2=.6
      XSCALE=1./DX2
      XADD=  -FX1/DX2
      YSCALE=1./DY2
      YADD=  -FY1/DY2
      XO=9.
      DO 3 I=1,6
      MV=0
      KN=1
      X=-HS(1)*JWRITE(1)
      IF(I.NE.1.AND.I.NE.4) GO TO 4
      IF(I.NE.1) GO TO 5
      IF (NB.EQ.1)  GO TO 9
      IF (NB.EQ.5)  GO TO 9
      IF (NB.EQ.9)  GO TO 9
      IF (NB.EQ.13) GO TO 9
      GO TO 7
    9 CONTINUE
      XO=2.
      YO=2.
      IF (NB.EQ.1)  GO TO 8
      CALL NEWPAGE
      GO TO 8
    7 CONTINUE
      YO=-13.
    8 CONTINUE
      CALL PLOT(XO,YO,-3)
      GO TO 4
    5 CONTINUE
      YO=13.
```

```
      CALL PLOT(.0,YO,-3)
    6 CONTINUE
      CALL AXIS(.0,.0,29H NORMAL DISTANCE FROM PLATE- ,-29.6,.0,FX1,DX2
     1)
      CALL AXIS(.0,.0,14HEIGENFUNCTIONS,14,10.,90., FY1,DY2)
      CALL SYMBOL (2.3,10.,.14,3HFIG,.0,3)
      CALL SYMBOL(1.,9.8,.14,3HPR=,.0,3)
      CALL SYMBOL(1.,9.5,.14,3HGR=,.0,3)
      CALL SYMBOL(1.,1.1,.14,18HWAVE NUMBER       =,.0,18)
      CALL SYMBOL(1.,.8 ,.14,18HPHASE VELOCITY CR=,.0,18)
      CALL SYMBOL(1.,.5 ,.14,18HPHASE VELOCITY CI=,.0,18)
      CALL NUMBER(1.42,9.8,.14,PR,.0,2)
      CALL NUMBER(1.42,9.5,.14,RR,.4,2)
      CALL NUMBER(3.56,1.1,.14,ALF,.0,6)
      CALL NUMBER(3.56,.8 ,.14,CSR,.0,6)
      CALL NUMBER(3.56,.5 ,.14,CSI,.0,6)
    4 CONTINUE
      DO 2 L=1,IX
      KL=NMAX(L)
      KM=JWRITE(L)
      DO 1 M=KN,KL,KM
      MV=MV+1
      X=X+HS(L)*KM
      XX(MV)=X
      YYR(MV)=REAL(YK(I,M))
      YYI(MV)=AIMAG(YK(I,M))
    1 CONTINUE
      KN=NMAX(L)+JWRITE(L+1)
    2 CONTINUE
      CALL ARKIST(XX,YYR,1,60,30,XSCALE,YSCALE,XADD,YADD,2,1)
      CALL ARKIST(XX,YYI,1,60,30,XSCALE,YSCALE,XADD,YADD,2,1)
    3 CONTINUE
      RETURN
      END
```

```
      SUBROUTINE PLOT2
      DIMENSION XX(100)
      DIMENSION YREY(360),YDIS(360),YBOU(360)
      DIMENSION  YRE(100),YDI(100),YBO(100)
      DIMENSION HS(10),NMAX(10)
      COMPLEX   YK(6,500 ),YH(6),Y(6),YG(6),YD(6),YL(6),YI(6,6),CONST(10
     1) ,A,B
      COMPLEX  GR,PR,CS,ALFAS,ALFAG,AGAMA,ABETA,ALFA
      COMMON/ST1/A,ERMINA,ERMINB,NC,NCMAX,B
      COMMON/ST2/DELMAX,IEXTEND,IPRINT,ISTEUP,
     1XXMAX,XMAX,JWRITE(10),ZMAX(10)
      COMMON/ST3/CONST,HS,NMAX,YI,IX
      COMMON/ST4/YK,YH,Y,YG,YD,YL
      COMMON/ST6/X,NHMG,M,N
      COMMON/ST9/ALFAG,ALFAS,AGAMA,ABETA,GR,PR,CS
      COMMON/ST10/NB,ND,DND
      COMMON/ST12/YREY,YDIS,YBOU
C**** ENERGY DISTRIBUTIONS.
      RB=AIMAG(GR)
      ALFA=CSQRT(ALFAS)
      ALF=REAL(ALFA)
      CSR=REAL(CS)
      CSI=AIMAG(CS)
      JWRITE(1)=10
      IX=3
      FX1=.0
      DX2=1.
      IF(NB.LE.8) DY2=.05
      IF(NB.LE.8)  FY1=-.2
      IF(NB.GT.8)  FY1=-.024
      IF(NB.GT.8) DY2=.004
      IF(NB.GT.11) DY2=.0018
      IF(NB.GT.11)  FY1=-.0126
      XSCALE=1./DX2
      XADD=  -FX1/DX2
      YSCALE=1./DY2
      YADD=  -FY1/DY2
      XO=9.
      MV=0
      KN=1
      X=-HS(1)*JWRITE(1)
      IF (NB.EQ.1)  GO TO 9
      IF (NB.EQ.9)  GO TO 9
      IF(FLOAT(NB)/2 .EQ.FLOAT(NB/2)) GO TO 5
      GO TO 7
    9 CONTINUE
      XO=2.
      YO=2.
      IF (NB.EQ.1)  GO TO 8
      CALL NEWPAGE
      GO TO 8
    7 CONTINUE
      YO=-13.
    8 CONTINUE
      CALL PLOT(XO,YO,-3)
      GO TO 6
    5 CONTINUE
      YO=13.
       CALL PLOT(.0,YO,-3)
```

```
6 CONTINUE
  CALL AXIS(.0,.0,29H NORMAL DISTANCE FROM PLATE- ,-29,6,.0,FX1,DX2
 1)
  CALL AXIS(.0,.0,37HREYNOLDS STRESSE,DISSIPATION,BUOYANCY,37,10.,90
 1.,FY1,DY2)
  CALL SYMBOL (2.3,10.,.14,3HFIG,.0,3)
  CALL SYMBOL(1.,9.8,.14,3HPR=,.0,3)
  CALL SYMBOL(1.,9.5,.14,3HGR=,.0,3)
  CALL SYMBOL(1.,1.1,.14,18HWAVE NUMBER       =,.0,18)
  CALL SYMBOL(1.,.8 ,.14,18HPHASE VELOCITY CR=,.0,18)
  CALL SYMBOL(1.,.5 ,.14,18HPHASE VELOCITY CI=,.0,18)
  CALL NUMBER(1.42,9.8,.14,PR,.0,2)
  CALL NUMBER(1.42,9.5,.14,RR,.4,2)
  CALL NUMBER(3.56,1.1,.14,ALF,.0,6)
  CALL NUMBER(3.56,.8 ,.14,CSR,.0,6)
  CALL NUMBER(3.56,.5 ,.14,CSI,.0,6)
  DO 2 L=1,IX
  KL=NMAX(L)
  KM=JWRITE(L)
  DO 1 M=KN,KL,KM
  MV=MV+1
  X=X+HS(L)*KM
  XX(MV)=X
  YRE(MV)=YREY(M)
  YDI(MV)=YDIS(M)
  YBO(MV)=YBOU(M)
1 CONTINUE
  KN=NMAX(L)+JWRITE(L+1)
2 CONTINUE
  CALL ARKIST(XX,YRE,1,60,30,XSCALE,YSCALE,XADD,YADD,2,1)
  CALL ARKIST(XX,YDI,1,60,30,XSCALE,YSCALE,XADD,YADD,2,1)
  CALL ARKIST(XX,YBO,1,60,30,XSCALE,YSCALE,XADD,YADD,2,1)
  RETURN
  END
```

```
      SUBROUTINE UPDATE
      DIMENSION FF(500),FFF(500),TT(500),FF(100),FFF(100),PP(100)
      DIMENSION HS(10),NMAX(10)
      COMPLEX   YK(8,500 ),YH(8),Y(8),YG(8),YD(8),YL(8),YI(8,8),CONST(10
     1)
      COMMON/ST2/DELMAX,IEXTEND,IPRINT,ISTEUP,
     1XXMAX,XMAX,JWRITE(10),ZMAX(10)
      COMMON/ST3/CONST,HS,NMAX,YI,IX
      COMMON/ST4/YK,YH,Y,YG,YD,YL
      COMMON/ST6/X,NHMG,M,N
      EXTERNAL  YGRD2
      IF (IEXTEND.EQ.1) GO TO 7
C**** EXTENSION OF EXISTING SOLUTION BY SIMPLE EXTRAPOLATION.
      IF(ISETUP.NE.0) GO TO 1
C**** SET UP THE INITIAL GUESS.
      RETURN
    1 DO 3  I=1,N
    3 Y(I)=YK(I,1)
C**** SET ALL VALUES OF THE Y,S AT THE SURFACE.
      M=1
      IX=5
C**** IX IS THE NUMBER OF CHANGES OF STEP.
      X=0.
      DO 6 L=1,IX
      H=HS(L)
      NMAX=NMAX(L)
C**** SET STEP LENGTH AND AHE NUMBER OF STEPS.
    4 M=M+1
      CALL RKINT (H,YGRD1)
C**** STEP TO NEXT POINT USING  THE NON-LINEAR EQUATIONS.
      DO 5  I=1,N
    5 YK(I,M)=Y(1)
C**** SET UP THE STORED FIRST APPROXIMATION TO THE SOLUTION.
      IF (M.LT.MMAX) GO TO 4
C**** IF WE HAVE NOT REACHED THE LIMIT OF STEPS,RETURN TO RKINT.
    6 CONTINUE
      WRITE(6,1000) ISETUP
      KN=1
      X=-HS(1)*JWRITE(1)
      DO 61 L=1,IX
      KL=NMAX(L)
      KM=JWRITE(L)
      DO 62 M=KN,KL,KM
      X=X+HS(L)*KM
   62 WRITE(6,1002) X,(YK(I,M),I=1,8)
      KN=NMAX(L)+JWRITE(L+1)
   61 CONTINUE
      ISETUP=0
      RETURN
    7 MA=NMAX(IX)
      IX=5
      IPRINT=1
      XMAX=XMAX+DELMAX
C**** UPDATE THE EFFECTIVE INFINITY.
      IF(XMAX.LE.XXMAX) GO TO 8
      IF(ISETUP.NE.0) GO TO 1
      RETURN
    8 NMAX(IX)=((XMAX-ZMAX(4))+1.E-5)/HS(5)+NMAX(4)
      MMAX=NMAX(IX)
```

```
C**** UPDATE NUMBER OF STEPS AT STEP LENGTH4.
      DO 9 I=1,N
      DO 9 M=MA,MMAX
    9 YK(I,M)=YK(I,MA)
   10 RETURN
 1002 FORMAT(1X,9(2X,F10.5))
 1009 FORMAT(1H1,1X,*NON-LINEAR INITIL VALUE PROBLEM *,5X, *ISTUP*,I5)
      END
```

```
      SUBROUTINE  ORTHO
      DIMENSION HS(10),NMAX(10)
      COMPLEX YHO(3,6,500),YI(6,6) ,CONST(10)
      COMPLEX ABHO(6),ABBH(6),ACHO(6),ACCH(6),ADHO(6),ADDH(6)
      COMPLEX  AYH(6),BYH(6),CYH(6),DYH(6),EYH(6),FYH(6),AHO(6),BHO(6) ,
     1CHO(6),AAHO(6),BBHO(6),CCHO(6 ),AY,BY,CY,DY,EY,FY,YHA(6),YHB(6),
     1YHC(6)
      COMMON/  / YHO
      COMMON/ST3/CONST,HS,NMAX,YI,IX
      COMMON/ST6/X,NHMG,M,N
C**** ORTHOGONALIZATION TECHNIQUE.
      DO 1 I=1,N
    1 AYH(I)=YHO(1,I,M)*CONJG(YHO(1,I,M))
      AY=CSQRT(AYH(1)+AYH(2)+AYH(3)+AYH(4)+AYH(5)+AYH(6))
      DO 2 I=1,N
      YHO(1,I,M)=YHO(1,I,M)/AY
      YI(1,I)=YI(1,I)/AY
    2 BYH(I)=YHO(1,I,M)*CONJG(YHO(2,I,M))
      BY=BYH(1)+BYH(2)+BYH(3)+BYH(4)+BYH(5)+BYH(6)
      RBY=REAL(BY)
      DO 4 I=1,N
      AHO(I)=RBY*YHO(1,I,M)
      AAHO(I)=YHO(2,I,M)-AHO(I)
    4 CYH(I)=AAHO(I)*CONJG(AAHO(I))
      CY=CSQRT(CYH(1)+CYH(2)+CYH(3)+CYH(4)+CYH(5)+CYH(6))
      DO 5 I=1,N
      ABHO(I)=RBY*YI(1,I)
      ABBH(I)=YI(2,I)-ABHO(I)
      YI(2,I)=ABBH(I)/CY
    5 YHO(2,I,M)=AAHO(I)/CY
      DO 6 I=1,N
    6 DYH(I)=YHO(1,I,M)*CONJG(YHO(3,I,M))
      DY=DYH(1)+DYH(2)+DYH(3)+DYH(4)+DYH(5)+DYH(6)
      RDY=REAL(DY)
      DO 7 I=1,N
      BHO(I)=RDY*YHO(1,I,M)
    7 EYH(I)=YHO(2,I,M)*CONJG(YHO(3,I,M))
      EY=EYH(1)+EYH(2)+EYH(3)+EYH(4)+EYH(5)+EYH(6)
      REY=REAL(EY)
      DO 9  I=1,N
      CHO(I)=REY*YHO(2,I,M)
      BBHO(I)=YHO(3,I,M)-BHO(I)
      CCHO(I)=BBHO(I)-CHO(I)
    9 FYH(I)=CCHO(I)*CONJG(CCHO(I))
      FY=CSQRT(FYH(1)+FYH(2)+FYH(3)+FYH(4)+FYH(5)+FYH(6))
      DO 10 I=1,N
      ACHO(I)=REY*YI(2,I)
      ACCH(I)=RDY*YI(1,I)
      ADHO(I)=YI(3,I)-ACCH(I)
      ADDH(I)=ADHO(I)-ACHO(I)
      YI(3,I)=ADDH(I)/FY
   10 YHO(3,I,M)=CCHO(I)/FY
      WRITE(6,6274)M
 6274 FORMAT(I5)
      WRITE(6,1000) (YHO(1,I,M),YHO(2,I,M),YHO(3,I,M),I=1,N)
      WRITE(6,1000) (YI(1,I),YI(2,I),YI(3,I),I=1,N)
 1000 FORMAT(6(3X,E17.10))
      RETURN
      END
```

```
      SUBROUTINE RKINT (H,YGRD)
      COMPLEX  ACO,BCO,CCO,DCO,ECO,GR,PR,CS, ALFAG,ALFAS,AGAMA,ABETA
      COMPLEX   YK(6,500 ),YH(6),Y(6),YG(6),YD(6),YL(6)
      DIMENSION AFF(500),AFFF(500),ATT(500)
      DIMENSION FF(500),FFF(500),TT(500),EE(100),EEE(100),PP(100)
      COMMON/ST4/YK,YH,Y,YG,YD,YL
      COMMON/ST5/AFF,AFFF,ATT
      COMMON/ST6/X,NHMG,M,N
      COMMON/ST7/ACO,BCO,CCO,DCO,ECO
      COMMON/ST8/FF,FFF,TT,EE,EEE,PP
      COMMON/ST9/ALFAG,ALFAS,AGAMA,ABETA,GR,PR,CS
C**** RUNGE-KUTA SINGLE STEP INTEGRATION ROUTINE.
      DO 1 J=1,N
    1 YD(J)=Y(J)
      ATT(M)=TT(M)
      AFF(M)=FF(M)
      AFFF(M)=FFF(M)
C**** FUNCTION EVALUATION AT POINT X.
      CALL YGRD
      DO 2 J=1,N
      YG(J)=YG(J)*H
    2 YH(J)=YG(J)
      X=X+0.5*H
      DO 4 I=1,2
      DO 3 J=1,N
    3 Y(J)=YD(J)+.5*YG(J)
      AFF(M)=(FF(M)+FF(M+1))/2.
      AFFF(M)=(FFF(M)+FFF(M+1))/2.
      ATT(M)=(TT(M)+TT(M+1))/2.
C**** FUNCTION EVALUATION AT  HALF STEP.
      CALL YGRD
      DO 4 J=1,N
      YG(J)=YG(J)*H
    4 YH(J)=YH(J)+2.*YG(J)
      X=X+0.5*H
      DO 5 J=1,N
    5 Y(J)=YD(J)+YG(J)
      AFF(M)=FF(M+1)
      AFFF(M)=FFF(M+1)
      ATT(M)=TT(M+1)
C**** FUNCTION EVALUATION AT X+H.
      CALL YGRD
      DO 6 J=1,N
C**** CALCULATION  OF THE CHANGE IN EACH Y.
      YH(J)=(YH(J)+H*YG(J))/6.
      YD(J)=YD(J)+YH(J)
C**** VALUE OF Y,S AT X+H
    6 Y(J)=YD(J)
      RETURN
      END
```

```
      SUBROUTINE YGRD1
      DIMENSION AFF(500),AFFF(500),ATT(500)
      DIMENSION FF(500),FFF(500),TT(500),EE(100),EEE(100),PP(100)
      COMPLEX   YK(6,500 ),YH(6),Y(6),YG(6),YD(6),YL(6)
      COMPLEX  ACO,BCO,CCO,DCO,ECO,GR,PR,CS, ALFAG,ALFAS,AGAMA,ABETA
      COMMON/ST4/YK,YH,Y,YG,YD,YL
      COMMON/ST5/AFF,AFFF,ATT
      COMMON/ST6/X,NHMG,M,N
      COMMON/ST7/ACO,BCO,CCO,DCO,ECO
      COMMON/ST8/FF,FFF,TT,EE,EEE,PP
      COMMON/ST9/ALFAG,ALFAS,AGAMA,ABETA,GR,PR,CS
C**** HOMOGENEOUS EQUATIONS.
C**** TRIAL-AND-ERROR TECHNIQUE.
      YG(1)=Y(2)
      YG(2)=Y(3)
      YG(3)=Y(4)
      CALL LIZEAN
      YG(4)=(ACO)*Y(3)-BCO*Y(1)-CCO*Y(6)
      YG(5)=Y(6)
      YG(6)= DCO*Y(5)-ECO*Y(1)
      RETURN
      END
```

```
      SUBROUTINE  LIZEAN
      DIMENSION AFF(500),AFFF(500),ATT(500)
      DIMENSION FF(500),FFF(500),TT(500),EE(100),EEE(100),PP(100)
      COMPLEX  ACO,BCO,CCO,DCO,ECO,GR,PR,CS,  ALFAG,ALFAS,AGAMA,ABETA
      COMMON/ST5/AFF,AFFF,ATT
      COMMON/ST6/X,NHMG,M,N
      COMMON/ST7/ACO,BCO,CCO,DCO,ECO
      COMMON/ST8/FF,FFF,TT,EE,EEE,PP
      COMMON/ST9/ALFAG,ALFAS,AGAMA,ABETA,GR,PR,CS
      ACO    =(ALFAG)*(AFF(M)-CS)+2*(ALFAS)
      BCO=(AFF(M)-CS)*(ALFAG)*(ALFAS)+(ALFAS)*(ALFAS)+(AFFF(M)*ALFAG)
      CCO    =(1.0,0.0)
      DCO    =ALFAS+(AFF(M)-CS)*(PR*ALFAG)
   13 ECO    =PR*ALFAG*ATT(M)
      RETURN
      END
```

```
      SUBROUTINE YGRD2
      DIMENSION AFF(500),AFFF(500),ATT(500)
      DIMENSION FF(500),FFF(500),TT(500),EE(100),EEE(100),PP(100)
      COMPLEX    YK(8,500 ),YH(8),Y(8),YG(8),YG(8),YL(8)
      COMPLEX  ACO,BCO,CCO,DCO,ECO,GR,PR,CS, ALFAG,ALFAS,AGAMA,ABETA
      COMMON/ST4/YK,YH,Y,YG,YD,YL
      COMMON/ST5/AFF,AFFF,ATT
      COMMON/ST6/X,NHMG,M,N
      COMMON/ST7/ACO,BCO,CCO,DCO,ECO
      COMMON/ST8/FF,FFF,TT,EE,EEE,PP
      COMMON/ST9/ALFAG,ALFAS,AGAMA,ABETA,GR,PR,CS
C**** LINEARIZED NON-HOMOGENEOUS EQUATIONS.
C**** QUASILINEARIZATION TECHNIQUE.
      YG(1)=Y(2)
      YG(2)=Y(3)
      YG(3)=Y(4)
      YG(4)=-Y(1)*YL(7)*YL(8)*(AFF(M)-CS)-Y(1)*YL(8)*YL(8)-Y(1)*YL(7)*
     1AFFF(M)+Y(3)*YL(7)*(AFF(M)-CS)+2*Y(3)*YL(8)-Y(6)+Y(7)*YL(3)*(AFF(M
     1)-CS)-Y(7)*YL(8)*YL(1)*(AFF(M)-CS)-Y(7)*YL(1)*AFFF(M)-YL(7)*YL(3
     1)*(AFF(M)-CS)+YL(7)*YL(8)*YL(1)*(AFF(M)-CS)+YL(7)*YL(1)*AFFF(M)
     1+2Y(8)*YL(3)-Y(8)*YL(1)*YL(7)(AFF(M)-CS)-2Y(8)*YL(8)*YL(1)-2YL(
     18)*YL(3)+YL(8)*YL(1)*YL(7)(AFF(M)-CS)-2YL(8)*YL(8)*YL(1)
      YG(5)=Y(6)
       YG(6)=-Y(1)*YL(7)*PR*ATT(M)+Y(5)*YL(7)*(AFF(M)-CS)*PR-Y(5)*YL(8)
     1+Y(7)*YL(5)*(AFF(M)-CS)*PR-Y(7)*YL(1)*PR*ATT(M)-YL(7)*YL(5)*(AFF(
     1M)-CS)*PR+YL(7)*YL(1)*PR*ATT(M)-YL(5)*Y(8)+YL(5)*YL(8)
      YG(7)=0.0
      YG(8)=0.0
      RETURN
      END
```

```
      SUBROUTINE YGRD3
      DIMENSION AFF(500),AFFF(500),ATT(500)
      DIMENSION FF(500),FFF(500),TT(500),EE(100),EEE(100),PP(100)
      COMPLEX   YK(8,500 ),YH(8),Y(8),YG(8),YG(8),YL(8)
      COMPLEX  ACO,BCO,CCO,DCO,ECO,GR,PR,CS,  ALFAG,ALFAS,AGAMA,ABETA
      COMMON/ST4/YK,YH,Y,YG,YD,YL
      COMMON/ST5/AFF,AFFF,ATT
      COMMON/ST6/X,NHMG,M,N
      COMMON/ST7/ACO,BCO,CCO,DCO,ECO
      COMMON/ST8/FF,FFF,TT,EE,EEE,PP
      COMMON/ST9/ALFAG,ALFAS,AGAMA,ABETA,GR,PR,CS
C**** HOMOGENEOUS EQUATIONS.
C**** QUASILINEARIZATION TECHNIQUE.
      YG(1)=Y(2)
      YG(2)=Y(3)
      YG(3)=Y(4)
      YG(4)=-Y(1)*YL(7)*YL(8)*(AFF(M)-CS)-Y(1)*YL(8)*YL(8)-Y(1)*YL(7)*
     1AFFF(M)+Y(3)*YL(7)*(AFF(M)-CS)+2*Y(3)*YL(8)-Y(6)+Y(7)*YL(3)*(AFF(M
     1)-CS)-Y(7)*YL(8)*YL(1)*(AFF(M)-CS)-Y(7)*YL(1)*AFFF(M)
     1  +2Y(8)*YL(3)-Y(8)*YL(1)*YL(7)(AFF(M)-CS)-2Y(8)*YL(8)*YL(1)
      YG(5)=Y(6)
        YG(6)=-Y(1)*YL(7)*PR*ATT(M)+Y(5)*YL(7)*(AFF(M)-CS)*PR-Y(5)*YL(8)
     1+Y(7)*YL(5)*(AFF(M)-CS)*PR-Y(7)*YL(1)*PR*ATT(M)-YL(5)*Y(8)
      YG(7)=0.0
      YG(8)=0.0
      RETURN
      END
```

BIBLIOGRAPHY

1. Tollmien, W., Nat. Adv. Com. Aero. TM 609 (1931).
2. Schlichting, H., Nachr. Ges. Wiss. Gott. Math. Phys. Kl. 181. (1933).
3. Shen, S.F., J. Aeronaut. Sci. 21, 62. (1954).
4. Schubauer, G.B. and Skramstad, H.K., Nat. Adv. Com. Aero. Rept. 909. (1948).
5. Polymeropoulos, C.E. and Gebhart, B., J. Fluid Mech., 30, 225 (1967).
6. Gebhart, B., J. Heat Transfer, 91, 293 (1968).
7. Colak-Antic, P., Jahrbuch der WGLR, pp.171-176 (1964).
8. Plapp, J.E., Ph.D. Thesis Calif. Instit. Tech. (1957).
9. Plapp, J.E., J. Aeronaut. Sci., 24, 318 (1957).
10. Szewczyk, A.A., Intern. J. Heat and Mass Transfer, 5, 903, (1963).
11. Nachtsheim, P.R., NASA, TN, D-2089, (1963).
12. Hieber, C.A. and Gebhart, B., J. Fluid Mech., 48, 625 (1971).
13. Griffiths, E. and Davis, A.H., Special Rept. No. 9 Food Investigation Board D.S.I.R. (1922).
14. Schmidt, E. and Beckman. Tech. Mech. Thermodynamics 1, 341, 391 (1930).
15. Schmidt, E., Forsch. G.b. Ingwes 3, 181, (1932).
16. Herman, R., Z. Physik. 33, 425 (1932).
17. Herman, R., Z. Angew. Math. Mech., 13, 433 (1933).
18. Saunders, O.A., Proc. Roy. Soc., A172, 55 (1939).
19. Saunders, O.A., Proc. Roy. Soc., A157, 278 (1936).
20. Eigenson, L.S., Compt. Rend. Acad. Sci. URSS, 26, 440, (1940).

21. Eckert, E.R.G. and Soehnghen, E., Proc. Gen. Discussion Heat Transfer, p.321. Inst. Mech. Engrs. London (1951).

22. Fujii, T., Bull. JSME. 2, 551 (1959).

23. Eckert, E.R.G., Hartnett, J.P. and Irvine, T.F., A.S.M.E. Paper No. 60.WA.250. (1960).

24. Tritton, D.J., J. Fluid Mech., 16, 417 (1963).

25. Dring, R.P. and Gebhart, B., J. Fluid Mech., 36, 446 (1969).

26. Cheesewright, R., J. Heat Transfer, 90, 1, (1968).

27. Vliet, G.C. and Liu, C.K., J. Heat Transfer, 91, 517 (1969).

28. Kurtz, E.F. and Grandall, S.H., J. Math. Phys., 41, 264 (1962).

29. Sparrow, E.M., Tsau, F.K. and Kurtz, E.F., Phys. Fluids, 8, 1559 (1965).

30. Knowles, C.P. and Gebhart, B., J. Fluid Mech., 34, 657 (1968).

31. Hieber, G.A. and Gebhart, B., J. Fluid Mech., 49, 557 (1971).

32. Mack, L.M., Methods in Computational Physics, vol.4, Academic Press (1965).

33. Bird, R.B., Stewart, W.E. and Lightfoot, E.N., "Transport Phenomena", John Wiley and Sons, New York, (1960), 3rd ed.

34. Schlichting, H., "Boundary Layer Theory", McGraw-Hill, New York (1968), 6th ed.

35. Lamb, H., "Hydrodynamics", Cambridge University Press, Cambridge (1932), 6th ed.

36. Curbe, N., "Laminar Boundary Layer Equations", Oxford University Press (1962).

37. Prandtl, L., Proc. 3rd Intern. Math. Congr. Heidelberg, (1904). Translated NACA TM 452 (1928).

38. Merk, H.J. and Prins, J.A., App. Sci. Pes., A4, 11 (1953).

39. Ostrach, S., NASA, TN 2635 (1952).

40. Sparro, E.M. and Gregg, J.L., J. Ht. Tr. (ASME), 80, 379 (1958).

41. Hellums, J.D. and Churchill, S.W., A.I.Ch.E.J., 10, 110 (1964).

42. Acrivos, A., A.I.Ch.E.J., 6, 584 (1960).

43. Schmidt, E. and Beckmann, W., Forsch. Ing. Wes., 1, 391 (1930).

44. Schlichting, H., NACA, TM 1265 (1950).

45. Bellman, R., Proc. Natl. Acad. Sci. U.S., 41, 743 (1955).

46. Kalaba, R.J., J. Math. Mech., 8, 519 (1959).

47. Bellman, R. and Kalaba, R.J., "Quasilinearization and Nonlinear Boundary-value problems", American Elsevier Publishing Co., New York (1965).

48. Beckenbach, E.F. and Bellman, R., "Inequalities", Springer, Berlin (1961).

49. Lee, E.S. and Fan, L.T., Can. J. Chem. Eng., 42, 200 (1968).

50. Lee, E.S., Chem. Eng. Sci., 21, 183 (1966).

51. Lee, E.S., "Quasilinearization and Invariant Imbedding", Academic Press, New York and London (1968).

52. Radbil, J.R. and McCue, G.A., "Quasilinearization and Nonlinear Problems in Fluid and Orbital Mechanics", American Elsevier Publishing Co., New York (1970).

53. Diplock, P.A., Ph.D. Thesis, University of London (1971).

54. Harris, J.B., M.Sc. Thesis, University of London (1970).

55. Kantorovich, L.V., Usp. Mat. Nawk 3, 89 (1948).

56. Kantorovich, L.V. and Krylov, V.I., "Approximate Methods of Higher Analysis", Wiley (Interscience), New York, (1958).

57. Kaplan, R.E., Mass. Inst. Tech. Aeroelastic and Structures Lab. TR116-1 (1964).

58. Bellman, R., Commun. ACM4, 222 (1961).

59. Bellman, R., Kalaba, R.J. and Kotkin, B., RM-3113-PR, RAND Corp, Santa Monica, California, April (1962).

60. Green, M.B., Ph.D. Thesis, University of London (1968).

61. Pandya, D.V., Ph.D. Thesis, University of London (1967).

62. Fox, L., "Numerical Solution of Ordinary and Partial Differential Equations", Pergamon, Oxford (1962).

63. Koppel, D.H., Tech. Dep. 86, Hudson Labs., Columbia University, pp.15-18 (1960).

64. Lock, G.S.H., Gort, C. and Pond, G.R., Appl. Scient. Res. Research 18, 171 (1967).

65. Polymeropoulos, C.E., Ph.D. Thesis, Cornell University (1966).

66. Brown, W.B., "Boundary Layer and Flow Control", Vol. 2, G.V. Lachman, ed., Pergamon Press, pp.913-923 (1961).

67. Hildebrand, F.B., "Method of Applied Mathematics", Prentice Hall, Englewood Cliffs, N.J. (1952).